Akt signalling in the human parasite *Schistosoma mansoni*

Thesis submitted in partial fulfilment of the requirements of Kingston University for the degree of Doctor of Philosophy

by

Maxine MCKENZIE

School of Life Science, Pharmacy and Chemistry
Kingston University
London

October 2017

Declaration

I Maxine McKenzie declare that all the work presented in this thesis is my own and does not contain any material that has been previously submitted for an award at an institute of Higher Education either in the UK or overseas.

Signed

……

Acknowledgements

Many people have helped during the course of this project and contributed to the final presentation of this thesis. My special thanks go to:

My supervisors Professor Tony Walker and Dr Ruth Kirk;
My friends and colleagues in the parasitology research group at Kingston University;
Dr Nuha Mansour and Professor Quentin Bickle at the London School of Hygiene and Tropical Medicine;
Dr Patrick Skelly at Tufts University, USA;
My friends and family for providing endless support.

Kingston University provided a studentship for the development of this work.

I dedicate this thesis to my Uncle Andy.

Publications

Mckenzie, M., Ruth, S. Kirk and Walker, A.J. (2017) Glucose uptake in the human pathogen *Schistosoma mansoni* is regulated through Akt/Protein Kinase B signalling. *The Journal of Infectious Diseases* **X(X)**: 1 – 13.

Presentations

British Society of Parasitology Spring Meeting, London, United Kingdom, April 2016. Akt signalling in the human parasite *Schistosoma mansoni*. Maxine Mckenzie, Ruth S. Kirk, Anthony J. Walker.

XIIth European Multicolloquium of Parasitology (EMOP), Turku, Finland, July 2016. From cercariae to adult worms; the story of Akt signalling in S*chistosoma mansoni*. Maxine Mckenzie, Ruth S. Kirk, Anthony J. Walker.

Abstract

The study of cell signalling in schistosomes is crucial in deepening our knowledge of the biology of these blood flukes, which affect hundreds of millions of people worldwide. Here, Akt/protein kinase B (PKB) signalling has been functionally characterised and mapped in *Schistosoma mansoni*; an Akt variant of approximately 52 kDa has been characterised and RNA interference of the *S. mansoni* Akt gene, resulted in an 84% reduction in Akt expression. The phosphorylation (activation) status of the characterised Akt protein was increased by host molecules, including insulin and L-arginine in somules and adult worms, and L-arginine and linoleic acid in cercariae. Akt phosphorylation (activation) was also attenuated by Akt Inhibitor X and herbimycin A treatment. Immunohistochemistry/confocal laser scanning microscopy revealed phosphorylated Akt in all *S. mansoni* human infective/resident life stages. Somules and adult worms displayed activated Akt primarily in the tegument, particularly the tubercles and gynaecophoric canal of adult males. Cercariae exhibited activated Akt in the nervous system and punctate regions along the length of the tail prompting investigation into the role of Akt in cercarial motility. Behavioural studies demonstrated a significant increase in cercarial swimming in response to host factors, which was attenuated following exposure to Akt inhibitor X. The striking activation of Akt observed in the tegument of adult worms stimulated research into its possible role in glucose uptake in this host-interactive layer. RNAi of Akt resulted in a 59% and 47% reduction in SGTP4 glucose transporter expression in male and female adult worms respectively with a concomitant reduction in glucose uptake by the parasite. In somules, the expression of SGTP4 and its evolution at the apical tegument membrane during transformation were significantly attenuated by Akt Inhibitor X; a 74% reduction in glucose uptake was also demonstrated following Akt inhibition. Bioinformatic analysis of *S. mansoni* Akt interacting proteins uncovered a putative connection between Akt and Rab vesicle trafficking proteins and a mechanistic model illuminating the possible role of Akt in the translocation of SGTP4 to the parasite surface was proposed. Collectively, this research highlights the significance of Akt in schistosome homeostasis and host-parasite interactions and thus demonstrates that Akt may be a suitable target for anti-schistosome drug development strategies.

Table of Contents

List of Figures

Chapter 1

Chapter 3

Chapter 5

Chapter 6

Chapter 7

List of Tables

Chapter 1

Chapter 2

Chapter 4

List of Videos

List of Abbreviations

aa	amino acid
ATP	adenosine triphosphate
BME	basal medium Eagles
BSA	bovine serum albumin
cAMP	cyclic adenosine monophospohate
Cdc42	cell division control protein 42
cm, mm, µm	centimetre, millimetre, micrometer
DMSO	dimethyl sulfoxide
EGF	epidermal growth factor
EGFR	epidermal growth factor receptor
ERK	extracellular regulated kinase
FCS	fetal calf serum
FTW	filtered tap water
g	gravitational acceleration
g, mg, µg	gram, milligram, microgram
GAP	GTPase-activating protein
GLUT4	glucose transporter 4
GO	gene ontology
GPCRs	G protein coupled receptors
GSK-3	glycogen synthase kinase-3
GTP	guanine triphosphate
h, min, sec	hours, minutes, seconds
HBSS	Hanks balanced salt solution
HRP	horseradish peroxidase
Hu	human
IC_{50}	50% inhibitory concentration
IGF-1	insulin-like growth factor
IGF-1R	insulin-like growth factor receptor
IP	immunoprecipitation
IR	insulin receptor
kDa	Kilodalton
l, ml, µl	litres, millilitres, microliters
LA	linoleic acid
M, mM, µM	molar, millimolar, micromolar
MAPK	mitogen activated protein kinase
mTOR	mechanistic target of rapamycin
NTD	neglected tropical disease
$p70^{S6K}$	70 kDa ribosomal protein S6 kinase 1
PBS	phosphate buffered saline
PDGF	platelet derived growth factor
PDK1	phosphoinositide-dependent protein kinase-1
PH	plecktstrin homology
PI3K	phosphoinositide 3-kinase
PIP_2	phosphatidylinositol 4,5-biphosphate

PIP_3	phosphatidylinositol 3,4,5 triphosphate
PK	protein kinase
PKA	protein kinase A
PKB	protein kinase B
PKC	protein kinase C
PMA	Phorbol myristate acetate
PTK	protein tyrosine kinase
PZQ	Praziquantel
RAC	Related A and C kinase
RIPA buffer	radio immunoprecipitation assay buffer
RNAi	ribonucleic acid interference
RPMI – 1640	Roswell park memorial institute – 1640 medium
RK	receptor kinase
RTK	receptor tyrosine kinase
Ser	serine
SGTP1/4	schistosome glucose transporter 1/4
SLK	Ste20-like kinase
Sm	*Schistosoma mansoni*
Smp	*Schistosoma mansoni* protein
Sos	son of sevenless
STK	serine/threonine kinase
TBS	tris-buffered saline
TGF-β	transforming growth factor-β
TK	tyrosine kinase
TGN	trans-Golgi network
Thr	threonine
Tris	tris[hydroxyimethyl] amino-methane
T-TBS	Tween-20 tris-buffered saline
Tyr	tyrosine
V	volts
VFT	venus flytrap
VKR	venus kinase receptor
WHO	World Health Organisation
ZAK1	cAMP-activated protein tyrosine kinase

1

Introduction

1.1 Schistosomiasis – A Neglected Tropical Disease

1.1.1 Epidemiology

Human schistosomiasis, one of the most prevalent neglected parasitic diseases, is predominantly tropical and subtropical affecting between 200-250 million people across 78 countries (Chitsulo *et al.*, 2004; Hu *et al.,* 2004; WHO, 2017) (Figure 1.1). Human schistosomiasis results from an infection of parasitic schistosomes; platyhelminth blood-dwelling flukes with a complex life cycle, that ultimately reside in the mammalian host. The primary human-infecting species are *Schistosoma mansoni* and *S. japonicum*, which cause intestinal schistosomiasis, and *S. haematobium* which causes urinary schistosomiasis. Two further species, *S. intercalatum* and *S. mekongi*, can also cause human intestinal schistosomiasis but do not feature greatly in schistosomiasis disease research. *S. mansoni* is endemic in 52 of the 78 affected countries[1], and the number of people at risk from *S. mansoni* infection has increased over time and currently stands at approximately 700 million. This has been largely due to population growth and subsequent water resource development projects such as dams and land reclamation (Chitsulo *et al*., 2000). Human schistosomiasis is caused by the parasite eggs becoming trapped in tissues, resulting in inflammation and obstruction in either the intestinal or urinary systems. Well known for its chronic nature, human schistosomiasis has a high morbidity rate, particularly in rural areas where individuals have had long-standing infections without treatment (Gryseels *et al.*, 2006). In sub-Saharan Africa alone, there are still an estimated 280,000 deaths each year as a direct result of infection by human schistosomes (Berriman *et al*., 2009).

1.1.2 Disease pathology

Human schistosomiasis can present as an acute or chronic infection. Acute schistosomiasis, or Katayama fever, is more commonly seen in tourists and travellers exposed to cercariae in endemic areas. The syndrome begins as a temporary rash at the site of skin penetration up to one week after exposure, progressing often to include pulmonary and abdominal symptoms, headache, and bloody diarrhoea two to ten weeks post-infection (Ross *et al.*, 2002; Bottieau *et al.*, 2006). The source of the Katayama symptoms has been suggested as an allergic reaction to antigens released into the blood during somule migration (Bailek and Knobloch, 1999). Repeated treatments with the drug praziquantel (PZQ) are commonly used against acute cases of schistosomiasis (Ross *et*

[1] http://www.who.int/mediacentre/factsheets/fs115/en/ [Accessed: March 31st, 2017]

al., 2002). Chronic schistosomiasis is found in endemic areas and can be characterised by intestinal lesions caused by eggs produced from the adult worms. Proteolytic enzymes and other molecules released from the eggs cause eosinophilic inflammatory and granulomatous reactions (Gryseels *et al.*, 2006), mediated by egg antigen-specific $CD4^+$ T helper (Th) lymphocytes (Stadecker, 1999). Collectively termed soluble egg antigens (SEA), eggs secrete a complex variety of glycoproteins and glycolipids (van Liempt *et al.*, 2007) *via* microscopic pores (Ashton *et al.*, 2001). The most abundant egg antigen is Sm-p40, making up 10% SEA (Nene *et al.*, 1986; Chikunguwo *et al.*, 1991). Characterised in mice, Sm-p40 is also immunogenic in humans (Stadecker, 1999), eliciting a Th1 biased immune response (Hernandez *et al.*, 1998). Other major egg antigens include omega-,1 kappa-5 and IPSE/alpha1 (Dunne *et al.*, 1986; Schramm *et al.*, 2003). Usually, granulomas develop where the accumulation of eggs is greatest; for infections by *S. mansoni* this is typically the intestines and the liver. During the early stages of infection, SEAs mediate a Th1 response, developing to a Th2 response as the infection advances (Pearce *et al.*, 1991; van Liempt *et al.*, 2007).

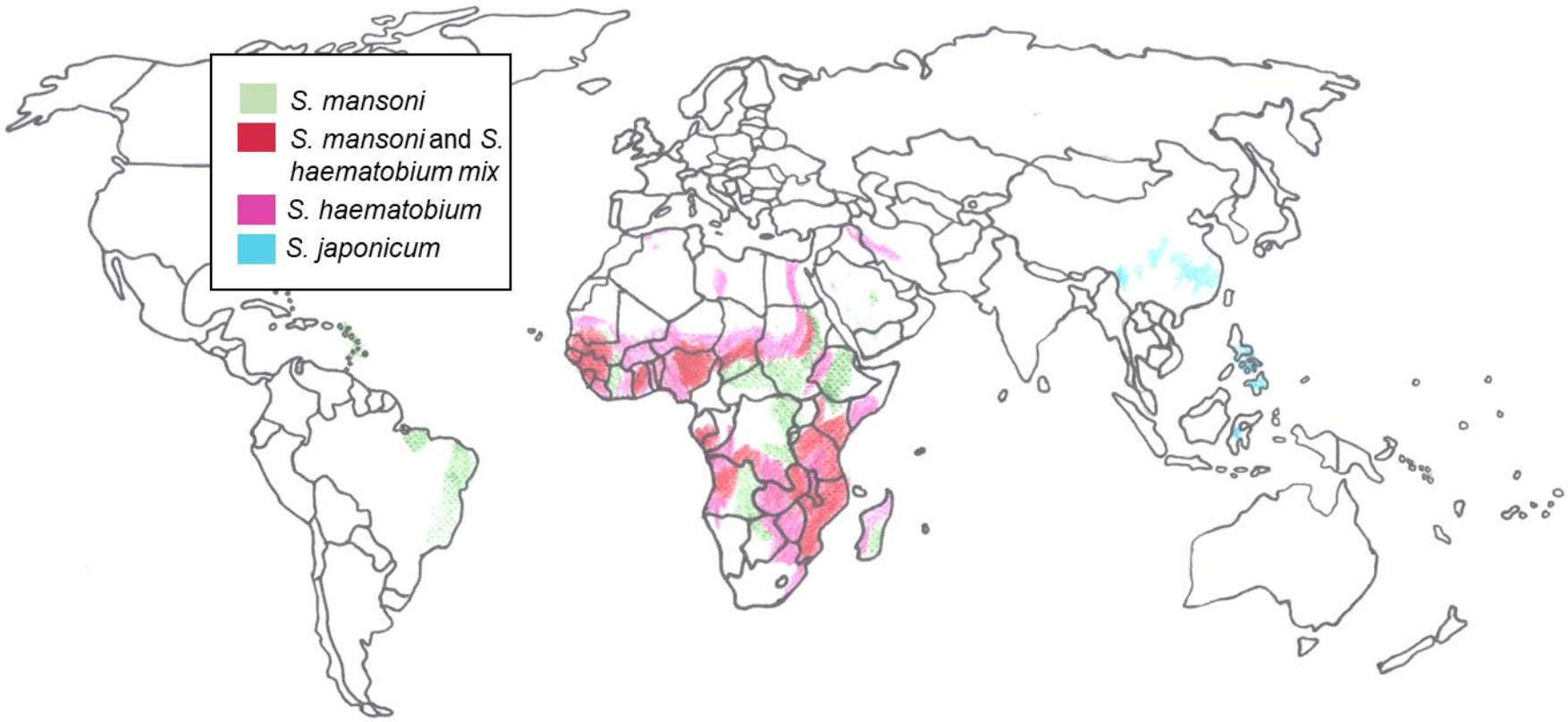

Figure 1.1 **The global distribution of human schistosomiasis.** Endemic regions of human schistosomiasis (as at 2006) caused by *S. mansoni, S. haematobium, S. and S. japonicum*. Adapted from Gryseels *et al.*, 2006

1.1.3 Schistosomiasis drug control strategies

Recent figures show that in 2015 at least 218 million people required preventative action for schistosomiasis, and 66.5 million were treated for the disease (World Health Organisation, 2017). In affected areas across Africa and South America, large-scale treatment programmes are running with PZQ as the only available drug to treat schistosomiasis of all species (Berriman *et al*., 2009; Fallon and Doenhoff, 1994). There are reports that drug resistance is developing after three decades of treatment exclusively with PZQ (Chitsulo *et al.*, 2004) and drug resistance can certainly be developed in a laboratory setting (Doenhoff *et al.*, 2002). Unfortunately, PZQ cannot prevent re-infection by the parasite and its efficacy is dependent on multiple parameters such as parasite gender and time of infection; juvenile schistosomes are not susceptible (Pica-Mattoccia and Cioli, 2004). There are also other possible reasons for treatment failures; PZQ has low water solubility and extensive first-pass metabolism through the liver, significantly decreasing the drug's bioavailability (Cioli *et al.*, 1995).

In the last decade, a few alternatives to PZQ have been found, although with less efficacy (reviewed by Cioli *et al.*, 1995). Oxamniquine has been used successfully in South America and Africa as a 'complementary drug' when PZQ treatment fails[2]. Oxamniquine is only effective against *S. mansoni,* but can be implemented at all stages of the disease with cure rates of 60-90 % (Bustinduy and King, 2014). Downsides of oxamniquine include its method of activation, which requires a schistosome sulfotransferase that is not present in drug-resistant worms (Pica-Mattoccia *et al.*, 2006). Another drug, Metrifonate (2,2,2-trichloro-1-hydroxyethyl dimethyl phosphonate), was developed in the 1950s originally as an insecticide (Lorenz *et al.*, 1955). Metrifonate is particularly effective against *S. haematobium* and has been used in the past to treat urinary schistosomiasis, although is it now no longer available (Pottinger and Jong, 2017).

1.1.4 The future of schistosomiasis

With the World Health Organisation having announced an ambitious target to eliminate global schistosomiasis by 2025, focus is turning to control of the intermediate host snail. The genome of the gastropod snail *Biomphalaria glabrata*, a host for *S. mansoni*, has recently been published (Adema *et al.*, 2017). This will facilitate new molecular research to help establish the mechanisms responsible for snail-schistosome host compatibility

[2]http://www.who.int/medicines/publications/essentialmedicines/20th_EML2017_FINAL_amendedAug2017.pdf?ua=1 [Accessed September 4th 2017].

and discover how the parasite evades the snail immune system. It is anticipated that in the future it may be possible to deploy genetically engineered snails in endemic areas that are refractory to schistosome infection/development. Given that PZQ does not guard against reinfection of schistosomes, halting transmission of the parasite at the snail host stage would aid enormously in the long-term aim to eradicate the disease. Although education and proper sanitation play an important part in an integrated control strategy to eliminate schistosomiasis, continued mass drug administration of PZQ combined with efforts to determine a novel drug or vaccine target against the schistosome and snail control methods are considered the best hope for achieving sustainable global elimination.

1.2 Schistosomes and Their Life Cycle

The life cycle of schistosomes is complex and each parasite life stage displays unique adaptations, allowing the parasite to make the difficult journey between intermediate snail and definitive human hosts and to survive within each host (Jones *et al.,* 2008). These remarkable adaptations are manifest during a striking array of morphological and physiological changes that occur in the life cycle (Figure 1.2). Adult female *S. mansoni* worms can produce hundreds of eggs per day, each containing a developing larva called

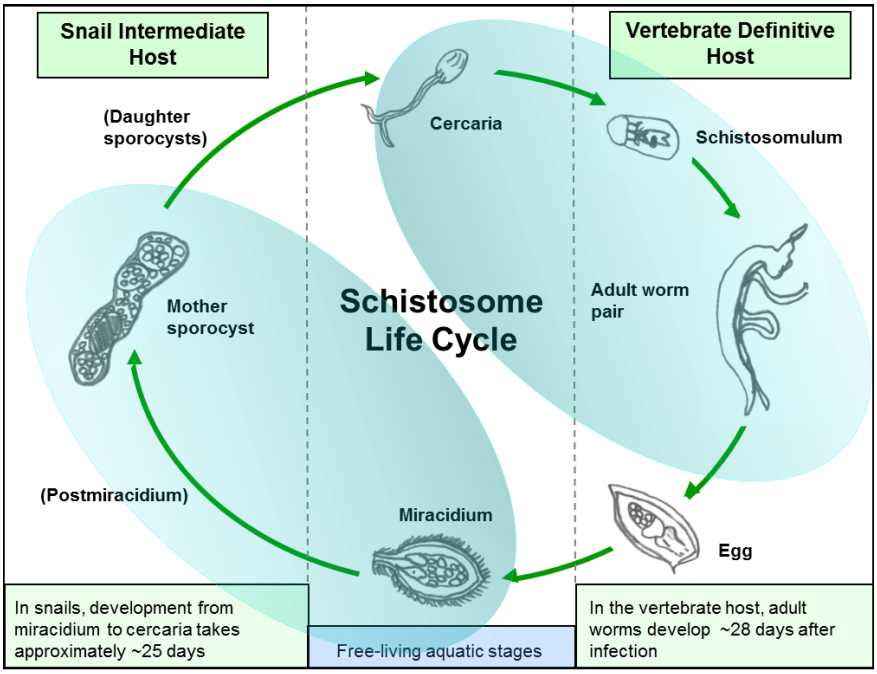

Figure 1.2 **Life cycle of *S. mansoni***. The parasite develops through various life stages that are adapted for the specific environment encountered (Reproduced with kind permission from A.J. Walker).

a miracidium. Those eggs destined for excretion migrate to the lumen of the intestine, where they are expelled from the host in the faeces. On contact with fresh water miracidia are released from their egg capsules and immediately start swimming (Gryseels *et al.*, 2006; Ressurreição *et al.*, 2011). The miracidium is approximately 150 µm long (Walker, 2011) and viable for up to 24 hours (Gryseels *et al.*, 2006). Miracidia use cilia to propel themselves through the water and search for their compatible intermediate host snails (e.g. *Biomphalaria*), aided by light, chemical signals and other environmental stimuli including water currents and temperature (Haas and Haberl, 1997; Gryseels *et al.*, 2006; Walker, 2011). *S. mansoni* miracidia swim fast and can infect snail hosts up to 9 m and 27 m away in standing and flowing water, respectively (Haas, 2003). The mechanism of penetration into the snail is unclear but is thought to result from a combination of proteases secreted from penetration glands of the miracidia and mechanical movement. After penetrating the snail, the miracidia shed their cilia and differentiate into asexually reproducing mother, and subsequently daughter, sporocysts, which eventually develop into cercariae (Walker, 2011). This asexual multiplication strategy ensures that large numbers of cercariae are produced from a single miracidium to provide optimal chances of definitive host infection.

Four to six weeks post-infection, the infected snail begins to shed cercariae. Shedding is influenced by light, happens mostly during the day and can last for months with infection caused by just one miracidia. At this early stage, the parasites are already sexually differentiated (Boissier *et al.*, 1999). Using their bi-furcated tails and glycogen reserves, the cercariae spin around and swim in the water for up to 72 hours, seeking a definitive host (Gryseels *et al.*, 2006). Miracidial and cercarial stages do not feed and therefore have limited energy reserves to swim and find a host. Consequently, these life stages have developed mechanisms for successful host location and penetration in order to survive (Haas and Haberl, 1997). Host location by cercariae is achieved using water turbulence and specific skin chemicals including linoleic acid (Ressurreição *et al.*, 2011). Attachment to the skin of the host is stimulated by L-arginine (Haas *et al.*, 2002), and cercariae will creep along the skin to find a suitable point of entry using heat gradients as small as 0.15 °C/mm (Haas, 2003). Cercariae penetrate the skin of the host by releasing proteases and mucus from the pre- and post-acetabular glands respectively. The contents of these glands aid attachment to the host skin, tissue digestion and immune evasion (Haas *et al.*, 1997). The tail is a temporary locomotion organ, which is shed once penetration has been achieved (Walker, 2011).

Cercariae start to develop into skin schistosomules (hereafter abbreviated to somules) when the tail is shed. At this point, several structural and physiological changes take place including release of the pre-acetabular gland contents, formation of a double bilayer outer membrane and production of new glycoproteins (Walker, 2011). The somules remain in the skin for an average 72 hours (for *S. mansoni*) before moving into the blood system, although movement has been reported to take up to 7 days (LoVerde *et al.*, 2004). The somules migrate through the pulmonary capillaries in the lungs from which they are able to enter systemic circulation. At this stage, they are young worms. Ultimately, the liver is where the worms begin to feed and pair up (Walker, 2011); full maturity is reached after a further 4-6 weeks in the hepatic portal vein (Gryseels *et al.*, 2006). Males grow considerably larger than the females and display higher levels of mitotic activity (Walker, 2011).

After maturing in the portal vein, the adult worms migrate to and settle in the mesenteric venous plexus, feeding on host blood and globulins *via* anaerobic glycolysis (Skelly and Shoemaker, 1995). The adult male flatworm is curled and appears cylindrical in shape, measuring an average 10 mm long (Machado-Silva *et al.*, 1995). The adult female measures longer than the male at up to 20 mm. Like all other blood-dwelling parasites, *S. mansoni* possess a unique tegument consisting of a single double-bilayer membrane surrounded by a syncytium of fused cells (Van Hellemond *et al.*, 2006). Other features include terminal suckers, a blind gut, and reproductive organs. The male worm curls round to form a gynaecophoric canal within which the thinner female lies, once pairing has occurred (LoVerde *et al.*, 2004). Once coupled, the females and males fully develop and the female lays eggs which either pass through the epithelium of the host to the intestinal system to be excreted, or collect in tissues including the liver causing granuloma and fibrosis (Berriman *et al.*, 2009). The sexual maturation of the female worm is crucially dependant on this pairing with the male, and very few other organisms make such permanent attachments, an example is *Diplozoon paradoxum*, where partners become fused at their point of contact (Kunz, 2001). The male schistosome regulates gene expression of the female *via* an uncharacterised mechanism (LoVerde *et al.*, 2004). Several female-specific genes, signalling pathways and receptors have been identified as having a role in female reproductive development (LoVerde *et al.*, 2009). The average life-span of an adult worm is 3-5 years but they have been recorded to live up to 30 years in some cases (Gryseels *et al.*, 2006).

1.2.1 Biology of cercariae

S. mansoni cercariae were first identified in 1915 in a specimen of *Planorbis boissyi* from Cairo (Khalil, 1922). *S. mansoni* cercariae are approximately 300 µm in length, comprising a body (head) and stage-specific tail ending in paired furcae. The head possesses a mouth at the anterior tip, an oral sucker, the acetabulum and acetabular glands (Mair *et al.*, 2003) (Figure 1.3). The pre- and post-acetabular glands, two and three pairs respectively, fill approximately two thirds of the body cavity (Collins *et al.*, 2011). Cercariae are coated in a surface layer called the glycocalyx, which is rich in sugars and covers the trilaminate membrane tegument (Dorsey *et al.*, 2002). The glycocalyx acts as a barrier against osmotic pressure in the cercariae's aquatic environment (Samuelson and Caulfield, 1982). In addition to the glycocalyx, cercariae are also covered in actin-rich spines and ciliated sensory papillae which aid in host location (Collins *et al.*, 2011). Sensory papillae are nerve terminals found at the surface of the tegument and allow the cercariae to connect to their environment. Located along the length of the whole parasite, unsheathed uni-ciliated papillae are the most abundant

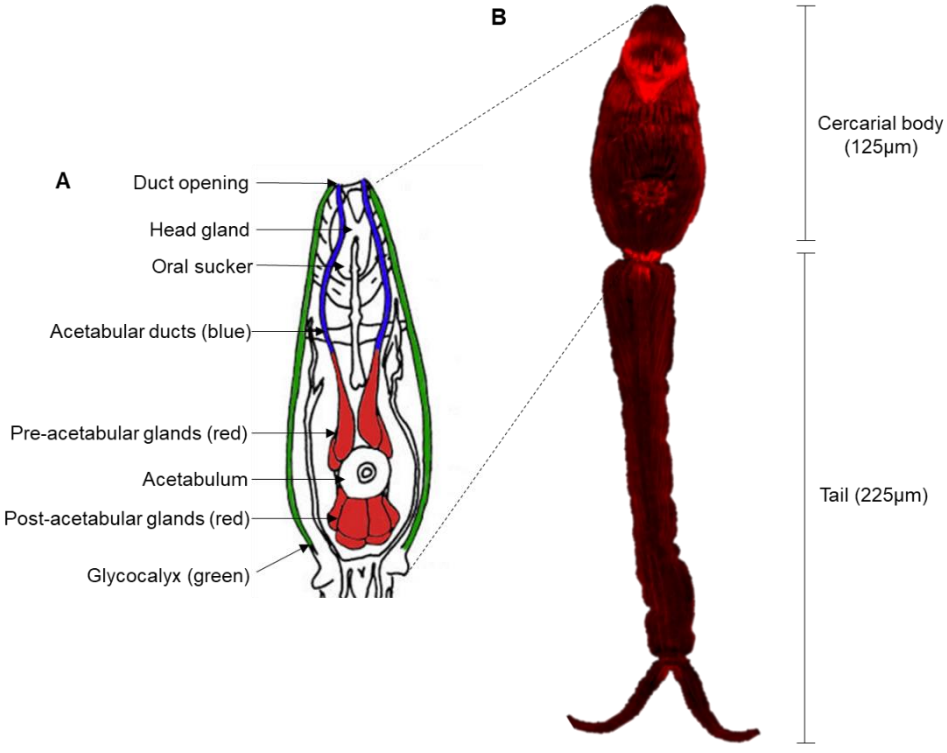

Figure 1.3 **The schistosome cercaria**. **A.** Schematic diagram of a cercariae showing the morphological features. (Ressurreicao, 2013, originally adapted from Dorsey *et al*., 2002). **B.** Fluorescence confocal image of a cercaria stained with rhodamine phalloidin to reveal various structures.

type of papillae, with a bulbous body and one projecting cilia approximately 7 μm wide anchored to a nerve fibre (Dorsey *et al.*, 2002). A comprehensive atlas of cercarial structures and musculature has been composed by Collins *et al.* (2011).

Beneath the tegument of cercariae lies a cytoplasmic layer containing three types of cells, connected to the surface membrane *via* cytoplasmic bridges (Hockley and McLaren, 1973). The most commonly distributed cell are the type 1 cytons; type 2 cytons are restricted to a small area in the dorso-anterior region of the cercarial body (Skelly and Shoemaker, 2001). The final subtegumental cell type is the head gland, which exists exclusively in the anterior organ (oral sucker) and possesses many connections to the tegument around the oral sucker (Dorsey, 1976). The membranous bodies contained within all three cell types migrate to the tegument through the cytoplasmic bridges during transformation from cercaria to somule.

The free-swimming cercaria has four distinct muscle types; circular, diagonal, longitudinal and striated fibres. The latter is located only in the tail with the other three types making up the body wall of the cercariae. Circular muscles form the outer muscle layer, with longitudinal and diagonal muscles interweaved underneath (Collins *et al.*, 2011). Some of the musculature is specific to the cercariae, such as the striated muscle in the tail, but some is similar or identical to the muscles seen in adult schistosomes, such as in the oesophagus and body wall. Other adult features including the reproductive organs have yet to develop (Mair *et al.*, 2003).

Provided with only a limited supply of glycogen reserves metabolised by anaerobic respiration (Tielens, 1997), it is imperative that the cercaria is efficient at locating a definitive host. Despite *S. mansoni* being a very successful species, little was known about the swimming behaviours until the last decade (Brachs and Haas, 2008). *S. mansoni* cercariae accumulate in a water depth of 20-30 cm, a suitable environment to encounter swimming humans (Haas *et al.*, 2008), but are seemingly generally unresponsive to shadow and light (Brachs and Haas, 2008). Brachs and Haas (2008) did report however, that higher light intensity induced longer active swimming phases and shorter passive phases. Active cercarial swimming is mainly backwards, with the tail facing the direction of travel. Forward travel is used to change direction. Passive phases involve the cercariae sinking head first. The swimming pattern displayed by *S. mansoni* cercariae is comparable to that of other species such as *Trichobilharzia ocellata* (Brachs and Haas, 2008).

Cercarial penetration through host skin has been the subject of much research dating back to the early 20th century (Fujinami and Nakamura, 1909), although the first study specifically on *S. mansoni* is not recorded until 1915 (Leiper, 1915). There are several stages to the process of penetrating the mammalian host, and each is stimulated by a different chemical cue derived from the skin. Initial attachment is promoted by L-arginine (Granzer and Haas, 1986), lingering on the skin by ceramides and acylglycerols (Woicke and Haas, 1989), and creeping to the point of entry stimulated by L-arginine (Haas *et al.*, 1989); penetration itself is stimulated by unsaturated fatty acids (Shiff *et al.*, 1972). The chemicals are thought to be detected by the sensory papillae on the syncytial tegument that surrounds both the head and tail sections of the cercariae (Granzer and Haas, 1986).

In addition to ceramides and acylglycerols, it is suggested that the contents of the post-acetabular gland may also support prolonged contact to the host's skin surface (Stirewalt and Kruidenier, 1961). The pre- and post-acetabular gland contents are released during creeping and penetration and contribute to host skin degradation, loss of the cercarial glycocalyx and protection against the host's immune system for the newly transformed somule (McKerrow and Doenhoff, 1988). Typically, acetabular gland secretion is stimulated by host skin lipids and occurs only when required during invasion (Haas *et al.*, 1997), but can also be induced by some chemical stimuli including PZQ (Matsumura *et al.*, 1990).

1.2.2 Biology of somules

There are three recognised stages of a somule: skin, lung and liver somule, indicating the locations through which the somules pass on their voyage to the liver. There has been some debate over how long somules take to pass through the skin although consensus is up to five days with an average of three days (He *et al.*, 2002; Wheater and Wilson, 1979). It was initially thought that cercariae utilised hair follicles as a route of entry into the skin, however research has shown that the parasites will penetrate any skin surface area (He *et al.*, 2002). During skin transit, Wheater and Wilson (1979) observed the somule distribution change from the epidermis towards the dermis and blood vessels contained within (Figure 1.4). Somules have been observed to slow down at the epidermal-dermal junction (basement membrane) which must be degraded using acetabular gland secretions, before the larvae can pass through (He *et al.*, 2002). The minimum time taken for somules to reach the blood is two days, after which time,

somules arrive in the lungs, locating themselves preferentially in the capillaries surrounding the pleural surface. This phase of somule migration can take anywhere from four to eighteen days and sees the somules elongate (Wheater and Wilson, 1979). Somules began to appear in branches of the hepatic portal vein as early as seven days post infection (He *et al.* 2002).

Several important morphological events occur during the transformation from cercaria and subsequent growth of the somule. The contents of all cercarial glands are released and the tail is shed. The glycocalyx that surrounds cercariae is replaced with the start of the double bilayer lipid membrane tegument (Samuelson and Caulfield, 1985; Skelly and Shoemaker, 2001). The development of the tegument at this crucial stage became of interest over four decades ago, when a detailed report hypothesised that the trilaminate cercarial membrane is replaced by a heptalaminate membrane within three hours of transformation (Hockley and McLaren, 1973). Hockley and McLaren (1973) observed that the additional layers of membrane were gained from membranous vesicles, originating in the sub-tegumental cells, fusing with the apical membrane. Since the preliminary research, additional data confirmed that the syncytial tegument of the developing somule consists of a tightly opposed double bi-layer membrane (McLaren and Hockley, 1977).

Figure 1.4 illustrates the passage of the somule through the skin layers and additionally the potential immune interactions occurring at each stage. Eight hours after infection, *S. mansoni* stimulates the production of cytokines IL-1 receptor agonist (IR-1ra), IL-10 and TNFα from Langerhans cells, keratinocytes and epidermal T lymphocytes in the epidermis (He *et al.*, 2002). It is possible that the residual components of the cercarial glycocalyx are partly responsible for eliciting this response (Jenkins *et al.*, 2005; Samuelson and Caulfield, 1982). Interestingly, infection by *S. japonicum* stimulates the production of many more cytokines, indicating a difference in immune response to a species, which migrates faster through the skin (Jenkins *et al.*, 2005). During traversal through the skin layers, somules secrete immunoregulatory products such as prostaglandin D2 (Angeli *et al.*, 2001) with the goal of suppressing the host immune system sufficiently for safe passage into the blood vessels (Fusco *et al.*, 1986; Salafsky *et al.*, 1987). Prostaglandin D2 inhibits the migration of Langerhans cells, preventing their departure from the epidermis and maturation into dendritic cells (Angeli *et al.*, 2001).

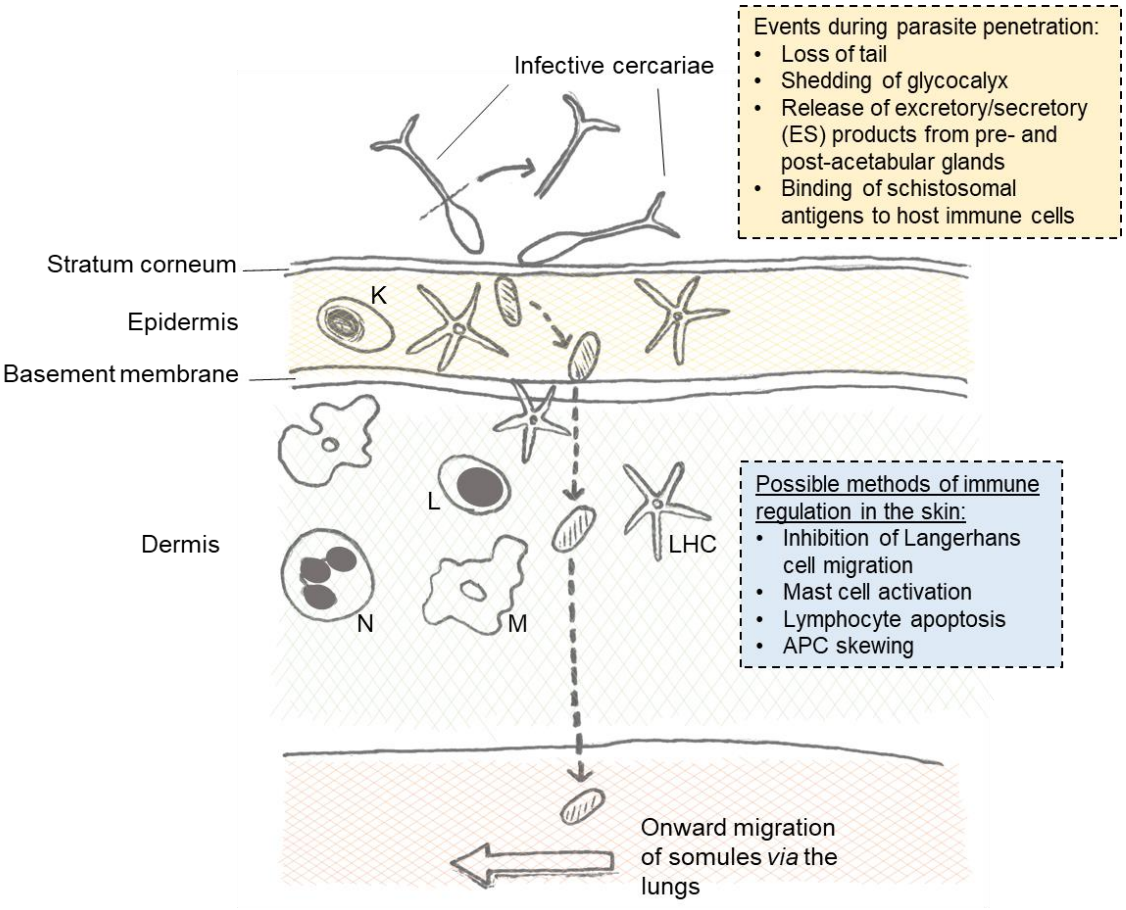

***Figure 1.4* The general stages of somule skin migration and the possible host immune responses encountered.** APC – antigen presenting cells; K – keratinocyte; L – lymphocyte; N – neutrophil; M – macrophage; LHC – langerhans cell. Adapted by the author from Jenkins *et al.* (2005).

1.2.3 Biology of adult worms

1.2.3.1 Sexual maturation and reproduction

Approximately 15 days post-exposure, somules reach the hepatoportal circulation where the maturation into adult male and female worms continues (LoVerde *et al.*, 2004). Schistosomes are sexually differentiated from as early as the miracidium stage (Boissier *et al.*, 1999) although it is not until adulthood that the sexes are morphologically discernible. Male *S. mansoni* are thicker and more muscular, although shorter, than the more slender females. Other morphological differences between the sexes are apparent upon inspection: male worms possess a tegument covered in tubercles, while the female surface is smooth. Males also form a gynaecophoric canal with which to hold the female worm once paired. Both sexes possess an oral and ventral sucker (Figure 1.5).

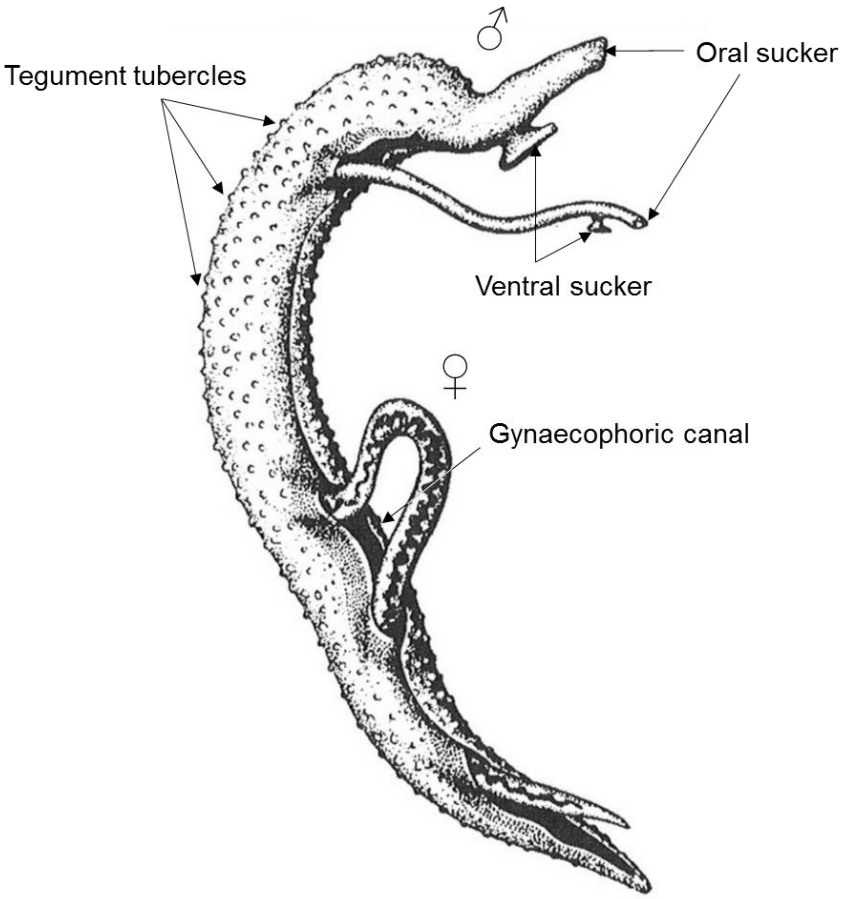

Figure 1.5 Drawing **of an adult female residing in the gynaecophoric canal of an adult male** (Beltran *et al.*, 2010).

From ~28 days post-infection, the adult worms begin to mate (LoVerde *et al.*, 2009). For female worms to reach and maintain sexual maturity, they must pair with a male worm and reside within its gynaecophoric canal (Popiel and Basch, 1984). When the worms become separated the female's ovary and vitelline gland regress, with other reproductive structures apparently unaffected (Erasmus, 1973). Mature male *S. mansoni* worms possess four to nine testes (Gönnert, 1955) which produce sperm that is subsequently passed to the enveloped female *via* a cirrus located at the top of the gynaecophoric canal. Once inside the female, sperm migrate through the reproductive tract to the seminal receptacle, positioned adjacent to the ovary (Collins *et al.*, 2011). From here, the sperm are able to fertilise the oocytes as they emerge from the ovary. Once passed through the oviduct, oocytes enter the vitelline duct, eventually reaching the Mehlis' gland. The Mehlis' gland is a cluster of secretory cells with several proposed roles within the reproductive process including uterus lubrication and egg shell biosynthesis (deWalick *et al.*, 2012). The eggs gain their shells from material synthesised in the

vitelline glands (Kunz, 2001) in the ootype before passing out of the female genital pore (Collins *et al.*, 2011).

1.2.3.2 The adult worm tegument

The success of schistosomes has been greatly reliant on their evolutionary-derived ability to 'hide' from the host by incorporating host antigens at the tegument surface, thereby effectively coating themselves in a protective barrier and suppressing the host immune response (Smithers *et al*., 1969). The tegument of *S. mansoni* is similar to previously described trematodes in that the outer syncytial layer is connected to sub-tegumental nucleated regions in the parenchyma (Morris and Threadgold, 1968). These oval shaped nucleated regions/cell bodies/cytons vary in size from 3 x 6 µm to 6 x 12 µm (Wilson and Barnes, 1974). The *S. mansoni* tegument is composed of a double lipid bilayer, which when viewed by electron microscopy, appears as two trilaminate membranes each with an electron-transparent layer sandwiched by electron dense layers, and varies in overall thickness from 0.9 - 3 µm (Wilson and Barnes, 1974). At the apical surface, the membrane is highly invaginated, forming pits and channels (Wilson and Barnes, 1974). Conversely, the tegument also features tubercles, small raised portions of the tegument present along the length of male worms although more densely in the dorsal region (Morris and Threadgold, 1968) (Figure 1.6). In addition to tubercles, cuticular spines approximately 2 µm long (Gobert *et al.*, 2003), are found at the surface of both male and female worms, including within the male gynaecophoric canal and suckers of both sexes (Hockley, 1968; Gobert *et al.*, 2003). Figure 1.7 details the components of the adult tegument and indicates the position of subtegumental cell bodies, spines, and mitochondria within the tegument.

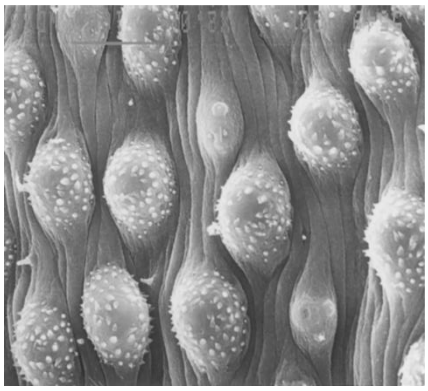

Figure 1.6 **The tegument surface of a male adult *S. mansoni* worm**. Multiple tubercle protrusions with spines are evident; image captured by scanning electron microscopy (Shuhua *et al.*, 2000).

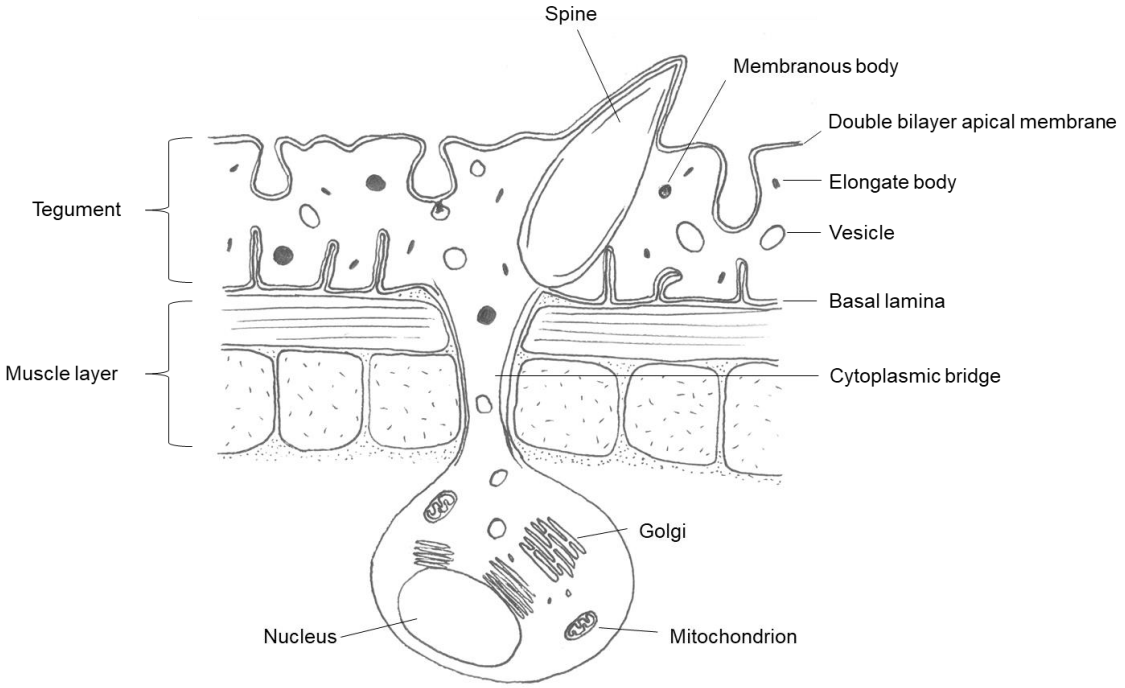

Figure 1.7 **Illustration of the adult *S. mansoni* tegument and associated cell body**. Adapted by the author from Braschi *et al.*, 2006a. Drawing is not to scale.

1.3 Cell Signalling in *S. mansoni*

The physiological complexity of schistosomes, which also differs between the morphologically distinct phases, renders this parasite a fascinating subject of research. Given that cellular signalling processes drive gene expression changes and modify cellular behaviour, investigating signalling in *S. mansoni* is critical to our understanding of the basic biology of this organism. As well as endogenous signalling, it is thought that schistosomes use cell signalling pathways to alter gene expression and cellular behaviour in response to external environmental stimuli such as host growth factors (Ressurreição *et al.*, 2011).

1.3.1 Protein kinases

Signalling in eukaryotic organisms is orchestrated by protein kinases (PKs). Protein phosphorylation by these pivotal regulatory enzymes occurs *via* the addition of a phosphate group from ATP or GTP to an amino acid, instigating a conformational change (Hanks *et al.*, 1988). Integrins, receptor tyrosine kinases (RTKs) and other receptors such as G-protein coupled receptors (GPCRs) bind ligands at the cell surface and their intracellular domains spark a chain of phosphorylations *via* PKs to effect changes at the molecular level (Beckman *et al.*, 2012).

There are two superfamilies of protein kinase, the majority belonging to the eukaryotic protein kinase superfamily (ePKs) and the remainder belonging to the atypical protein kinase superfamily (aPKs) (Hanks *et al.*, 1988). Within the ePKs there are eight groups: AGC (cAMP-dependent protein kinase/protein kinase G/protein kinase C extended), CAMK (Calcium/Calmodulin regulated kinases), CK1 (Cell Kinase I), CMGC (Cyclin-dependent kinases), RGC (Receptor Guanylate Cyclases), STE (MAP Kinase cascade kinases), TK (Protein Tyrosine Kinase) and TKL (Tyrosine Kinase Like) but broadly, PKs can be divided into two classes based on their phosphorylation preferences, serine/threonine kinases (STKs) or tyrosine kinases (TKs)[3] (Andrade *et al.*, 2011). Structurally, PKs contain at minimum, a catalytic domain and a regulatory domain. The ~250-300 amino acid catalytic domain contains residues capable of binding and phosphorylating target proteins (Andrade *et al.*, 2011).

PKs are now commonly used as targets against human diseases (Parasido *et al.*, 2017) and consequently, are also of interest in the search for novel drug targets against schistosomiasis, although research is faced with several challenges, primarily the capacity for PKs to hold multiple functional roles within the different life stages (Walker, 2011). The publication of the *S. mansoni* genome and kinome (Andrade *et al.*, 2011; Berriman *et al.*, 2009; Protasio, *et al.*, 2012) has revealed 252 putative protein kinase genes, facilitating research into schistosome form and function and enabling comparisons to be made with other species. However, elucidating the precise functional roles for the kinases derived from these genes, remains a significant challenge.

1.3.2 Protein kinases in S. mansoni

Although 252 putative protein kinases have been identified in *S. mansoni* (Andrade *et al*., 2011), which is a similar number to those present in *S. haematobium* (Stroehlein *et al.*, 2015), only a selection have been investigated in any detail. Amongst the first kinases to be studied in *S. mansoni* was receptor kinase 1 (SmRK1), discovered by Davies *et al.* (1998) (Table 2.1). Their hypothesis that schistosomes can detect host-derived signals *via* membrane-bound receptor proteins was inspired by previous work suggesting that in order for the complete and successful maturation of adult schistosomes, male and female worms must receive signals from their host and from each other (Basch and Rhine, 1983). SmRK1 is an STK and forms part of the Transforming Growth Factor-β (TGF-β) family of receptors. In 2001, Kapp *et al.* isolated SmTK5, the first *S. mansoni*

[3] http://kinase.com/kinbase/ [Accessed August 10th 2017].

protein tyrosine kinase (PTK). PTKs play a major role in forwarding extracellular signals to a variety of internal signalling pathways. Of the 252 protein kinases identified in *S. mansoni,* 90 have been classified as PTKs and approximately 43 as tyrosine-like kinases (Andrade *et al.*, 2011). To date, SmTK3, SmTK4, SmTK5, SmTK6 and SmFes have been investigated in *S. mansoni* (Bahia *et al.*, 2006) and roles for these SmTKs include reproduction, mitogenic activity, female egg production and larval transformation (reviewed in You *et al.*, 2011). The first kinase of the AGC superfamily to be discovered in schistosomes was protein kinase C1 (PKC1) (Bahia *et al.*, 2006). Since then, protein kinase A (PKA) and most recently, protein kinase B (PKB/Akt) have also been researched in *S. mansoni* (Swierczewsk and Davies, 2009; Morel *et al.*, 2014a). Since work began on *S. mansoni* signalling proteins in 1991, at least one new kinase has been investigated almost anually. Table 1.1 lists *S. mansoni* signalling proteins in chronological order of their discovery. Many signalling pathways remain that have not been investigated in *S. mansoni*; the research described here focuses on the Akt signalling pathway.

Signalling Proteins Studied in *S.mansoni*	**Reference**
S. mansoni epidermal growth factor receptor (SER)	Ramachandran *et al.*, 1996
S. mansoni mitogen-activated protein kinase (MAP kinase)	Schuessler *et al.*, 1997
S. mansoni GTPase activating protein (GAP)	Schuessler *et al.*, 1997
S. mansoni receptor kinase (SmRK1)	Davies *et al.,* 1998
S. mansoni tyrosine kinase 5 (SmTK5)	Kapp *et al.*, 2001
S. mansoni tyrosine kinase 4 (SmTK4)	Knobloch *et al.*, 2002
S. mansoni receptor tyrosine kinase 1 (SmRTK1/SmVKR1)	Vicogne *et al.*, 2003
S. mansoni receptor kinase 2 (SmRK2)	Forrester *et al.*, 2004
S. mansoni tyrosine kinase 3 (SmTK3)	Kapp *et al.*, 2004
S. mansoni protein kinase C (SmPKC1)	Bahia *et al.*, 2006
S. mansoni cytoplasmic protein-tyrosine kinase (SmFes)	Bahia *et al.*, 2007
S. mansoni insulin receptor 1 and 2 (SmIR1, SmIR2)	Khayath *et al.*, 2007
S. mansoni Ste20-like kinase (SmSLK)	Yan *et al.*, 2007
S. mansoni cAMP-dependant protein kinase (SmPKA-C)	Swierczewsk and Davies, 2009
S. mansoni protein kinase C β (PKCβ)	Ludtmann *et al.*, 2009
S. mansoni tyrosine kinase 6 (SmTK6)	Beckmann *et al.*, 2011
S. mansoni p38 mitogen-activated protein kinase (p38MAPK)	Ressurreição *et al.,* 2011
S. mansoni venus kinase receptor 1 (SmVKR1)	Gouignard *et al.*, 2012
S. mansoni venus kinase receptor 2 (SmVKR2)	Gouignard *et al.*, 2012
S. mansoni polo-like kinase 2 (SmSak)	Long *et al.*, 2012
S. mansoni cAMP-dependant protein kinase (PKA)	de Saram *et al.*, 2013
S. mansoni fibroblast growth factor receptor (Smfgfr)	Collins *et al.*, 2013
S. mansoni extracellular signal regulated Kinase (ERK)	Ressurreição *et al*., 2014
S. mansoni nucleotide kinases – deoxyriboside, uridine, cytidine	Naguib and Kouni, 2014
S. mansoni protein kinase B/Akt (SmAkt)	Morel *et al.,* 2014a

Table 1.1 **Protein kinases identified and studied in *S. mansoni* listed in chronological order of investigation.** Adapted from Ressurreição (2009) and updated.

1.3.2 Protein kinase B/Akt

1.3.2.1 Discovering Akt

Akt, also known as Protein Kinase B (PKB) (Alessi *et al.*, 1996a), is an STK belonging to the AGC subfamily of protein kinases (Yang *et al*., 2002). Akt is critical to signalling in all higher eukaryotic cells (Manning and Cantley, 2007), and can be traced back to early metazoans (Bozulic and Hemmings, 2009). Originally discovered as a proto-oncogene in humans (Jones *et al.*, 1991; Bellacosa *et al.*, 1991; Coffer and Woodgett, 1991), Akt has since been implicated in various cellular processes such as insulin signalling, glucose metabolism, cell-cycle progression, apoptosis, transcriptional regulation and cancer progression[4] (Brazil *et al.*, 2004). There are three human isoforms of Akt; Akt-1, Akt-2 and Akt-3 (PKBα, PKBβ and PKBγ, respectively) (Manning and Cantley, 2007). Akt-1 is the cellular homologue of a protein known as v-Akt, which was isolated from rodent T-cell lymphoma in the genome of AKT-8 acute transforming retrovirus (Alessi *et al*., 1996b).

1.3.2.2 Structure and activation mechanism of the Akt protein

All currently characterised forms of Akt have the same configuration: an N-terminal pleckstrin homology (PH) domain, a catalytic domain and a short C-terminal tail containing a hydrophobic motif (Bozulic and Hemmings, 2009). In humans, the catalytic domain displays 65% and 75% similarity to PKA and PKC respectively. Mammalian Akt signalling can be initiated by a variety of receptors including RTKs, integrins, B and T cell receptors (BCRs), cytokine receptors and GPCRs, among others. Each of these stimuli result in the activation of phosphoinositide 3-kinase (PI3K) and consequently, the production of phosphatidylinositol 3,4,5 triphosphate (PIP3). Accumulation of PIP3 at the plasma membrane provides docking sites for PH domains, as are found in Akt and its upstream kinase, phosphoinositide-dependent protein kinase-1 (PDK1). PDK1 mediates the phosphorylation of Akt at the T-loop on residue Thr^{308} (Alessi *et al.*, 1997; Brazil *et al.*, 2004; Mora *et al.*, 2004) (Figure 1.8). Complete activation of Akt requires a series of phosphorylations, including on Ser^{473} in the hydrophobic motif and Thr^{308} found in the catalytic domain (Alessi *et al.*, 1996a). However, prior to these events, tyrosine phosphorylation is also required at Tyr^{315}/Tyr^{316} (in human Akt1/Akt2, respectively) (Chen *et al.*, 2001). Once active, the effects of Akt on cell behaviour can last up to several hours (Alessi *et al.*, 1997). The downstream targets of Akt vary depending on the function required. For instance, cell survival is mediated by Bcl-2-associated death promoter

[4] http://www.cellsignal.com/reference/pathway/Akt_PKB.html [Accessed November 18th 2015].

(BAD) and Forkhead Box O (FOXO), whereas Glycogen Synthase Kinase 3 (GSK3) is a target for metabolism (Norrmén and Suter, 2013). In humans, Akt can also exert effects on synaptic signalling, and other pathways (Figure 1.9).

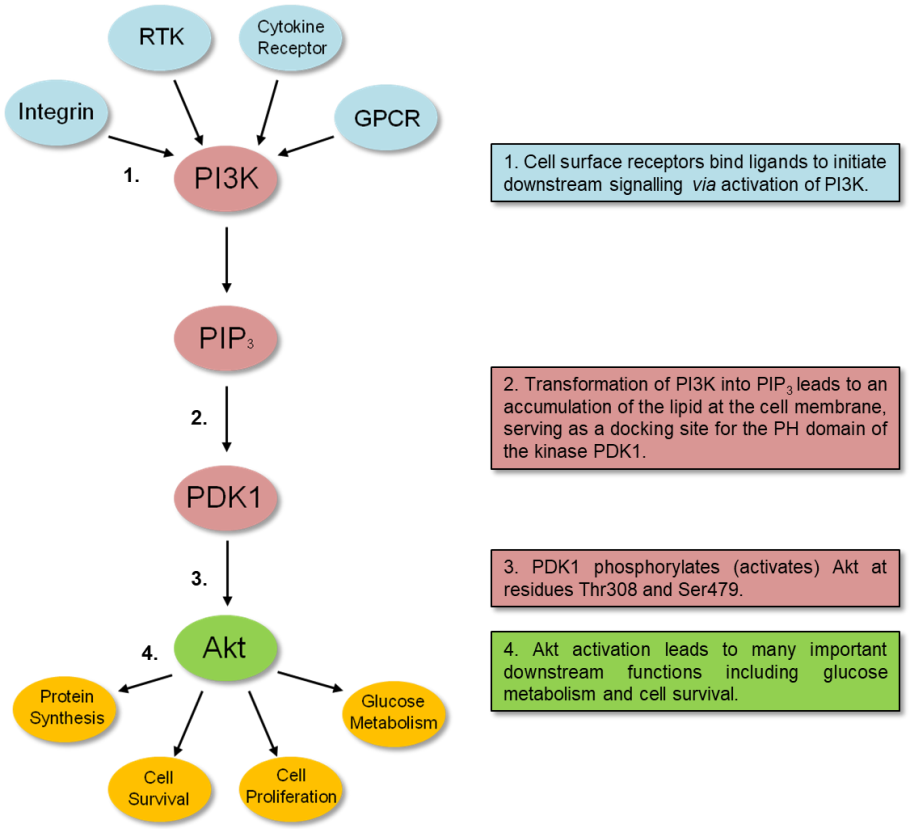

***Figure 1.8* Simplified diagrammatic representation of human Akt activation.**
A flow diagram with explanatory boxes indicating the chain of events leading to the phosphorylation (activation) of human Akt.

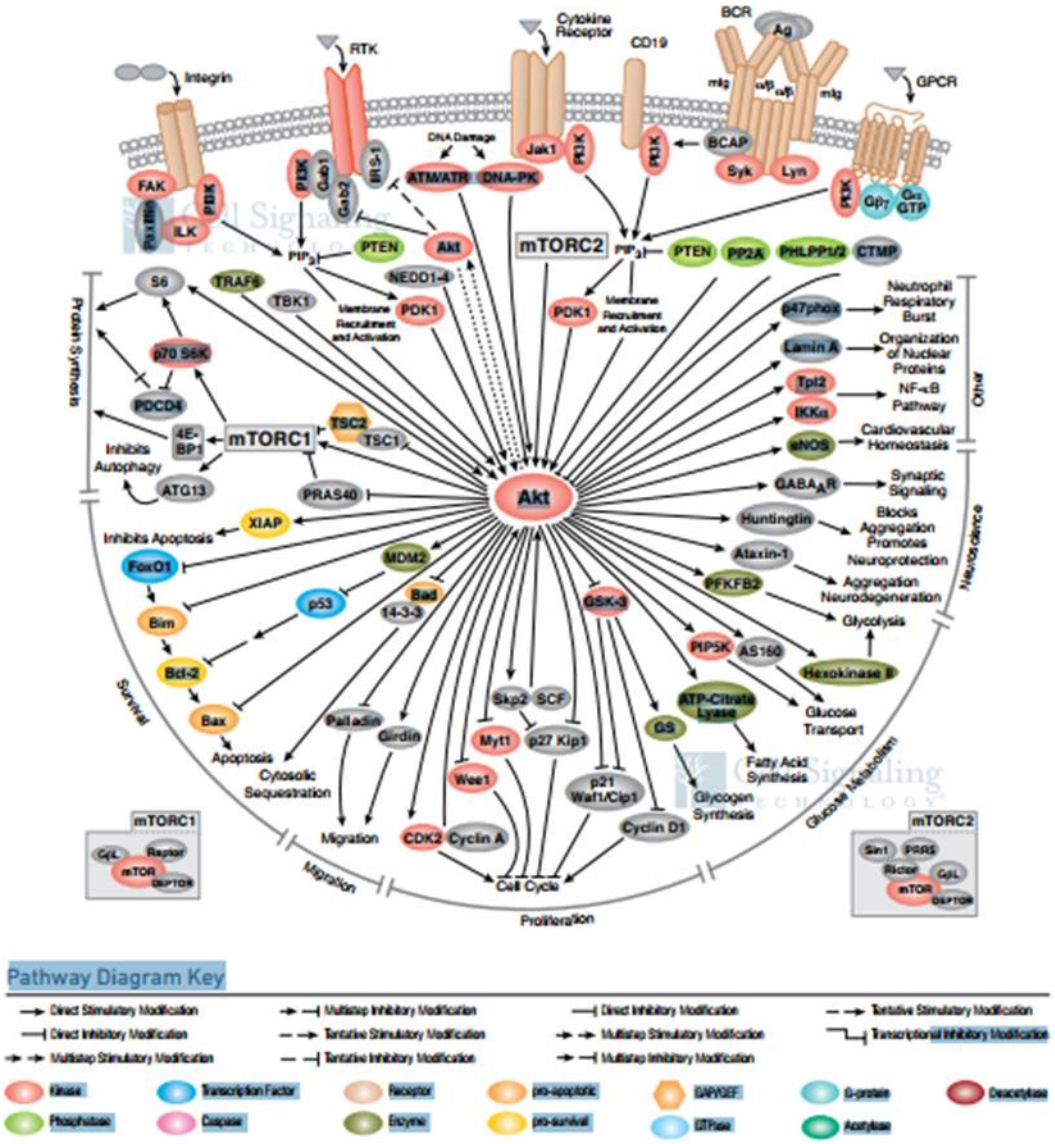

Figure 1.9 **Diagrammatic representation of the human Akt signalling network** (http://www.cellsignal.com/reference/pathway/Akt_PKB.html, [Accessed October 10th 2017]).

1.3.2.3 Akt in other organisms

Most of the knowledge regarding Akt emanates from investigations on the human protein. However, several orthologues of Akt containing a PH domain have been identified in non-mammalian species, including *Drosophila melanogaster* (Andjelkovic *et al.*, 1995), *Dictyostelium discoideum* (Meili *et al.*, 1999) and *Caenorhabditis elegans* (Paradis and Ruvkun, 1998). In *C. elegans* there are two Akt genes: Akt-1 and Akt-2, with Akt1 giving rise to two splice variants, Akt-1a and Akt-1b (Paradis and Ruvkun, 1998). *C. elegans* Akt-1 is regulated by phosphorylation sites equivalent to the human Thr^{308} and Ser^{473} residues, whereas the Akt-2 protein is activated only by the former,

indicating that the two proteins are potentially differentially regulated (Paradis and Ruvkun, 1998). The *D. melanogaster* homologue of Akt (*DAkt1*) encodes two proteins of different sizes, a shorter protein of 66 kDa and a longer form measuring 85 kDa. Both proteins possess kinase activity and are differentially expressed between embryo and adult life stages, indicating putative functional differences (Andjelkovic *et al.*, 1995).

1.3.2.4 Akt in *S. mansoni*

During this PhD investigation, one article regarding Akt in *S. mansoni* was published (Morel *et al.*, 2014a), with none existing previously. Morel *et al.* (2014a) confirmed the presence of Akt in *S. mansoni* and showed it to be a well conserved kinase, implicated in adult pairing and female worm egg laying. Their study focused on exposing the parasite to commercially available PK inhibitors and monitoring the physiological effects. The three inhibitors found to be most effective on adult worms and somules were Akt Inhibitor IV, Akt Inhibitor VIII and Akt Inhibitor X. In somules, 100 % parasite kill was observed with 1 µM Akt Inhibitor IV after 24 h. Although Morel *et al.* (2014a) assigned a likely functional role of Akt in worm reproduction and somule survival, the variety of Akt functions in mammals provided a rationale to investigate the importance of *S. mansoni* Akt in other cellular processes. An in depth biochemical validation of Akt signalling in *S. mansoni* was also warranted.

1.4 Insulin Signalling

Insulin is a polypeptide hormone crucial to normal metabolism and growth regulation (Dupont *et al.*, 2001). Insulin plays a role in a wide range of processes in mammals including gene expression and protein degradation, glucose and lipid metabolism, cell growth, and DNA synthesis (Figure 1.10). The insulin pathway is stimulated by the binding of extracellular insulin or insulin-like growth factor (IGF) to transmembrane RTKs. These receptors are constitutively assembled heterotetramers consisting of an extracellular α-subunit and a membrane spanning β-subunit ($\alpha_2\beta_2$), joined by a disulphide bridge (Huang *et al.*, 1994, Khayath *et al.*, 2007). Autophosphorylation of several tyrosine residues in the β-subunit is stimulated after ligand binding to the receptor. One of these residues makes up a well-conserved NPXY-motif, to which bind intracellular adaptor proteins such as those possessing a Src-homology 2 (SH2) motif (Teleman, 2010). Studies on the differences between insulin and IGF stimulation indicate that when the two bind to the same receptor, more than one intracellular pathway may be activated at the same time. Hence, there may be significant differences in the biological effect of these two ligands (Pandini *et al.*, 2003). Hormone-receptor binding triggers various

pathways (Figure 1.8), the two major ones being the mitogen-activated protein kinase (MAPK) and the phosphatidylinositol 3-kinase (PI3K) pathways (You *et al.*, 2009).

Class II RTKs, including IR and IGF-1R, are among the most ancient proteins and are conserved across a wide range of organisms, from sponges to mammals (Schäke *et al.*, 1994, Khayath *et al.*, 2007). In *S. mansoni*, two insulin receptors have been identified, SmIR-1 and SmIR-2 (Khayath *et al.*, 2007), each with distinct properties. Both receptors have been found present in all major stages of the parasite; miracidia, sporocysts, cercariae, somules and adult worms, and can be detected on western blots with molecular weights of 140 kDa (SmIR-1) and 115 kDa (SmIR-2). SmIR-2 is generally more abundant in *S. mansoni* than SmIR-1 and is expressed at the same level throughout parasite development whereas SmIR-1 shows a stronger presence in cercariae and somules when compared with other stages (Khayath *et al.*, 2007). Differences have also been found in the location of the two receptors; immunolocalisation reveals that SmIR-1 is specifically located in the musculature, intestinal epithelium and basal membrane of adult worms and at low levels in the tegument of somules (Khayath *et al.*, 2007). SmIR-2 is more greatly expressed in the parenchyma of adult worms and somules, but cannot be seen in the tegument. Although present in SmIR-2, all mammalian insulin signalling systems and model organisms *C. elegans* and *D. melanogaster*, the NPXY and SH2 motifs could not be identified in SmIR-1 (Khayath *et al.*, 2007).

1.5 Glucose Uptake in *S. mansoni*

The link between insulin signalling and glucose uptake in mammals is well known and the role of Akt in each of these processes has been investigated in detail (reviewed by Schultze *et al.*, 2012). In schistosomes, research has confirmed the presence of these processes (Clemens and Basch, 1989; Skelly *et al.*, 1998; Khayath *et al.*, 2007), yet the lack of knowledge surrounding Akt in these parasites means functional homology has not yet been ascertained. Since *Schistosoma* glucose transporter proteins were characterised over two decades ago (Skelly *et al.*, 1994), glucose uptake in *S. mansoni* has been researched thoroughly by Skelly and colleagues (Zhong *et al.*, 1995; Skelly and Shoemaker, 1996; Skelly and Shoemaker, 2001), leading to a comprehensive understanding on the location and expression of schistosome glucose transporters, SGTP1 and SGTP4. SGTP4 presents at the apical membrane surface, binding extracellular glucose (Skelly and Shoemaker, 1996) and importing it into the tegument, while SGTP1 is located uniquely in the basal membrane, transporting glucose into the underlying tissues (Zhong *et al.*, 1995).

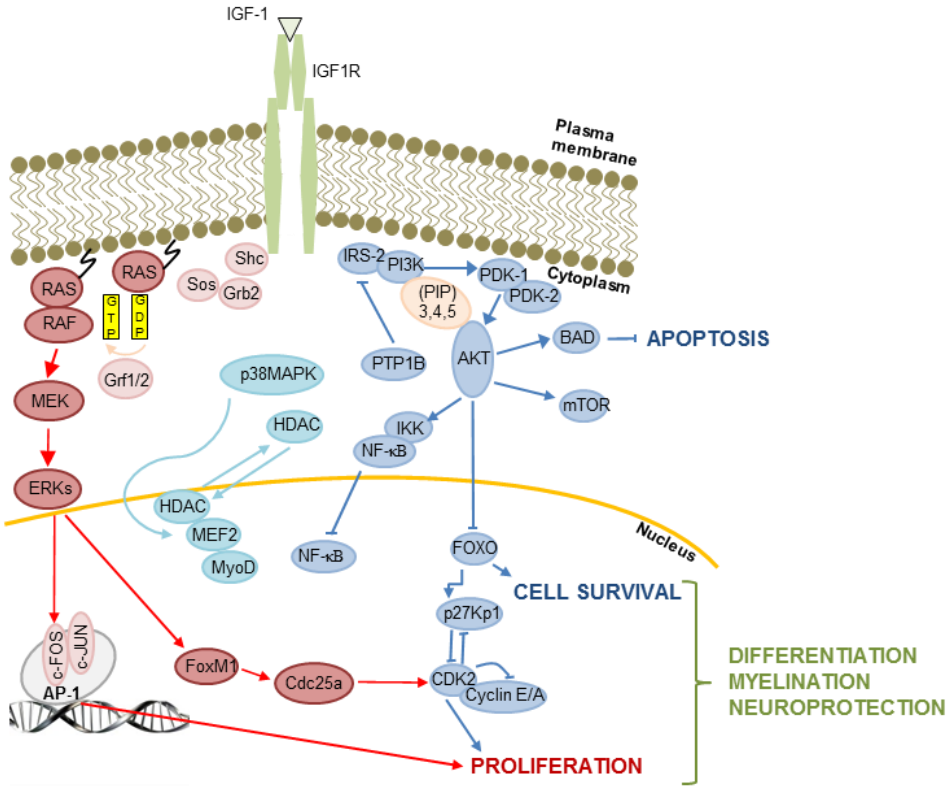

Figure 1.10 **Schematic diagram of Insulin and IGF signalling in humans** (Murillo-Cuesta *et al*., 2011).

1.6 Study Context, Contribution to Knowledge and Research Aims

Given that the current status of schistosomiasis as an NTD remains second only to malaria in terms of morbidity, research into novel anthelmintic drug targets and strategies is of crucial importance. Of particular interest are the stages paramount to human host invasion and residency: cercariae, somules and adult worms. As the parasite develops through these three life stages, many distinct changes take place both biochemically and morphologically. Namely the development of the adult tegument, from trilaminate in cercariae to fully formed adult double lipid bilayer, is of great significance as the interacting barrier between parasite and host.

Although steady progress is being made concerning schistosome cell signalling, little is known on the molecular systems within the tegument. As a fundamental protein in the insulin signalling network, Akt is a prime candidate for furthering knowledge of cell signalling within *S. mansoni*, to discover its role not only in insulin signalling, but also putative related pathways. Previous work on the effect of host molecules on the parasite (Ressurreição *et al.*, 2015), and the publication of schistosome genomes, has set the

framework for this and future projects to investigate the importance of protein kinases in the complex developmental and metabolic processes during the life cycle of *S. mansoni*. A greater understanding of the mechanisms that control parasite homeostasis is of vital importance in the search for novel drug targets.

Consequently, the aims of this study were to:

i. Identify/detect an evolutionarily conserved Akt protein in *S. mansoni* life stages, using commercially available anti-Akt antibodies; validate antibodies to determine the activation status of the parasite Akt.
ii. Determine the effect of host factors and signalling blockade on activated Akt in three mammalian infective and resident life stages: cercaria, somule and adult worms.
iii. Investigate the potential downstream importance of Akt signalling within *S. mansoni* by localising putative substrates within the parasite and performing bioinformatic analysis on putative substrates and interacting proteins.
iv. Identify a functional role(s) for Akt in *S. mansoni* human resident life stages.
v. Investigate a possible role for Akt in cercarial host detection/penetration.
vi. Contribute to the overall knowledge of *S. mansoni* cell signalling mechanisms and their role in schistosomes, from cercariae to the mature parasite.

2

Materials and Methods

2.1 Materials

2.1.1 Antibodies

The anti-AKT 1/2/3 (total) polyclonal antibody (#126811) was obtained from Abcam (Cambridge, UK), Alexa Fluor 488 goat anti-rabbit IgG (#A11008) from Life Technologies (Thermo Fisher Scientific, Loughborough, UK), and the anti-phospho GSK3α/β (Tyr^{279}/Tyr^{216}) polyclonal Clone SG-2F (#05413) was purchased from Millipore (Watford, UK). The horse radish peroxidase (HRP)-conjugated actin (1-19) pAb; sc1616 (#B1815) and anti-phospho Akt 1/2/3 ($Tyr^{315/316/312}$) pAb (#29309) were bought from Santa Cruz Biotechnology (Heidelberg, Germany) and the anti-SGTP4 antibody was kindly provided by Patrick Skelly (Tufts University, USA). The remaining antibodies used throughout the project were all obtained from Cell Signalling Technology (New England Biolabs, Hitchin, UK); anti-mouse IgG HRP-linked antibody (#7076) anti-rabbit IgG HRP-linked antibody (#7074) anti-rabbit IgG conformation-specific mouse mAb (#3678) anti-phospho Akt (Thr^{308}) Rabbit mAb (#2965) anti-phospho Akt Substrates (RXXS*/T*) rabbit mAb (#9614) anti-phospho Akt (Thr^{308}) XP rabbit mAb (#13038) anti-phospho p70 S6 Kinase (Thr^{389}) rabbit mAb (#9234) and anti-phospho GSK-3α/β ($Ser^{21/9}$) rabbit mAb (#9327).

2.1.2 Kits

The Glucose Uptake-Glo™ assay was obtained from Promega (Southampton, UK), the Pierce Crosslink immunoprecipitation (IP) kit was bought from Thermo Fisher Scientific and the Akt Kinase Assay kit from Cell Signalling Technology. The lambda protein phosphatase components were purchased from New England Biolabs. The Proteome profiler array 96 (human phospho kinase array 1) was bought from R&D systems (Abingdon, UK).

2.1.3 Stimulants and Inhibitors

Akt Inhibitor X was obtained from Merck (Nottingham, UK). The LY294002 inhibitor was bought from Cell Signalling Technology. Fetal bovine serum (FBS) was obtained from Gibco (Thermo Fisher Scientific), insulin (human) recombinant expressed in yeast, and SC79 were bought from Tocris (Abingdon, UK), and L-arginine, human serum, linoleic acid and the GSK2334470 inhibitor were purchased from Sigma Aldrich (Dorset, UK). siRNAs, labelled Akt_3 and Akt_16, were obtained from Integrated DNA Technology (IDT) (London, UK).

2.1.4 Other Reagents

Radioimmunoprecipitation (RIPA) Buffer (x10), cell lysis buffer (x10) and protein A agarose beads (50% slurry) were obtained from Cell Signalling Technology. Amersham ECL Prime western blot detection reagent and Amersham Protran 0.45µm nitrocellulose blotting membrane were sourced from GE Healthcare (Chalfont St. Giles, UK). Gibco (Thermo Fisher Scientific) was the source for media: MEM vitamins solution (100x), Basal Medium Eagles (BME), RPMI Medium 1640 and OPTI-MEM®. The DS scrambled negative control sequence and siRNAs were obtained from IDT. Bolt™ 4-12% Bis-Tris Plus 15-well and 10-well gels were from Invitrogen (Thermo Fisher Scientific). 10% normal goat serum was bought from Life Technologies (Thermo Fisher Scientific), Dried skimmed milk powder was Marvel, and 18 x 18mm or 20 x 20mm cover slips were purchased from Menzel-Gläser (Thermo Fisher Scientific). Bolt LDS sample buffer (4x), Bolt sample reducing agent (10x), See Blue Plus 2 pre-stained markers and Bolt MES SDS running buffer (20x) were from Invitrogen. Bradford reagent, antibiotic/antimycotics solution (100x) stabilized Hanks Balanced Salt Solution (HBSS), bovine serum albumin (BSA), lactalbumin hydrolysate solution (50x), rhodamine phalloidin and HistoChoice® clearing agent were purchased from Sigma Aldrich (Dorset, UK). GelCode Blue stain reagent, Super Signal molecular weight protein standards, Restore™ western blot stripping buffer, Halt™ protease and phosphatase inhibitor cocktail, SuperSignal West Pico chemiluminescent substrate, 20x TBS Tween-20 (TTBS) buffer, 10% formaldehyde solution methanol free, glass slides and Histoplast PE paraffin, Whatman grade GB004 botting paper and phosphate buffered saline (PBS) tablets were obtained from Thermo Fisher Scientific. Vectashield mounting medium for fluorescence was bought from Vector Laboratories (Peterborough, UK), ethanol absolute from VWR (Lutterworth, UK), and Immersol from Zeiss (Cambridge, UK).

2.2 Ethics Statement

Laboratory animal use was within a designated facility regulated under the terms of the UK Animals (Scientific Procedures) Act 1986, complying with all requirements therein. The University of Nottingham Ethical Review Committee approved experiments involving mice and work was carried out under Home Office licence 40/3595.

2.3 Snail Husbandry

Infected intermediate host snails for *S. mansoni*, *B. glabrata* (M-line), were provided by the Biomedical Research Institute (USA) *via* the National Institute of Health – National

Institute of Allergy and Infectious Disease (HIH-NIAID) Schistosomiasis Resource Center under (NIH-NIAID) Contract No. HHSN272201000005I. Additional M-line snails (when required) infected with the same strain (PR-1) of *S. mansoni* were kindly provided by Nuha Mansour/Quintin Bickle from the London School of Hygiene and Tropical Medicine (LSHTM, UK).

Snails were maintained in 1.5 l transparent plastic containers from 'Really Useful Box' until patency, approximately 35 days post-infection. Snails from the BRI were kept ~50 per box with approximately 1 l of tap water filtered through a Brimark carbon filtration unit (Silverline UK; Devon, UK), and fed with dried round lettuce and fish food (Tetramin) twice a week. Snails from LSHTM were kept in approximately 1 litre of distilled water with 1 ml added salts (100 g calcium carbonate, 10 g magnesium carbonate, 10 g sodium chloride, 2 g potassium chloride dissolved in 3 litres of distilled water)[5] and fed also with dried round lettuce and fish food twice a week.

All snail boxes were thoroughly cleaned once a week although the water was changed twice weekly. Discarded water was carefully decanted into buckets containing 2 % Virkon (Thermo Fisher Scientific) and left for a minimum of 5 days before disposal. Dead snail shells were removed from the boxes daily to prevent any potential bacterial infection spreading to the remaining population. Under normal conditions, the boxes containing infected snails were kept in an LMS incubator at 26°C under constant light. During patency, snails were kept in the dark by placing the boxes into larger, black, plastic boxes as from the Really Useful Box Company.

2.4 Adult Schistosomes

Adult worms were supplied by Bioglab (c/o Professor Mike Doenhoff, University of Nottingham, UK). Upon receipt, worms were transferred to a Petri dish and equilibrated in RPMI medium containing antibiotics/antimycotics (x4) for 1 - 2 h at 37°C/5% CO_2 prior to use.

2.5 Isolation of Cercariae and Mechanical Transformation into Somules

Patent snails were transferred from their boxes into a 100 ml glass beaker containing 50 ml of filtered water and were left under direct light from a fluorescent table lamp for between 60 - 120 min. After this time, snails were returned to fresh boxes, fed and placed back in the dark for the next shed (a minimum of three days later). By keeping the beaker

[5] Salt recipe kindly provided by Nuha Mansour at LSHTM

under light, cercariae emerged and swam to the top of the beaker and were therefore easier to transfer by sterile pipette into three 15 ml screw cap Falcon tubes (Thermo Fisher Scientific). The tubes containing the cercariae were incubated on ice for no more than 30 min while two 20 ml volumes of BME with antibiotic/antimycotic were placed at 37°C. The tubes were then centrifuged (Eppendorf - 5702) for 10 min at 0.5 x *g* (rcf), and the supernatant removed down to 3 ml. 3 ml of warmed BME was then added to provide a total of 6 ml. Following this, the tubes were vortexed (Vortex Genie 2) for approximately 10 min to mechanically transform the cercariae, then 1 ml of HBSS was added. Tubes were returned to ice for a further 7 min then centrifuged again, this time for 2 min at 0.5 x *g* to separate the cercarial heads from the tails. The supernatant was removed down to 3 ml. Somules were re-suspended by briefly vortexing the tubes and the contents were poured into a high-sided Petri dish. Under a microscope, the dish was gently swirled to form a clump of somules in the centre. These were transferred to a new 15 ml tube. This process was repeated until as many somules as possible had been collected, then the volume was made up to the next nearest ml with BME. To count the somules, the tube was vortexed and taking from the middle of the tube, three aliquots of 1 µl each were transferred into a small glass dish, making sure to vortex between each sample. The somules contained in each aliquot were enumerated and the mean calculated. (total no. somules = (mean somule count x 1000) x total volume (ml) collected).

The transformed somules were then placed in an incubator at 37°C, 5%CO_2 for 18 - 24 h before use in experiments.

2.6 Exposure of Parasites to Host Molecules or Kinase Inhibitors

Stimulation and inhibition experiments were performed on cercariae, somules and adult worms. The treatments included human serum, insulin, L-arginine, linoleic acid (LA) and SC79 as potential stimulants, and Akt Inhibitor X, Herbimycin A, GSK2334470 and LY294002 as inhibitors.

Samples of freshly shed cercariae were collected using a 1 ml pipette and transferred into wells of a 48 well tissue culture plate. During collection, the beaker was kept under light to promote concentration of cercariae at the water surface, allowing for easier and more consistent collection to try to achieve similar numbers of cercariae per well. Cercariae were then exposed to either 100 µM L-arginine (0-45 min) or 10 µM Akt Inhibitor X (0-60 min) by adding each compound directly to each well for the desired time. To expose cercariae to LA, a 48 well plate was pre-coated with this fatty acid; 500 µl of 26.6 µg/ml LA in methanol was placed in each well and allowed to evaporate over 72 h

at 4 °C. 1 ml cercariae suspension was then added for increasing durations (0-45 min). Cercariae treatments were performed at room temperature to mimic natural conditions. At the appropriate duration, cercariae were transferred to pre-chilled 1.5 ml microfuge tubes and placed on ice for 5 min. Samples were then processed for western blotting, immunohistochemistry or immunoprecipitation.

Approximately 1000 somules cultured overnight for ~18 h in 1 ml BME per well in a 48 well tissue culture plate (Nunc) were exposed to 10 % human serum (0 - 30 min), 1 µM bovine/human insulin (0 - 30 min), 100 µM L-arginine (0 – 30 min), 26.6 µg/ml LA (0 – 45 min), 1 - 100 µM Akt Inhibitor X (0 - 60 min), 12 µM herbimycin (60 - 120 min), 1 – 50 µM LY294003 (1 h) or 1 – 50 µM GSK2334470 (2 h). Treatments were halted by transferring the somules into pre-chilled microfuge tubes and placing on ice for 5 min. An additional wash in 1 ml ice-cold PBS was performed when somules treated with serum. During exposures, somules were incubated at 37°C/5 % CO_2. Samples were then processed for western blotting, immunohistochemistry or immunoprecipitation.

Adult worms were exposed to compounds either as individual sexes or in pairs, which was determined by the experiment. After receipt, adult worms were placed in a Petri dish at 37°C for 1 h to equilibrate. Worms were then gently transferred to microfuge tubes using flat-ended tweezers and exposed to 1 µM insulin (10 - 30 min), 1 µM L-arginine (30 - 45 min), 1 – 100 µM Akt Inhibitor X (60 min) or 12 µM Herbimycin (60 - 120 min). To end treatment, tubes were placed directly in ice for 5 min. Samples were then processed for western blotting, immunohistochemistry or immunoprecipitation.

2.6.1 Sample preparation for western blotting

After 5 min incubation on ice, the somules or cercariae were centrifuged at full speed (12,045 x *g*; Eppendorf minispin) for 45 s and the supernatant removed, leaving ~20µl with the pellet. Parasites were then solubilised in 1 x LDS-PAGE sample buffer, and 1 x sample reducing agent was added. Samples were then heated to 95°C for 5 min on a thermomixer compact (Eppendorf) and sonicated (Fisherbrand) for ~1 min. At this stage, samples were either loaded directly onto a gel for electrophoresis, or frozen at -20°C with the addition of 1 x protease and phosphatase inhibitors.

After 5 min incubation on ice, worms were transferred to new pre-chilled tubes containing RIPA buffer (20 µl/worm pair) and homogenised on ice using a motorised pestle (VWR). Worms were then centrifuged at full speed for 45 s and the supernatants collected in new microfuge tubes. 1 x LDS PAGE sample buffer and 1 x sample reducing agent were

next added. Samples were then heated to 95°C for 5 min and sonicated for ~1 min. At this stage, samples were either loaded directly onto a gel for western blotting, or frozen at -80°C with the addition of 1 x protease and phosphatase inhibitors.

In some cases, protein estimations (on samples in RIPA buffer) were performed on the extracted proteins using the Bradford microassay and using the manufacturer's instructions with BSA (0 – 1.5 mg/ml) as the protein standard.

2.6.2 Sample preparation for immunohistochemistry

After treatment and incubation on ice for 5 min in microfuge tubes, the water, BME or RPMI medium was removed from cercariae, somules or adult worms respectively, leaving ~100 µl, and replaced with 300 µl 4% paraformaldehyde (approximately 75%). Parasite were incubated at 4°C for 1 – 2 h then the paraformaldehyde was washed out and parasites stored in PBS.

2.6.3 Sample preparation for immunoprecipitation with kinase assay

Somules (24 h, ~10,000 per sample) were placed in a microfuge tube in 200 µl BME. Somules were treated with 10% human serum for 10 min then placed on ice for 5 min. Somules were washed twice with 500 µl ice-cold PBS and twice with 500 µl cell lysis buffer, centrifuging at full speed (12,045 x *g*; Eppendorf minispin) for 30 s between each wash. After the final spin, the supernatant was collected in a new microfuge tube and protease and phosphatase inhibitors added (1:100). Samples were stored at -80°C.

Adult worm pairs (~20) were placed in a microfuge tube containing 500 µl RPMI medium. Worms were treated with 10% human serum for 10 min then placed on ice for 5 min. Worms were washed twice in ice-cold PBS, then suspended in 500 µl cell lysis buffer and homogenised on ice using a motorised pestle. Parasites were centrifuged at full speed for 3 min in a pre-chilled rotor (Eppendorf minispin) and the supernatant collected in a new tube. The pellet was re-suspended in 200 µl cell lysis buffer and the homogenising and centrifuging repeated, adding the supernatant to the previously collected sample. Protease and phosphatase inhibitors were added (1:100) and the samples were stored at -80°C.

2.6.4 Sample preparation for cross-linked immunoprecipitation

Typically, two microfuge tubes were prepared per assay, each containing ~10,000 18 h somules in 200 µl BME; somules were then treated with 1 µM insulin for 10 min before placing on ice for 5 min. Samples were then centrifuged at 1000 rpm (Eppendorf

minispin) for 5 min, supernatants discarded, and washed once in 1 ml PBS re-centrifuged. 500 µl ice-cold IP lysis/wash buffer containing 1:100 protease and phosphatase inhibitors was added to each pellet and somules resuspended. After 5 min incubation on ice, samples were centrifuged at full speed for 10 min and supernatants collected. Protease and phosphatase inhibitors were re-added and samples stored at -80 °C.

2.7 Tegument Stripping

Adult worm pairs (10 – 20) were placed in a microfuge tube with 500 µl RPMI medium. Human insulin (1 µM) was added (or not, control) and worms were incubated for 10 min before being transferred into tubes containing 100 µl ice-cold PBS and placed on ice for 5 min. Ensuring the lids were firmly closed, the tubes were immersed in liquid nitrogen for 15 min. After removing from the liquid nitrogen, parasites were thawed initially at room temperature until almost defrosted (approximately 8 min) then put on ice until fully thawed. Worms were washed in ice cold PBS (1 ml) and incubated on ice for a further 5 min. The tubes were then vortexed (20 x 1 s pulses). Once worms had settled to the bottom of the tubes, the supernatant was collected and kept on ice. The supernatants were then centrifuged at 16,000 x *g* for 30 min at 4°C (Hettich Zentrifugen EBA12R). The supernatant was removed but retained, and the pellet resuspended in RIPA buffer (40 µl per 10 worms). An aliquot of the pellet was taken for protein estimation and the remaining sample was prepared for western blotting. A portion of the supernatant (i.e. non-particulate fraction) was also prepared for western blotting.

2.8 Proteome Profiler Assay

After parasites were subjected to the desired treatment(s) (without further processing) in microfuge tubes, they were washed in 1 ml PBS, leaving as little PBS as possible in each tube. The buffers detailed below are as specified in the kit. Parasites were suspended in lysis buffer 6 (10 µl/per worm pair or 1000 somules). Adult worms were homogenised on ice using the motorised pestle, centrifuged at full speed (12,045 x *g*; Eppendorf minispin) for 2 min, then the supernatant was transferred to a clean microfuge tube on ice. For somules, ~2000 were treated (or not, control) then placed on ice for 5 min. Samples were then centrifuged at full speed for 30 s and the supernatants discarded. The pellet was washed in 1 ml ice-cold PBS and re-centrifuged. The pellet was then re-suspended in 40 µl lysis buffer 6, protease and phosphatase inhibitors were added (1:100), and the samples sonicated for ~20 s. A small portion (5 µl) of each sample was taken for a protein estimation. 5 - 50 µg of total protein, as determined by protein estimation, was diluted in

Array Buffer 1. The lysate could not exceed 20% of the final reaction volume. Once diluted, 50 - 100 µl lysate was added to each well of the 96 well assay plate. The plate was covered with parafilm and incubated overnight (~ 18h) at 4°C on a horizontal orbital microplate shaker (Eppendorf, Stevenage, UK) set at approximately 500 rpm. After incubation, as much lysate as possible was removed and each well was washed four times with 400 µl wash buffer. After the final wash, the plate was inverted on tissue to wick the remaining buffer. Reconstitution of the detection antibody cocktail was done in 100 µl distilled water. Per pair of wells, 1.67 µl of this cocktail was made up to 100 µl in Array Buffer 2. 50 µl of diluted detection antibody cocktail was then added to each well, the parafilm was replaced and the plate incubated for 1 h at room temperature on the microplate shaker. The washing procedure was repeated. Streptavadin-HRP was next diluted according to instructions, 50 µl was added to each well and samples incubated for 30 min at room temperature on the microplate shaker. Washing was repeated a final time, 50 µl of mixed Substrate Solution was added to each well and incubated for at least 30 s prior to imaging. A Syngene Gbox imaging system (Syngene, UK) and associated software were used to image the plate. The iris and focus settings were tested before imaging using the template on the mousemat provided.

2.9 Western Blotting

Samples from storage at -20°C were placed on a hot block at 95°C for 5 min, allowed to cool to room temperature and centrifuged on a short pulse (10 s) to remove any liquid in the lids of the microfuge tubes. Meanwhile, running buffer (1x Bolt running buffer, diluted in distilled water) was poured into the electrophoresis cell and the Bolt Bis-Tris SDS-PAGE gel (10 or 15 well; 10% or 4 – 12% gradient gel) inserted and clamped. Using a graduated Hamilton syringe, wells were carefully loaded with pre-stained molecular weight marker and the samples. Gels were run at 165v and 280mA using a Hoefer powerpack until the marker reached the bottom of the gel.

Blotting paper and Protran nitrocellulose membrane were next prepared. Wearing gloves, 4 pieces of blotting paper per gel and one piece of membrane were cut into 7.5 x 9 cm rectangles. These were placed in blotting buffer (3 g tris, 15 g glycine and 200 ml MeOH, made up to 1 l with distilled water). Gels were carefully removed from their cassettes, and placed in the blotting buffer to equilibrate for 5 min. The semi-dry transfer apparatus was then set up: blotting paper (x2), nitrocellulose membrane, gel, and two further pieces of blotting paper. A roller was used to lightly roll over the stack, removing

any residual bubbles. Excess buffer was mopped up from around the stack and a semi-dry electrotransfer performed for 90 min at 15 v and 280 mA.

After transfer, the gel and membrane were removed together from the stack and excess membrane cut away around the gel. The gel was removed and discarded, and the membrane washed once in distilled water before being incubated in Ponceau S stain for 1 min to check for homogeneous transfer. The membrane was washed with distilled water three times to remove excess Ponceau S, until clear bands were visible. Any membrane trimming/cutting was done at this stage while lanes were visible, using a scalpel. Membranes were then washed three times for 5 min each in 1 x TTBS in a plastic tub. Membranes were then blocked for a minimum of 1 h in ~5 ml 1 % BSA blocking buffer at room temperature with gentle agitation. A 1:1000 dilution (5 µl) of appropriate primary antibody was added directly into the blocking solution and left to rock at 4°C overnight followed by a further 1 h at room temperature. The washing procedure was repeated (3 x 5 min with TTBS) then the membrane was transferred to a solution (1:3000 dilution) of appropriate secondary antibody in TTBS, and incubated for 120 min at room temperature with gentle agitation. Washing was repeated then the membrane was rinsed briefly in distilled water ready to be visualised.

Equal amounts of the Supersignal West Pico chemiluminescent substrate components were mixed; to cover a membrane, approximately a 1 ml was required. One membrane at a time was laid on the imaging tray of the CCD GeneGnome chemiluminescence imaging system (Syngene, Cambridge, UK) and the substrate was added, ensuring total coverage and no air bubbles. Membranes were imaged and typically 10 images were captured with 30 s between exposures. Images were saved as Syngene files and also as .tiff files to allow import into Microsoft Office. When imaging for actin, five images were typically captured as the signal was strong. Bands were quantified for analysis using associated GeneTools software with appropriate background correction.

2.10 Lambda Phosphatase Treatment

Post electrophoretic transfer, membranes were washed briefly twice in distilled water then blocked for 1 h in 5 ml TTBS with 1 % BSA at room temperature. After blocking, 2 mM $MnCl_2$ and, where de-phosphorylation was required, 400 U/ml λ-phosphatase was added and incubated overnight at 4°C with constant agitation. The membranes were then washed in TTBS for 5 min and rinsed in distilled water 5 times before continuing with the western blot protocol.

2.11 Immunoprecipitation (IP) – Kinase Assay

Samples were retrieved from -80°C storage, defrosted and kept on ice. Tubes were centrifuged in a pre-chilled rotor for 3 min at full speed (12,045 x *g*; Eppendorf minispin). The volume of each sample was determined before splitting the sample equally between two 2ml screw-cap tubes. 10% of each sample was removed and retained as the 10% of I.P. input (control). A 1:50 dilution of anti-phospho Akt (XP) antibodies was added to one tube with the second acting as the no antibody control. All samples were then placed on the rocker at 4°C for overnight incubation.

The contents of each screw-cap tube were transferred into microfuge tubes and placed on ice (samples were transferred at this stage before the addition of agarose beads). Protein A agarose beads were mixed and a volume (10 % of the total sample volume) added to both the negative control and the I.P. tube. All samples were incubated at 4°C for 1 h. Samples were pulse centrifuged in a pre-chilled rotor at full speed for 30 s and the supernatant removed and discarded, being careful not to disturb the pellet. The pellet was washed twice in 500 µl of ice-cold cell lysis buffer and then a further two times in 500 µl ice-cold kinase buffer. Tubes were kept on ice at all times. Each pellet was re-suspended in 50 µl of kinase buffer, then 1 µl of 10 mM ATP and 1 µg of kinase substrate (GSK-3 α/β fusion protein) was added. In the 10% input tube, double the quantity of assay components were added. All three sample tubes were placed in a Eppendorf thermomixer at 30°C at 700 rpm for 1 h. After this time, 12.5 µl of 5x sample buffer was added to the negative control and IP tubes and 20 µl to the 10% input tube. Tubes were vortexed for 10 s each, pulse centrifuged at full speed for 30 s then heated at 95°C for 5 min. The samples were then subjected to western blotting (section 2.4) with the following modifications:

- After transfer, membranes were blocked in 5% non-fat dried milk in TTBS then washed and placed in a 5% BSA solution containing the primary anti-phospho GSK-3α/β ($Ser^{21/9}$) antibody at 1:1000 dilution.
- The secondary antibody was diluted in 5% non-fat dried milk instead of TTBS and incubated with the membrane for 1 h.
- To visualise bands, 0.5 ml of each LumiGLO substrate component was mixed into 9 ml of distilled water and incubated with the membrane for 1 min at room temperature with gentle agitation before exposing as normal on the GeneGnome imaging system.

2.12 Crosslink Immunoprecipitation

The crosslinked IP was performed using the Pierce Crosslink Immunoprecipitation Kit following the manufacturers recommendations.

To bind the anti-phospho Akt (Thr^{308}) antibodies to the agarose beads, 20 µl of evenly suspended Pierce Protein A/G Plus Agarose was added to a Pierce Spin Column. The column was centrifuged at 1000 rpm (Eppendorf minispin) for 1 min and the flow-through discarded. The resin was washed twice with 200 µl 1x coupling buffer, re-centrifuged and the flow-through discarded. After removing any excess liquid from the bottom of the column, the plug was inserted. To each tube of washed resin, 10 µl of antibody, 5 µl of 20x coupling buffer and 85 µl of distilled water was added. These columns were incubated for 60 min at room temperature on a rocker to ensure continued suspension. The plugs were removed and the columns centrifuged at 1000 rpm for 1 min. The resin was washed once with 100 µl 1x coupling buffer, then twice with 300 µl 1x coupling buffer before re-inserting the plugs. To each tube, 2.5 µl 20x coupling buffer, 9 µl 2.5 mM disuccinimidyl suberate (DSS) and 38.5 µl distilled water was added. This solution was incubated for 60 min at room temperature on a rocker. The plug was then removed and the column centrifuged; 50 µl elution buffer was added to the resin and re-centrifuged. Two washes were completed with 100 µl elution buffer and two with 200 µl IP lysis/wash buffer, centrifuging at 1000 rpm for 1 min after each wash.

The sample lysate was pre-cleared using control agarose beads. 80 µl control agarose resin slurry was transferred to a spin column and centrifuged, then washed with 100 µl 1x coupling buffer, centrifuged and the flow-through discarded. The previously prepared 500 µl lysate was added to the column and incubated on a rocker for 60 min at 4 °C. The column was then centrifuged and the flow-through collected to be added to the cross-linked antibody.

Pre-cleared lysate (300–600 µl) was added to the column containing the antibody-crosslinked resin. The column was incubated overnight at 4°C on a rocker. The plug and cap were removed and the column centrifuged at 1000 rpm for 1 min. The spin column was placed in a fresh collection tube and the resin washed three times with 200 µl IP lysis/wash buffer, and once with 100 µl 1x conditioning buffer, centrifuging after each wash. The column was then placed in a fresh collection tube and centrifuged with 10 µl elution buffer. A further 50 µl elution buffer was added and incubated for 5 min at room temperature. The column was then centrifuged a final time at 1000 rpm for 1 min and the flow-through collected for analysis by western blot analysis (section 2.9).

2.13 Fractioning samples

Each 24 h somule sample (~20,000; treated/untreated) was lysed in 250 µl cell lysis buffer (Cell Signalling Technology) with protease and phosphatase inhibitors in a microfuge tube. Samples were left on ice for 5 min before centrifuging at full speed (12,045 x *g*; Eppendorf minipsin) for 1 min and the supernatants collected. This lysis step was repeated with each pellet to extract as much protein as possible and supernatants combined for each sample. 500 µl was then transferred to a Vivaspin 500 column and each column was centrifuged at 15,000 rpm, 15°C for 10 min in a Hettich Zentrifugen (EBA12R). The flow-through was retained and the upper fraction transferred from the column to another microfuge tube, making up the upper fraction a similar volume to the lower fraction with cell lysis buffer. Each sample was then divided into two, antibody added to one, with the other as a control. Samples were placed at 4°C overnight with constant agitation. From this point, the protocol for IP (section 2.11) was followed.

2.14 RNAi

2.14.1 Designing small interfering RNA

Small interfering RNAs (siRNAs) were designed using the IDT online design tool (https://www.idtdna.com/site/order/designtool/index/DSIRNA_CUSTOM). Initially, the Akt FASTA sequence was input and a basic local alignment search tool (blast) was used against human. Two of the resulting siRNAs were chosen based on their position in the gene; each within a single exon rather than spanning two. The two resulting target sequences were: SmAkt siRNA1 5'-ATTGTTGGATAAAGATGGTCATATA-3' which spans bp 1119 – 1143 of the SmAkt coding region, and SmAkt siRNA2 5'-AAGTGATCATGAAGTCTTATTTGAG-3' which spans bp 1332 – 1356. The design tool was used specifically to create a 25-mer siRNA product that spanned close to the Thr^{308} phosphorylation motif (bp 1188 – 1218). The siRNA target sequences were blasted against the *S. mansoni* genome and no matches were found other than those for Akt. A control siRNA was also obtained which shares no similarity with any part of the *S. mansoni* genome, DS Scrambled Negative Control, with the sequence siRNA 5'-CTTCCTCTCTTTCTCTCCCTTGTGA-3'.Of the six available designs, two were chosen.

2.14.2 Performing RNAi

Adult worms were carefully transferred directly into an electroporation cuvette containing 100 µl Optim-MEM using flat-ended tweezers. 2.5 µg of each siRNA was added to each cuvette. 2.5 µg of scrambled control was added to the negative control samples.

Parasites were electroporated at 120V for 20 ms before being transferred into individual wells of a clean 48 well plate. To avoid risk of contamination, separate plates were used for samples that were to be processed on different days. Wells were made up to 1 ml containing approx. 930 µl Opti-MEM, 20 µl antibiotic/antimycotic and 50 µl FBS. Parasites were maintained at 37°C, 5% CO_2 for 3 - 7 days. Knockdown was then measured by western blot.

2.15 Immunohistochemistry

Parasites were transferred to wells of a 24 well tissue culture plate, PBS was removed and parasites incubated in 1% glycine solution for 10 min. Next, the glycine solution was replaced with 0.3% Triton X-100 in PBS and incubated for 1 h. Parasites were then washed in PBS three times each for 10 min, each time removing as much PBS as possible. The parasites were next blocked in 10% normal goat serum for 2 h, (300 µl per well). The washing procedure was repeated and the parasites incubated with the primary antibody (1:50 dilution in 1% BSA) with constant agitation for 3 days at 4°C. The parasites were then washed in PBS three times for 30 min each. Following the final wash, parasites were re-suspended in 1 ml PBS, Alexafluor 488 secondary antibody (1:500 in PBS) and rhodamine phalloidin (5 µM/ml) was added and parasites left to incubate for 2 days in the dark at 4°C. Following this, parasites were washed three times for 30 min each. After the last wash, as much PBS as possible was removed and the remaining PBS was carefully pipetted with the parasites (cercariae or somules) onto a silane prepared slide. For cercariae and somules, slides were checked under the microscope to ensure a sufficient and even distribution of parasites, before placing them on a hot plate at 60°C for approximately 30 min or until the liquid had evaporated. For adult worms, 100 µl PBS was pipetted directly onto an untreated glass slide, then worms were carefully placed in the droplet using flat-ended tweezers. Once dry, 1-2 drops of Vectashield mounting medium was placed over the adherent parasites and a coverslip gently placed on top, ensuring no air bubbles. The cover slip was sealed around the edges with transparent nail polish and left flat in the fridge overnight to dry in a slide magazine.

Specimens were visualised on a Leica TCS SP2 AOBS confocal laser scanning microscope using 20x dry, 40x or 63x oil immersion objectives and images captured. Laser levels were maintained within experiments between negative control and stained samples.

2.16 Bioinformatics

2.16.1 Gene alignment

Akt gene sequences from *H. sapiens, D. melanogaster, C. elegans* and *S. mansoni* were aligned using Multiple Sequence Comparison by Log-Expectation (MUSCLE) software, available at: http://www.ebi.ac.uk/Tools/msa/muscle/. The sequences were entered in FASTA format, retrieved from NCBI or GeneDB for the *S. mansoni* gene. Output format ClustalW was selected and the results were copied into Microsoft Powerpoint, where colours were added to indicate the level of homology between the four species; white to black for increasing homology.

2.16.2 STRINGdb

The identifier for Akt (Smp_073930.2) was entered into STRINGdb (http://string-db.org/) (December, 2015). The parameters at the bottom of the page were altered to give either medium confidence (≥0.40) or high confidence (≥0.70), and to produce a maximum of 500 results; the option, 'Disable Structure Previews inside Network Bubbles' was selected. An image of the medium confidence map was saved (Save > Image (Low Res)) but the nodes on the high confidence map were moved so that all Smp numbers were visible.

2.16.3 Blast2GO

Blast2GO Pro was downloaded as a local trial copy. The Smp identifier data obtained through STRING was downloaded as a Fasta file, then imported to Blast2GO. A Cloudblast (blastp) was conducted to identify potentially homologous sequences from public protein databases. The settings for blast were: Number of blast hits – 20, Blast expectation value – 1.0E-3, HSP length cut off – 33. Next, the mapping function was employed to match the sequence IDs obtained in the blast step against the Gene Ontology (GO) annotation database. The data was then annotated, evaluating the information from the previous two steps and assigning the most reliable GO terms to each sequence. The parameters for running the annotation were: Annotation cut off – 55, GO weight – 5, Filter by GO taxonomy – Nematodes, Hit filter – 500.

To begin analysing the data, charts were created (Charts > Make Statistics > Annotation). All options in the 'Annotation Statistics' window were selected, GO distribution by level was set to three and maximum number of terms to display in Direct

GO Count for Biological processes, Molecular function and Cellular component was set to 20.

To create pie charts of the GO data, a combined graph was made (Graphs > Make Combined Graph > Run). All GO categories were automatically included. In the charts section of the side toolbar for each graph, 'Make level pie chart' was selected and level 3 chosen. Pie charts for Biological process, Molecular function and Cellular component at level 3 were made in this way.

2.16.4 Kinasephos phosphorylation site prediction

To identify potential phosphorylation sites within Akt interacting proteins, the entire list of high confidence STRING predicted functional Akt partners was transferred into Microsoft Excel. Using the interactive list at STRINGdb, the amino acid sequence for each protein (FASTA format), was submitted to kinasephos (http://kinasephos.mbc.nctu.edu.tw/). Using the drop down menu, protein kinase B was selected, the prediction specificity was set to 95%, and the box for tyrosine residue prediction was unselected. If results were retrieved, details from the first four columns (Locations, Phosphorylated Sites, HMM Bit Score and E-value) were pasted the into the Excel spreadsheet. This process was repeated individually for each of the proteins. (http://metazoa.ensembl.org/biomart/martview)

2.17 Histology

Adult worms were placed in plastic histology cassettes, fixed in approximately 50 ml 10% neutral buffered formalin for 2 h in 120 ml plastic tubs (Sigma), then stored in 70% industrial methylated spirits (IMS) in clean tubs. The processing was done manually due to the small size of the parasites. Watch-glasses with lids were used to hold the parasites for dehydration. Worms were transferred from the IMS storage containers into the watch-glasses using flat-ended forceps. Two washes of 90% ethanol, each for 1 h were performed, during which time 3 drops of eosin was used to pre-stain the worms. Two further washes in 100% ethanol were carried out before two washes in HistoChoice clearing agent. Meanwhile, Histoplast PE paraffin wax was melted at 57°C in 300 ml glass containers, one for each sample. Worms were transferred into histology cassettes, one for each sample, and submerged in the wax for 1 h, twice. One at a time, worms were encased in wax blocks using a HistoStar wax block maker. Blocks were left to cool for 1 h on the cold plate, removed from the moulds, and then stored in the fridge overnight.

A microtome (Leica, RM2235) was used to slice the worms into 5 µm sections, which were then expanded using a water bath at 45°C and mounted on polysine slides. The slides were left upright in a slide holder for approximately 10 min to remove excess water then placed on a slide drying bench for up to 4 h at 40°C. Slides were placed horizontally in an oven set at 40°C overnight to dry completely before staining.

Slides were placed in a slide holder and immersed in two baths of Histochoice for 5 min each to de-wax the slides. Slides were hydrated through 90% IMS, 70% IMS and distilled water, each for 2 min. Haematoxylin stain was used for 15 min then slides were rinsed in distilled water and immersed in alkaline tap water for 2 min to 'blue' the slides. Slides were placed in 70% IMS for 2 min, dropped in eosin and immediately transferred to 90% IMS. Longer incubation in eosin was not required due to the pre-staining during tissue processing. Slides were moved to 100% ethanol for 5 min then Histochoice for a final clearing before being mounted using DPX and 20 x 60mm cover slips. Finished slides were dried overnight in the oven at 40°C then stored in a slide magazine at room temperature.

2.18 Measurement and Analysis of Tegument Tubercles

2.18.1 Tubercle analysis of Akt Inhibitor X treated worms

Adult male worms were placed (five/well) in a 48 well tissue culture plate, containing 1 ml RPMI medium. Worms were treated with 0.1, 1 or 10 µM Akt Inhibitor X or not (control) and incubated for five days at 37°C/5% CO_2. Images were captured daily of worm tubercles using a LEICA microscope/tablet image capture system using a x 10 objective lens. As much as possible images were captured of the dorsal surface to maintain consistency between worms. To analyse, images were imported into Image J, the area of tubercles (n > 40) was determined using the measurement function and means calculated.

2.18.2 Tubercle analysis of histology worms

After histological preparation, slides were viewed using a Nikon microscope (Eclipse Ni) imaging system. Images were captured at x 40 magnification of tubercles on the dorsal surface of worms. Using the Nikon software, the diameter of ~50 tubercles per treatment was measured and the means calculated.

2.19 SGTP4 Expression at the Somule Tegument During Transformation

To determine the effect of Akt inhibition on the expression of SGTP4 in somules during transformation from cercariae, pre-incubation was required with Akt Inhibitor X at the cercarial stage. Snails were shed and approximately 1 ml of cercariae suspension (in water) was collected using a Pasteur pipette and transferred to a microfuge tube. Control and inhibitor-treated parasites were investigated for each time point studied. 10 µM of Akt Inhibitor X (or not, control) was incubated with cercariae for 1 h at room temperature. Following this, tubes were vortexed for 2 min on a platform attachment (Vortex Genie 2) to induce transformation of the cercariae into somules, then parasites were cooled on ice for 5 min. The parasites were then centrifuged at full speed (12,045 x *g*; Eppendorf minispin) for 45 s and the supernatant removed to leave approximately 20 µl parasite suspension; 1 ml of RPMI medium containing 10 µM of Akt inhibitor X (or not, control) were added and parasites incubated at 37 °C in 5% CO_2 for 30, 60 or 120 min. At each time point, parasites were processed for western blotting or immunohistochemistry/confocal laser scanning microscopy with anti-Akt or anti-SGTP4 antibodies as detailed in sections 2.5.1 and 2.5.2.

For microscopy, at each time point, a single confocal Z-scan through the centre of a parasite was captured (30 somules, 15 each treated and non-treated). Post capture, images were analysed using Leica confocal quantification software. Two digital lines were drawn across each somule, one anterior and one posterior approximately ¼ and ¾ through the parasite, respectively. Effort was made to keep the lines perpendicular through the somules and to extend past the somule by equal distance at each end. Graphs were generated by the software displaying the signal intensity along the lines. The peak fluorescence intensity at the two intersections of the lines with the tegument were recorded. Settings were altered to show only the green channel of each line on the graphs, and an example image from each time point was captured.

2.20 Glucose Uptake Assay – Promega Glucose uptake Glo Assay

All kit components were thawed at room temperature. Once thawed, the luciferase reagent, stop buffer and neutralization buffer were kept at room temperature, while all other reagents were placed on ice. Prior to use, thawed components were mixed to ensure homogenous solutions. The 2DG6P detection reagent (Table 2.1) was prepared 1 h before use to minimize assay background. The 2DG6P detection reagent had to be made fresh and used on the day of preparation.

Component	Per Reaction	Per 10 ml
Luciferase Reagent	100 µl	10 ml
$NADP^+$	1 µl	100 µl
G6PDH	2.5 µl	250 µl
Reductase	0.5 µl	50 µl
Reductase Substrate	0.0625 µl	6.25 µl

Table 2.1 **Reagents and volumes required to make up the *2DG6P* detection reagent as detailed in the Promega Glucose uptake Glo assay protocol.**

Somules were treated (or not, control) with Akt Inhibitor X as detailed in Section 2.6; a blank well was set up with only 1 ml RPMI medium to act as a background control. For the assay, somules were then washed twice in pre-warmed PBS (37°C) then resuspended in 50 µl PBS with 10 µM Akt Inhibitor X. This wash removed any components in the PRMI that may have interfered with the assay. The blank well was treated in the same way. Parasites were then transferred into a clean, white, 96 well plate (Nunc). For adult worms, parasites were washed in 100 µl warmed PBS then transferred to fresh wells containing 50 µl PBS. A 10 mM solution of 2DG was prepared from the 100 mM stock solution accounting for the number of reactions needed (5 µl per reaction). 5 µl 2DG was added to each well, mixed briefly and the plate incubated at room temperature for 20 min. After 20 min, 25 µl of stop buffer was added and the plate manually shaken for 30 s to kill the parasites and lyse the surface cells (the parasites appeared intact under the dissecting microscope). After a further 5 min at room temperature the plate was shaken again for 30 s. Immediately after adding the neutralization buffer, 100 µl of 2DG6P was added to each well, the plate shaken for a further 30 s and incubated for 30 min at room temperature before taking the initial reading. Luminescence was measured using a 0.5 – 1 s integration on a BMG Fluorstar Optima plate reader. A second luminescence reading was taken after 1 h incubation with the 2DG6P. The signal of the blank well was subtracted from all other wells to account for any background reading.

2.21 Cercarial Video Analysis

Freshly shed cercariae were transferred by pipette in a 100 µl drop into the bottom of a 48 well tissue culture plate. Treatments of 1 µM L-arginine, 100 µM LA or 10 µM Akt Inhibitor X were added *via* 1 µl of appropriately diluted reagent. Movies were captured using a Canon DSLR camera attached to a Leica stereo dissecting light microscope. The focus was set to the bottom of the well plate and the zoom adjusted so the majority of the droplet was in focus. Treatments were performed in a staggered manner to allow

enough videoing time between treatments. For 0 min captures, the well was placed under the camera and the recording initiated immediately after the 1 µl reagent was added; 30 s movies were captured at 0, 1, 5, 10, 20, 30 and 45 min for each treatment.

For analysis, 30 individual cercariae were randomly chosen from each video and the number of seconds each swam was measured. Contracting movements were not counted as active swimming.

In addition to the above analysis, movies captured for cercariae treated with 10 µM Akt Inhibitor X were also analysed for the number of parasites swimming at certain time points. The camera was focused on the bottom of the plate therefore any settled, non-swimming cercariae were clearly visible and these were enumerated at 0, 10, 30 and 45 min. At 45 min, no cercariae were swimming at all, so the number counted for this time point was taken as the total. Movies were paused for enumeration at the start of each 30 s clip for consistency.

2.22 Statistical Analysis

Where appropriate, statistical differences between means were tested for by ANOVA using Fisher's multiple comparison post-hoc test with Minitab 16. All data is expressed as mean ± standard deviation (SD) with the values $p \leq 0.001$, 0.1 or 0.5 to indicate statistical significance.

3

Results 1 – Characterisation of functionally active Akt in *S. mansoni*

Exploring cell signalling in the human-infective/resident life stages of schistosomes may eventually result in the identification of a much-needed novel drug target against the parasite. Research in this area also provides valuable knowledge of the host-parasite relationship on a molecular level. Although several signalling pathways have been studied in *S. mansoni,* our overall understanding of molecular communication in schistosomes remains poor. Recent studies have identified roles for several protein kinases in *S. mansoni*, such as TK6, PKC and PKA (Table 1.1). Akt has also been studied in schistosomes (Morel *et al.*, 2014a) although only from the perspective of parasite control, and not functional biology. Furthermore, a novel insulin-like peptide has been recently characterised in *S. japonicum* (Du *et al.*, 2017), which could have important applications for future work on schistosome Akt. This chapter concerns the validation and application of commercially available antibodies and pharmacological Akt inhibitors and activators for use in *S. mansoni*. RNAi of Akt was also performed and phosphorylated Akt was functionally mapped in various schistosome life stages to demonstrate the *in situ* localisation of the activated kinase. A proteome profiler kit was trialled in early work to assess the viability of this approach for screening selected *S. mansoni* kinase activities.

3.1 Proteome Profiler 96 Kit

Initial experiments were performed using a Proteome Profiler kit (Human Phospho-Kinase Array 1) to ascertain whether schistosome extracts could be screened for multiple phosphorylated (activated) kinases simultaneously. The chosen array contained targets associated with MAPK and Akt signalling. Such pre-designed arrays have been used successfully in human cancer research (Bordinhão *et al.*, 2016; Wang *et al.*, 2016). Although such arrays are commercially available only for mammalian species, given the generally good interspecies conservation of phosphorylation motifs, this array was trialled with the rationale that the employed antibodies might react suitably with the *S. mansoni* kinases. The Profiler kit is a two-site sandwich ELISA-based kinase array. The specific capture antibodies spotted in each well bind to the protein kinases in the homogenate. An HRP-conjugated detection antibody is then added, which binds to a different (phosphorylated) motif on each kinase, allowing measurement of the phosphorylated proteins by chemiluminescence. The targets of the assay and their phosphorylation sites are illustrated in Figure 3.1.

The aim was to monitor the activities of the different kinases in parallel, and ascertain their responses to various stimulants. Adult worms were exposed to three different

treatments (anisomycin, EGF, or PMA) before total proteins were extracted and 50 µg protein applied to each array. Anisomycin is a known activator of $p70^{S6K}$, p38 MAPK and ERK1 (Cano *et al.*, 1994; Kardalinou *et al.*, 1994), EGF is a commonly known stimulant of multiple signalling pathways including ERK1/2 (Adamson and Rees, 1981), and PMA activates protein kinases such as PKC (Castagna *et al.*, 1982). Not all antibodies on the array reacted with the schistosome extracts (Figure 3.2). In all cases phosphorylated (activated) ERK was detected and, in all but one experiment (Figure 3.2 B), $p70^{S6K}$ was also activated after stimulation. However, phosphorylated -Akt, -JNK, and -Src were not detected in adult worm extracts irrespective of treatment (Figure 3.2 A-C). To ascertain if protein quantity affected detection, 25 µg and 100 µg total protein from PMA-treated adults were applied to each array (Figure 3.2 C). Increased levels of phosphorylated GSK-3β and $p70^{S6K}$ were detected with 100 µg protein, however -Akt, -JNK, and -Src remained unreactive (Figure 3.2 C). Finally, the array was screened using somule protein extracts to ascertain whether a different *S. mansoni* life stage would demonstrate greater immunoreactivity. Although phosphorylated Src was detected (Figure 3.2 D), this spot also presented in the non-treated control. There was little observable difference between treatments and the results were consistent across replicate experiments, with one exception (Figure 3.2 B). Overall, results from the Profiler kit were inconclusive, likely due to the incompatibility of the anti-human total kinase (capture) and/or phospho-kinase (detection) antibodies with the *S. mansoni* proteins. As a result, a different approach was taken, aiming to focus on Akt signalling in *S. mansoni* using different methodologies.

A

Target	Phosphorylation Site
Akt1	S473
ERK1/ERK2	T202/Y204
GSK-3β	S9
JNK Pan Specific	T183/Y185
p38α	T180/Y182
p70S6K	T421/S424
Src	Y416
HSP60	-

B

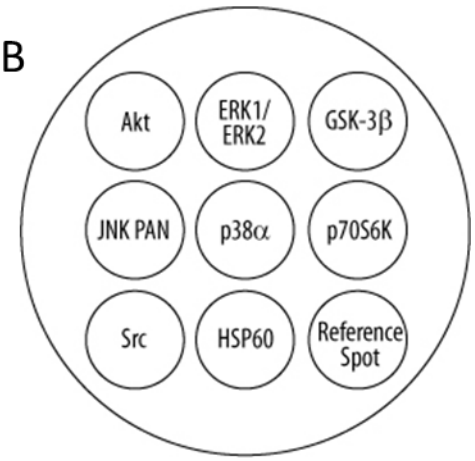

Figure 3.1 **Composition of the Proteome Profiler kit (Human Phospho-Kinase Array 1). A.** The phosphorylation sites for each kinase target represented on the array. **B.** Layout of the pre-spotted capture antibodies on the base of each well in the 96 well plate. A cocktail of antibodies directed against the phosphorylated target proteins was used to detect the active kinases.

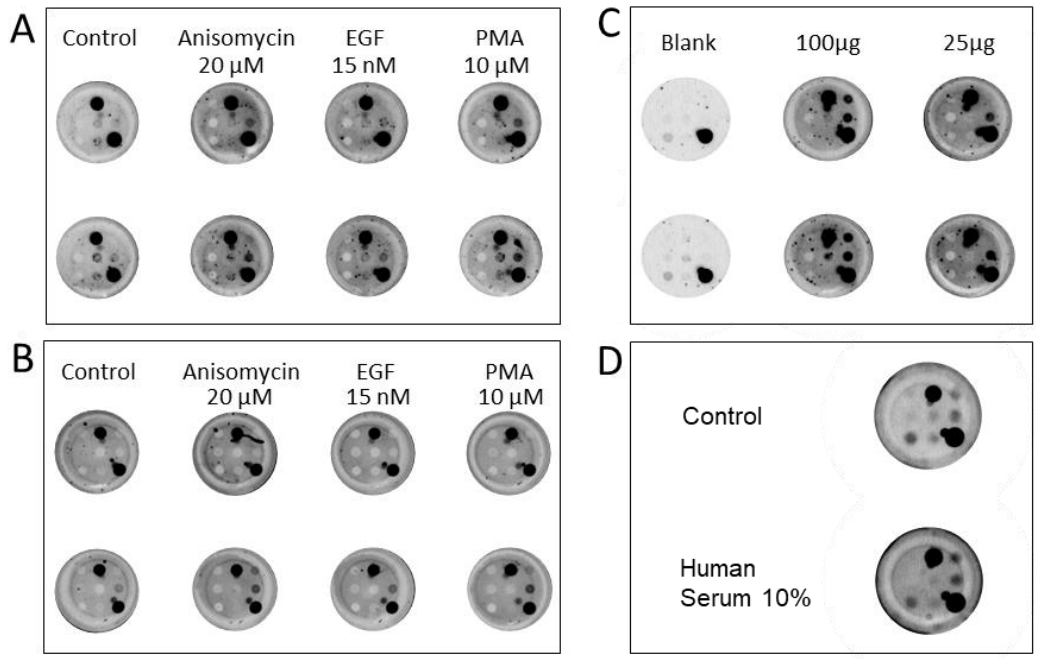

Figure 3.2 **Multiple phosphorylated *S. mansoni* kinases are captured and detected by the Human Phospho-Kinase Array 1. A**. Adult *S. mansoni* were treated with anisomycin (20 µM) for 30 min, EGF (15 nM) for 5 min, PMA (10 µM) for 30 min, or left untreated (control). Worm protein extracts (50 µg) were incubated in wells of the plate overnight at 4°C. **B.** Replicate experiment performed as in A, but with samples incubated for 5 h at room temperature. **C**. Adult worms treated with PMA, but with different protein amounts used. **D**. 24 h somules incubated with 10% human serum for 10 min, or not (control).

3.2 Initial Detection of Phosphorylated Akt in *S. mansoni*

Prior to screening commercially available anti-Akt antibodies against *S. mansoni* protein extracts, a multiple pair-wise alignment of the predicted *S. mansoni* Akt protein against Akt proteins from *H. sapiens*, *D. melanogaster* and *C. elegans* was created using MUSCLE. Human Akt1 was chosen to facilitate selection of appropriate antibodies for testing based on sequence similarity between species; *D. melanogaster* and *C. elegans* Akt were selected as comparator proteins due to the status of these species as invertebrate model organisms and because each species possesses an Akt homologue with a pleckstrin homology (PH) domain (Vanhaesebroeck and Alessi, 2000). The protein sequences for alignment were sourced from NCBI with the exception of the *S. mansoni* Akt sequence, which was retrieved from Ensembl Metazoa. SmAkt possesses 79% homology with both human Akt1 and *D. melanogaster* Akt1A sequences, and 80% homology with *C. elegans* Akt. Figure 3.3 outlines the three key protein domains; the PH,

kinase, and regulatory domains. Also highlighted are the residues that are phosphorylated in human, *D. melanogaster* and *C. elegans* Akt that may be conserved for Akt activation in *S. mansoni*. Notably, the *S. mansoni* Akt gene contains a long leader sequence at the N-terminus, a feature not shared by the human, *D. melanogaster* or *C. elegans* homologues.

The PH domain, a motif approximately 100 amino acids (aa) long, was first identified over two decades ago (Haslam *et al.*, 1993). This region appears in number of signalling proteins, many of them protein kinases. The PH domain in Akt has been implicated in binding to PIP_2 and PIP_3 in the context of Akt membrane localisation (Lietzke *et al.*, 2000; Vanhaesebroeck and Alessi, 2000). *S. mansoni* and human Akt share 57.5% homology in the PH domain (Figure 3.3).

The Akt catalytic kinase domain generally ranges from 250 – 300 amino acids in length (depending on species) and can be further separated into several major sub-domains (Hanks *et al.*, 1988). In *S. mansoni* Akt, the kinase domain is 264 amino acids long. The human Akt kinase domain is conserved with those of PKA and PKC, 65% and 75% respectively (Coffer and Woodgett, 1991; Alessi *et al.*, 1996b), hence why Akt is also known as PKB. Additionally, the kinase domain contains the Asp-Phe-Gly (DFG) motif. This motif marks the start of the activation loop, which is 20-30 amino acids long and is commonly involved in kinase activation (Hanada *et al.*, 2004). The *S. mansoni* Akt kinase domain shares 73.1%, 71.9% and 69.6% similarity with human, *D. melanogaster* and *C. elegans* kinase domains, respectively (Figure 3.3).

The regulatory domain is located at the carboxyl terminal end of the protein and contains the crucially important hydrophobic motif. The hydrophobic motif consists of F-X-X-F/Y-S/T-Y/F, where X is any amino acid, and is found in all proteins of the AGC superfamily (Peterson and Schreiber, 1999). Phosphorylation of the serine/threonine residue in this motif is critical for protein activation (Alessi *et al.*, 1996a).

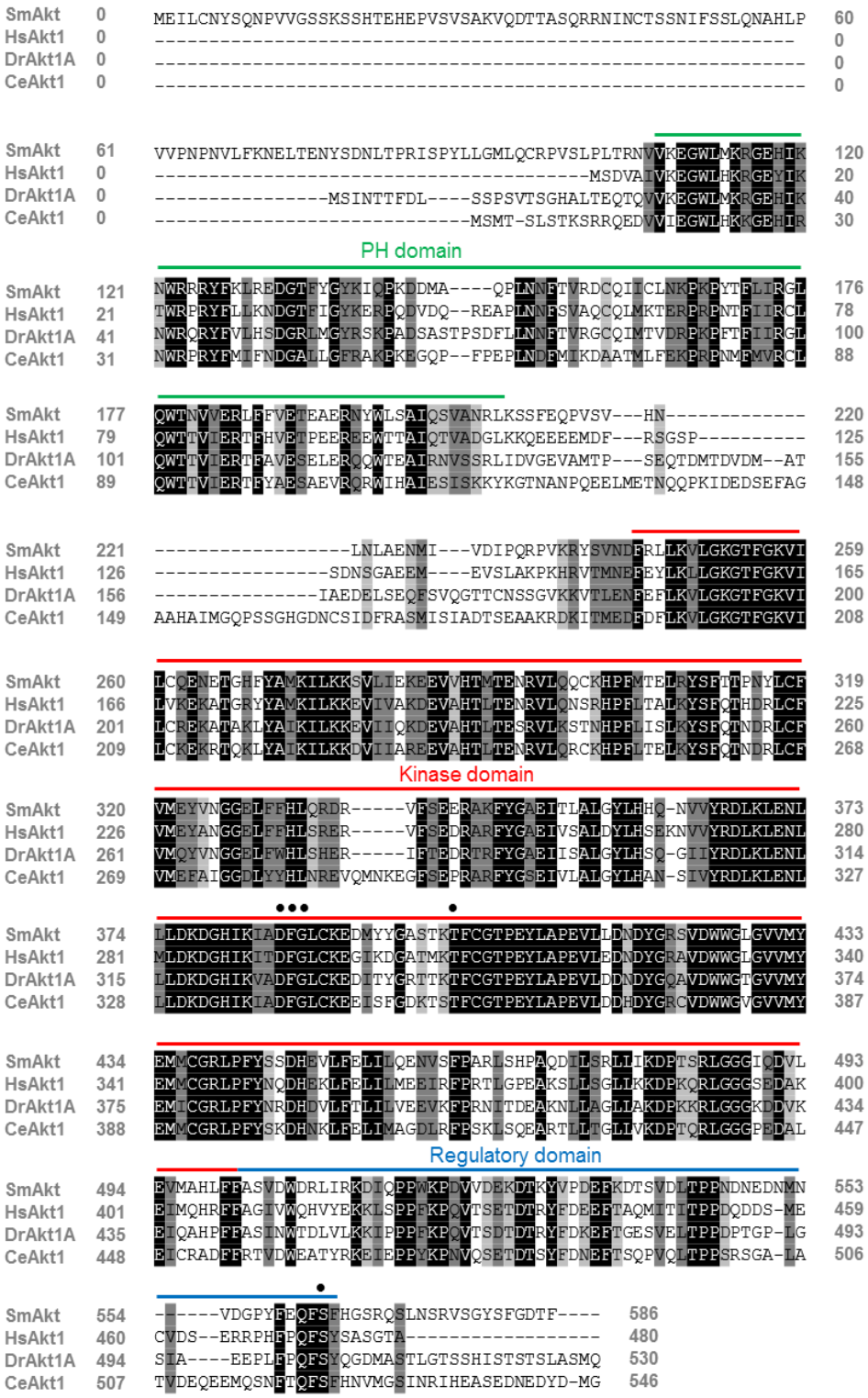

Figure 3.3 **Full multiple pair-wise alignment of *S. mansoni* Akt with Akt proteins from three other organisms.** *S. mansoni* (Smp_073930), *H. sapiens* (NP_00104432.1), *D. melanogaster* (AHN57352.1) and *C. elegans* (O18178.4) alignment created using MUSCLE. The pleckstrin homology (PH) domain is indicated in green, the kinase domain in red, and the regulatory domain in blue. The black dots indicate important conserved residues for phosphorylation of Akt, the DFG motif of the ATP binding site, Sm (Thr^{401}) and Sm (Ser^{565}). The colours range from light grey to black showing least conserved to most conserved amino acids, respectively, as determined by MUSCLE.

As discussed in Chapter 1 (Section 1.2), for activation, Akt must be phosphorylated not only on the Thr^{308} residue in the activation loop, but also the Ser^{473} residue in the hydrophobic motif (human numbering) (Alessi *et al.*, 1996a), as is also the case for *D. melanogaster* (Sarbassov *et al.*, 2005) and *C. elegans* (Paradis *et al.*, 1999) Akt. However, western blotting with anti-phospho Akt (Ser^{473}) antibodies raised against a phosphorylated peptide surrounding this residue failed to reveal any immunoreactive bands in *S. mansoni* extracts (data not shown). This is likely due to the low level of amino acid similarity surrounding Ser^{473} between the *S. mansoni* and human protein, as revealed by bioinformatic analysis (Figure 3.4). By comparison, the residues surrounding Thr^{308} and Tyr^{315} (human numbering) showed almost complete conservation. Initial western blots performed with monoclonal anti-phospho Akt (Thr^{308}) antibodies that recognise exclusively the phosphorylated (activated) form of human Akt, revealed an immunoreactive protein of approximately ~52 kDa in extracts from *in vitro* cultured *S. mansoni* somules and a weaker immunoreactive protein of ~70 kDa (Figure 3.5A). This antibody recognises the sequence: 5'-GATMK**T**FCGTP-3' (Figure 3.4). Tyr^{315} is thought to be phosphorylated prior to phosphorylation of Thr^{308} and Ser^{473} (Chen *et al.*, 2001) and is also important to Akt catalytic activation. The anti-phospho Akt (Tyr^{315}) antibodies recognise the highly conserved sequence 5'-CGTPE**Y**LAPEV-3'; these antibodies also detected the ~52 kDa in extracts from *S. mansoni* somules (Figure 3.5A). λ-phosphatase treatment was employed to release phosphate groups from proteins on the blot; the lack of antibody binding following treatment (Figure 3.5A) demonstrates that the anti-phospho Akt (Thr^{308}) and (Tyr^{315}) antibodies specifically recognise the phosphorylated Akt-like protein.

During multiple initial experiments using these anti-phospho antibodies in somules, it was noted that the stronger and more consistently immunoreactive band for Akt was that of ~52 kDa. The current *S. mansoni* genome (Protasio *et al.*, 2012) predicts Akt to be 68 kDa and does not indicate that there may be different isoforms, as occurs in other organisms such as *C. elegans*. (Paradis and Ruvkun, 1998; Manning and Cantley, 2007). Thus, an important aim became to determine the identity of this ~52 kDa Akt-like protein.

In addition to the two anti-phospho antibodies, a 'total' Akt (anti-Akt1/2/3) antibody was tested which detects all Akt protein present, regardless of phosphorylation status (Figure 3.5 B). This anti-Akt antibody recognises the 'PEYLA' region in the amino acid sequence, therefore overlapping the Tyr^{315} site (Figure 3.4). In somules, this antibody recognised a band at 50 kDa and at 70 kDa, with the latter being stronger than when detected with the anti-phospho Akt (Thr^{308}) and (Tyr^{315}) antibodies. This supports the possibility that there

are two forms of Akt in *S. mansoni,* with one (50 kDa) having a greater basal level of activation than the other (70 kDa).

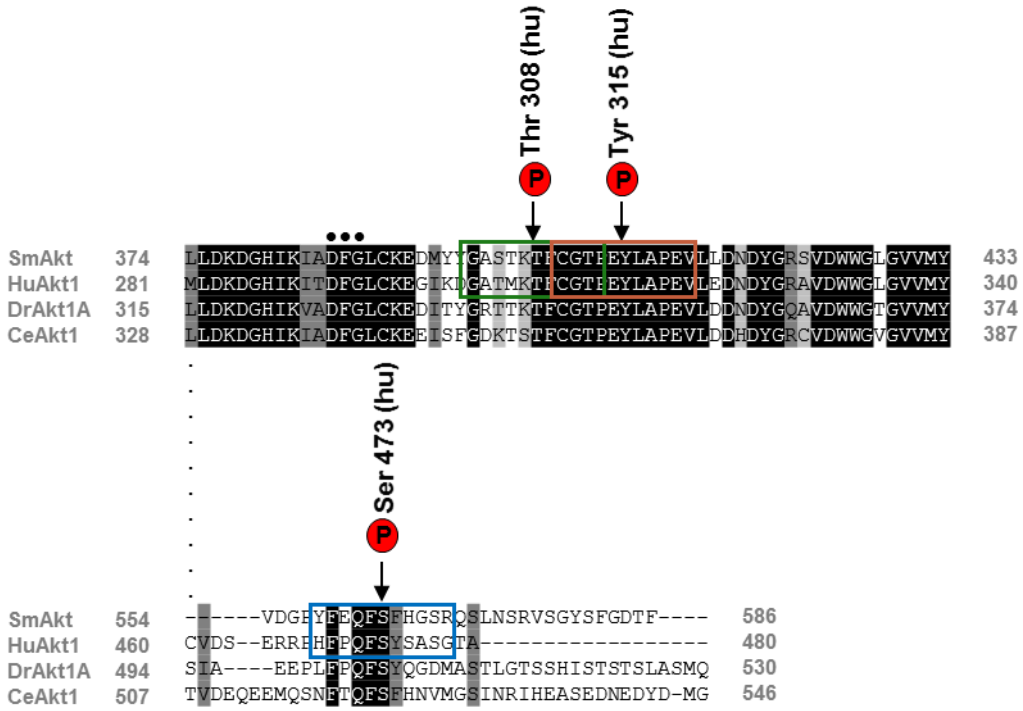

Figure 3.4 **Partial pair-wise alignment of *S. mansoni* Akt and Akt from three other organisms shows homology of important phosphorylation motifs.** Predicted *S. mansoni* (Sm) Akt sequence and the comparative alignment of relevant Akt sequences from human (Hu), *D. melanogaster* (Dr) and *C. elegans* (Ce). The amino acid sequences shown span the anti-phospho antibody recognition sites for the antibodies that bind Thr^{308}, Tyr^{315} and Ser^{473} residues (human numbering). These antibodies only recognise the phosphorylated kinase and typically identify a total of 10-12 residues around the phosphorylated amino acid (green, orange and blue boxes). The recognition site around the Ser^{473} residue shows poor conservation between the Sm and Hu sequences. Three dots signify the DGF motif of the ATP binding site. This alignment was created using MUSCLE with sequences imported from NCBI and Ensembl Metazoa.

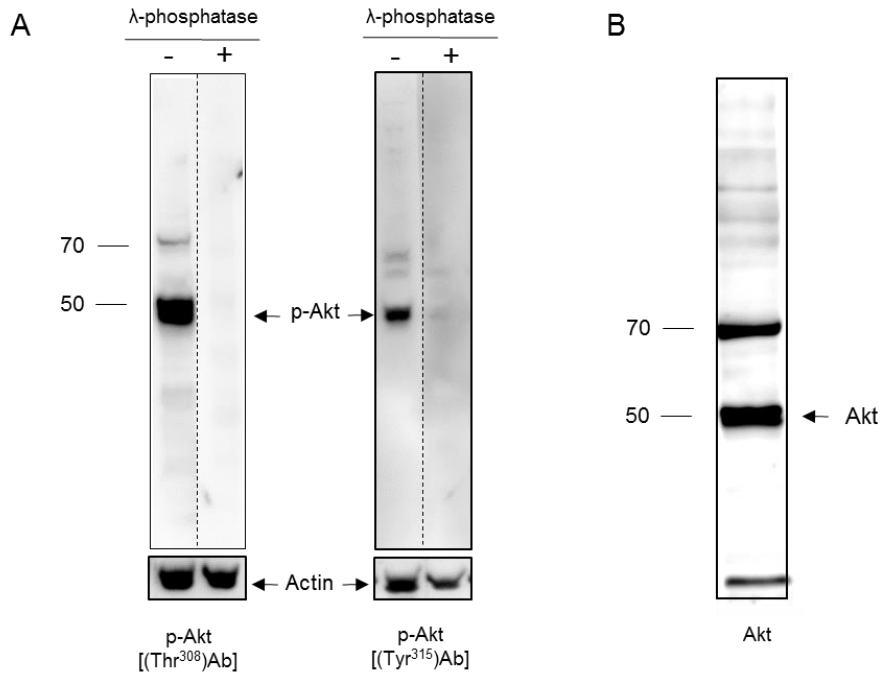

Figure 3.5 **Detection of an Akt-like protein in *S. mansoni*.** Somules (~1000 per lane) were processed 18 h post transformation. **A.** The blot was cut into four pieces, two of which were treated with $MnCl_2$/λ-phosphatase overnight (+). Western blotting using anti-phospho Akt (Thr^{308}) and anti-phospho Akt (Tyr^{315}) antibodies was then performed on all blots. Blots were also probed with anti-actin antibodies to reveal the presence of protein in all lanes. **B.** The membrane was probed with 'total' anti-Akt antibodies that recognise Akt irrespective of its phosphorylation status. The positions of the relevant molecular weight markers are indicated. The blots shown are representative of those obtained in at least two independent experiments.

Having characterised two anti-phospho Akt antibodies and a total Akt antibody using somule extracts, cercariae and adult worm protein extracts were also screened. Each antibody recognised a band of similar molecular weight (~52 kDa) across the three life stages, indicating that all antibodies were recognising a similar protein (Figure 3.6). This was expected based on the sequence alignment (Figure 3.4). The anti-Akt antibody also sometimes revealed a weakly immunoreactive band above the putative Akt band in cercariae and adult worms. This was attributed to non-specific background binding as it was not seen consistently across experiments.

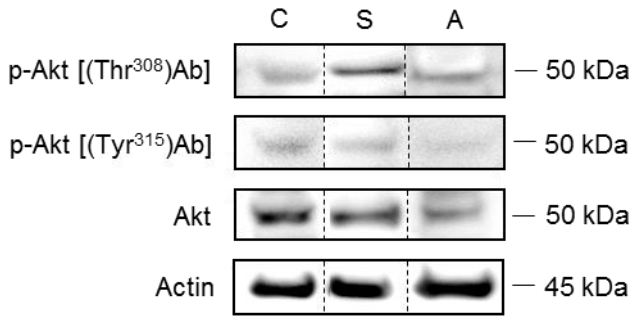

Figure 3.6 **Different *S. mansoni* life stages show similar banding profiles when blotted with antibodies against Akt.** Cercariae (C) (~1000), somule (S) (~1000) and adult worm (A) (~ 1 pair) proteins were processed for western blotting with anti-phospho Akt or anti-Akt antibodies as indicated. Blots were also stripped and re-probed with anti-actin antibodies. Blots are representative of results obtained in two independent experiments.

3.3 Immunoprecipitation of SmAkt and Activity Assay

Immunoprecipitation (IP) and Akt activity experiments were performed with adult worm and somule extracts to ascertain whether the putative phosphorylated Akt protein detected by western blotting possessed Akt activity. To conduct these experiments, an Akt activity assay kit was used, which included a GSK-3α/β kinase substrate peptide known to be specifically phosphorylated by human Akt. This assay was selected due to the good conservation between human and *S. mansoni* GSK-3 proteins (Chapter 4, section 4.4.3). The assay kit employs the 'classical' method of IP whereby the antibody is incubated directly with the sample containing the target protein to form an antigen-antibody complex. Post complex formation, protein A agarose beads are added to 'pull down' the target protein by binding to the Fc region of the IP antibody (Kaboord and Perr, 2008). This method results in both the antigen of interest and the antibody being released from the beads during the elution stage. Phosphorylated GSK-3α/β fusion protein is then detected by western blotting after kinase assay.

Anti-phospho Akt XP (Thr^{308}) antibodies were able to precipitate protein from serum-treated somules and adults, that phosphorylated the GSK-3α/β fusion protein substrate (Figure 3.7). There was minimal immunoreactivity in the negative control (no antibody) lanes against phosphorylated GSK-3α/β, demonstrating that the immunoprecipitations were reasonably specific and that the immunoprecipitated protein possesses Akt-like activity.

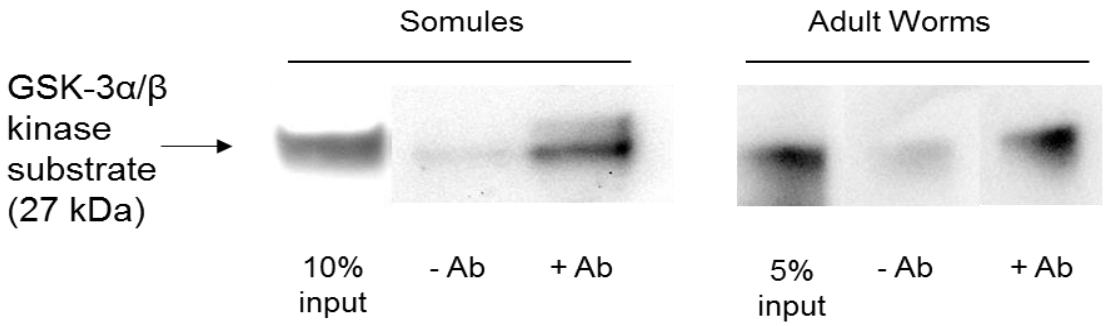

Figure 3.7 **Phosphorylation of the GSK-3 substrate by an immunoprecipitated *S. mansoni* Akt-like protein.** Somules (~20,000) or adult worm pairs (~20) were homogenised, separated into equal amounts and subjected to immunoprecipitation using monoclonal anti-phospho Akt (Thr^{308}) XP antibodies (+Ab) or not (control, -Ab). Immunocomplexes were then subjected to an Akt assay, with GSK-3α/β fusion protein as the Akt substrate. Phosphorylation of GSK-3α/β by Akt was then detected by western blotting using anti-phospho GSK-3α/β (ser9/21) antibodies. Results are representative of three independent experiments.

Given the successful IP, the anti-phospho Akt (Thr^{308}) XP antibody was used to attempt to isolate enough protein for sequencing. An alternative to the classical IP method was used, the oriented affinity method (Kaboord and Perr, 2008), because the Akt-like protein shared a similar molecular weight (~50 kDa) to the antibody heavy chain. The oriented affinity method employs DSS to covalently crosslink the antibody to the agarose beads, thereby preventing it from eluting with the antigen and interfering with analysis. After gel staining, three potential bands were cut from the gel run with the IP eluates and sent for sequencing at Nottingham University. However, the results were negative, presumably due to low protein abundance. Nevertheless, the oriented IP protocol was used for reciprocal IPs of the Akt antibodies used (Figure 3.8). Three antibodies (anti-phospho Akt (Thr^{308}) XP, anti-phospho-Akt (Thr^{308}) and anti-Akt) were used as the IP antibody in separate experiments and the resulting immunocomplexes were processed for western blotting with reciprocal antibodies (Figure 3.8). In all cases the same molecular weight band was observed, further supporting that each antibody is recognising the same target protein.

Finally, 50 kDa spin columns (Vivaspin 500) were used to isolate proteins of ~50 kDa or less from the somule protein homogenate prior to IP and kinase assay. This was done to ensure that Akt kinase activity (Figure 3.7) was due to a ~50 kDa Akt rather than larger (~70 kDa) Akt form(s) that might have been immunoprecipitated although not detected by blotting (Figure 3.8). After immunoprecipitation and kinase assay, the 0-50 kDa

fraction demonstrated phosphorylation of the GSK-3α/β substrate which could only have been achieved by an Akt-like protein (Figure 3.9).

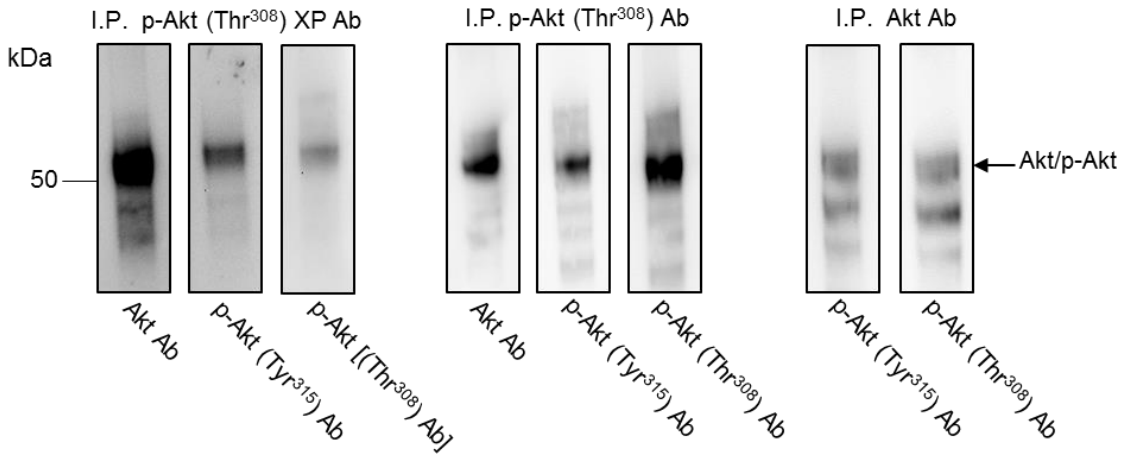

Figure 3.8 **Reciprocal immunoprecipitation (IP) of *S. mansoni* Akt.** 24 h somules (~10,000 per IP) were homogenised, pre-cleared and immunoprecipitated with one of three antibodies; anti-phospho Akt (Thr^{308}) XP, (Thr^{308}), and Akt antibodies (Ab). Subsequent western blotting of the pulled down protein was performed with anti-Akt, anti-phospho Akt (Tyr^{315}), and (Thr^{308}) Ab.

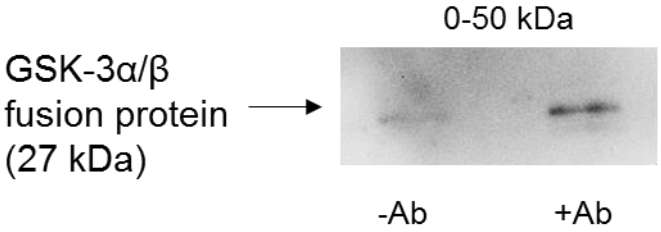

Figure 3.9 **Fractionation columns reveal Akt-like activity in 0 - ~50 kDa fraction of *S. mansoni* homogenates.** Somules (~20,000) were homogenised and the homogenate was processed through a Vivaspin 500 column with a 50 kDa cut-off. The flow through was separated into equal amounts and subjected to immunoprecipitation using monoclonal anti-phospho Akt (Thr^{308}) XP antibodies (+Ab) or not (control, -Ab). Immunocomplexes were then subjected to an Akt assay, with GSK-3α/β fusion protein as the Akt substrate. Phosphorylation of GSK-3α/β by Akt was then detected by western blotting using anti-phospho GSK-3α/β (ser9/21) antibodies. Results are representative of three independent experiments.

3.4 RNAi Knockdown

To provide further evidence that the detected Akt-like protein results from the annotated *S. mansoni* Akt gene, RNA interference (RNAi) was performed. RNAi by electroporation has become a routine tool for the suppression of protein expression in *S. mansoni* (Beckmann *et al.*, 2010; Kasinathan *et al.*, 2014; Morel *et al.*, 2016). The siRNAs were designed and sourced from IDT using their online custom design tool. Protein knockdown was measured by western blotting after 5 days culture of worms in Opti-MEM. The

validated anti-total Akt antibodies facilitated detection of total expressed Akt before and after RNAi, and the anti-phospho (Thr^{308}) antibodies allowed for the estimation of remaining activated Akt. From three independent experiments, a significant 83% ($p \leq 0.001$) reduction in total Akt expression was observed after RNAi compared to control worms (Figure 3.10), demonstrating that the detected Akt protein is derived from the annotated Akt gene. Although significant, there was only a reduction of 26% ($p \leq 0.05$) in the phosphorylated protein levels, suggesting that the remaining Akt might be hyperactivated (Figure 3.10).

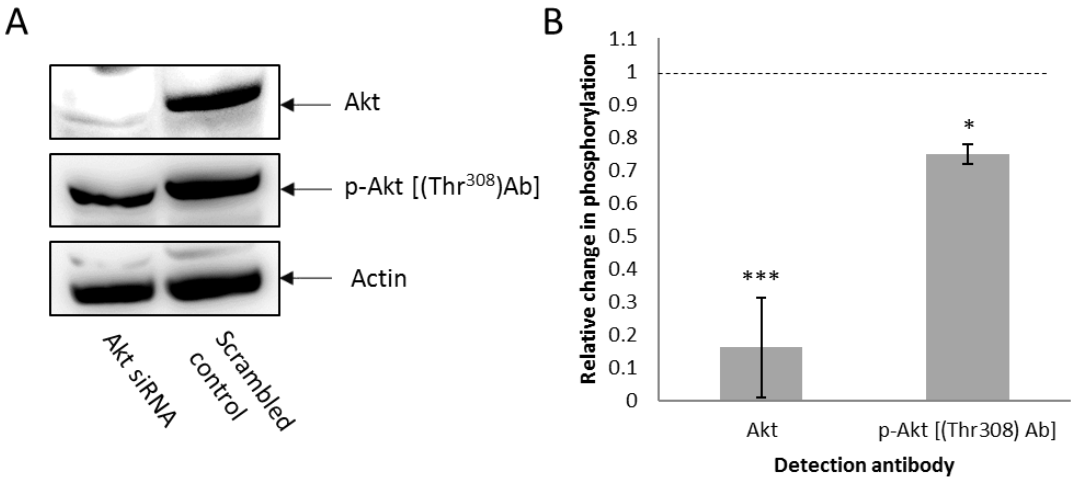

Figure 3.10 **Knockdown of Akt expression in adult *S. mansoni*. A.** Adult worms (5 pairs) were electroporated with either 2.5 µg SmAkt siRNA or 2.5 µg scrambled control siRNA. After culture for 5 days, worms were prepared for western blotting and the resulting membranes were probed with anti-Akt antibodies, then stripped and re-probed with anti-phospho Akt (Thr^{308}) antibodies; blots were also probed with anti-actin antibodies to assess protein loading between lanes. **B.** The mean (+/- S.D., n=3) relative change in band intensity following treatment was determined (GeneTools) over three independent experiments when compared with controls (indicated by the dotted line). *$p \leq 0.05$ and ***$p \leq 0.001$ (ANOVA).

3.5 Immunolocalisation of Akt and Activated Akt in *S. mansoni*

Previous work in our laboratory has employed anti-phospho antibodies and confocal laser scanning microscopy to localise phosphorylated (activated) protein kinases in intact *S. mansoni* (de Saram *et al.*, 2013; Hirst *et al*, 2016). Having established that the anti-phospho Akt and total Akt antibodies recognise *S. mansoni* Akt, experiments were undertaken to map Akt and functionally activated Akt in the parasite. Cercariae, somules and adult worms, were stained with antibodies and mounted for microscopy, without treatment, to visualise the basal localisation of both phosphorylated and non-phosphorylated Akt, and to evaluate any differences between the two. Negative control

parasites labelled only with the secondary Alexafluor 488 antibodies and rhodamine phalloidin, which stains the actin filaments revealed that non-specific binding did not occur (Figure 3.11).

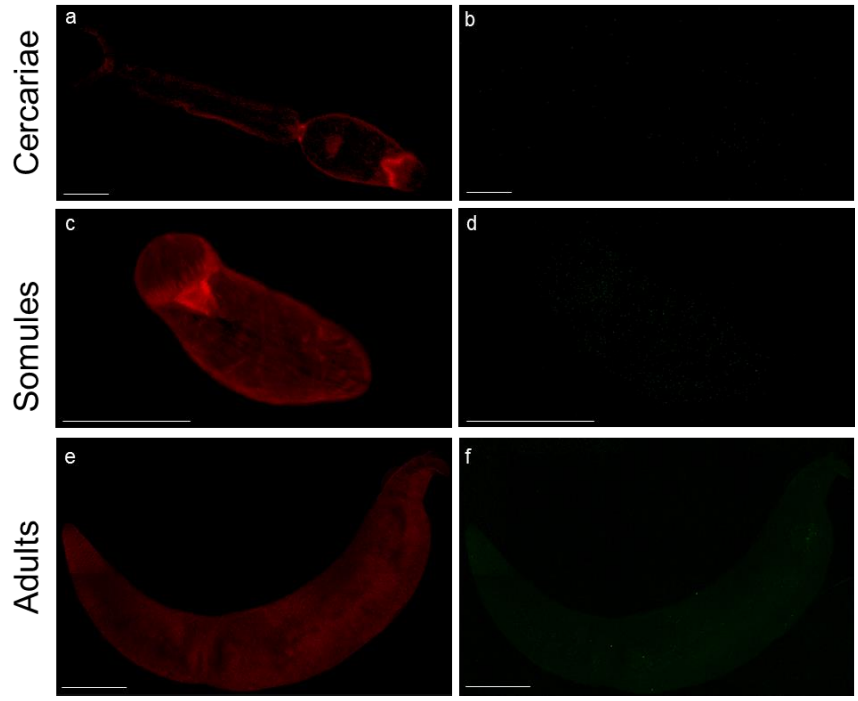

Figure 3.11 **Negative control parasites display little non-specific binding of the secondary antibody.** The red channel **(a, c, e)** is visible as rhodamine phalloidin binds directly to actin, whereas the Alexafluor 488 secondary antibodies (green) bind to the primary antibody only. There is no background non-specific binding of this antibody to either parasite life stage **(b, d, f)**. Laser levels for all subsequent confocal microscopy were set according to those employed for negative control scans. Bars: 50 µm except e-f, 200 µm.

3.5.1 Immunohistochemistry of Akt in cercariae

Freshly shed, actively swimming cercariae were immediately fixed and processed for immunohistochemistry. Activated Akt was particularly found in the nervous system of the head region and could also be seen localised to distinctive punctate regions along the tail (Figure 3.12 a-c). In individual 'z' sections, these latter spots of activation appeared in pairs, progressing towards the tail furcae as demonstrated in adjacent z-sections (Chapter 6, section 6.1). This activated Akt could signify the presence of sensory receptors in the tail, possibly important in host invasion and/or cercarial locomotion. The presence of Akt in the nervous system of the cercariae again indicates a possible sensory function. In several cases, the tail/head junction of the cercariae displayed activated Akt, as did the oral tip. Anti-Akt antibodies used to label total Akt expression

(Figure 3.12 d-f), revealed additional expression, particularly at the oral tip which presented as six individual structures, shaped in a circle around the tip; Akt here is not active as the structures were not seen with anti-phospho Akt antibodies.

3.5.2 Immunohistochemistry of Akt in somules

When stained with anti-phospho Akt (Thr^{308}) antibodies, 24 h *in vitro* cultured somules showed activated Akt at the tegument and underlying musculature, and more general staining of the pre-acetabular glands within the parasite (Figure 3.12 g-i). Interestingly, 24 h 'somules' retaining tails that had not detached (Figure 3.12 g), showed less Akt activation in the tails when compared to cercariae, indicating a potential importance of Akt in swimming/host location. Somules stained with the anti-Akt antibodies (Figure 3.12 j-l) showed a similar general Akt localisation profile at the parasite surface and musculature, with additional signal noted particularly associated with the pre-acetabular glands (Figure 3.12 k-l) and concentrated sub-tegumental regions, identified possibly as cytons (Figure 3.12 j). Cytons are cell bodies that lie within the parenchyma and are connected to the tegument by cytoplasmic tubules (Skelly and Shoemaker, 2000).

3.5.3 Immunohistochemistry of Akt in adult worms

Adult worms were processed with all three antibodies, anti-phospho Akt (Thr^{308}) (Figure 3.13), anti-phospho Akt (Tyr^{315}) (Figure 3.14) and anti-Akt (Figure 3.15). Staining with the anti-phospho Akt (Thr^{308}) antibodies resulted in highly detailed adult worm images, with phosphorylated Akt present primarily in the tegument, gynaecophoric canal, oesophageal sphincter, and in some cases, the oral sucker. The adult males displayed greater activated Akt levels than female worms, which in turn showed little activated Akt except in the oesophageal sphincter (Figure 3.13 c). Deep scanning of the female worms also revealed no phosphorylated Akt signal at laser levels appropriate for Akt detection in male worms. Immunolocalisation using anti-phospho-Akt (Tyr^{315}) or anti-Akt antibodies revealed a similar overall distribution to the anti-phospho-Akt (Thr^{308}) antibodies, although the anti phospho-Akt (Tyr^{315}) antibodies produced a generally weaker signal. When stained with anti-Akt antibodies, there were no additional locations of Akt compared with the two anti-phospho antibodies, suggesting that the Akt is predominantly located in these areas in adult worms regardless of phosphorylation status.

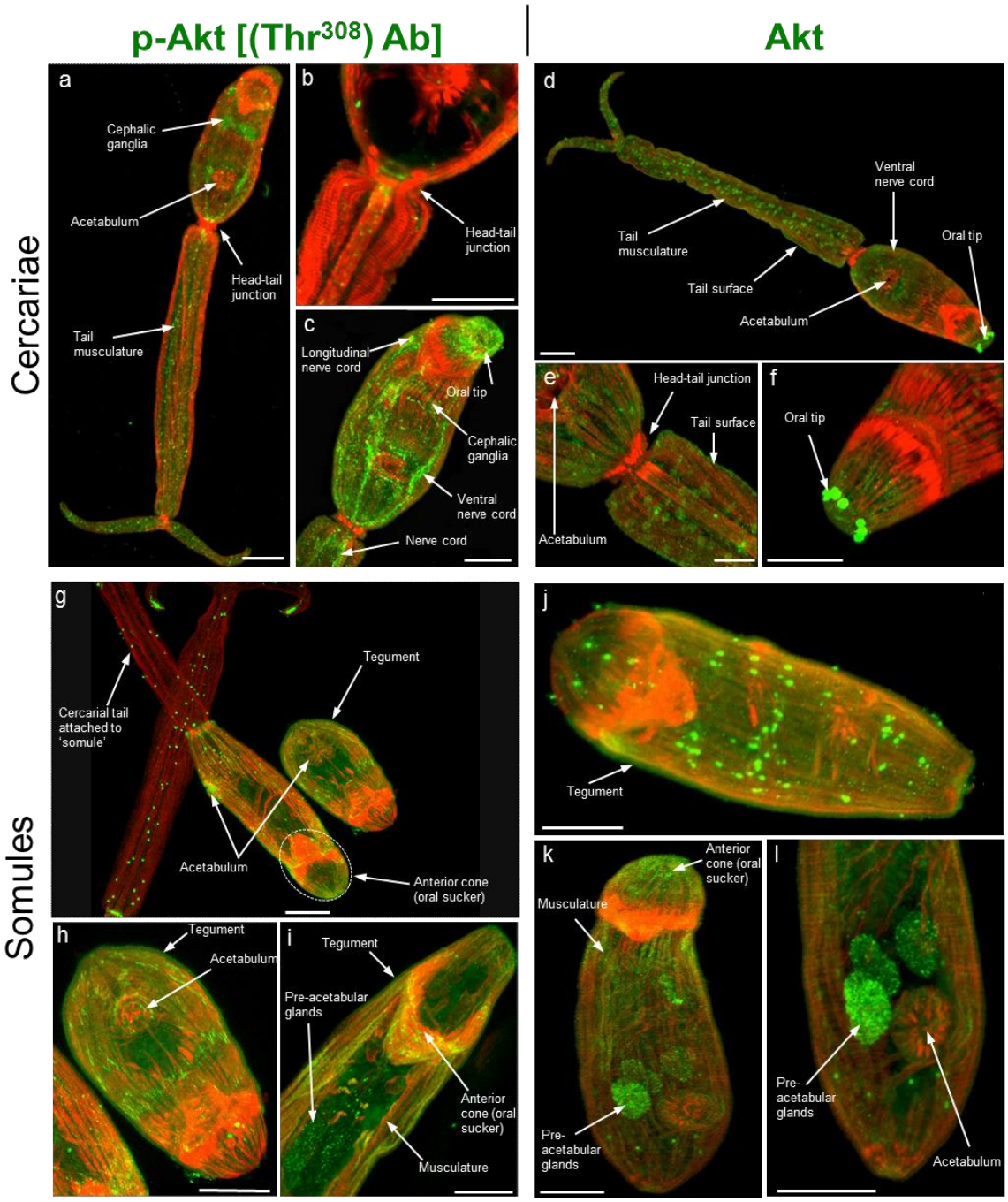

Figure 3.12 **Immunolocalisation of Akt and phosphorylated Akt in cercariae and somules. (a-c)** Anti-phospho Akt (Thr^{308}) antibodies (Ab) reveal phosphorylated Akt (p-Akt) throughout the nervous system, head-tail junction and at the parasite surface of the oral tip. 'Spotting' along the length of the tail could indicate sensory receptors. **(d-f)** Total Akt staining with anti-Akt Ab in cercariae reveals the same pattern of Akt localisation in the tail and additionally shows brightly stained structures at the oral tip, not seen with phospho-Akt Ab. **(g-i)** Somules stained with anti-phospho Akt (Thr^{308}) Ab reveal a relatively high presence of p-Akt at the parasite surface and underlying musculature compared to cercariae. **(j-l)** Total Akt staining of somules with anti-Akt Ab reveals non-phosphorylated Akt in the pre-acetabular glands and in the tegument in the form of spots, possibly cytons. Rhodamine phalloidin was used to stain filamentous actin (red), all images are maximum projections with the exception of **(b)** and **(l)**. Scale bars = 25 µm.

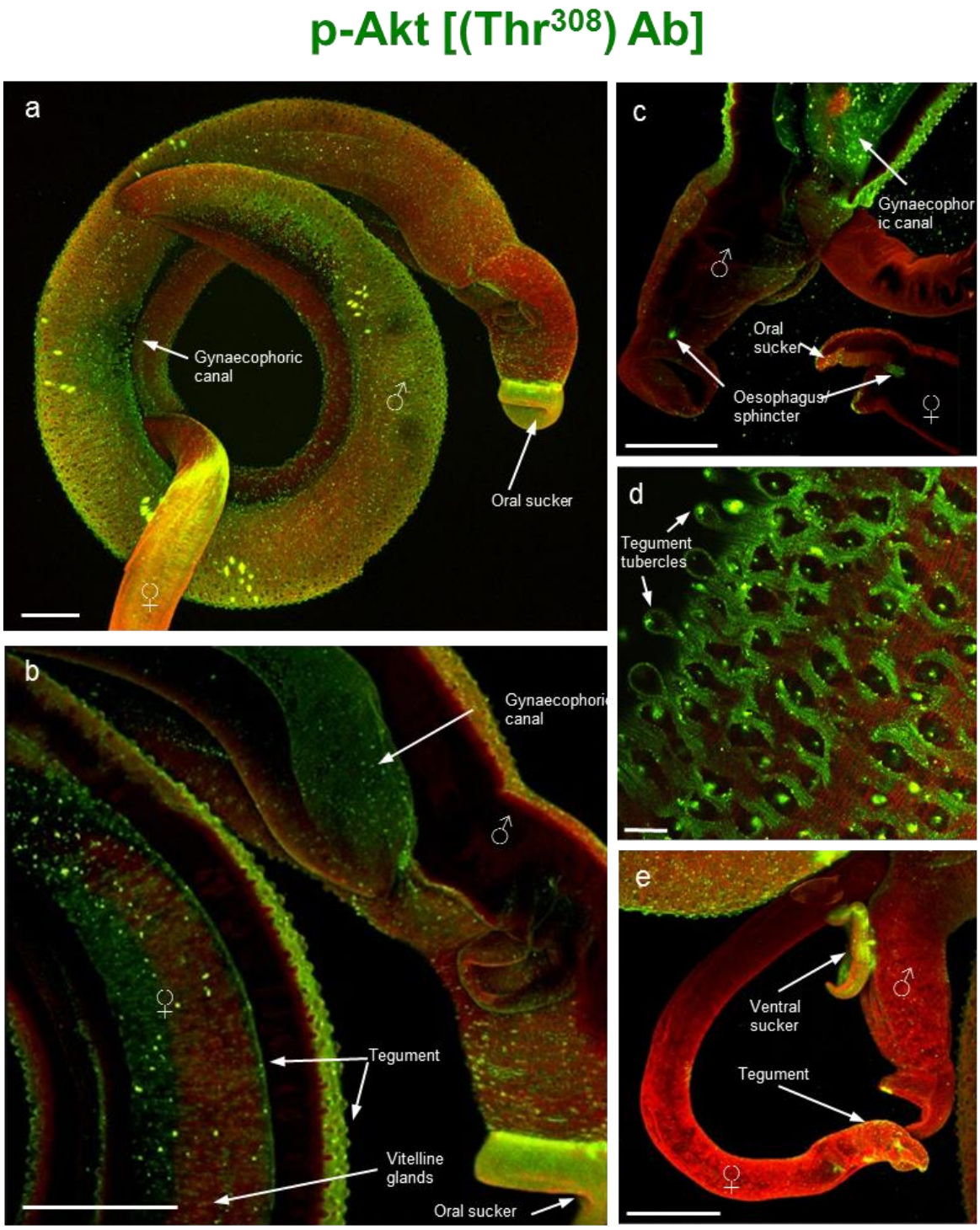

***Figure 3.13 In situ* immunolocalization of phosphorylated (activated) Akt in intact *S. mansoni* adults.** Adult worm pairs were fixed and incubated with anti-phospho Akt (Thr^{308}) **(a-e)** followed by Alexa Fluor 488 secondary Ab (green); specimens were also stained with rhodamine phalloidin to reveal actin filaments (red)**.** All images are of z-axis projections displayed in maximum pixel brightness mode except **(d)** which is derived from a single surface scan. **(a)** Whole male and female worms in copula; **(b-e)** detailed scanning of activated Akt and total Akt in worms. Bar: 200 µm, except **d** = 20 µm.

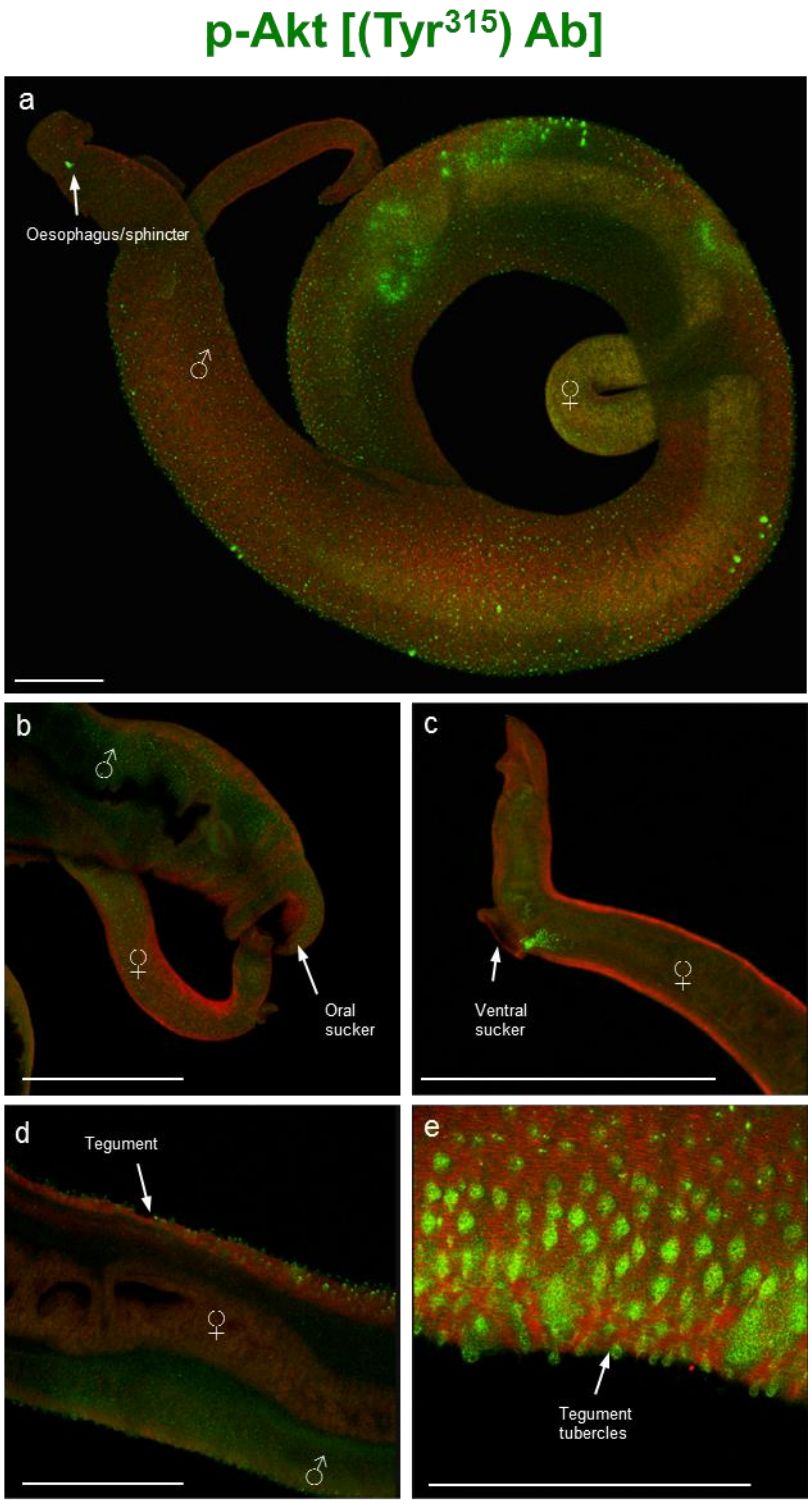

***Figure 3.14 In situ* immunolocalization of phosphorylated (activated) Akt in intact *S. mansoni* adults.** Adult worm pairs were fixed and incubated with anti-phospho Akt (Tyr^{315}) **(a-e)** primary antibodies (Ab) followed by Alexa Fluor 488 secondary Ab (green); specimens were also stained with rhodamine phalloidin to reveal actin filaments (red)**.** All images are of z-axis projections displayed in maximum pixel brightness mode. **(a)** Whole male and female worms in copula; **(b-e)** detailed scanning of activated Akt and total Akt in worms. Bar: 300 µm.

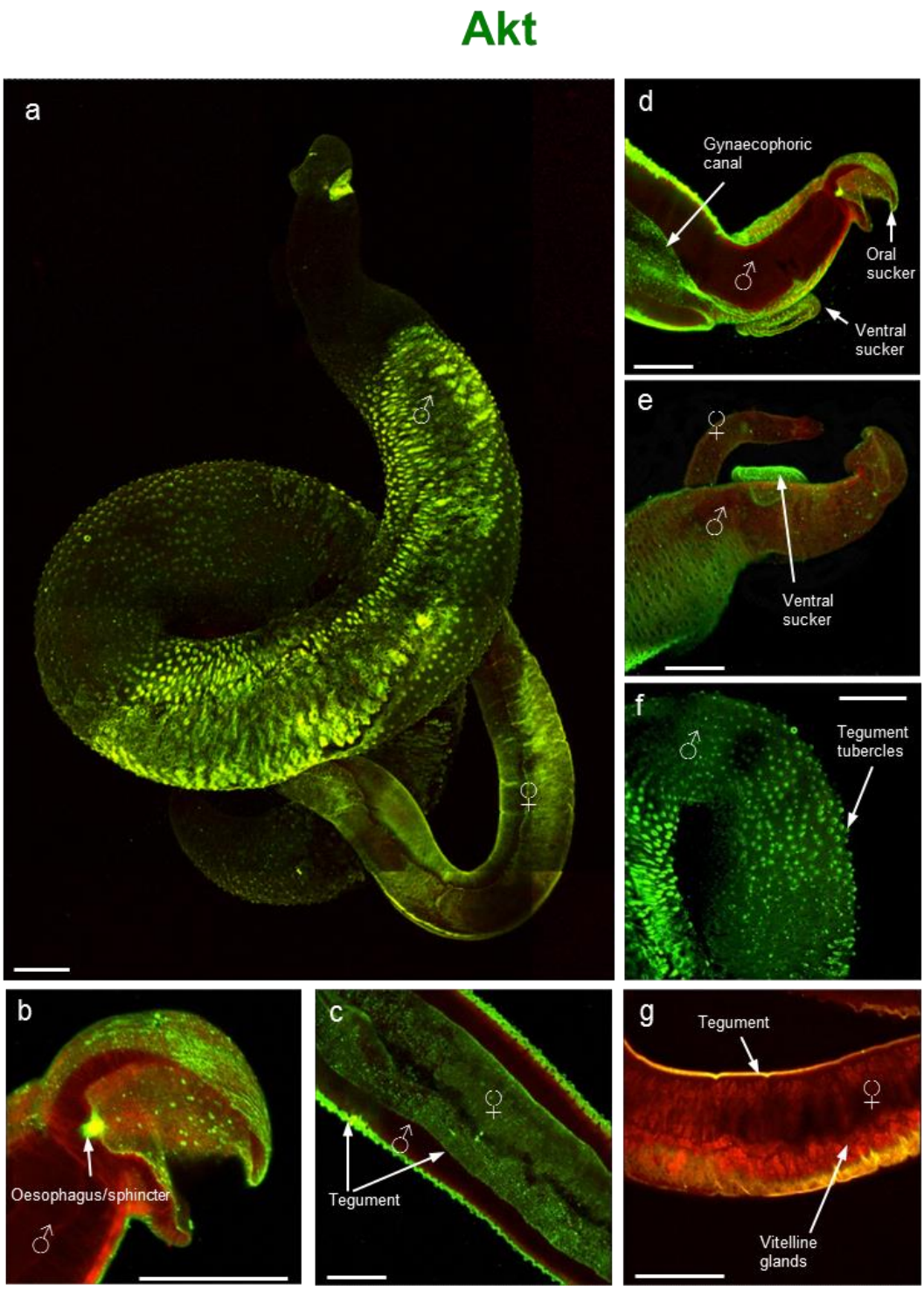

***Figure 3.15 In situ* immunolocalization of total Akt in intact *S. mansoni* adults.** Adult worm pairs were fixed and incubated with anti-Akt primary antibodies (Ab) **(a-g)** followed by Alexa Fluor 488 secondary Ab (green); specimens were also stained with rhodamine phalloidin to reveal actin filaments (red)**.** All images are of z-axis projections displayed in maximum pixel brightness mode. **(a)** Whole male and female worms in copula; **(b-g)** detailed scanning of total Akt in worms. Bar: 200 µm.

3.6 Effect of Human Host Factors and Other Agents on *S. mansoni* Akt Phosphorylation

When *S. mansoni* enters the skin of the human host it will encounter for the first time in its life cycle blood factors and other molecules that might stimulate Akt signalling in the parasite. Somules were therefore transformed mechanically and cultured overnight in BME only. They were then exposed to serum, insulin, or L-arginine for increasing durations, or the chemical compound SC-79. Proteins were extracted and processed for western blotting to ascertain whether these components stimulated Akt phosphorylation (activation) in the somules.

3.6.1 Effect of serum on S. mansoni *Akt phosphorylation*

Treatment of somules with human serum was investigated with the rationale that Akt phosphorylation may increase upon exposure. Initial results showed that serum treatment resulted in increased Akt phosphorylation (activation) at 5 and 10 min declining to below basal levels at 30 min (Figure 3.16). However, subsequent experiments with serum revealed that in many cases, the anti-phospho Akt (Thr^{308}) antibody bound to a human serum component resulting in a double-band effect making interpretation difficult; human serum alone also reacted with anti-phospho Akt (Thr^{308}) antibodies (data not shown). Thus future experiments focused on better-defined stimulants.

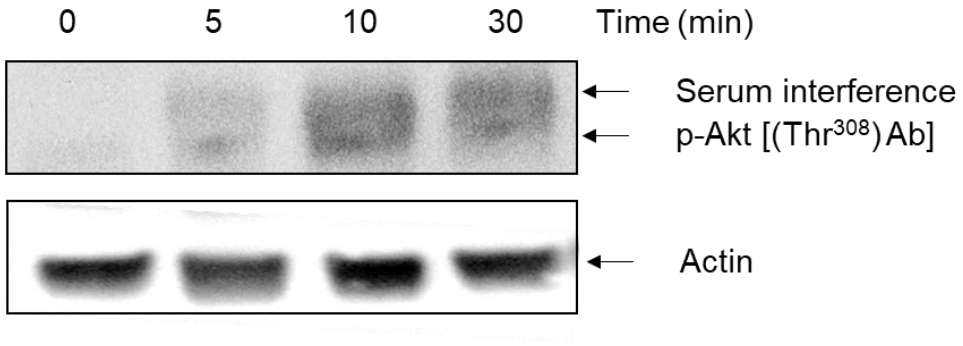

Figure 3.16 **Serum treatment induces Akt activation in *S. mansoni* somules at 5-10 min.** 24 h somules (~1000) were treated with 10% human serum at 37 °C, 5% CO_2 for the times indicated. Protein samples were processed for western blotting with anti-phospho Akt (Thr^{308}) antibodies, then stripped and re-probed with anti-actin antibodies to determine protein loading between lanes. Above blot is representative of 5 blots.

3.6.2 Effect of insulin on S. mansoni *Akt phosphorylation*

Given that insulin receptors exist in *S. mansoni* (Kayath *et al.*, 2007; Vanderstraete *et al.*, 2013) and that in humans Akt is modulated by insulin signalling (Alessi *et al.*, 1996a), the effect of insulin on Akt activation in *S. mansoni* somules was explored. *In vitro* transformed somules were treated with insulin (bovine; 1 µM) and somule extracts blotted with anti-phospho Akt (Thr^{308}) antibodies. Although somewhat variable between individual experiments, analysis of blots revealed that over several replicates, 10 min insulin treatment increased Akt phosphorylation by 43% (p≤0.001) when compared to 0

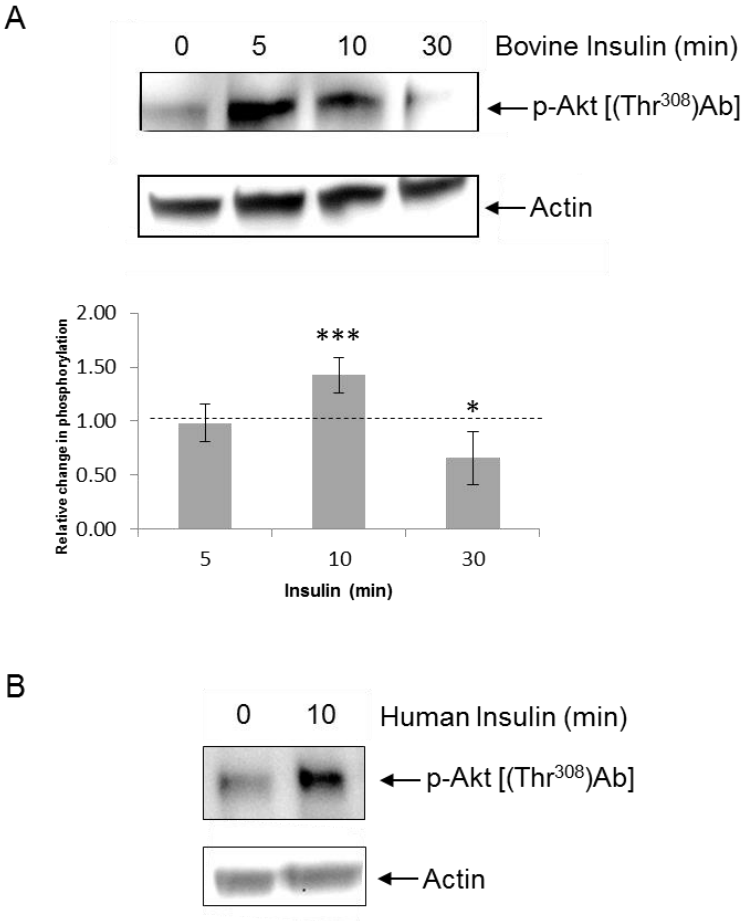

Figure 3.17 **Exogenous insulin activates Akt in intact *S. mansoni*. A.** Somules (~1000) were treated with 1 µM recombinant bovine insulin for the indicated durations and protein samples processed for western blotting with anti-phospho Akt (Thr^{308}) antibodies. Blots were then stripped and re-probed with anti-actin antibodies to determine protein loading in each lane**.** Immunoreactive bands from seven independent experiments were analysed for mean intensity (±S.D.; n=5) using GeneTools and the change in phosphorylation calculated relative to phosphorylation levels of controls (0) that were assigned a value of 1 (also shown as dotted line). *p≤0.05, and ***p≤0.001 (ANOVA). **B.** Somules (~1000) were treated with 1 µM human insulin for 10 min and protein samples processed for western blotting with anti-phospho Akt (Thr^{308}) antibodies. Blots were then stripped and re-probed with anti-actin antibodies to determine protein loading in each lane. The blot in B is representative of those from four independent experiments.

min controls (Figure 3.17 A). Across four blots, similar results (47% increase) were obtained for human insulin at the same concentration (Figure 3.17 B).

3.6.3 Effects of L-arginine on S. mansoni *Akt phosphorylation*

Skin lipids have long been known to stimulate the penetration of host skin by cercariae (Stirewalt, 1971) with the amino acid L-arginine being specifically recognised as a factor by Granzer and Haas (1986). More recently, L-arginine has been shown to stimulate SmVKRs expressed in *Xenopus* oocytes (Gouignard *et al.*, 2012). Thus to investigate if L-arginine modulated Akt activation in *S. mansoni*, somules were exposed to this amino acid at the same concentration (100 µM) as used by Gouignard *et al.* (2012) for increasing durations similar to those for insulin (Figure 3.18). L-arginine exposure resulted in an increase in somule Akt phosphorylation, culminating with a significant 1.84 fold increase compared to the control at 30 min ($p \leq 0.001$). Over several experiments, L-arginine produced a stronger and more reproducible stimulation than insulin. Consequently, for further experiments, insulin and L-arginine were used concurrently,

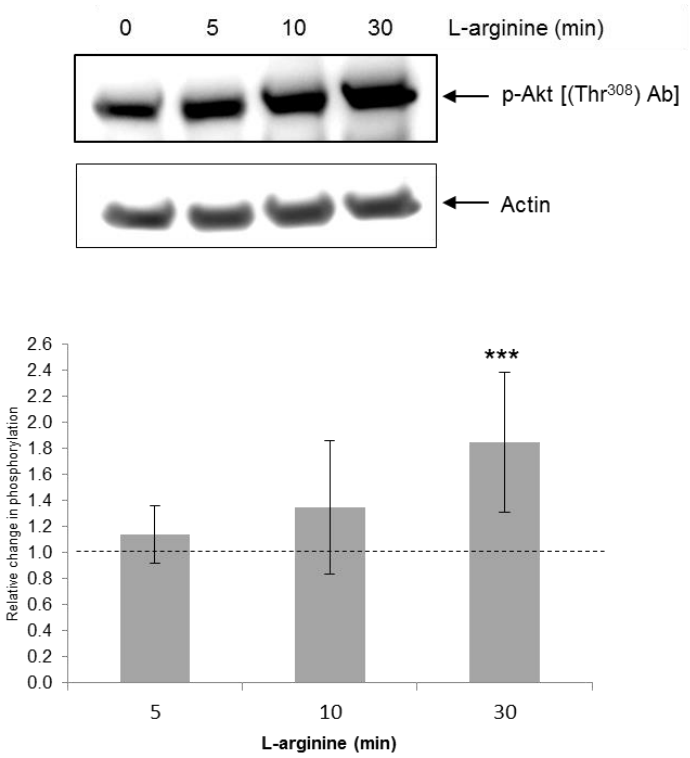

Figure 3.18 **L-arginine activates Akt in *S. mansoni* somules.** **A.** Somules (~1000) were treated with 100 µM L-arginine for increasing durations and samples were processed for western blotting with anti-phospho Akt (Thr^{308}) antibodies. Membranes were stripped and re-probed with anti-actin antibodies to determine protein loading. **B.** Immunoreactive bands from three independent experiments were analysed for mean intensity (±S.D.; n=7) using GeneTools and the change in phosphorylation calculated relative to phosphorylation levels of controls (0) that were assigned a value of 1 (also shown as dotted line). ***$p \leq 0.001$ (ANOVA).

with the nature of the experiment dictating the preferred stimulator. For example, L-arginine, being a skin surface component, was more appropriate in experiments involving cercariae (Chapter 6) whereas insulin was preferentially used in somule and adult worm studies.

3.6.4 Effect of alternative Akt pathway stimulators on S. mansoni *Akt*

As well as serum, insulin and L-arginine, a relatively new Akt stimulator, SC79, was tested, with little effect seen on Akt phosphorylation (Figure 3.19). SC79 was first reported as a specific Akt stimulant by Jo *et al.* (2012). Originally screening for Akt inhibitors, Jo *et al.* discovered that while SC79 suppresses Akt plasma membrane translocation, it also simultaneously enhances cytosolic Akt phosphorylation. Phosphorylation of both the Thr^{308} and Ser^{473} residues was increased and activation was demonstrated in cells both with and without serum treatment, indicating a strong level of stimulation (Jo *et al.*, 2012). However, as shown in Figure 3.19, there was no evidence of increased Akt phosphorylation in *S. mansoni* somules until used at 100 µM, but this was found to be non-reproducible in subsequent experiments.

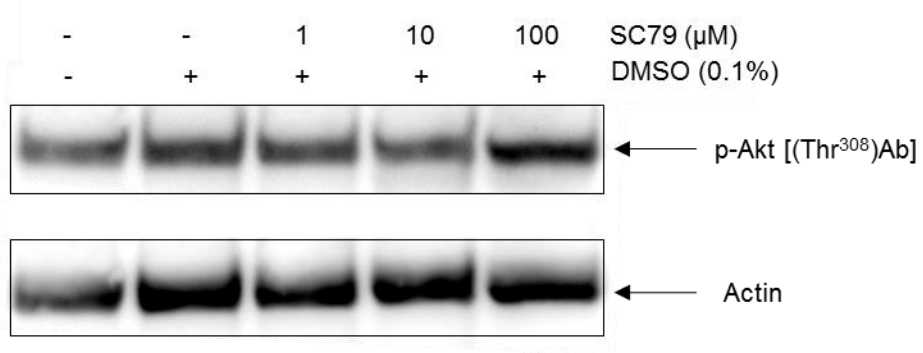

Figure 3.19 **SC79 does not consistently stimulate *S. mansoni* Akt.** 24 h somules (~1000) were treated for 2 h with SC79 (1µM, 10 µM and 100 µM) or DMSO (vehicle, control) at 37 °C, 5% CO_2. Samples were processed for western blotting with anti-phospho Akt (Thr^{308}) antibodies, then membranes were stripped and re-probed with anti-actin antibodies to confirm similar protein loading between lanes.

3.7 The Effects of Akt Pathway Inhibitors on *S. mansoni* Akt Phosphorylation

3.7.1 The effect of LY294002 on S. mansoni *Akt phosphorylation*

In total, four inhibitors of the Akt pathway were tested: LY294002, GSK2334470, Akt Inhibitor X and Herbimycin A. LY294002 is a specific phosphatidylinositol 3-kinase (PI3K) inhibitor, reported to prevent PI3K activity with an IC_{50} value of 1.4 µM in human and rabbit cells (Vlahos *et al.*, 1994). During *in vitro* experiments with live somules, LY294002

did not consistently block phosphorylation of Akt at the concentrations used (1 μM, 10 μM and 50 μM) after 3 h pre-incubation (Figure 3.20). After actin equalisation, no significant change in Akt phosphorylation (activation) could be determined. This experiment was conducted prior to the discontinuation of serum as a stimulator, hence the double band is apparent as discussed earlier (Section 3.5.1).

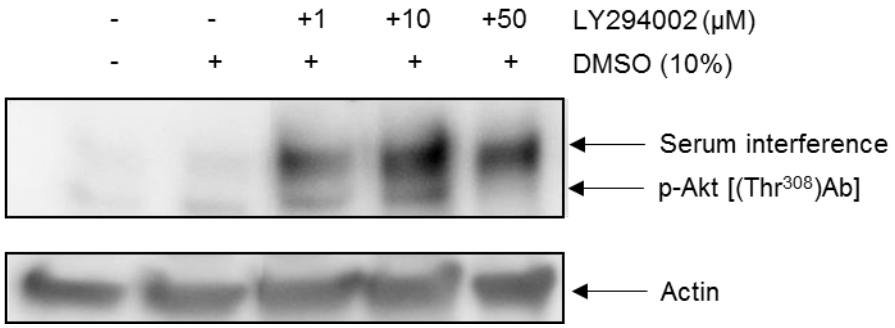

Figure 3.20 **LY294002 shows inconsistent inhibition of *S. mansoni* Akt.** Somules (~1000) were incubated for 180 min at 37°C with 1 μM, 10 μM or 50 μM LY294002 then exposed to 10% human serum for 10 min. Somules were processed for western blotting with anti-phospho Akt (Thr^{308}) monoclonal antibodies. Membranes were stripped and re-probed with anti-actin antibodies to determine protein loading differences between lanes.

3.7.2 The effect of GSK2334470 on S. mansoni *Akt phosphorylation*

GSK2334470 is a specific PDK1 inhibitor (Najafov *et al.*, 2011). PDK1 activates Akt by phosphorylating the Thr^{308} residue in the activation loop, in keeping with 22 other AGC kinases, which are also phosphorylated on a serine/threonine residue in the activation loop (Mora *et al.*, 2004). GSK2334470 was incubated with somules at three concentrations, initially for 1 h. When this yielded no inhibition, incubation was increased to 2 h. Although there was variability between experiments, analysis of blots revealed that over three experiments, a significant decrease ($p \leq 0.05$) in Akt phosphorylation (activation) was observed after 2 h treatment with 20 μM GSK2334470.

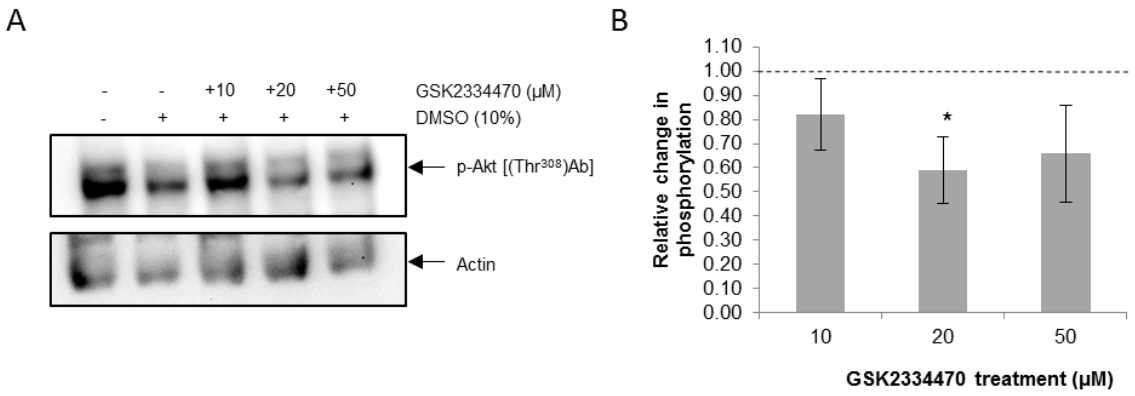

***Figure 3.21* GSK2334470 shows moderate inhibition of *S. mansoni* Akt. A.** Somules (~1000) were incubated for 120 min at 37°C with 10 μM, 20 μM or 50 μM GSK2334470, DMSO (vehicle), or not (-) then stimulated for 10 min with 1 μM human insulin. Parasites were processed for western blotting with anti-phospho Akt (Thr^{308}) antibodies. Membranes were stripped and re-probed with anti-actin antibodies to determine protein loading. **B.** Immunoreactive bands were analysed and mean intensity (±S.D.; n=3) determined using GeneTools and the change in phosphorylation calculated relative to phosphorylation levels of controls (-) that were assigned a value of 1 (also shown as dotted line). *p≤0.05 (ANOVA).

3.7.3 The effect of Akt Inhibitor X on S. mansoni *Akt phosphorylation*

Despite the decreased Akt phosphorylation achieved with GSK2334470, trials with this inhibitor were halted when greater efficiency and consistency of inhibition was found with Akt Inhibitor X. In contrast to LY294002 and GSK2334470, which inhibit kinases upstream of Akt, Akt Inhibitor X directly inhibits the Akt protein. Akt Inhibitor X was first used in *S. mansoni* by Morel *et al.* (2014a) who showed that, among other inhibitors, Akt Inhibitor X reduced the pairing and egg laying capabilities of adult worms *in vitro*. Morel *et al.* also demonstrated a 100% reduction of germinal vesicle breakdown (GVBD) in constitutively active mutant SmAkt L_{150}R expressing *Xenopus* oocytes after treatment with 5 μM Akt inhibitor X for 15 h.

As no data was available regarding the efficacy of Akt inhibitor X towards *S. mansoni* Akt in intact parasites, a dose response was performed. Live somules were treated with increasing concentrations (1 μM - 50 μM) of Akt Inhibitor X for 1 h then treated for 10 min with 1 μM human insulin. Blots were probed with both anti-phospho Akt (Thr^{308}) and (Tyr^{315}) antibodies. Incubation of somules with 50 μM Akt Inhibitor X for 1 h significantly reduced the phosphorylation of Akt following insulin stimulation (p≤0.01), although clearer inhibition was observed at 10 μM over multiple experiments when probed with anti-phospho Akt (Tyr^{315}) antibodies (Figure 3.22). At 50 μM, Akt inhibitor X reduced mean Akt phosphorylation by 34% and 46% when detected with anti-phospho Akt (Thr^{308}) and (Tyr^{315}) antibodies, respectively. The subtle difference in mean levels of inhibition detected by the two antibodies is possibly due to the different routes by which

each antibody target residue is phosphorylated; Tyr^{315} being activated by Src (Chen *et al.*, 2001) compared with the Thr^{308} residue which is activated by PDK1 (Alessi *et al.*, 1997).

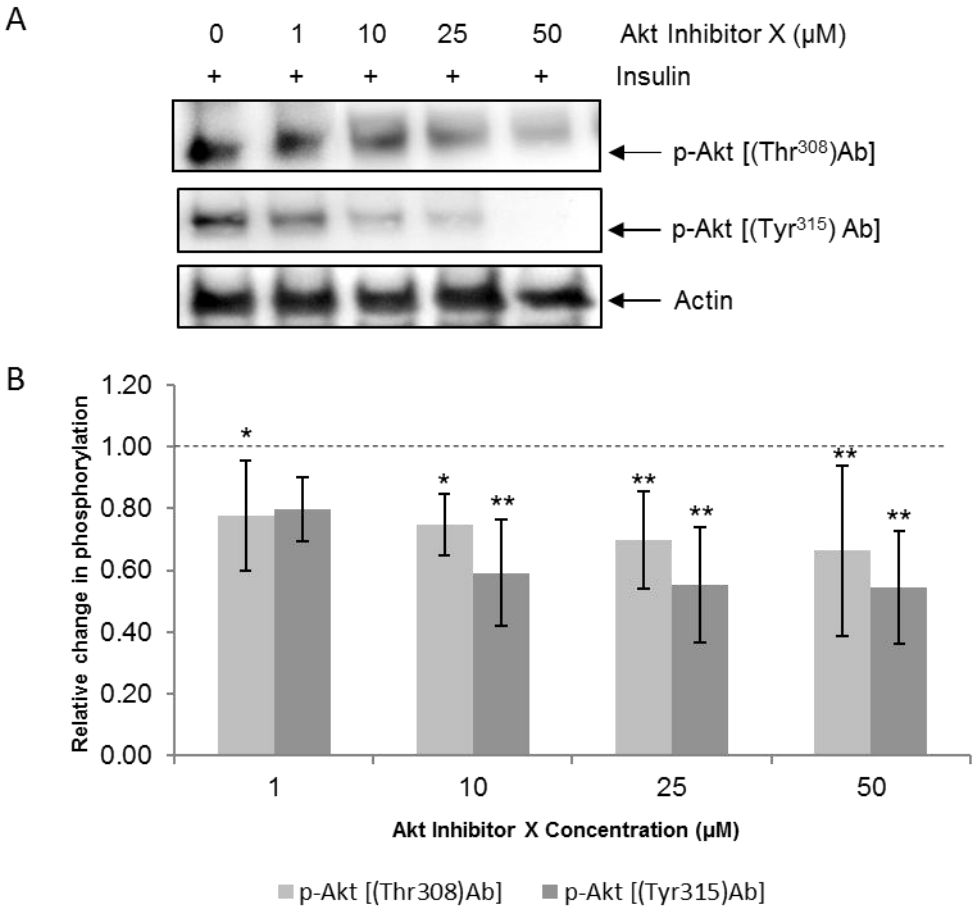

Figure 3.22 **Akt Inhibitor X blocks Akt activation in *S. mansoni* somules. A.** Somules (~1000) were incubated for 1 h at 37°C with Akt Inhibitor X at four different concentrations, then for 10 min with 1 μM human insulin. Parasites were processed for western blotting with anti-phospho Akt (Thr^{308}) or (Tyr^{315}) antibodies. Blots were then stripped and re-probed with anti-actin antibodies to determine protein loading. **B.** Immunoreactive bands were analysed for mean intensity (±S.D.; n≥3) using GeneTools and the change in phosphorylation calculated relative to phosphorylation levels of controls (0) that were assigned a value of 1 (also shown as dotted line). *p≤0.05, **p≤0.01 (ANOVA).

3.7.4 Effect of Herbimycin A on S. mansoni *Akt phosphorylation*

Herbimycin A is a selective Src inhibitor. Given that Src phosphorylates the Tyr^{315} residue in human Akt, herbimycin was employed to assess its effects on *S. mansoni* Akt activation using anti-phospho Akt (Tyr^{315}) antibodies. This inhibitor was previously used

in schistosomes to suppress mitotic activity in adult female worms (Knobloch *et al.*, 2006).

Herbimycin A was used at 12 µM as this is its IC_{50} value (Knobloch *et al.*, 2006). Somules were incubated for increasing durations (30 - to 120 min) with the inhibitor, then stimulated for 10 min with human insulin. Similar to Akt Inhibitor X, herbimycin A significantly decreased phosphorylation of Akt following stimulation with human insulin (Figure 3.23). After 120 min, mean phosphorylation levels were reduced by 27% compared to the control samples ($p \leq 0.01$) (Figure 3.23). This implicates Src as the upstream kinase responsible for phosphorylation of Tyr^{408} in *S. mansoni*.

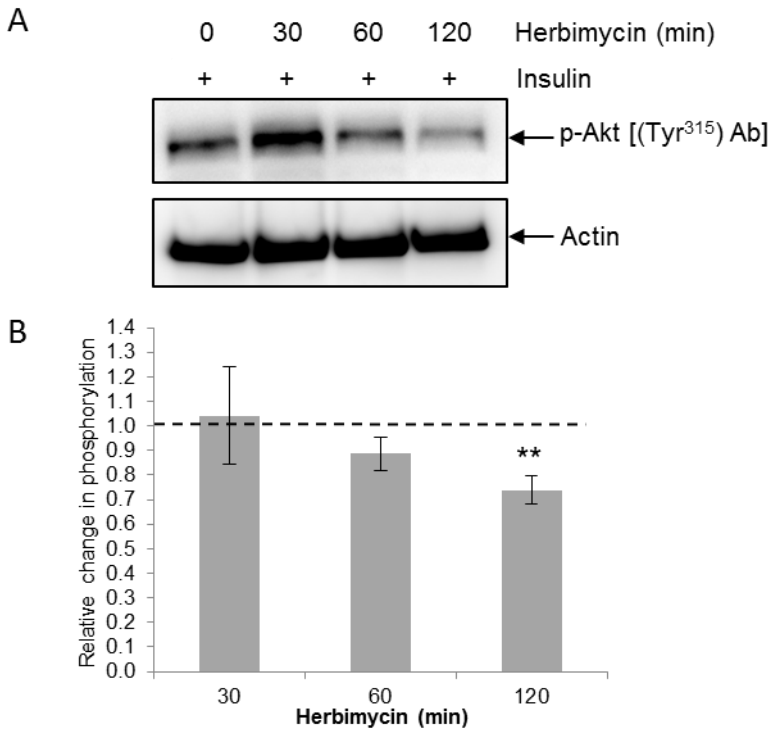

Figure 3.23 **Herbimycin A inhibits Tyr^{315} phosphorylation in S. mansoni somules, implicating Src as an upstream kinase. A.** Somules (~1000) were incubated for 30 min, 60 min, or 120 min at 37°C with 12 µM herbimycin A, then 10 min with human insulin. Parasites were processed for western blotting with anti-phospho Akt (Tyr^{315}) antibodies. Membranes were stripped and re-probed with anti-actin antibodies to determine protein loading. **B.** Immunoreactive bands were analysed for mean intensity (±S.D.; n=3) using GeneTools and the change in phosphorylation calculated relative to phosphorylation levels of controls (0) that were assigned a value of 1 (also shown as dotted line). **p≤0.01 (ANOVA).

Summary

This chapter reports the validation of three antibodies for studying Akt in *S. mansoni*. Anti-phospho Akt (Thr^{308}) and (Tyr^{315}) antibodies and the anti-Akt antibodies all recognise the same molecular weight *S. mansoni* Akt-like protein at ~52 kDa, across cercariae, somules and adult worms. Reciprocal immunoprecipitation experiments confirmed that each of the antibodies was binding the same protein target at ~52 kDa and Akt activity assays revealed that the immunoprecipitated protein possessed Akt-like activity. RNAi (employing siRNA) of the predicted *S. mansoni* gene was successfully performed and western blotting with anti-Akt antibodies revealed an 84% Akt knockdown in adult worms.

Immunolocalisation studies across the different *S. mansoni* life-stages revealed where Akt is present in the parasite and where it is activated. Phosphorylated (activated) Akt was predominantly present in the tegument and tubercles of the adult worms but also in the tegument of somules. Other notable areas of phosphorylated Akt were the cercariae nervous system and oral tip, the preacetabular glands and cytons in somules, and the gynaecophoric canal and oesophageal sphincter in adult worms.

Studies employing host molecules that *S. mansoni* could interact with during infection revealed that insulin and L-arginine stimulated Akt in somules, with maximal activation occurring at 10 min and 30 min, respectively. By far the most effective inhibitor tested was Akt Inhibitor X, which caused a 35% and 42% decrease in Akt phosphorylation when probed with anti p-Akt (Thr^{308}) and anti p-Akt (Tyr^{315}) antibodies, respectively. Herbimycin A also proved to be an efficient inhibitor of Akt activation in somules.

This chapter confirms the presence of an evolutionarily conserved Akt protein in *S. mansoni*, which can be stimulated and inhibited with known mammalian Akt pathway effectors. The level of conservation between *S. mansoni*, *C. elegans*, *D. melanogaster* and human sequences indicates a functionally conserved role for Akt in the parasite, and the response to insulin stimulation raises further possibilities about as yet unknown functions of the protein.

4

Results 2 – Downstream Akt Signalling in *S. mansoni*

Having demonstrated the presence of activated Akt in various *S. mansoni* life stages (Chapter 3) an investigation into putative downstream Akt interacting proteins and substrates was undertaken in an attempt to better understand the biology of the parasite. As discussed in previous chapters, minimal data is available on Akt signalling in *S. mansoni*; this is particularly the case for Akt substrates. Conversely, substrates of Akt in humans have been well characterised and these are involved in diverse cellular processes from metabolism and cell proliferation, to glucose uptake (Manning and Cantley, 2007). By employing Akt substrate antibodies and bioinformatic approaches this chapter aims to map global substrate activity and illuminate putative Akt interactions within the parasite.

4.1 Akt Substrate Localisation in *S. mansoni*

4.1.1 Akt substrate immunoblotting in three life stages

Akt exclusively phosphorylates substrates at Ser/Thr residues and has substrate specificity to proteins that possess an arginine residue at the -5 and -3 positions relative to the Ser/Thr phosphorylation site (i.e. RXRXXS*/T*) (Alessi *et al.*, 1996b). The anti-phospho Akt substrate antibodies used here have preference for Ser/Thr residues preceded by Arg at the -5 and -3 positions, but may also detect motifs containing Arg at only the -3 site; the Ser/Thr residue must also be phosphorylated for detection[6].

To compare the overall profile of Akt substrates in cercariae, somules and adult worms, a western blot was done with samples from all three life-stages, including adult male and female worms individually, as well as an adult pair (Figure 4.1). With the exception of the female worm lane, all other samples contained comparable levels of protein (based on actin immunoreactivity), facilitating comparison between samples. The results indicate that as the parasite develops and matures in the definite host, more putative Akt substrates become phosphorylated (excepting female worms), suggesting that Akt becomes more active in cellular processes. Cercariae displayed less substrate phosphorylation by western blot compared to somules, which in turn had a reduced global phosphorylation when compared with adult worms. Although weaker in total signal, the female worms showed a similar banding pattern to the male worms, with only a few bands absent, notably at ~15 kDa, ~20 kDa and ~45 kDa (Figure 4.1). Additionally, adult worm pairs were treated with increasing concentrations of Akt Inhibitor X for 1 h to monitor the effect of Akt inhibition on the substrate phosphorylation profile (Figure 4.2).

[6] www.cellsignal.com [Accessed: January 13th 2016]

As the concentration of inhibitor increased, many of the substrates displayed weaker phosphorylation despite similar protein levels (based on actin immunoreactivity). This demonstrates that the detectable proteins are sensitive to Akt Inhibitor X, thus supporting that they are Akt substrates.

4.1.2 Immunolocalisation of Akt substrates in cercariae, somules and adult worms

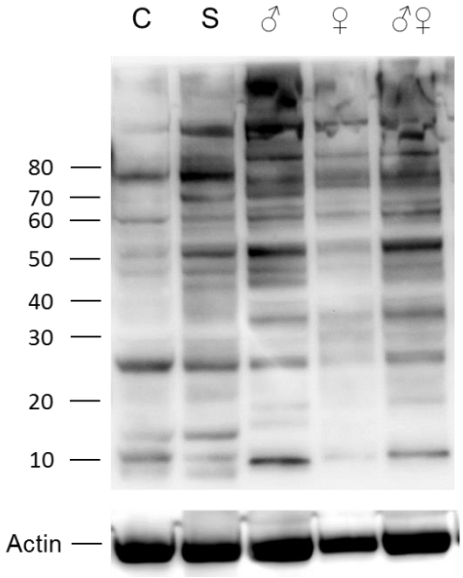

Figure 4.1 **Akt phosphorylates more cellular substrates as *S. mansoni* matures.** Western blotting of the human-infective/resident life stages of *S. mansoni* using anti-Akt substrate antibodies. Lanes contain from left to right; ~1000 cercariae, ~1000 somules, 1 adult male worm, 2 adult female worms and 1 pair of adult worms. The membrane was stripped and re-probed with anti-actin antibodies to determine protein loading.

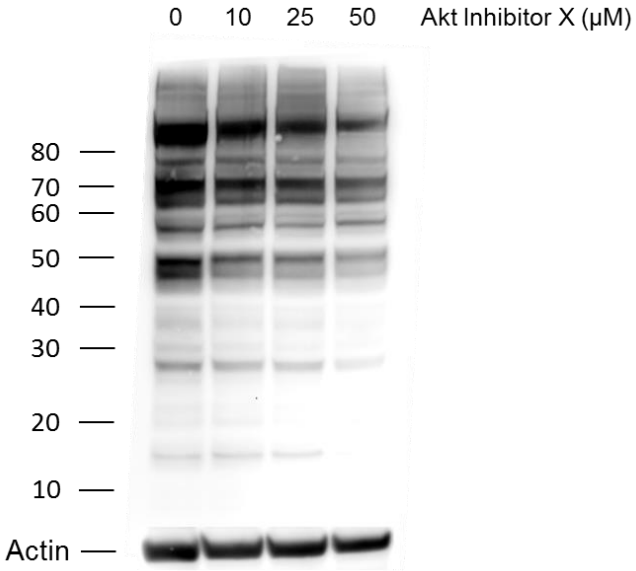

Figure 4.2 **Akt-directed phosphorylation of putative Akt substrates is reduced by Akt Inhibitor X.** Western blotting of *S. mansoni* adult worms (1 pair per lane) using anti-Akt substrate antibodies. Worms 24 h post-perfusion were treated for 1 h with 10, 25 or 50 μM Akt Inhibitor X at 37 °C, 5% CO_2. The membrane was stripped and re-probed with anti-actin antibodies to determine protein loading.

In order to map Akt substrates within the parasite, confocal microscopy was conducted on freshly shed cercariae, *in vitro* cultured (~24 h) somules and adult worms that were processed for immunohistochemistry with anti-phospho Akt substrate antibodies. In cercariae (Figures 4.3 a-c) the nervous system in the head displayed strong immunoreactivity and the pattern of staining observed was similar to that seen with cercariae stained for phosphorylated (activated) Akt (Figure 3.12), with the cephalic ganglia and ventral nerve cords particularly evident. Detailed analysis of individual z-sections revealed that the nervous system of the tail contained phosphorylated Akt substrates and that regions of substrate phosphorylation were also evident towards the tail surface (Figure 4.3 c); such localisation raises the possibility that Akt, and its substrates, are implicated in cercarial movement and possibly host penetration.

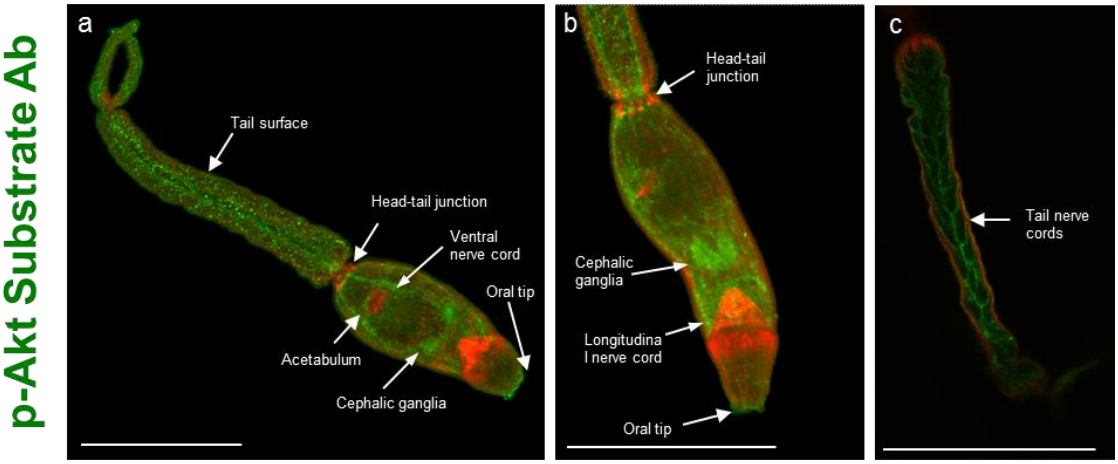

Figure 4.3 **Cercariae display phosphorylated Akt substrates in the nervous system and other anatomical regions.** Freshly shed cercariae were fixed and stained with anti-phospho Akt substrate antibodies (green) and rhodamine phalloidin (red) to reveal filamentous actin and were imaged by confocal microscopy. **(a)** Whole cercariae showing phosphorylated Akt substrates throughout the parasite but particularly at the oral tip, nervous system and tail surface. **(b)** Close-up projection of the head reiterates the substrate phosphorylation in the nervous system, clearly seen in the cephalic ganglia/longitudinal nerve cords. **(c)** A deep tissue scan (single z-section) of the cercaria tail reveals highly specific staining of the tail nerve cords. a, b = maximum projections; bar: 100 µm.

Unlike cercariae, the distribution of phosphorylated Akt substrates in somules was more heterogenous when compared to that of phosphorylated Akt (Figure 4.4 c.f. Figure 3.12). The phosphorylated substrates in somules appeared to be primarily localised internally and the distribution was quite general throughout the parasite (Figure 4.4 a-c). However, deep scanning (Figure 4.4 b) revealed a layer of punctate sub-tegumental staining in addition to a halo of immunoreactivity surrounding the tegument surface. The single 'z'

scan (Figure 4.4 c) revealed the preacetabular gland in the centre of the parasite with slightly greater Akt substrate phosphorylation than the surrounding tissue.

As with cercariae, the overall distribution of phosphorylated Akt substrates in adult worms

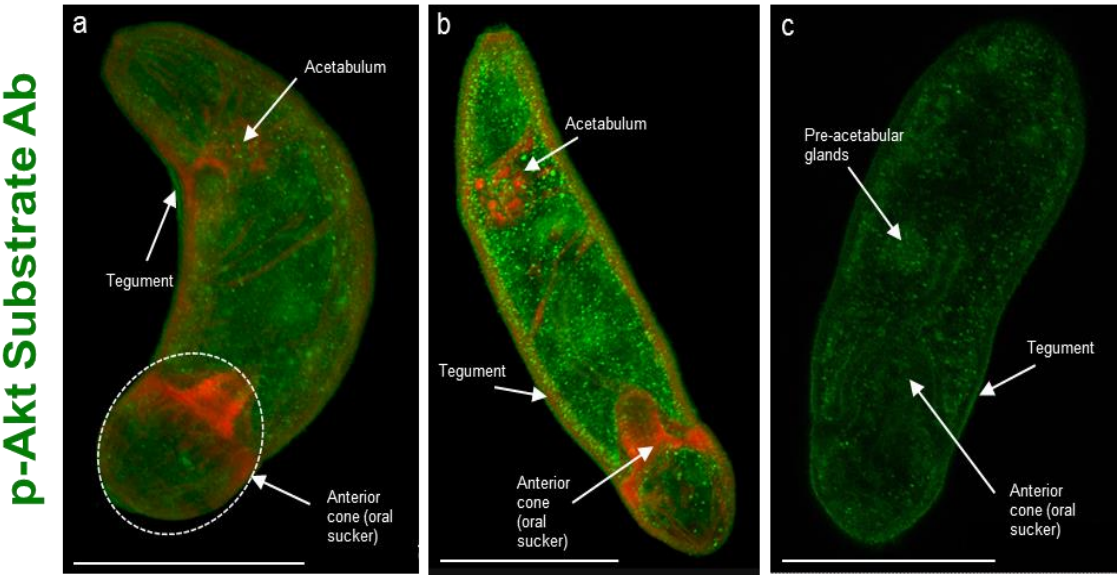

Figure 4.4 **Somules display considerable internal signal for phosphorylated Akt substrates.** 24 h somules were fixed and stained with anti-phospho Akt substrate antibodies (green) and rhodamine phalloidin (red) to reveal filamentous actin, then imaged by confocal microscopy. **(a)** Maximum projection displaying general localisation of phosphorylated Akt substrates within the somule. **(b)** Deep tissue scan of the central portion of a somule illustrating the general localisation of substrate phosphorylation. **(c)** A single z-section through the somule centre showing only the phosphorylated Akt substrates (no actin). Bar: 50 µm.

revealed using anti-phospho Akt substrate antibodies was comparable to that achieved with anti-phospho Akt antibodies. Substrate staining was seen in the tegument tubercles, oral and ventral suckers, and the gynaecophoric canal (Figure 4.5 a-d). The tegument tubercles did not appear to be stained as intensely as with the anti-phospho Akt antibodies (Figures 3.13 and 3.14) although as the two sets of images were captured on different occasions, using different antibodies and with different laser settings, direct comparisons cannot be drawn. One observation that can be made however is the lack of substrate phosphorylation in the presumed oesophageal sphincter (Figure 4.5 c.f.

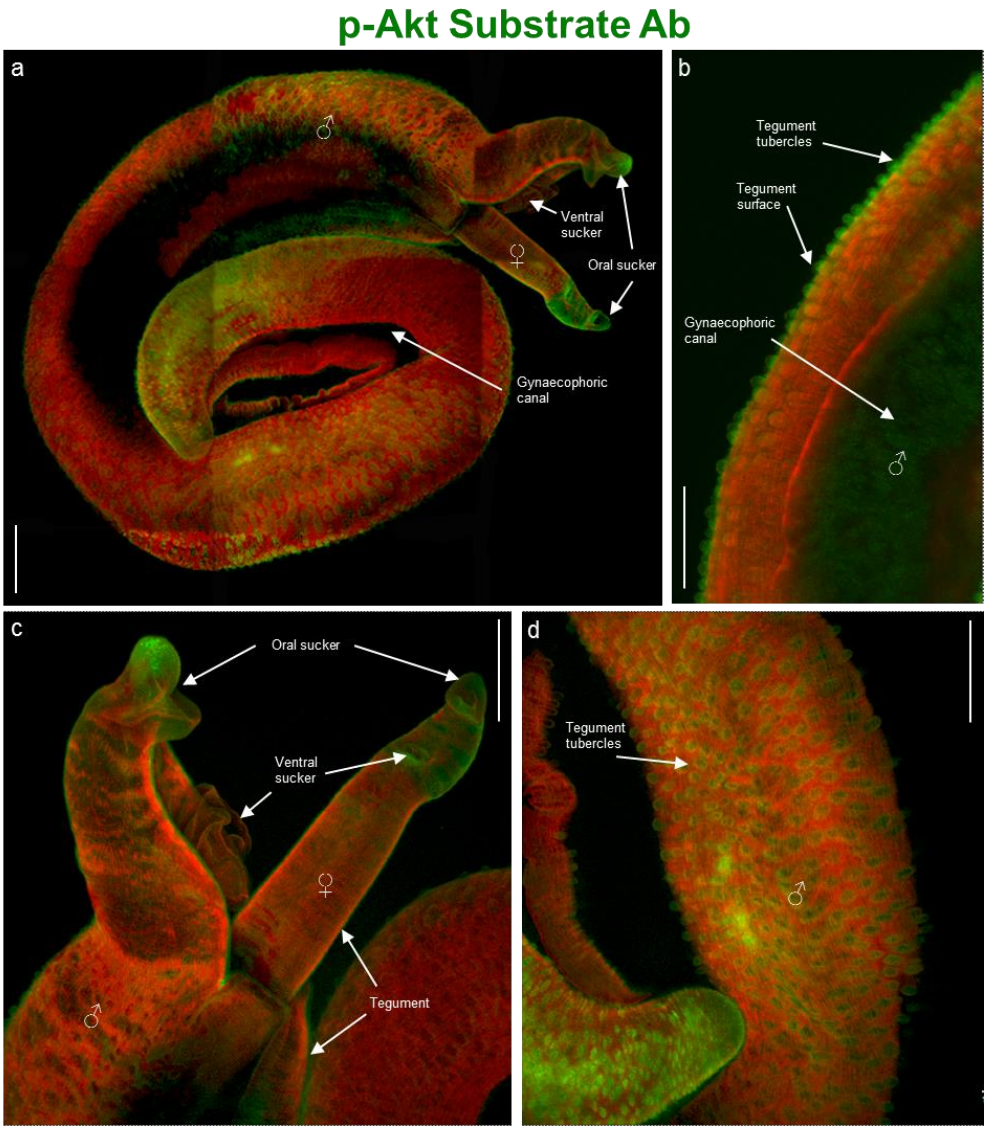

Figure 4.5 **Adult worms display phosphorylated Akt substrates in the tegument.** Approximately 24 h post-perfusion, adult worms were fixed and stained with anti-phospho Akt substrate antibodies (green) and rhodamine phalloidin (red) to reveal filamentous actin, then imaged by confocal microscopy. **(a)** Tiled maximum projection of an adult worm pair showed substrate activity in the tegument and oral suckers of both male and female worms. **(b)** Deep tissue scanning of the male dorsal region revealed phosphorylated Akt substrates localised at the gynaecophoric canal surface and in the tegument tubercles. **(c)** A higher magnification maximum projection of the male and female heads shows in greater detail the substrates in the oral suckers and the 'halo' of substrate phosphorylation at the worm teguments. **(d)** A maximum projection of the male dorsal region revealed specific localisation of phosphorylated Akt substrates to the tegument tubercles. This activity increased towards the tail tip where the tubercles are greater in density. Bars: 150 µm.

Figure 3.13). The female worm displayed phosphorylated Akt substrates in the head region from the ventral sucker upwards towards the tip of the oral sucker (Figure 4.5 a, c). Detailed observations could not be easily made on other features of the female worm as she resided within the male. However, deep scans of the pair revealed little to no

internal substrate staining other than the surface of the gynaecophoric canal (Figure 4.5 b).

4.2 Akt in the *S. mansoni* Genome

When the first version of the *S. mansoni* genome was published (Berriman *et al.*, 2009), the predicted Akt was annotated as being 776 amino acids (aa) long. The current prediction, 586 aa, excludes a sequence encoding gluterodoxin 5 (190 aa) which had been incorrectly included in the original protein prediction (Figure 4.6). The original predicted protein identifier, Smp_073930 was changed to Smp_073930.1 for Akt and Smp_073930.2 for the larger protein that also contained gluterodoxin 5[7]. For approximately 18 months, Akt was removed from GeneDB and NCBI. When relisted, it had a new identifier, Smp_243630. The functional protein association network analysis tool, STRING, was used to predict interactions between Akt and other *S. mansoni* proteins. However, at the time of analysis (Spring 2016) and writing (Summer 2017) the STRING database only contained the larger Smp_073930.2. Therefore, any proteins identified in the STRING interaction map that were exclusively interacting with gluterodoxin 5 were manually removed; only two proteins were predicted to be interactors with gluterodoxin 5, Smp_012050 and Smp_139630.

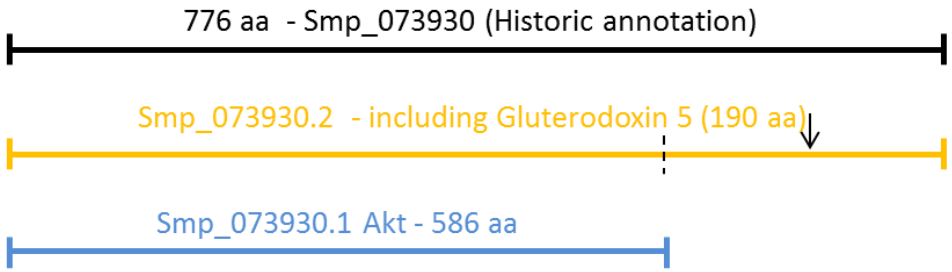

***Figure 4.6* Corrections have been made to the originally annotated Akt gene product.** Historically (Berriman *et al.*, 2009), Akt was annotated in the genome as being 776aa. Revision of the genome (Protasio *et al.*, 2012) resulted in a revised annotation (Smp_073930.2), which includes a 190aa Gluterodoxin 5 protein.

4.3 Protein Interactions with Akt in *S. mansoni*

In any organism, the variety and volume of protein interactions is astonishing. In order to further understand the role of Akt in *S. mansoni*, it is necessary to study the specific connections between Akt and other proteins of the parasite, and what purpose they might serve. To begin to unravel the complexity of potential Akt protein-protein interactions,

[7] http://www.genedb.org [Accessed February 22nd, 2016]

STRING (Szklarczyk *et al.*, 2011) was used with Smp_073930.2 as input sequence. STRING associations are largely derived from predictions or from transferring associations/interactions between organisms ('interlog transfer'); nevertheless STRING provides a snapshot of possible interactions with probabilistic confidence scores. The maps created with STRING provide a visual perspective of the putative protein network and can provide a large amount of data in a relatively short space of time. Initially, a map of medium confidence (≥0.40) interactions was constructed with a maximum limit of 500 proteins (Figure 4.7). The density of interactions shown in the medium confidence map indicates the likely importance of Akt

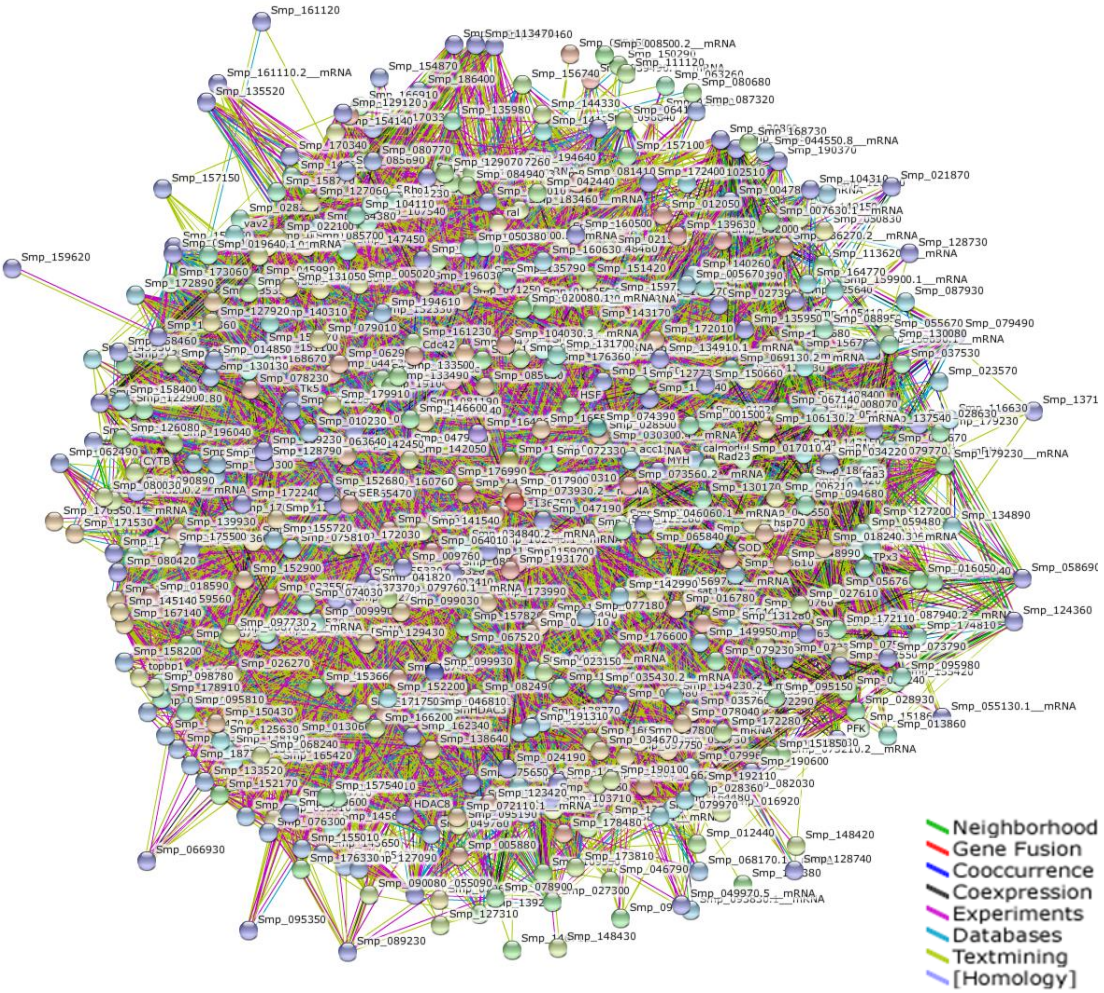

Figure 4.7 **Medium confidence putative protein interaction map for *S. mansoni* Akt.** A map was created in STRINGdb (evidence mode) using Smp_073930.2 as input and parameters set to maximum 500 interactions at medium confidence (STRING Global Score ≥ 0.40). Smp_073930.2, coloured red, appears towards the network centre. The colour code indicates the sources for the predicted interactions.

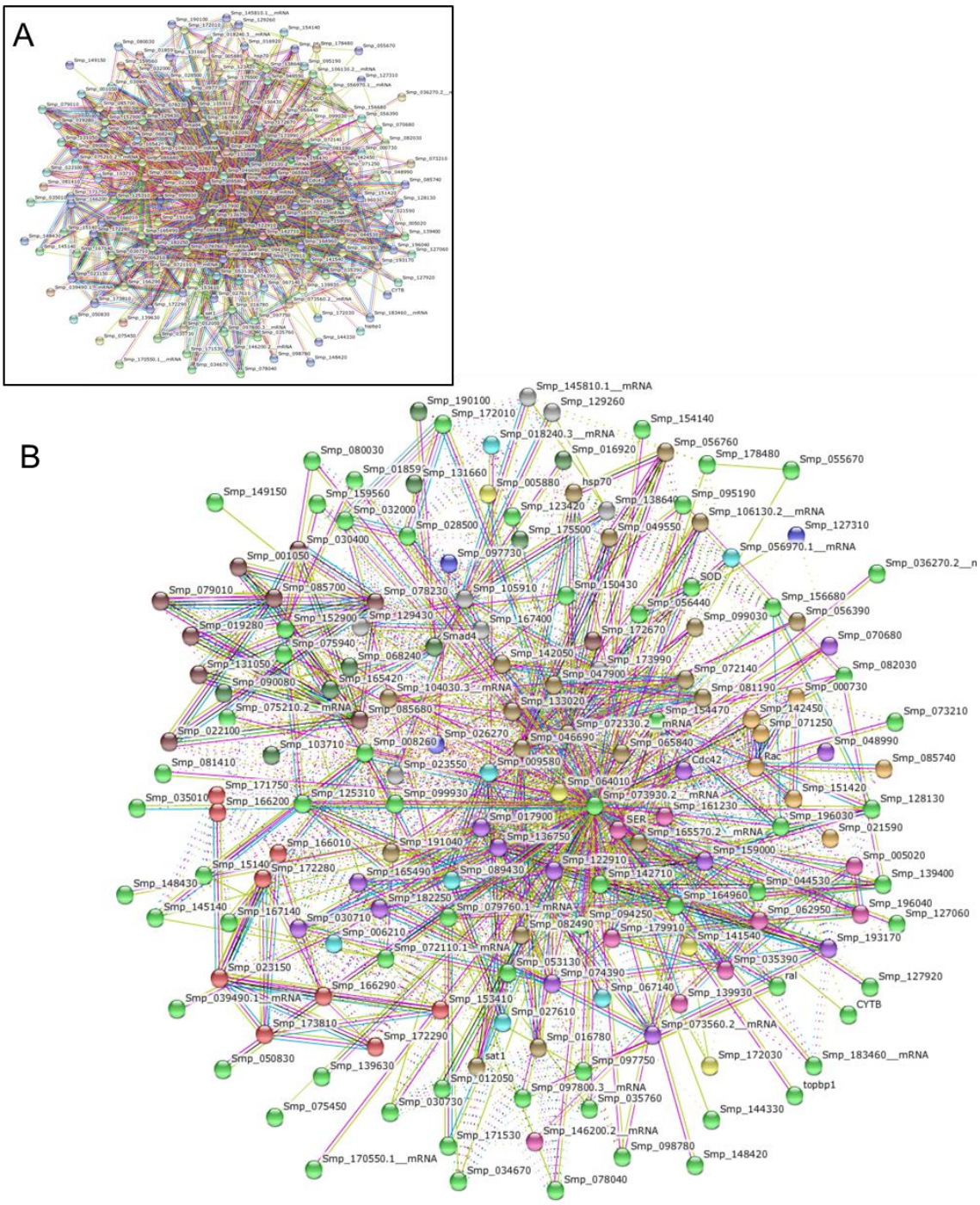

Figure 4.8 **High confidence putative protein interaction map for *S. mansoni* Akt classified in 12 categories. A.** Map in 'evidence mode' created in STRINGdb using Smp_073930.2 as input and parameters set to maximum 500 interactions at high confidence (STRING Global Score **≥ 0.70)**. **B.** A view of the same interaction map but with 12 interaction clusters (each with a different colour) defined using the KMEANS algorithm; inter-cluster edges are shown with dashed lines, interacting proteins with high Global Scores appear in the same cluster (colour). Smp_073930.2, coloured green, appears towards the network centre.

in many biological processes in *S. mansoni*. The confidence parameter was then raised from ≥0.40 (medium) to ≥0.70 (high). The resulting output table (Appendix 2) comprising mapped proteins was saved for further analysis in which putative phosphorylation sites were investigated (Section 4.4.1). The high confidence map is clearer to interrogate but still reveals a 158 potential Akt protein-protein connections (Figure 4.8 A).

To begin to understand better the putative protein-protein interactions, an interaction map was created categorising the proteins into 12 clusters using the K-Means algorithm within STRING (Figure 4.8 B). K-Means analysis aims to determine groups within a data set based on the features of each data point without any prior parameters being set[8]. Each colour on the K-Means map represents a different grouping, with the majority of proteins being grouped together as green. The STRING software provides no further information on the defined groupings but the exercise does provide a useful basic visual reference prior to Gene Ontology (GO) analysis.

4.4 Gene Ontology with High Confidence Akt-Interacting Protein Sequences

Gene Ontology is a method to meaningfully annotate genes and their products from any organism (Ashburner *et al.*, 2000). The three key non-overlapping domains which form the basis of GO are present in all organisms and thus make suitable categories: 'biological process', 'cellular component' and 'molecular function'. Biological process is defined as a biological objective contributed to by a gene or gene product. A biological process often results in a chemical or physical change, requiring a series of molecular functions. Examples of biological process terms range from 'cell growth and maintenance' at high level, to 'cAMP biosynthesis' at specific low-level classification. Molecular function is described as a gene product's biochemical activity, or potential activity, and details only the function itself, not the location or method of the function. Terms including 'transporter', 'enzyme' or 'Toll receptor ligand' would be found in a list of molecular functions. Finally, cellular component refers to the location of the gene product activity within a cell. Examples include 'nuclear membrane', 'ribosome' and 'Golgi apparatus'. The terms within this domain are representative of eukaryotic cell structure knowledge and not all terms can be applied to every organism (The Gene Ontology Consortium, 2000). GO annotation is a highly useful tool for determining

[8] https://www.datascience.com/blog/introduction-to-k-means-clustering-algorithm-learn-data-science-tutorials [Accessed August 3rd 2017].

biological significance within large data sets or to aid in sorting data from novel genomes (The Gene Ontology Consortium, 2006).

To begin GO of the high confidence putative Akt interacting proteins, a list of the high confidence Smp numbers retrieved from STRING was imported into Ensembl Metazoa and an output table of gene ontology created. The table listed every "GO term name" allocated to each Smp number, resulting often in many output terms per protein; from a list of 158 high confidence proteins, 940 output terms were received with only six proteins not recognised. The basic GO domain data was used to visualise the distribution between the three Level 1 GO categories: biological process, cellular component and molecular function. The chart reveals that over half of all protein classifications within the list of high confidence putative Akt interacting proteins fall under the molecular function domain (54%), followed by 32% biological process and 14% cellular component (Figure 4.9).

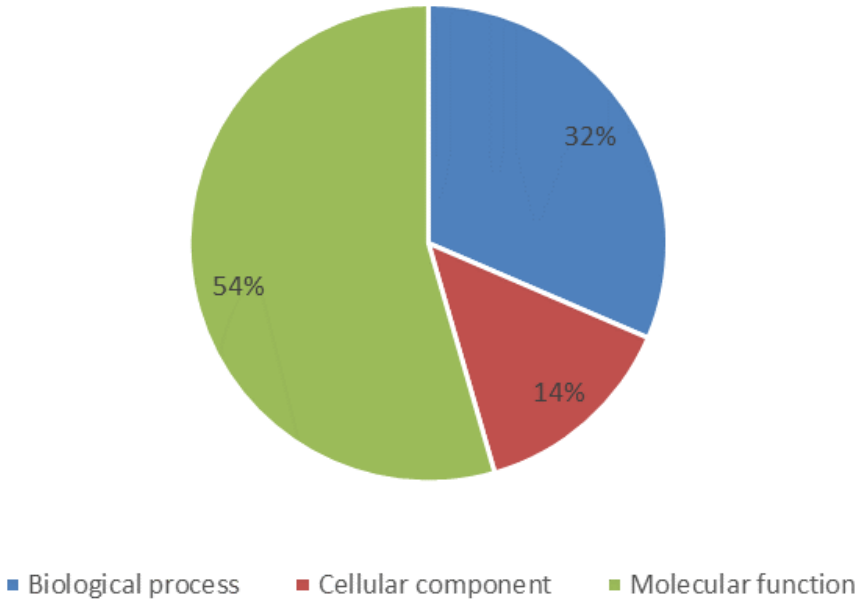

Figure 4.9 **Over half the putative Akt interacting proteins are categorised under the GO term 'molecular function'.** The initial categorisation using Ensembl Metazoa, of 158 high confidence Akt interacting proteins taken from STRINGdb into the three GO parent domains; biological process (32%), cellular component (14%) and molecular function (54%).

4.4.1 Blast2GO analysis

The high confidence putative Akt interacting protein list derived from STRING was also imported into Blast2GO[9], a platform which provides GO data in several forms and allows for statistical analysis. Figure 4.10 displays the number of GO terms assigned to each protein sequence. The majority of proteins (82%) were assigned 10 GO terms or less, contrasting with only 6% which received 20 or more GO terms.

Blast2GO also produces data regarding the number of annotations per GO level (Figure 4.10). GO is represented in a direct acyclic graph (DAG) and shows the parent-child relationships between terms. Each child term is more specific than its parent term although a child term can have more than one parent. These 'generations' of terms form Levels, so that a data set GO can be studied as whole or cut at a specific level. This allows for detailed analysis to be made efficiently. Analysis of levels revealed that Level 3 was the most suitable for further GO annotation as this level had the highest number of annotations across all three domains together (Figure 4.11).

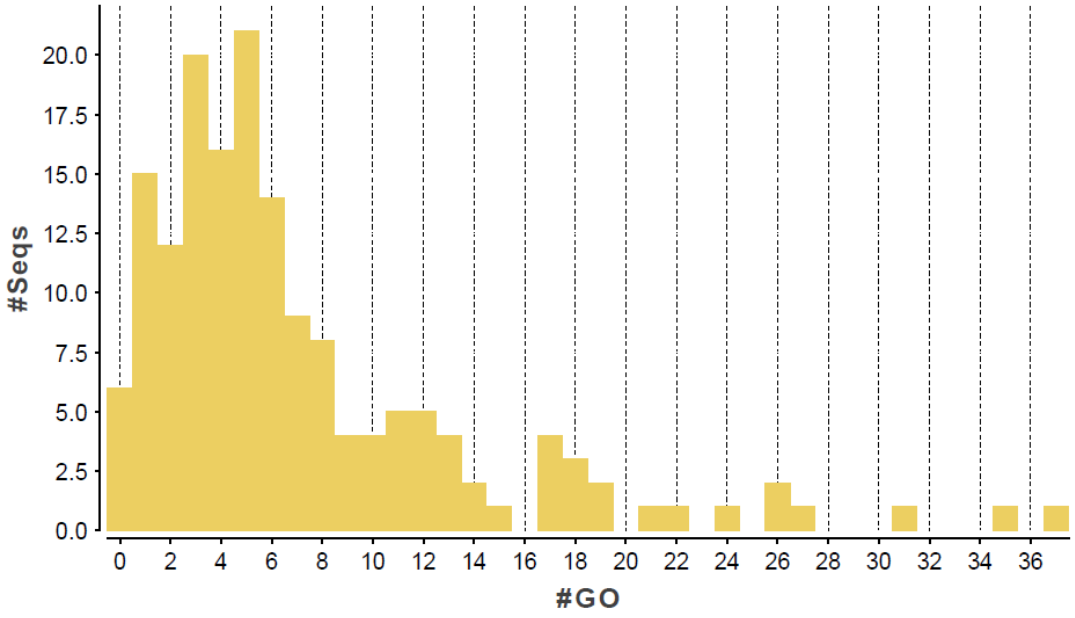

***Figure 4.10* 82% of putative Akt interacting sequences have 10 or less GO annotations.** The distribution of GO terms across the imported high confidence sequences suggests that many proteins within the data set have specific functions as opposed to being implicated in several areas of cell biology. Chart derived using Blast2GO; Charts > Make Statistics > Annotation.

[9] https://www.blast2go.com/blast2go-pro [Accessed August 3rd 2017].

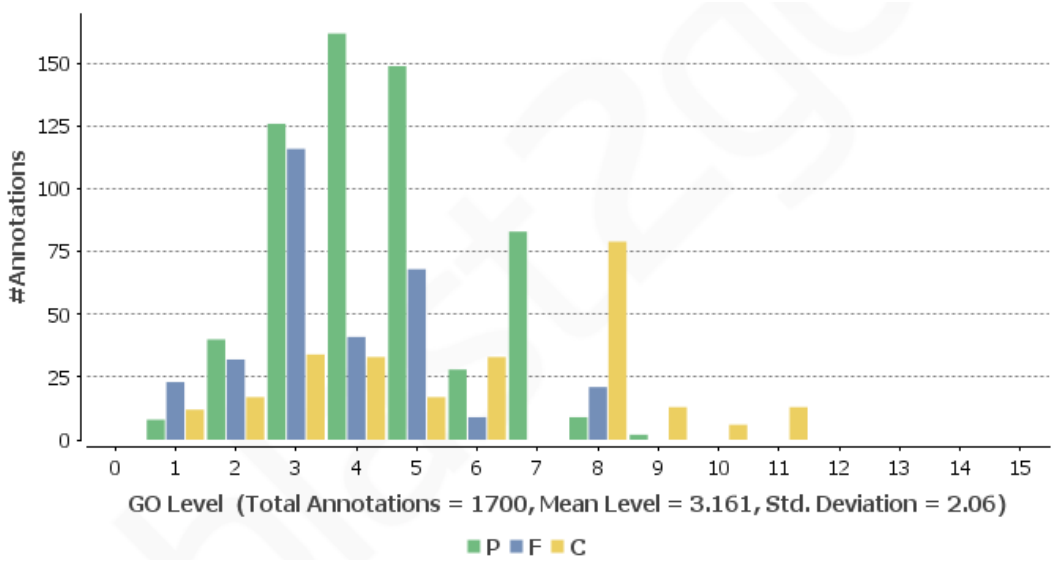

Figure 4.11 **GO Level 3 contains the greatest number of annotations across the three domains at once.** Within the 'Make Statistics' function of Blast2GO, data was retrieved on the number of annotations per GO level. Biological processes (P) dominate the lower levels while cellular component (C) terms are those remaining at high levels; molecular function (F) appear more normally distributed. Level 3 was chosen as the most useful for further analysis. Chart derived using Blast2GO; Charts > Make Statistics > Annotation.

Before investigating GO at a specific level, overview graphs of each domain were created. Direct GO count graphs display the most commonly annotated terms, regardless of GO hierarchy. The top term descending from the biological process root was 'cellular protein modification process' with 61 sequences annotated (Figure 4.12). This term is defined as "The covalent alteration of one or more amino acids occurring in proteins, peptides and nascent polypeptides (co-translational, post-translational modifications) occurring at the level of an individual cell. This also includes the modification of charged tRNAs that are destined to occur in a protein (pre-translation modification)" and has 63 potential child terms (EMBL-EBI, 2017). In this data set, this term is found at Level 6 (Appendix 3). The most annotated molecular function term (81 sequences) was 'ion binding' (Figure 4.13), defined as "Interacting selectively and non-covalently with ions, charged atoms or groups of atoms." (EMBL-EBI, 2017). This term is found at Level 3 in the data set and has no child terms (Appendix 4). Finally, the top term for cellular component was 'protein complex' (Figure 4.14) - "A stable macromolecular complex composed (only) of two or more polypeptide subunits along with any covalently attached molecules (such as lipid anchors or oligosaccharide) or non-protein prosthetic groups (such as nucleotides or metal ions)" (EMBL-EBI, 2017) (34 sequences). In this data set, this term features at Level 3 and has no child terms (Appendix 5).

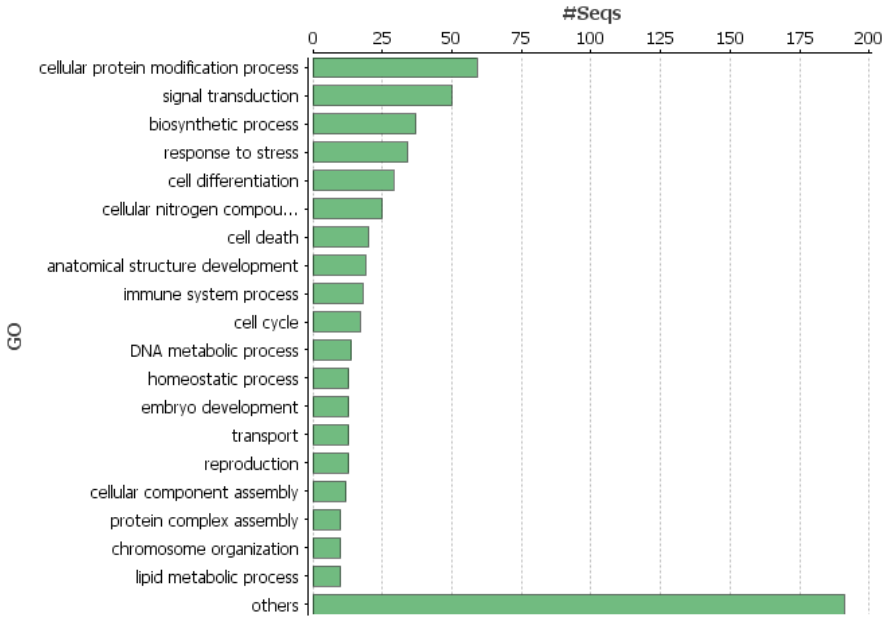

Figure 4.12 **Direct GO count for the high confidence Akt interacting proteins within the biological process (BP) domain.** The top 20 most annotated terms across the entire BP domain are displayed, regardless of GO hierarchy. Created in Blast2GO; Charts > Make Statistics > Annotation.

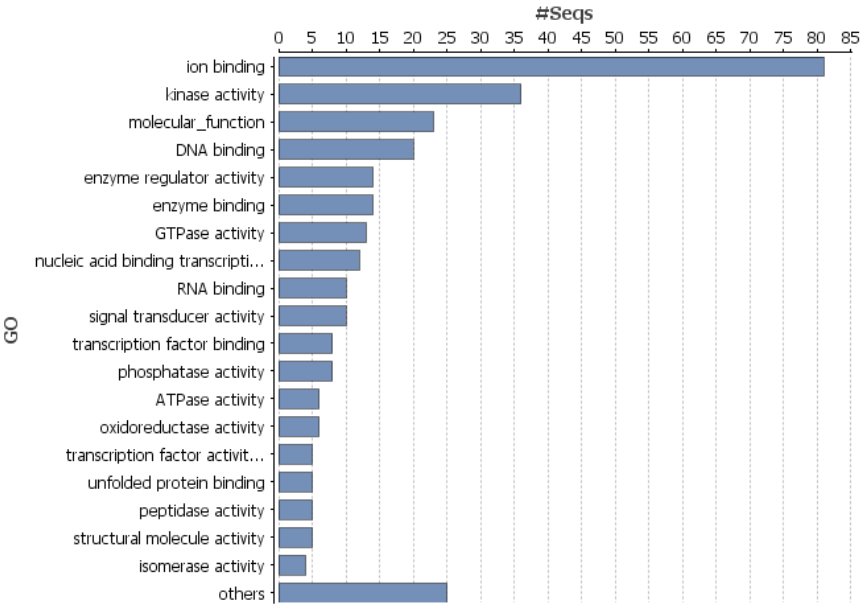

Figure 4.13 **Direct GO count for the high confidence Akt interacting proteins within the molecular function (MF) domain.** The top 20 most annotated terms across the entire MF domain are displayed, regardless of GO hierarchy. Created in Blast2GO; Charts > Make Statistics > Annotation.

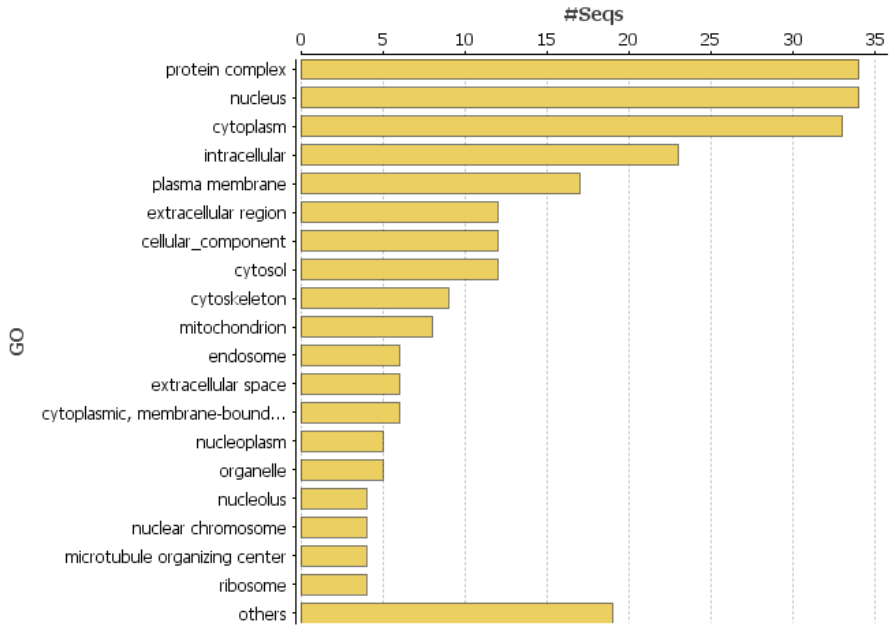

Figure 4.14 **Direct GO count for the high confidence Akt interacting proteins within the cellular component (CC) domain.** The top 20 most annotated terms across the entire CC domain are displayed, regardless of GO hierarchy. Created in Blast2GO; Charts > Make Statistics > Annotation.

At Level 3, the top 20 terms for each of the three root domains are represented in Figure 4.15. This gives a cross-sectional overview of the GO and provides detail on the specificity of the terms at this level. The most annotated term at Level 3 in the biological process domain, with 87 sequences, is 'cellular metabolic process' (GO:0044237: "The chemical reactions and pathways by which individual cells transform chemical substances." (Blast2GO, 2017)). At Level 3, this term is a parent to several more specific terms, in this case; 'heterocycle metabolic process', 'cellular aromatic compound metabolic process', 'cellular nitrogen metabolic process' and 'cellular macromolecule metabolic process' (Appendix 3). In the molecular function domain, the most annotated term (53.3% of sequences) is 'ion binding' (GO:0043167:, "Interacting selectively and non-covalently with ions, charged atoms or groups of atoms." (Blast2GO)). Here, this term does not have any child terms (Appendix 4). The localisation term which received the most annotations in Level 3 of the cellular components domain was 'intracellular' (GO:0005622: "The living contents of a cell; the matter contained within (but not including) the plasma membrane, usually taken to exclude large vacuoles and masses of secretory or ingested material. In eukaryotes it includes the nucleus and cytoplasm." (Blast2GO, 2017)). Of the 32 possible child terms linked with this term, this data set

contained 3; ‘intracellular organelle’, ‘intracellular part’ and ‘intracellular nonmembrane bound organelle’ (Appendix 5).

Next, pie charts were created from combined graphs (Appendix 3-5), which are designed to allow the combined annotation of a group of sequences to be visualised together. The pie charts show the number of sequences per GO node at a specific level from the combined graph of each domain; biological process (Figure 4.16), molecular function (Figure 4.17) and cellular component (Figure 4.18), representing similar information as Figure 4.14 but in a different format.

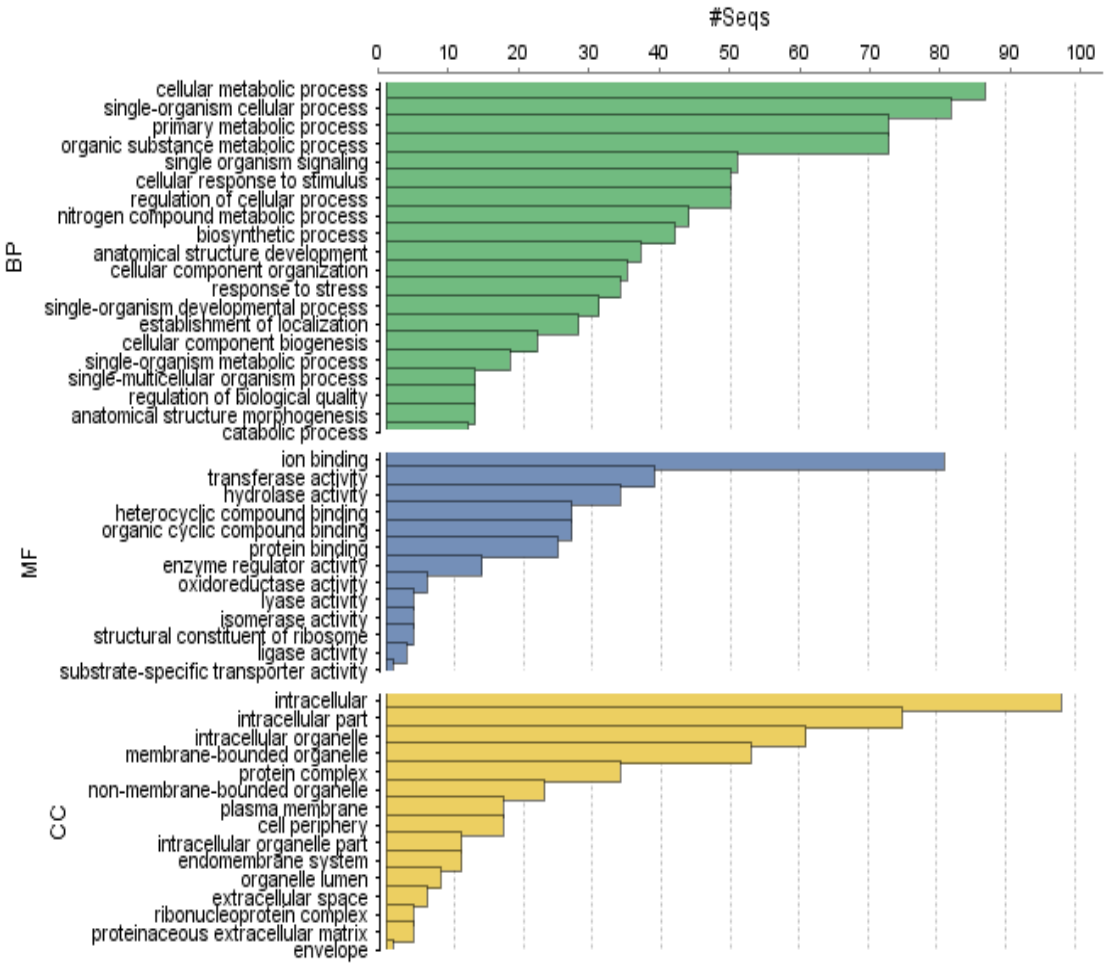

Figure 4.15 **The biological process domain contains the most terms at Level 3 for the high confidence Akt interacting proteins.** A GO distribution by level graph created through the annotation statistics feature of Blast2GO. A maximum term number of 20 was set.

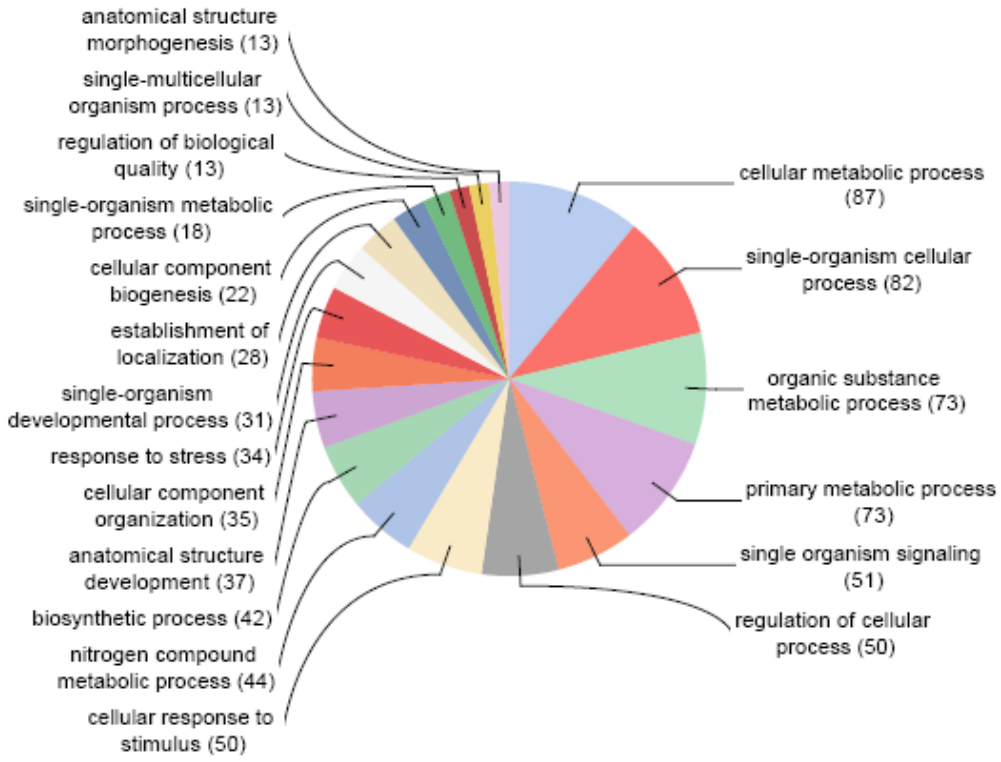

Figure 4.16 **Level 3 biological processes domain contains 19 nodes.** Level 3 pie chart created from a combined graph with the parameters; Sequence filter – 13, Nodescore filter – 0.00, Nodescore alpha – 0.60. A total of 19 nodes each with a minimum of 13 sequences annotated. The nodescore is calculated as the sum of sequences associated to a GO term, directly or indirectly, each weighted by the distance of the term to the term of direct association. Created in Blast2GO

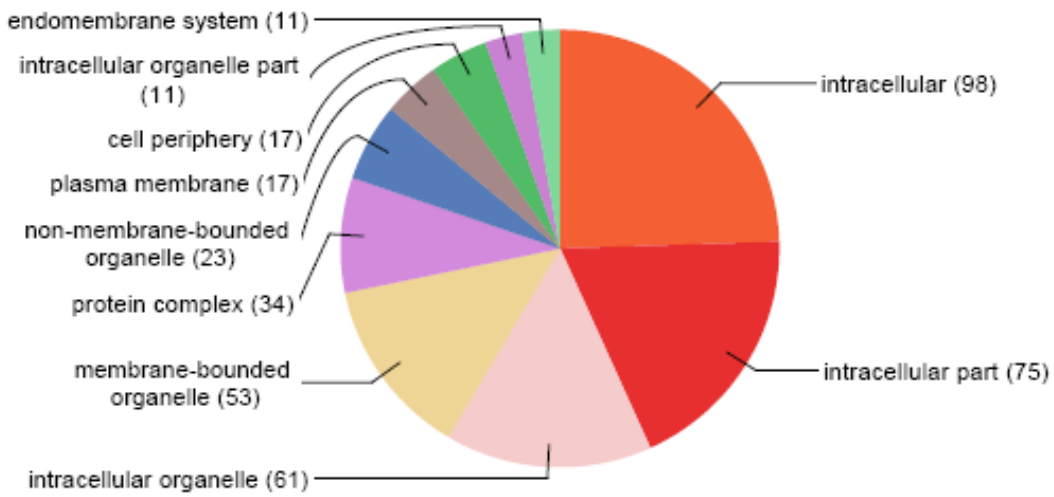

Figure 4.18 **Level 3 cellular components domain contains 10 nodes.** Level 3 pie chart created from a combined graph with the parameters; Sequence filter – 11, Nodescore filter – 0.00, Nodescore alpha – 0.60. A total of 10 nodes each with a minimum of 11 sequences annotated. Created in Blast2GO

4.4.2 Gene Ontology with medium confidence Akt protein interactions

In addition to GO analysis of the high confidence putative protein connections with Akt, analysis was repeated with the additional proteins generated using STRING Global Score **≥** 0.40 (medium confidence). Addition of these proteins did not alter the general distribution of basic GO terms; biological process, cellular component and molecular

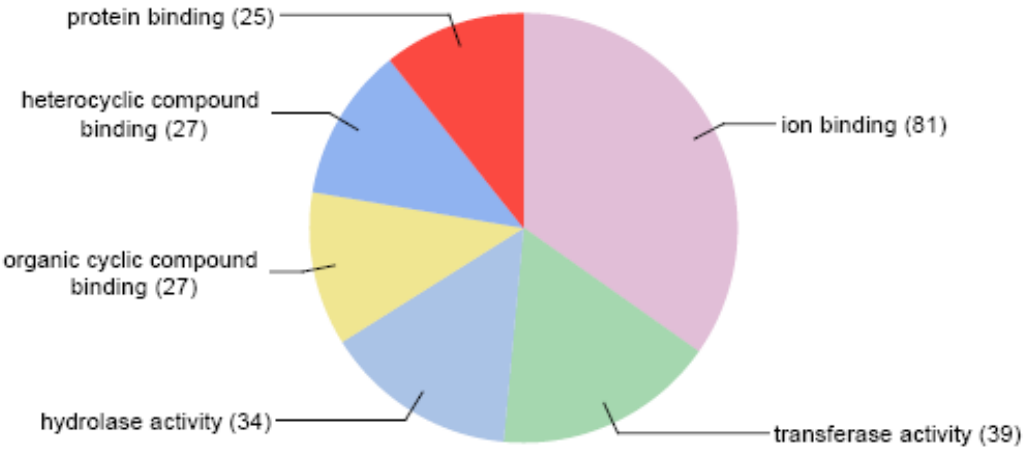

Figure 4.17 **Level 3 molecular function domain contains 6 nodes.** Level 3 pie chart created from a combined graph with the parameters; Sequence filter – 15, Nodescore filter – 0.00, Nodescore alpha – 0.60. A total of 6 nodes each with a minimum of 15 sequences annotated, although in this case each term had at least 25 annotated sequences. Created in Blast2GO

function (data not shown) as seen in Figure 4.8. However, interrogation of the interacting protein list with regard to Akt signalling highlighted some interesting findings. At 0.694 confidence are listed three putative glucose transporter proteins. One of these (Smp_105410) is listed in GeneDB[10] as GTP4. Also in the list are members of the Ras superfmily, Rab, Rac and Rho. These proteins are known to play a role in vesicle trafficking, amongst other things (reviewed by Bustelo *et al.*, 2007).

4.5 Analysis of Downstream Substrate Proteins

4.5.1 Bioinformatic analysis of putative substrates

The list of high confidence (STRING Global Score ≥ 0.70) Akt interacting proteins was used to determine which proteins might be actively involved in Akt signalling as substrates based on potential Akt phosphorylation sites present within each. In total, three phosphorylation prediction platforms were used: KinasePhos, ScanSite3 and HRPD (Appendix 3). For each protein, the full (predicted) aa sequence was queried for the presence of motifs that comply with Akt phosphorylation requirements; a Ser or Thr residue with Arg at -3 and -5 positions (RXRXXS/T). Potential phosphorylation sites were tabulated and compared between the prediction platforms. Table 4.1 lists 32 proteins, which generated 48 putative Akt phosphorylation sites common across at least two of the three databases. The protein with the most putative phosphorylation motifs was Smp_036270.2_mRNA – arginine/serine-rich splicing factor, putative.

[10] http://www.genedb.org/Homepage/Smansoni [Accessed September 10th 2017].

Table 4.1

Protein ID	Protein Name	Amino Acid	Predicted Phosphosite
Smp_053130	40S ribosomal protein S6 (248 aa)*	235	SRSHSLRES
Smp_099930	F-box and wd40 domain protein, putative (863 aa)	289	SRTQSIPFS
Smp_064010	Camp-response element binding protein-related (825 aa)	210 614	RRSSTLAPP QRRRSVFTA
Rac	Rac gtpase, putative (188 aa)	71	LRPLSYPQT
Smp_039490.1_ mRNA	Expressed protein (954 aa)	832 887 929 938 947	KRRYSKTDS RRSSSNRPS RRSRSFNQR HRSRSTDRR DRSSSNRYR
Smp_156680	Fyve finger-containing phosphoinositide kinase, fyv1, putative (2289 aa)*	591 995 1756	MRDCSLESL SRVKSLNKM ARTHSNSIS
Smp_104030.3_ mRNA	Scribble complex protein (Cell polarity protein) (1456 aa)	74 848	IRLLTLSDN ARIQSKTAD
Smp_105910	CREB-binding protein 1 (SmCBP1) (2093 aa)	1499	RRISTMHRG
Cdc42	Cell polarity protein (Regulator of photoreceptor cell morphogenesis) (195 aa)	75	LRPLSYPQT
Smp_036270.2_ mRNA	Arginine/serine-rich splicing factor, putative (371 aa)	189 233 304 316 337 339	SRSGSYRSR QRSESGNDS SRSRSISHS SRSRSVESR SRSRSMSHR SRSMSHRSE
Smp_062950	Growth factor receptor-bound protein, putative (234 aa)	155	NRLLTLVDL
Smp_150430	Forkhead protein/ forkhead protein domain, putative (504 aa)	181	RRTNSLQRS
Smp_017900	Serine/threonine kinase (806 aa)*	794	VRAKSILTN
Smp_136750	Serine/threonine kinase (1767 aa)*	423 697	SRRRSGISS KRLISAASE
Smp_082030	Family C56 non-peptidase homologue (C56 family) (184 aa)	123	KRLTSYPGF
Smp_072110.1_ mRNA	Programmed cell death, putative (534 aa)	520	KRFISETDS
Smp_035390	Protein tyrosine phosphatase n11 (Shp2), putative (708 aa)	708	PRTKS****
Smp_139400	Tensin, putative (1704 aa)	1121	GRAFSGSPT
Smp_196030	GTPase activating protein,putative (745 aa)	503	NRSNSFSES
Smp_131050	Camp-dependent protein kinase type II regulatory subunit, putative (301 aa)	254	PRAASAYAV
Smp_021590	Rac gtpase activating protein, putative (610 aa)	181	GRASSVSHT
Smp_050830	Synaptojanin, putative (526 aa)	468	HRKNSVSSA
Smp_065840	DNA topoisomerase 2 (1599 aa)	1482	GRQFSAPPK
Smp_141540	Thymidine kinase, putative (945 aa)	54	QRRWSVPFQ
Smp_183460_m RNA	Map/microtubule affinity-regulating kinase 2,4, putative (108 aa)	95	RRRSSLDTS
Smp_016920	Putative uncharacterized protein (203 aa)	153 162	RRTRSIGPS RRSNSMNIF
Smp_148430	Expressed protein (738 aa)	570	SRSSSLCYN
Smp_148420	Expressed protein (974 aa)	597 766	KRLDSLTDE RKTISMPPN
Smp_166200	Axis inhibition protein, axin, putative (1142 aa)	635	SRSYSMAEH
Smp_085740	Abl-binding protein-related (583 aa)	288	SRKSSGSSG
Smp_149150	Acyl-CoA-binding protein (Acbp) (Diazepam binding inhibitor) (Dbi) (343 aa)	125	DRGFSLSKV
Smp_161230	Ras GTP exchange factor, son of sevenless, putative (1518 aa)	541	RRSTSTTAT

Table 4.1 **Several putative Akt interacting proteins possess one or more potential Akt phosphorylation sites.** An exert taken from appendix 3 showing those phosphorylation sites of high confidence proteins (>0.70) which were in accordance across at least two of the three phosphorylation site prediction platforms, KinasePhos, ScanSite3 and HRPD.

4.5.2 S. mansoni *homologues of human Akt substrates –Glycogen Synthase Kinase -3*

Akt has many known substrates in humans (Figure 1.7). To begin to assess if any of those substrates have *S. mansoni* homologues, experiments were designed to study glycogen synthase kinase-3 α/β (GSK-3α/β) within the parasite.

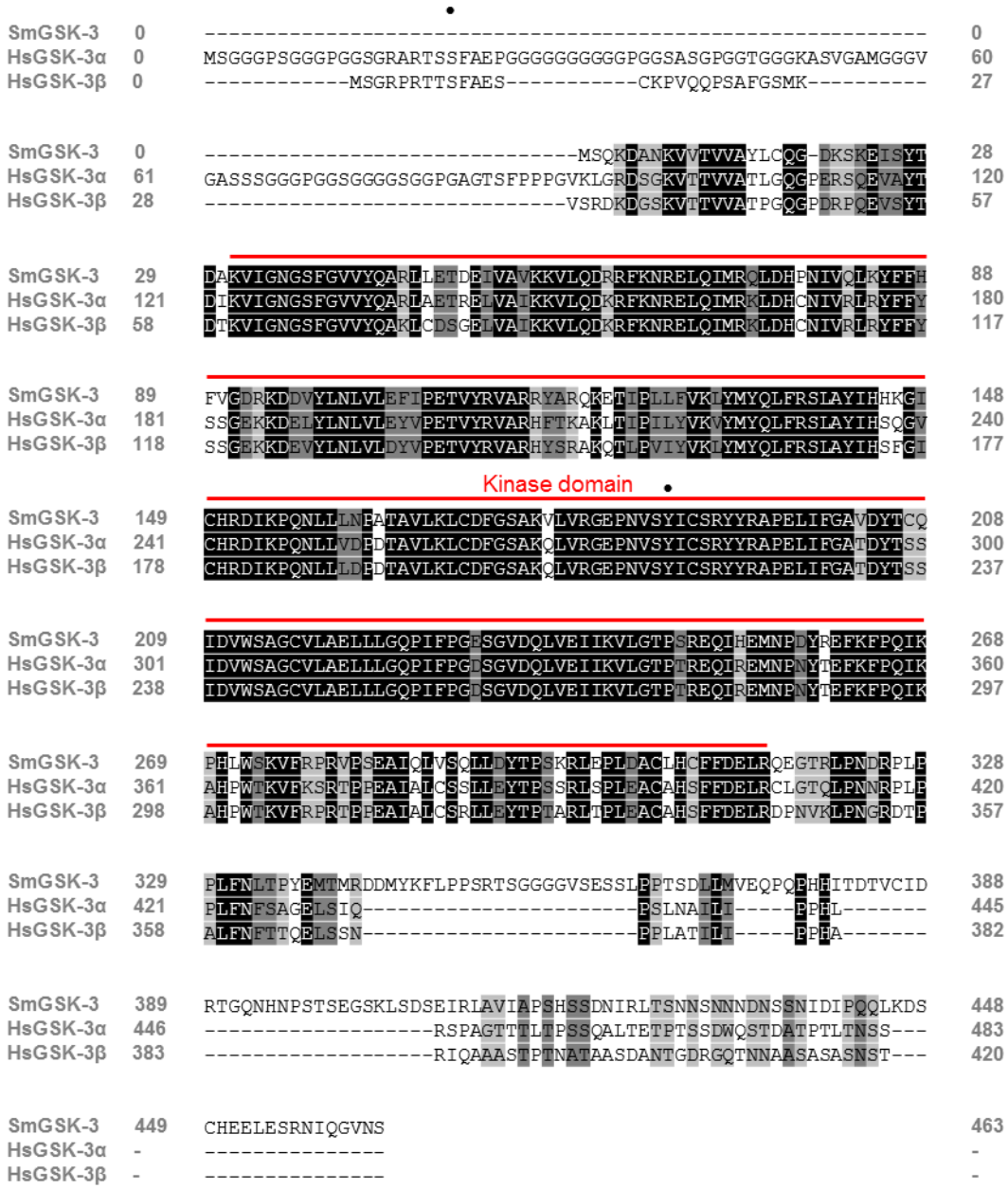

Figure 4.19 **Multiple pairwise alignment of *Schistosoma mansoni* (Sm)GSK-3 with human (Hs)GSK-3α/β proteins.** Alignment of the GSK-3 protein to compare *S. mansoni* (CCD75971.1), *H. sapiens* GSK-3α (NP_063937.2) and *H. sapiens* GSK-3β (NP_001139628.1). The alignment was created using MUSCLE. The Kinase domain is shown in red and the black dots indicate important conserved residues for phosphorylation of GSK-3; Hs(Ser$^{9/21}$) and Hs(Tyr$^{216/279}$). The colours range from light grey to black showing least conserved to most conserved residues, respectively, as determined by the MUSCLE software.

GSK-3 is involved in the regulation of many signalling pathways including those implicated in glucose metabolism, cell cycle regulation, and innate and adaptive immunity (Beurel *et al.*, 2010; Giambelluca *et al.*, 2013). GSK-3 lies downstream of Akt and is present as two distinct isoforms in humans, GSK-3α and GSK-3β (Zhao *et al.*, 2013). Unusually, GSK-3 is constitutively active until phosphorylated in response to external signals; for example, inactivation by Akt occurs when stimulated by insulin (Cross *et al.*, 1995). GSK-3α and GSK-3β are phosphorylated at Ser^{21} and Ser^{9} respectively (Dajani *et al.*, 2001). In addition to GSK-3α/β in humans, several GSK-3 proteins have been identified in other organisms, such as in *Saccharomyces cerevisiae* and *D. melanogaster* (Osolodkin *et al.*, 2011). Bioinformatic analysis of GSK-3β across parasites performed by Osolodkin *et al.* (2011), revealed that *S. mansoni* GSK-3 possesses 88% kinase domain similarity to human GSK-3β. Figure 4.19 shows a multiple pair-wise alignment between SmGSK-3, HsGSK-3α and HsGSK-3β. As the alignment demonstrates, the currently annotated/predicted *S. mansoni* protein is shorter than its human counterparts at the N-terminus. Within these additional human residues is $Ser^{9/21}$, which HsGSK-3α/β requires be phosphorylated to inactivate the protein. With this residue missing from the annotated SmGSK-3, it is unsurprising that the antibody against

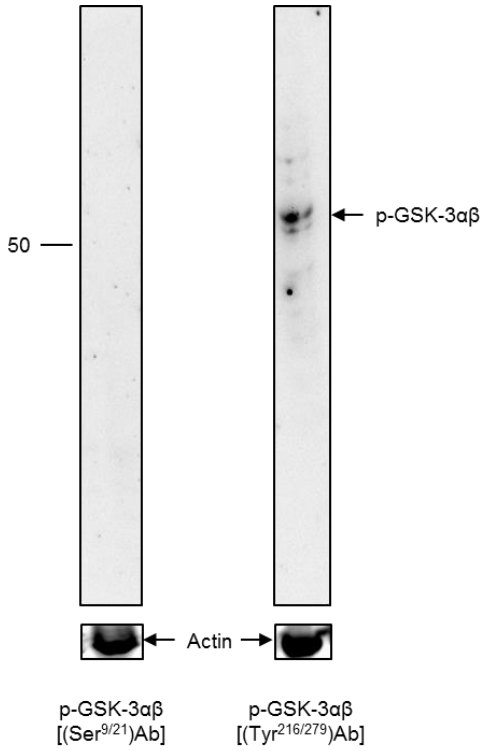

Figure 4.20 **Detection of GSK-3α/β in *S. mansoni*.** ~1000 untreated, 24 h somules were processed for western blotting with either anti phospho-GSK-3α/β ($Ser^{9/21}$) or anti phospho-GSK-3α/β ($Tyr^{216/279}$) antibodies. Membranes were then stripped and re-probed with anti-actin antibodies to determine protein loading. Relevant molecular weight markers are indicated. Blots are representative of two experiments.

Ser$^{9/21}$ (human) was unsuccessful when tested with *S. mansoni* parasite material (Figure 4.20). However, antibodies against phosphorylated GSK-3α/β (Tyr$^{216/279}$) successfully detected a GSK-like protein at the predicted molecular weight (53 kDa) in *S. mansoni* somules (Figure 4.19). Further troubleshooting using the anti- GSK-3α/β (Ser$^{9/21}$) was therefore not undertaken.

Using anti-phospho GSK-3α/β (Tyr$^{216/279}$) antibodies, western blotting confirmed that, as in humans, *S. mansoni* GSK-3 is inversely activated by Akt. When somules were incubated in the stimulants insulin and L-arginine, GSK-3 signal was no more apparent than in the control samples (Figure 4.21). However, when treated with Akt Inhibitor X, somules displayed increased GSK-3 activation.

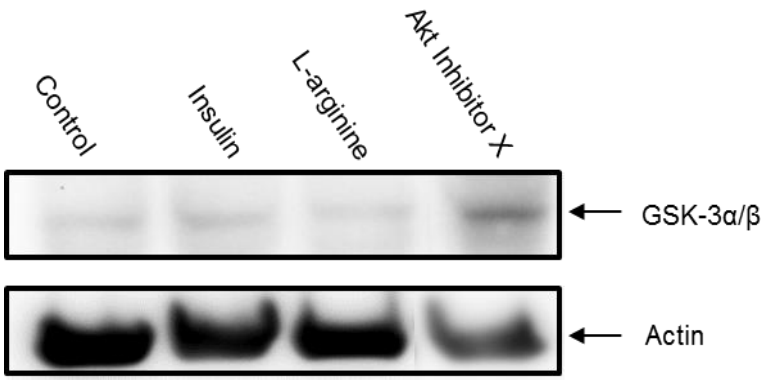

***Figure 4.21 S. mansoni* GSK-3α/β phosphorylation (activation) is increased when Akt is inhibited.** 24 h somules (~1000) were treated with 1 μM insulin (10 min), 100 μM L-arginine (30 min) or 10 μM Akt Inhibitor X (60 min). Samples were processed for western blotting with anti-phospho GSK-3α/β (Tyr$^{216/279}$) antibodies. Membranes were then stripped and re-probed with anti-actin antibodies to determine protein loading between lanes. The blot is representative of results obtained in three experiments.

Summary:

This chapter has reported the global distribution of Akt substrates in *S. mansoni* human-infective/resident life stages and has considered the identity of putative Akt interacting proteins *via* bioinformatic analysis.

Western blotting with anti-phospho Akt substrate antibodies revealed approximately twelve Akt-like substrates detectable in cercariae, somules and adult male and female worms. These substrates were then mapped within each parasite stage, and the phosphorylated Akt substrate distribution broadly mirrored that of activated Akt, with the exception of somules, which displayed a more general substrate phosphorylation throughout the parasite.

Given the potential for a large Akt signalling network being present in *S. mansoni*, as is the case in mammals, a bioinformatic analysis was performed to help unravel the nature of signalling downstream of Akt in schistosomes. Initially, STRING analysis defined 158 putative Akt interacting proteins at a high confidence (STRING Global Score ≥ 0.70). Gene ontology of those proteins highlighted the wide range of cellular processes that SmAkt is potentially involved in.

Analysis of potential phosphorylation sites within the putative high confidence Akt interactors revealed 32 sequences that possessed one or more specific motif requirements for Akt phosphorylation.

Finally, a known substrate of human Akt, GSK-3α/β, was tested for in *S. mansoni* somules. Conservation of the two species genes was high at 88% and immunoblotting supported that Akt in *S. mansoni* blocks GSK-3 activity as it does in humans.

This chapter has highlighted the central position of Akt within *S. mansoni* cell signalling and has opened potentially important avenues for future research.

5

Results 3 – Akt in the tegument: A role in glucose uptake from the host

As discovered during the immunolocalisation work (Chapter 3), activated Akt localises to the tegument of somules and adult worms. Numerous studies have been dedicated to researching the schistosome tegument as it is the point of contact with the mammalian host blood and therefore has the potential to possess novel drug targets (van Balkom *et al.*, 2005; Braschi *et al.*, 2006b; Braschi and Wilson, 2006; Loukas *et al.*, 2007; Castro-Borges *et al.*, 2011; Collins *et al.*, 2016). Given the possibility of targeting Akt in schistosomes for parasite control, this chapter focused on investigations into the role of Akt in this parasite host-interactive layer.

Having validated Akt Inhibitor X for use in schistosomes to supress Akt activation, initial experiments focused on evaluating the possible effects of this inhibitor on tegument structure/morphology, particularly given that the tegument is known to turn over rapidly *in vitro* and *in vivo* (Van Hellemond *et al.*, 2006). Subsequently, a functional application for Akt in the tegumental layer was identified *via* experiments exploring the connection between Akt and the facilitated glucose transporter protein, SGTP4.

5.1 Activation of Akt in the Tegument of *S. mansoni*

In Chapter 3, activated Akt had been identified in the tegument *via* immunolocalisation. Thus, tegument stripping was performed to demonstrate the presence of Akt in this structure by western blotting; the effect of human insulin on phosphorylation of tegumental Akt was also determined. Stripping the tegument from adult worms involved snap-freezing them in liquid nitrogen and vortexing to remove the outer layer of the worms (Roberts *et al.*, 1983); samples were then centrifuged to isolate the particulate membranous fraction. Male and female adult worms were treated with or without human insulin and their teguments stripped and processed for western blotting with anti-phospho Akt (Thr^{308}) antibodies. Phosphorylated Akt was detected in both the membranous particulate fraction and the cytoplasmic fraction, and the total pool of phosphorylated Akt increased approximately 2.1 fold and 1.5 fold ($p \leq 0.01$), respectively when worms were treated with human insulin compared with the controls (Figure 5.1).

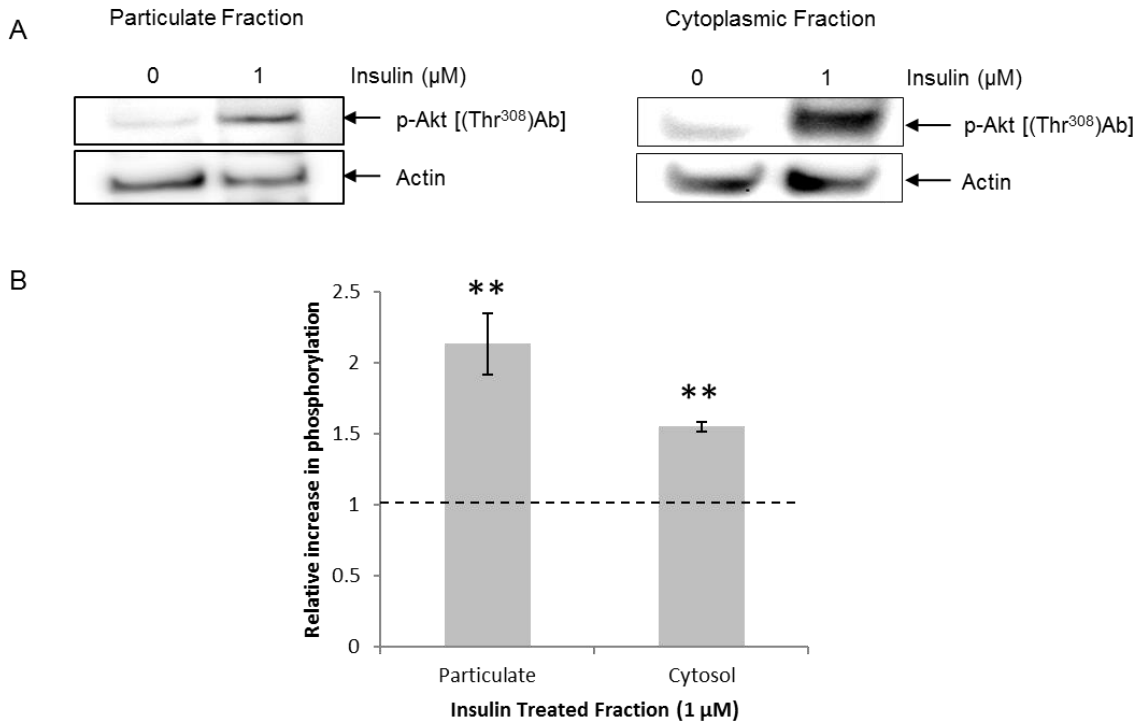

Figure 5.1 **Akt is present in the tegument of adult *S. mansoni* and can be activated by human insulin. A.** Mixed populations of male and female worms (10 worms/treatment) were treated with human insulin (1 μM) for 10 min or not and their teguments stripped and the membranous particulate fraction isolated. The fractions containing the particulate and cytoplasmic samples were western blotted with anti-phospho Akt (Thr308) antibodies. Blots were also stripped and re-probed with anti-actin antibodies to ascertain protein loading levels. **B.** Blots from 3 independent experiments were analysed using GeneTools and the mean relative increase in Akt phosphorylation (±S.D.) in response to insulin calculated with respect to actin. **p≤0.01, when compared with control levels (represented by the dotted line)

5.2 Inhibition of Adult *S. mansoni* Akt by Akt Inhibitor X

5.2.1 The role of Akt in S. mansoni *tegument morphology*

To ascertain the effects of Akt inhibition on the gross phenotype of the parasite, an observational study of adult worms incubated with 10 μM Akt Inhibitor X was conducted over five days with daily inhibitor replenishment. Observations under high-power light microscopy revealed that the tubercles on the tegument of male worms appeared larger after 48 h. Their appearance was swollen and less uniform in comparison to those on the control worms, which were small, neat and close together. Also 'blebbing' was observed at the tegument surface from day three, a phenomenon previously noted in the literature in response to drug treatments (Becker *et al.*, 1980; Manneck *et al.,* 2010). Other observations made included the longitudinal uncurling of male worms in the presence of the inhibitor. Rather than being curled around in their normal shape, the

worms flattened and appeared ribbon-like. After 24 h in 10 μM Akt Inhibitor X, the male worms were also seen to be more active, displaying a greater frequency of twisting, turning and whip-like movements. This was not seen with the lower doses of the inhibitor. Also after ~24 h, worms became increasingly opaque the longer they remained in the inhibitor, a phenomenon thought to indicate pending parasite death, although some worms were observed for several days in this state. Finally, Akt Inhibitor X seemed to induce shrivelling of the oral and ventral suckers, and initially was thought to affect the worm's ability to adhere to the culture plate surface, but this observation was not seen consistently.

An experiment was thus designed to quantify the response of the tubercles to Akt Inhibitor X by capturing photomicrographs and analysing them with ImageJ to measure the area of the tegument protrusions with and without treatment. Representative images from control and 10 μM Akt Inhibitor X treated worms are displayed in Figure 5.2 A. The outcomes of this experiment were not striking but an upward trend in the size of the tubercles was apparent after treatment with 10 μM Akt Inhibitor X (Figure 5.2 B). Additionally, there was a marked decrease in the mean tubercle area over the five days treatment with 1 μM Akt Inhibitor X.

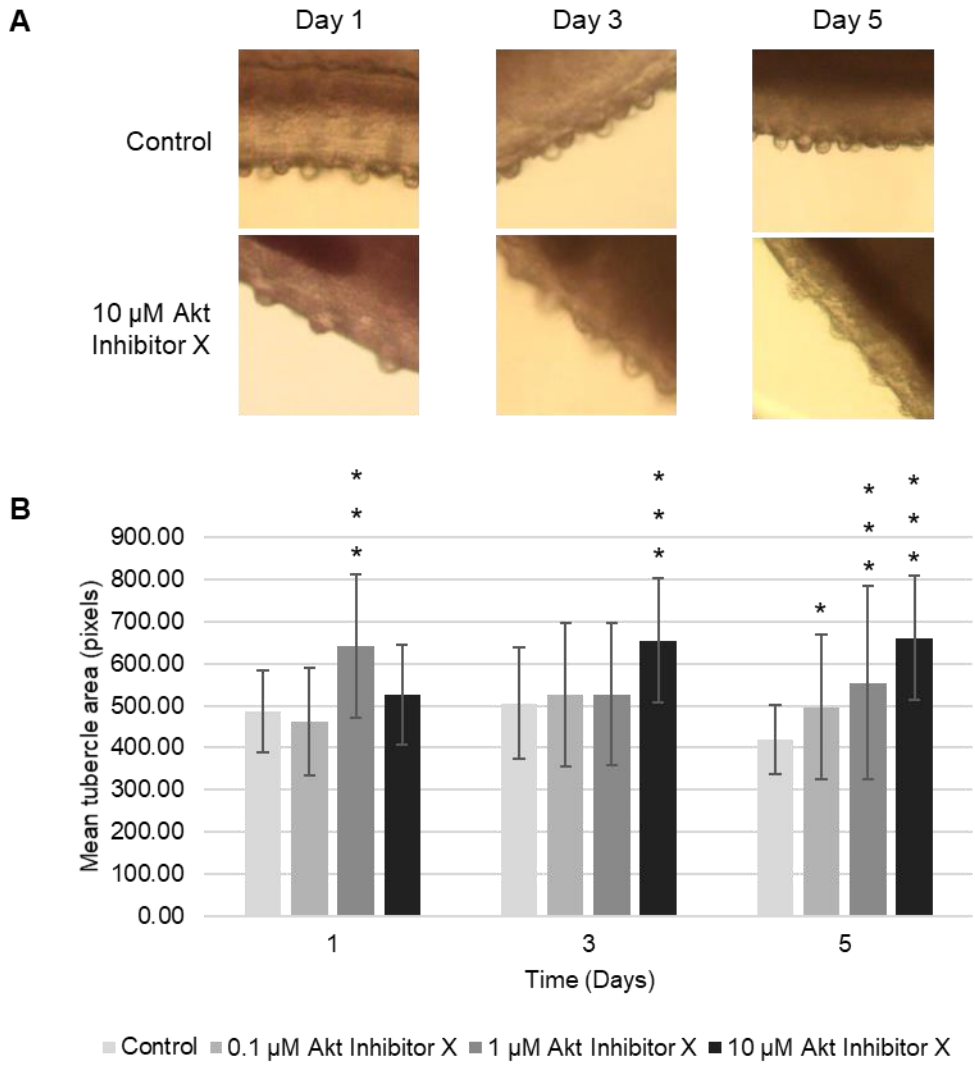

Figure 5.2 **Incubation of adult worms in Akt Inhibitor X promotes increased tubercle size over 5 days.** Male adult worms (5 per well) were maintained in RPMI and increasing concentrations of Akt Inhibitor X or not (control) for up to 5 days. **A.** Worms were photographed daily using LEICA microscope/tablet image capture system (x10 objective). The light intensity was adjusted to view the tubercles clearly but was maintained constant for each day. **B.** The mean tubercle area (±S.D., n ≥ 45) was then calculated by analysing micrographs using ImageJ.* p≤0.05, *** p≤0.001.

5.2.2 The effect of Akt inhibition on worm phenotype by histological analysis

In an attempt to better analyse the tubercle size following treatment, worms were processed for histology so that the tegument tubercles could be observed in cross section. Based on the previous observations (Figure 5.2), male worms were treated with 1 μM or 10 μM Akt Inhibitor X and incubated for four days with daily media/inhibitor replenishment. Worms were fixed, sectioned, and processed for histology, sections visualised under a Nikon Ni-E microscope and images captured for analysis. Images of tubercles only on the anterior dorsal surface of the males were captured to control for possible regional differences between individual worms. Nikon NIS-Elements BR software was used to measure the diameter in μm across the base of tubercles in each image. This approach was chosen because measuring the height of the tubercles was impractical given there is no clear starting point from which to measure. The analysis revealed that there was an upward trend in mean diameter size following treatment with

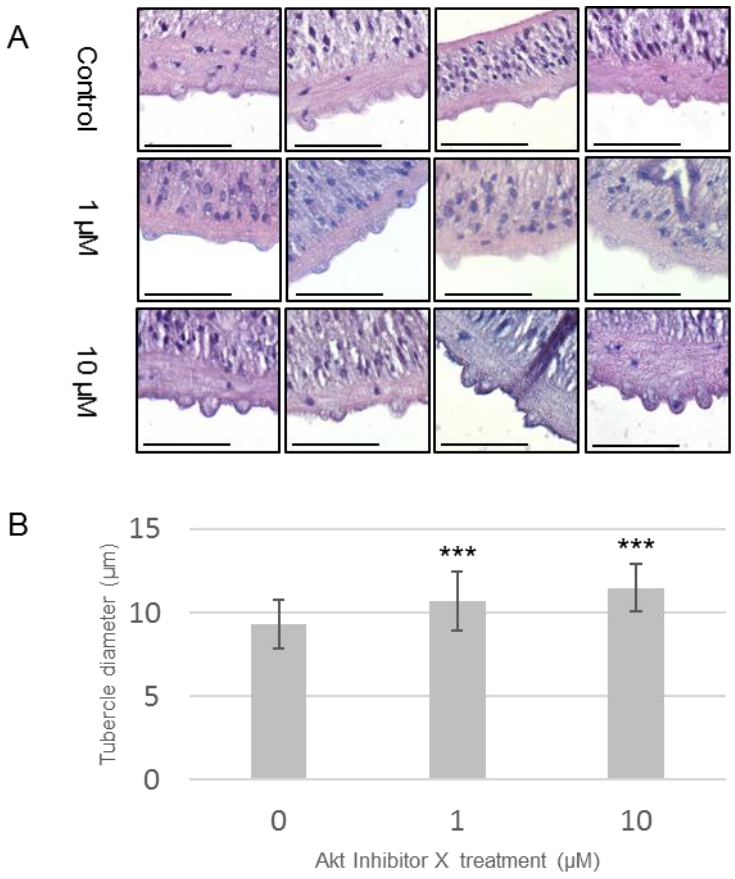

Figure 5.3 **Male adult worm tubercle morphology is affected by treatment with Akt Inhibitor X. A.** Male adult worms (5 per well) were incubated for 4 days in RPMI and increasing concentrations of Akt Inhibitor X or not (control), replenished daily. Worms were fixed in 10% neutral buffered formalin and processed for histology. Images were captured at x40 magnification and tubercle diameter was measured using Nikon software. **B.** The mean tubercle diameter (±S.D., n ≥ 40) was calculated. ***p≤0.001, when compared with control levels.

1 μM and 10 μM Akt Inhibitor X increasing tubercle diameter by 14.9 % and 23.5 % respectively ($p \leq 0.001$) (Figure 5.3). Figure 5.3 A shows representative images for each treatment and it is apparent that the tubercles of worms treated with 10 μM Akt Inhibitor X protrude further from the tegument surface.

5.3 A Role for Akt in Glucose Transport in *S. mansoni*

It is well documented that schistosomes rely on a supply of blood glucose to survive (Rogers and Beuding, 1975; Uglem and Read, 1975). Each adult worm metabolises its dry weight in glucose every ~5 h, sourced from the host blood (Bueding, 1950). Glucose transporter proteins (GTPs) exist in almost all organisms, with the exception of anaerobic bacteria, to carry essential glucose across the hydrophobic membrane into cells for metabolism. In schistosomes, four glucose transporters have been identified in the genome, SGTP1, 2, 3 and 4, with SGTP1 and SGTP4 being the focus of studies as the only two displaying functional glucose transport activity (Skelly *et al*., 1994). SGTP1 is found in the majority of schistosome life stages, whereas SGTP4 is specifically present in the definitive host resident life stages (somules to adult worms) (Skelly and Shoemaker, 1996). Whilst both transporters are found in the tegument of somules and adult worms and their distribution appears consistent along the length of male and female adult worms, there is a crucial difference in their specific localisation within these life stages. SGTP1 is located at the basal tegument membrane and within the parasite body, whereas SGTP4 is found specifically at the apical tegument membrane, indicating that SGTP4 interacts initially with host glucose at the parasite surface to facilitate diffusion into the worm (Skelly and Shoemaker, 1996).

5.3.1 SGTP4 in the apical tegument membrane

Close examination of overlay images showing SGTP4 and filamentous actin confirm that in *S. mansoni* somules and adult worms, SGTP4 is expressed exclusively in the apical membrane (Figure 5.4) as reported by Skelly and Shoemaker (1996). At 1 h post-transformation, SGTP4 was observed in discontinuous patches around the apical membrane of somules. During this stage of SGTP4 evolution at the parasite surface, areas could be identified where the glucose transporter was erupting from sub-tegumental cytons (Figure 5.4 (inset)).

In adult worms, SGTP4 expression at the apical membrane is well established and single z scans of the male and female tegument reveal a narrow space between SGTP4 localisation and the sub-tegumental muscle layer, indicating that no SGTP4 is present in the basal tegument membrane adjacent to the muscle.

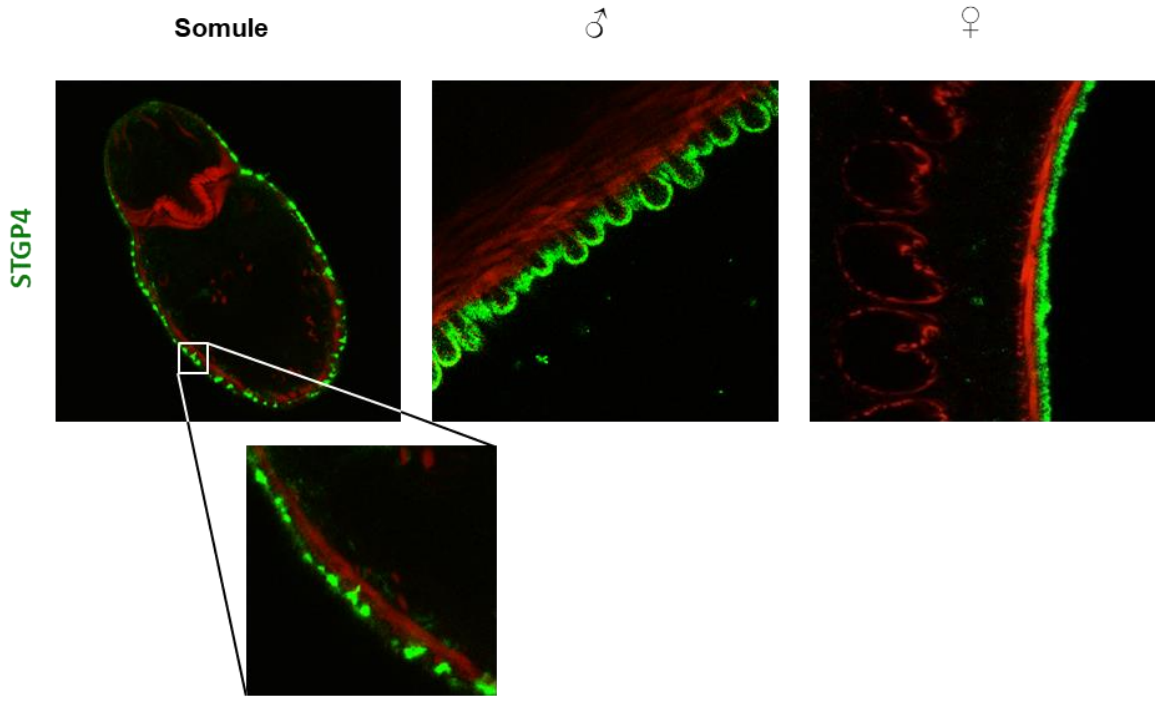

***Figure 5.4* SGTP4 is expressed exclusively in the apical tegument membrane of *S. mansoni* somules and adult worms.** Single z scans of a somule, male and female adult worms stained with anti-SGTP4 antibodies (green) and filamentous actin (red).

Having demonstrated that Akt in *S. mansoni* host-resident life stages is primarily localised within the parasite tegument and is activated by host insulin (Chapter 3), the possibility that Akt is linked to the expression of SGTP4 and schistosome glucose uptake was explored. This hypothesis was further supported by evidence of the immediate evolution of SGTP4 at the somule surface after transformation (Skelly and Shoemaker, 1996), and the fact that human Akt is already known to play a role in glucose uptake (Schultze *et al.*, 2012).

5.3.2 Akt regulates the surface expression of SGTP4 in somules

As reported by Skelly and Shoemaker (1996), SGTP4 expression begins after cercariae have started to transform into somules with SGTP4 evolving at the surface of the parasite within hours. Hence, to establish whether or not Akt influences SGTP4 expression, freshly-shed cercariae were incubated in water at room temperature with Akt Inhibitor X for 60 min to enable the inhibitor to penetrate the cercaria prior to transformation. Following tail detachment, somules were suspended in RPMI and Akt Inhibitor X, incubated at 37 °C, and samples at 30, 60 and 120 min post-transformation processed for western blotting with anti-SGTP4 and anti-phospho Akt (Thr^{308}) antibodies. The

temperatures used aimed to replicate the conditions the parasite would experience during host location/infection. At 30 min, there was a relatively low level of SGTP4 expression in the absence of the inhibitor, which increased substantially after 60 min. However, treatment of somules with 10 µM Akt Inhibitor X, which reduced Akt activation, resulted in a striking suppression of SGTP4 expression 60 min and 120 min post transformation (Figure 5.5), when compared to those not exposed to the inhibitor. These results provided the first indication of a link between Akt and SGTP4 expression in the developing parasite.

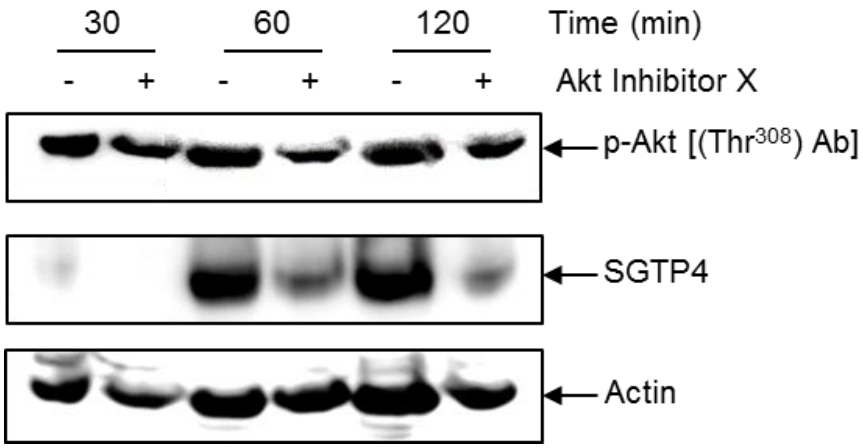

Figure 5.5 **Inhibition of Akt reduces SGTP4 expression in *S. mansoni* somules.** Cercariae were treated for 1 h with Akt Inhibitor X (10 µM) (or not, control) at room temperature immediately after being shed from snails. The cercariae were then subject to mechanical transformation and were placed in RPMI along with 10 µM Akt Inhibitor X or not. The samples were then incubated at 37°C, 5% CO_2, for increasing durations. Somule proteins were then processed for western blotting with anti-phospho Akt (Thr^{308}) antibodies before re-probing with anti-SGTP4 antibodies; Blots were also probed with ant-actin antibodies to confirm similar protein loading between samples. The blot shown is representative of four experiments.

5.3.3 Inhibition of Akt blunts SGTP4 expression at the somule surface

To determine the effect of Akt inhibition on the localisation of SGTP4 in somules immunohistochemistry and confocal laser scanning microscopy were employed. Over the three times points studied (30, 60 and 120 min), in the control samples SGTP4 expression was seen to evolve across the somules in an anterior to posterior direction, after which it appeared to migrate from the sub-tegumental cyton network to the tegument surface (Figure 5.6). This was concurrent with previous research by Skelly and Shoemaker (1996). In contrast, the parasites treated with 10 µM Akt Inhibitor X showed little to no SGTP4 expression until 120 min, where low levels of SGTP4 appeared to remain in the sub-tegumental cyton network (Figure 5.6). Thus Akt inhibition appears to

supress not only the expression of SGTP4 but its transport to the parasite surface over 120 min.

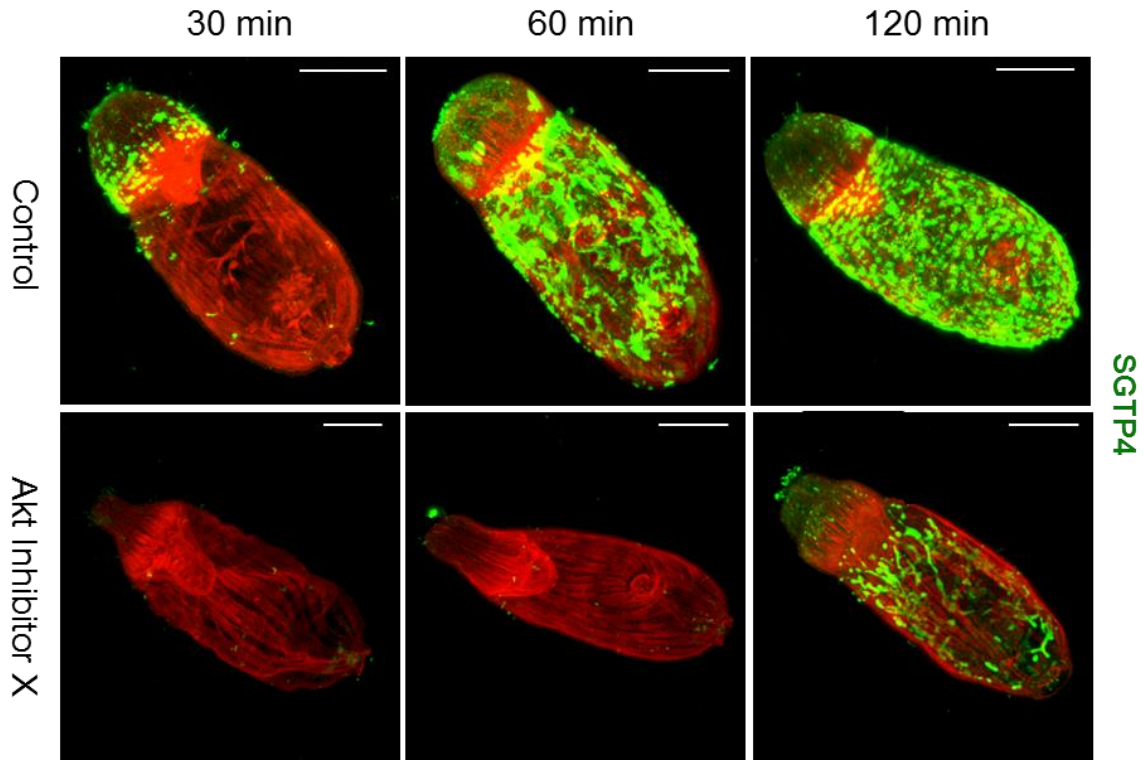

Figure 5.6 **Inhibition of Akt supresses the expression of SGTP4 at the *S. mansoni* somule surface during transformation.** Cercariae were treated for 1 h with Akt Inhibitor X (10 µM) or not (control), at room temperature immediately after being shed from snails. The cercariae were then subject to mechanical transformation and were placed in RPMI containing 10 µM Akt Inhibitor X or not. The samples were then incubated at 37°C, 5% CO2, for increasing durations. Somules were fixed in 4% paraformaldehyde and processed for immunohistochemistry with anti-SGTP4 antibodies (green); rhodamine phalloidin was also used to stain filamentous actin (red). Maximum projection images were captured for somules at each time point and for each treatment. Laser setting were maintained the same throughout. Bar: 25 µm.

To quantify the development of SGTP4 at the tegument of somules, individual z-sections were captured through 30 somules at each time point (15 control/15 inhibited) and Leica image analysis software used to determine the intensity of the signal from the SGTP4 staining at the tegument. To illustrate the overall variability in SGTP4 staining pattern between treatments, at each duration, a montage of all z-sections was constructed for comparison (Figure 5.7). For quantification, lines were drawn through the anterior and posterior quarters of each somule and the fluorescence intensity recorded (Figure 5.8 A); the charts under each image (Figure 5.8 A) represent the signal intensity measured across each line, with peaks at both ends indicating the increase in signal at the intersection with the tegument. Analysis of the fluorescence intensity data (Figure 5.8 B),

revealed that Akt Inhibitor X significantly reduced SGTP4 expression at the somule tegument ($p \leq 0.001$) at both anterior and posterior ends (by 75% and 88%, respectively at 120 min), with the exception of the 30 min time point where the posterior of the somule showed minimal SGTP4 signal in the control.

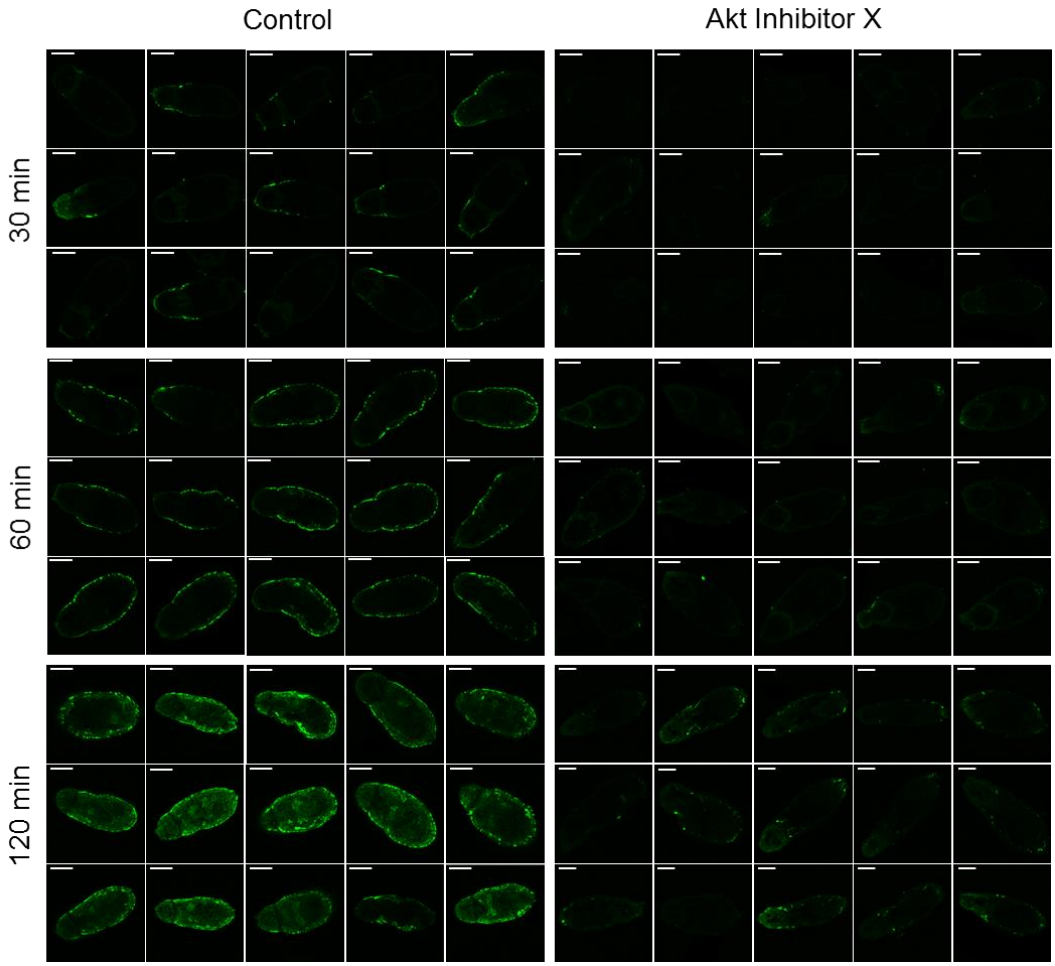

***Figure 5.7*SGTP4 localisation is consistent across all 15 individual *S. mansoni* somules.** Displaying only the green laser channel, z-section images were captured through 30 anti-STGP4 stained (green) somules per time point (15 control/15 treated). Tiling of images demonstrates the consistency of SGTP4 expression with and without inhibition. Bar: 25 µm.

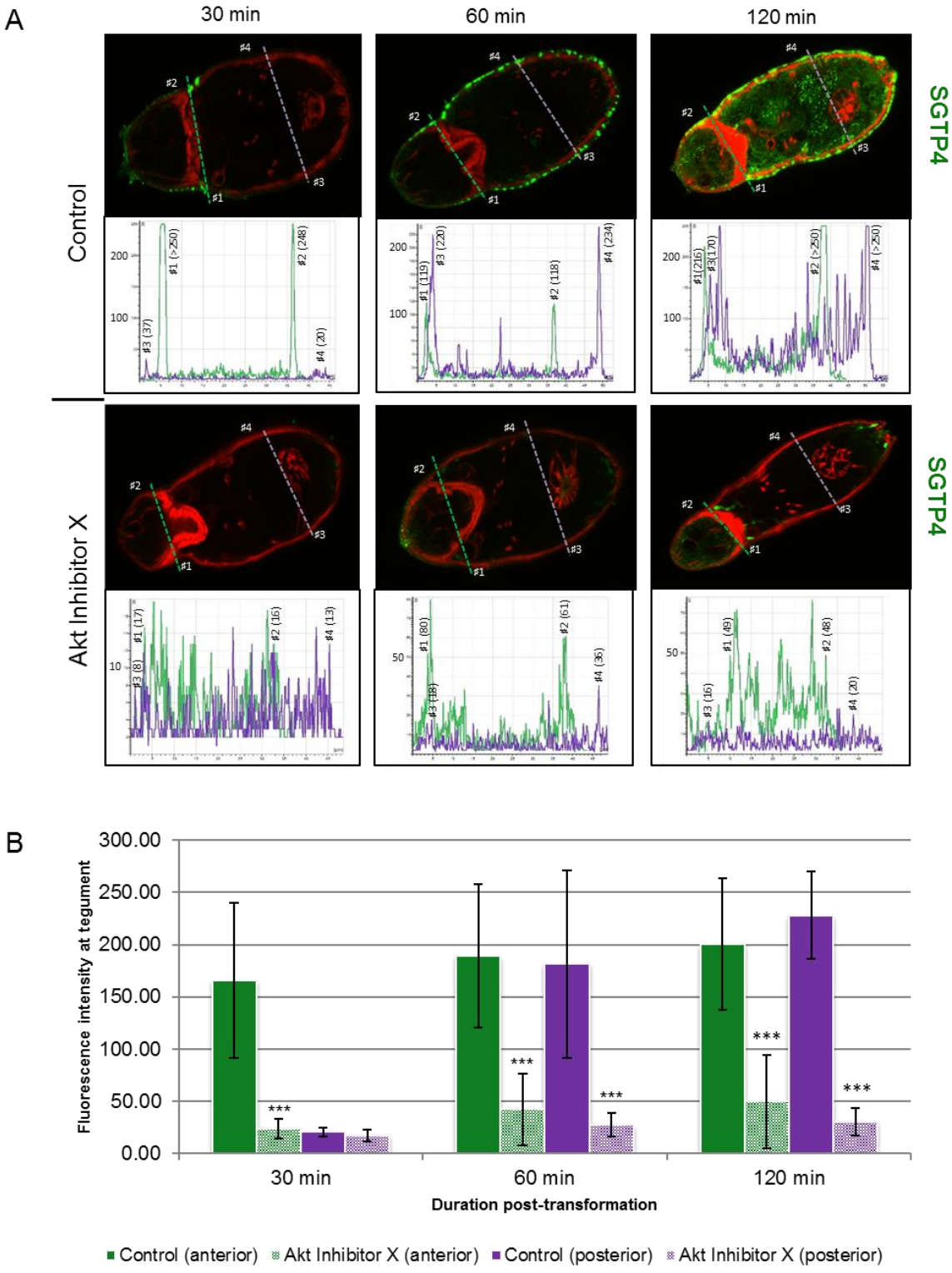

Figure 5.8 **Akt Inhibitor X attenuates SGTP4 expression in *S. mansoni* somules.** **A.** Immunohistochemistry and expression analysis of SGTP4 at the tegument towards the anterior (lines ♯1 - ♯2) and posterior (lines ♯3 - ♯4) of the transforming somules, images are single z-sections through the centre of somules. **B.** Mean fluorescence intensity of SGTP4 expression at the tegument was calculated over time (graph; mean ±S.D., n=30 per treatment); ***p≤0.001 (ANOVA).

5.3.4 Glucose Assay in Somules

Having established that the developmental expression of SGTP4 in somules could be impeded by treatment with Akt Inhibitor X, a glucose assay was used to monitor glucose uptake, with and without inhibitor treatment. A plate-based Glucose Uptake-Glo bioluminescence assay was used to measure the ability of the parasites to import glucose based on the detection of 2-deoxyglucose-6-phosphate (2DG6P); 2DG6P is processed by mammalian cells in the same manner as glucose (Yoshiyama *et al.*, 1995).

Here, somules were treated as for the immunohistochemistry experiments although only 60 min and 120 min time points were done. Over three independent assays, Akt inhibitor X treatment supressed mean relative glucose uptake by 56% and 74% at 60 min and 120 min respectively (Figure 5.9; p≤0.001).

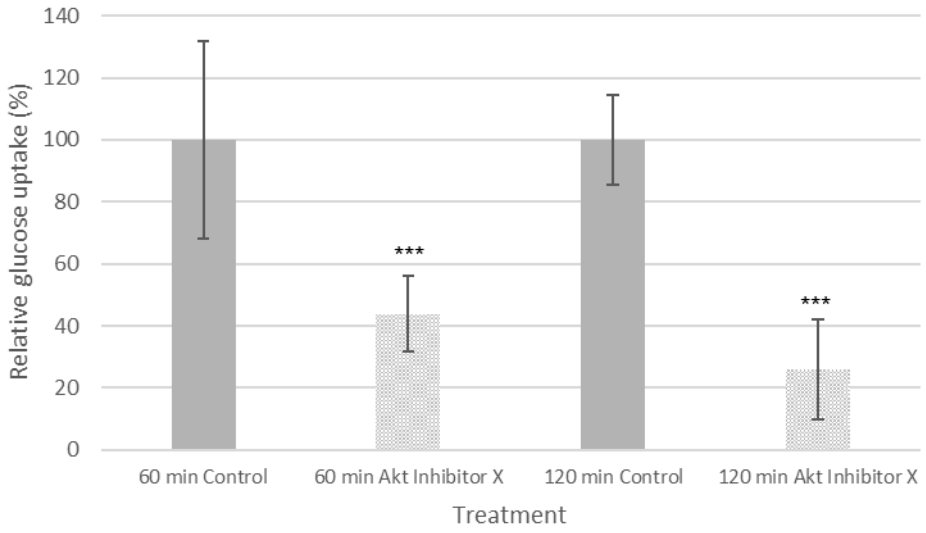

Figure 5.9 **Akt Inhibitor X reduces glucose uptake over time in *S. mansoni* somules.** Cercariae (1000 per treatment) were treated for 1 h with Akt Inhibitor X (10 μM) or not (control), at room temperature immediately after being shed from snails. The cercariae were then subject to mechanical transformation and were placed in RPMI containing 10 μM Akt Inhibitor X or not. The samples were then incubated at 37°C, 5% CO_2, for 60 min or 120 min, washed in PBS and subjected to glucose uptake assay in the presence of Akt Inhibitor X. Luminescence readings were taken at 1h. Mean relative glucose uptake was calculated from three independent experiments (±S.D.); *** p≤0.001 (ANOVA).

5.4 The Role of SGTP4 in Adult *S. mansoni*

5.4.1 RNAi of Akt attenuates SGTP4 expression in adult worms

To definitively show that Akt signalling is linked to SGTP4 expression, RNAi of Akt was performed. Male and female adult worms were separately electroporated with siRNAs targeting Akt (see section 3.4) and were then maintained in Opti-MEM for five days. In both sexes, knockdown of Akt protein expression was successful (Figure 5.10). Furthermore, knockdown of Akt resulted in a marked reduction in SGTP4 expression (Figure 5.10) - 59% and 47% in male and female worms, respectively based on duplicate experiments. This demonstrates that SGTP4 expression is influenced by signalling *via* the Akt pathway.

5.4.2 SGTP4 in adult S. mansoni *is affected by Akt inhibition*

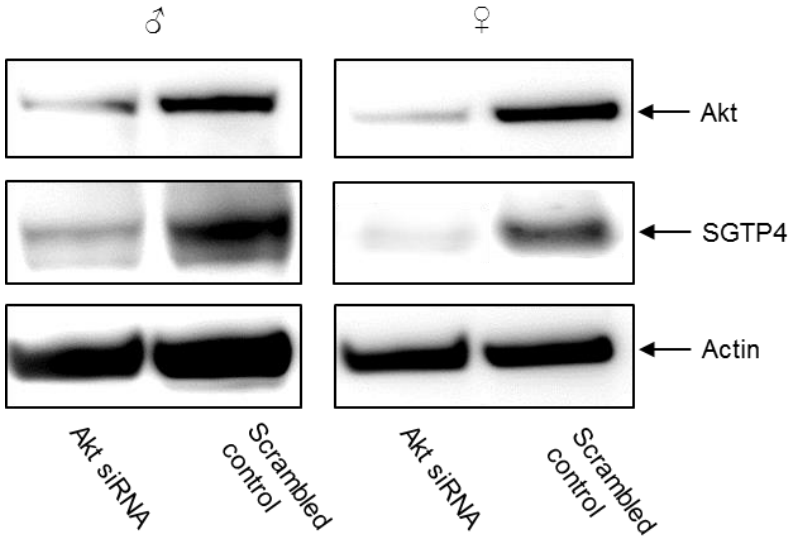

Figure 5.10 **SGTP4 expression is reduced in adult *S. mansoni* by the knockdown of Akt.** Adult male and female worms were processed separately for RNAi. Worms were electroporated with SiRNA targeting Akt and after 5 days, worms were processed for western blotting with anti-Akt antibodies before stripping the membranes and re-probing with anti-SGTP4 and subsequently anti-actin antibodies, with anti-actin used as a loading control. The blot is representative of results obtained in two independent experiments.

Experiments next aimed to determine whether Akt plays a role in glucose uptake in adult worms by affecting the overall expression of SGTP4 and its maintenance at the parasite surface. Male and female worms were separated and treated overnight (20 h) with 10 µM Akt Inhibitor X. Because of the tegumental turnover that exists in adult schistosomes, it was hypothesised that existing SGTP4 would be shed from the parasite surface, and that new de novo expression of SGTP4 would be supressed by this longer-term Akt inhibition. Inhibition of SGTP4 expression was more apparent in the adult female worms compared to the males despite Akt not being completely inhibited (Figure 5.11). The

reduced inhibition of Akt is likely due to the low basal level of Akt present in female worms. In male worms, an apparent decrease in both phosphorylated Akt and SGTP4 expression was observed over two experiments.

As with the somules, the next experiments aimed to evaluate the effects of Akt inhibition on the localisation of SGTP4 at the parasite surface. Male and female worms were incubated for 20 h in Akt Inhibitor X then fixed and processed for immunohistochemistry using anti-SGTP4 antibodies. Confocal laser scanning microscopy revealed that in both sexes, SGTP4 was observed primarily in the tegument (Figure 5.12). Akt Inhibitor X-treated worms displayed a weaker signal although SGTP4 expression at the parasite surface was not completely supressed. This mirrors the outcomes of the expression analysis by western blotting (Figure 5.11). Thus, the residual SGTP4 expression observed could be due to partial Akt inhibition or sustained presence of SGTP4 at the tegument surface due to low levels of tegumental turnover in culture, or both.

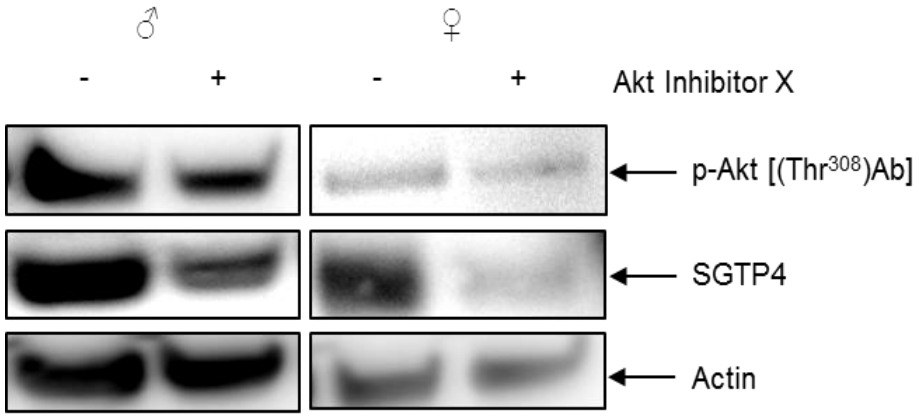

***Figure 5.11* SGTP4 expression is inhibited in adult *S. mansoni* by Akt Inhibitor X.** Adult male and female worms were separated approximately 24 h post perfusion. 10 worms were treated (or not) with 10 µM Akt Inhibitor X in RPMI overnight (20 h) and incubated at 37°C, 5 % CO_2. Worms were washed, homogenised and processed for western blotting with anti-phospho Akt (Thr^{308}) antibodies before stripping and re-probing with anti-SGTP4, and anti-actin antibodies to confirm that similar amounts of protein were loaded from each sample. The blot shown is representative of those obtained in two independent experiments.

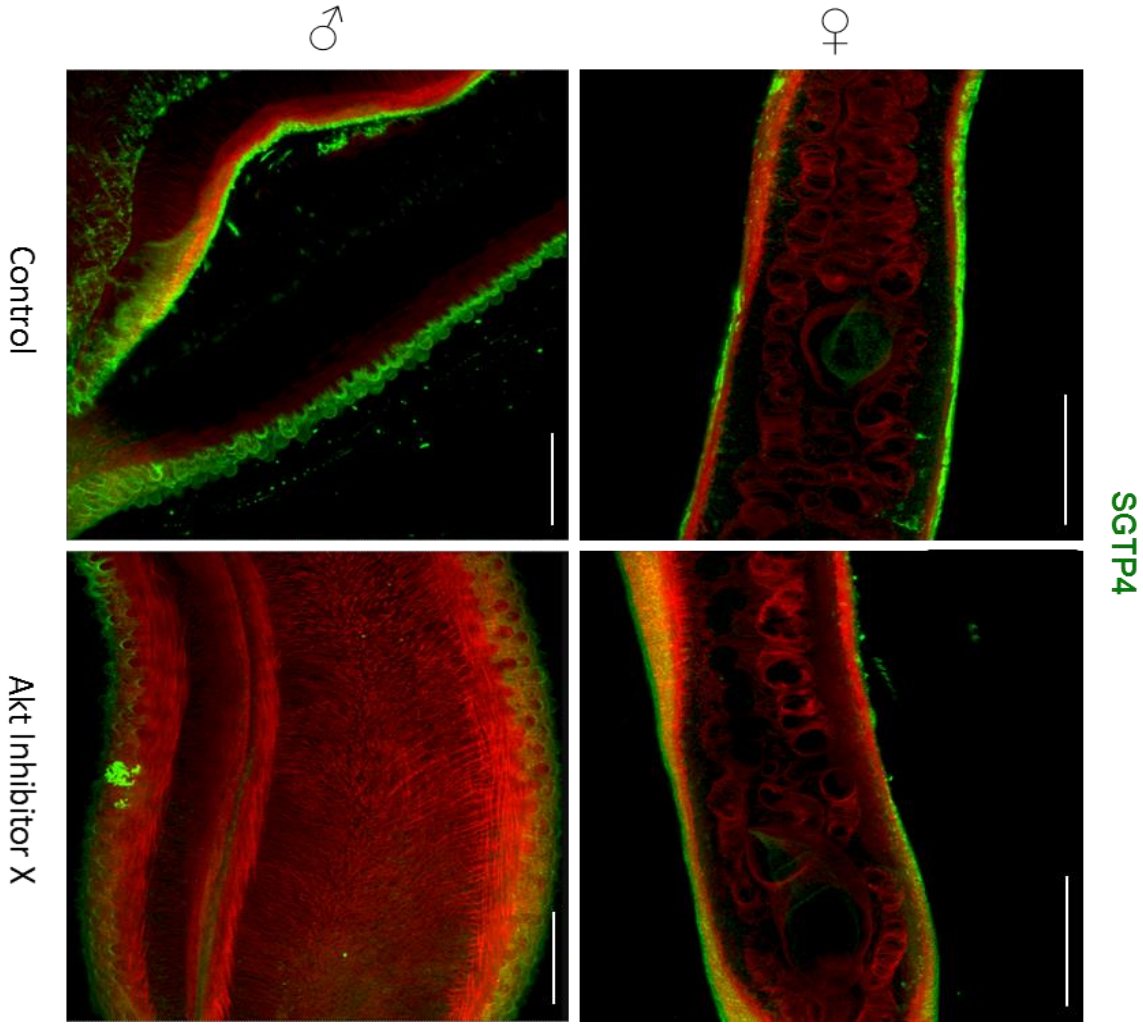

Figure 5.12 **Akt Inhibitor X reduces SGTP4 expression at the surface of adult *S. mansoni*.** Adult male and female worms were treated separately for 20 h in RPMI supplemented with 10 µM Akt Inhibitor X. Worms were fixed and processed for immunohistochemistry with anti-SGTP4 antibodies (green). Rhodamine phalloidin was used to stain filamentous actin (red). Bar: 75 µm.

5.4.3 Glucose Assay in Adult Worms

The Glucose Uptake-Glo bioluminescence assay was next used with adult worms to

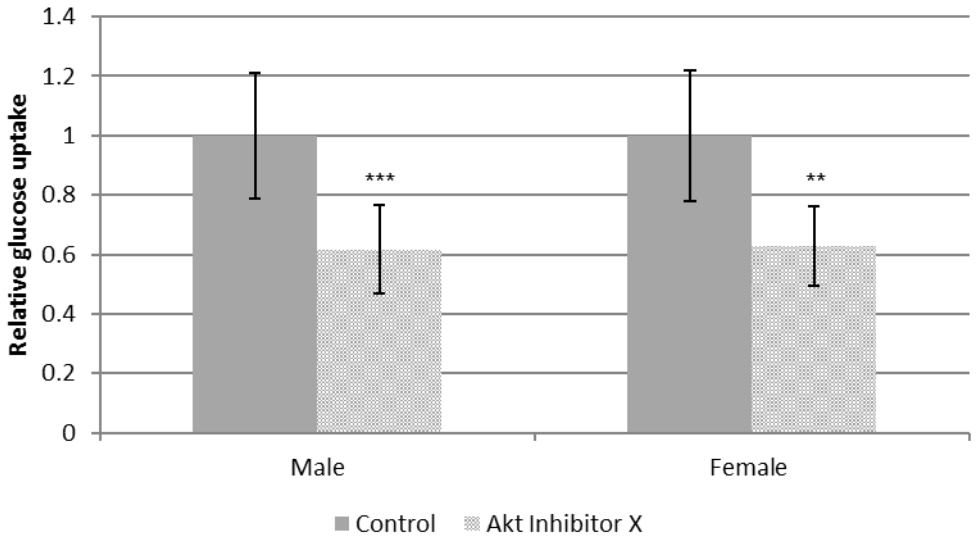

Figure 5.13 **Glucose uptake in adult *S. mansoni* is reduced by Akt Inhibitor X treatment.** Males and female worms were incubated separately overnight (20 h) in 10μM Akt Inhibitor X or not (control), at 37°C, 5% CO_2. Worms were then subjected to a glucose uptake assay in the presence of Akt Inhibitor X or not. Luminescence readings were taken at 30 min and mean relative glucose uptake was calculated compared to the controls (±S.D.; n=4 for males, n=5 for females). **p≤0.01, ***p≤0.001 (ANOVA).

measure glucose uptake in both sexes when subjected to Akt inhibition. Worms were incubated for 20 h with Akt Inhibitor X then assayed (1 male or 3 females per well). A significant decrease in glucose uptake of 38 % ($p \leq 0.01$) and 37 % ($p \leq 0.01$) was observed in male and female worms, respectively (Figure 5.13). To determine protein levels between male and female worms in the assay, the same worms were processed for western blotting with anti-actin antibodies, and the glucose uptake assay results were adjusted accordingly.

Summary:

This chapter has encompassed novel research conducted on the schistosome tegument. Initial observations revealed that in somules and adult worms, phosphorylated Akt is localised primarily in the tegument (Chapter 3, section 3.4). This discovery prompted further investigation into the role that Akt might be playing in this host-interactive layer.

Initially, western blotting of adult worm tegument membrane fractions confirmed the presence of Akt in this layer and demonstrated that insulin significantly increased tegumental Akt phosphorylation. Following this, observational studies using light microscopy revealed that the tegument surface is disrupted following treatment with increasing concentrations of Akt Inhibitor X. Specifically, the tubercles in worms exposed to 10 μM inhibitor appeared larger and less uniform than their untreated counterparts.

Next a possible link between Akt activation in the tegument and schistosome glucose transporter expression was evaluated. In somules, SGTP4 expression at the tegument surface was significantly supressed following Akt inhibition, as observed using immunolocalisation/confocal microscopy and western blotting. Further analysis confirmed that the intensity of SGTP4 expression at both anterior and posterior ends of the somules was substantially attenuated by incubation in Akt inhibitor X. Furthermore, glucose uptake assays revealed that Akt Inhibitor X treatment reduced glucose transport in somules with 74% less glucose imported into the parasite after a 2 h incubation with the inhibitor.

In adult worms, RNAi established a definitive link between the activated Akt kinase and expression of the facilitated glucose transporter, SGTP4. SiRNA-mediated knockdown of female and male worm Akt resulted in reduced expression of the transporter protein (47% and 59% respectively). Western blotting demonstrated inhibition of SGPT4 expression after treatment with Akt Inhibitor X and immunohistochemistry demonstrated the apparent reduction in SGTP4 at the tegument surface. As with somules, glucose uptake in adults was reduced significantly, by 38% and 37% in male and female worms respectively, following Akt inhibitor X treatment.

Collectively these results demonstrate a novel role for Akt in *S. mansoni* glucose import processes, which significantly advances our understanding of schistosome biology, particularly in relation to host-parasite interactions.

6

Results 4 – A putative role for Akt in *S. mansoni* cercariae host invasion

Of all the schistosome life cycle stages, cercariae have possibly the most challenging task – to infect a mammalian definitive host, especially given that this larval stage is viable for up to 72 h (Gryseels *et al.*, 2006). How the parasite finds and enters the host was unknown until three decades ago, when studies began characterising the chemical and environmental signals, including various host skin elements, sensed by cercariae (Granzer and Haas, 1986; Ressurreição *et al.*, 2015). Among the chemical skin elements, cercariae behaviour is influenced by L-arginine and fatty acids such as linoleic acid (LA) (Haas *et al.*, 2002; Ressurreição *et al.*, 2015). Also known to be a key factor in host penetration is the cercarial tail, serving a purely motor-functional role (Walker, 2011). Given that L-arginine has been demonstrated to be an effective stimulator of Akt activation (Chapter 3), and that activated Akt/phosphorylated Akt substrates (Chapter 4) have been shown to be present in the tail, the possible link between Akt activation status and cercarial movement/host sensing was explored.

6.1 *S. mansoni* Cercariae Display Distinct Phosphorylated Akt Localisation Patterns

During immunohistochemical analysis of cercariae (Chapter 3), single z scans through the parasite revealed distinct spots of phosphorylated Akt close to the surface of the parasite that appeared in pairs. Two pairs of spots were consistently seen in the head region, with the anterior pair somewhat larger than the posterior pair (Figure 6.1 A1 c.f. A2). Given previous work on the structure of schistosome life stages (Senft *et al.*, 1961; Bahia *et al.*, 2006), these spots were presumed to be flame cells. Flame cells are ciliated cells, localised in the basal membrane, forming part of the protonephridial system (Sato *et al.* 2002). The protonephridium functions as a means of excreting waste products (Valverde-Islas *et al.*, 2011) and the flame cells are the cellular termini, producing excretory vesicles (Sato *et al.* 2002). Knowledge of this excretory system is limited due to lack of techniques to study excretion (Valverde-Islas *et al.*, 2011).

Along the length of the cercaria tail, a number of ‘hotspots’ of phosphorylated Akt were also observed, with approximately six pairs seen in all samples visualised. A pair was also noted close to the head-tail junction, although this was seen less consistently. Given that phosphorylated Akt was also observed in the tail nervous system (Chapter 3) the possibility remains that the identified punctate regions of intense Akt activation (Figure 6.1 B) could be due to the presence of sensory receptors indicating that the tail may also participate in host localisation in response to certain cues.

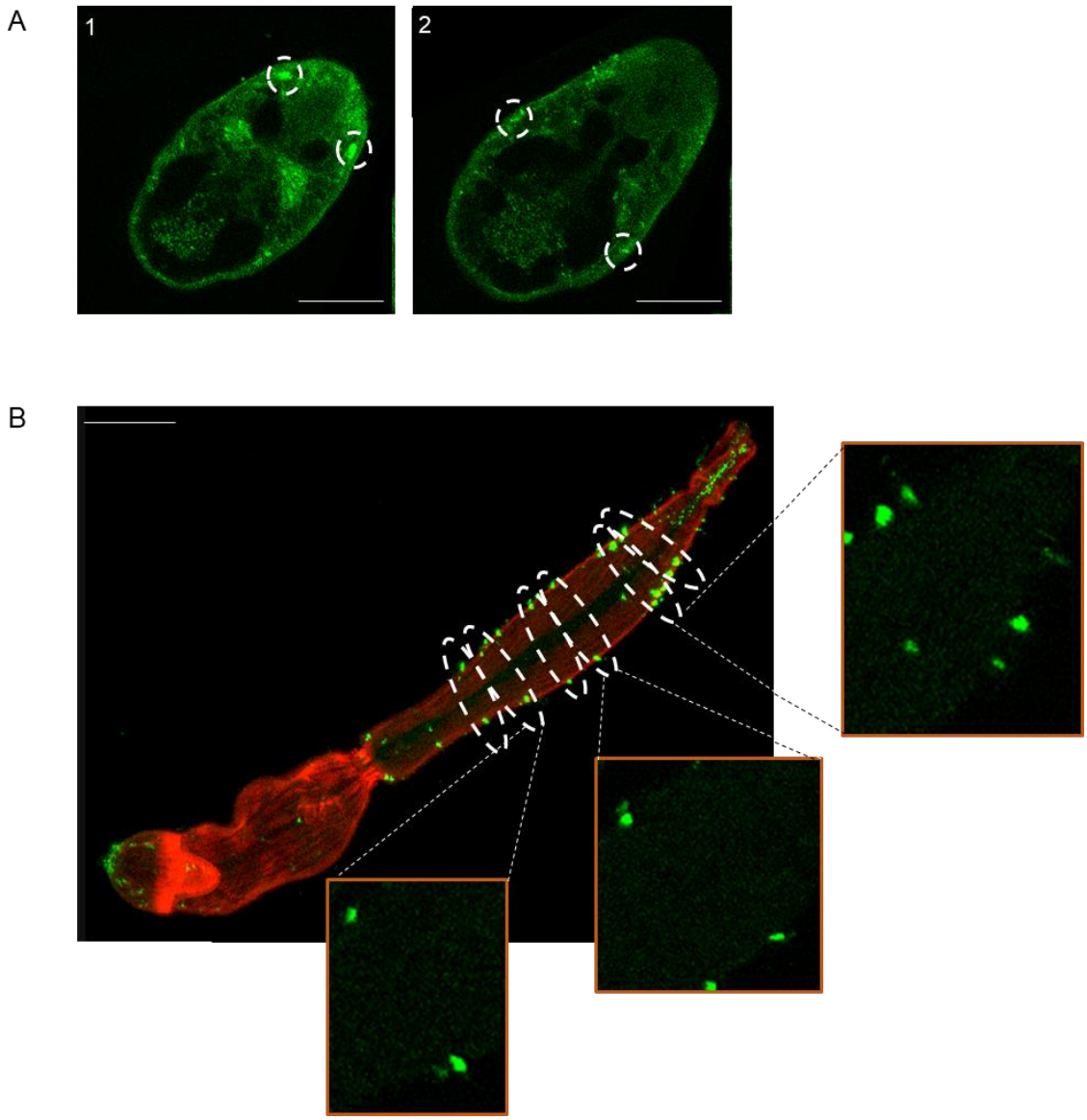

Figure 6.1 **Akt activation near the surface of cercariae occurs in multiple distinct punctate regions.** Freshly shed cercariae were processed for immunohistochemistry with anti-phospho Akt (Thr^{308}) primary and Alexa Fluor 488 secondary antibodies (green). Rhodamine phalloidin was used to stain filamentous actin (red). **A1.** A pair of distinct punctate regions at the anterior of the head. **A2.** A second pair of punctate regions located posteriorly. **B.** Pairs of punctate Akt activity in the cercarial tail. The images are representative of the staining pattern observed across multiple specimens in several independent experiments. Bar: 50 µm.

6.2 Exposure of Cercariae to Host Factors

6.2.1 The effects of L-arginine on Akt phosphorylation in cercariae

As a mammalian skin component, L-arginine has been reported to play an important role in the location and penetration of suitable hosts by cercariae (Granzer and Haas, 1986; Haas *et al.* 2002). In previous assays using L-arginine, the optimum time point for

stimulation of Akt in mechanically transformed 24 h somules when measured by western blotting was 30 min (Chapter 3, Section 3.5.3). To understand how cercariae might respond differently to somules, cercariae were exposed to L-arginine for increasing durations and processed for western blotting and immunohistochemistry. The results from immunohistochemical analysis indicated a minor increase in the phosphorylation of Akt from 1 – 10 min (Figure 6.2 A). The increased Akt activation occurred mainly in the tail although at 10 min, Akt in the head region also appeared more phosphorylated. From 15 min onwards, levels of phosphorylated Akt appeared comparable to the control. In contrast, western blotting revealed that the phosphorylation of Akt increased at 5 min exposure and was sustained until 30 min, declining to basal levels thereafter (Figure 6.2 B).

6.2.2 The effects of linoleic acid on Akt phosphorylation in cercariae

Linoleic acid (LA) is a polyunsaturated fatty acid component of human skin, which has been shown previously to stimulate signalling *via* more than one kinase pathway in *S. mansoni* (Ressurreição *et al.*, 2015). Given that Akt had been located at the oral tip of cercariae (Chapter 3, section 3.4.1) it was hypothesised that Akt may be stimulated within cercariae upon contact with LA.

As with L-arginine, the effect of LA on cercariae Akt activation was investigated using both western blotting and immunohistochemistry. Confocal laser scanning microscopy of stained cercariae revealed inconsistent localisation of phosphorylated Akt. There are noticeable increases in Akt activity at 5 min and 15 min compared to the control, with minimal Akt activation seen at the remaining time points (Figure 6.3 A), raising the possibility that Akt is activated in waves in response to L-arginine rather than continuously. The increase in Akt phosphorylation at 5 and 15 min was seen exclusively in the tail and at the oral tip of the cercariae, highlighting the possible importance of these areas in the series of events leading to host invasion. At 15 min, the structures at the oral tip are present as a ring of small nodules, clearly displaying phosphorylated Akt. Previously, these structures were only seen with anti-Akt antibodies (section 3.5). Western blot results showed only a moderate increase in Akt phosphorylation up to 30 min before levelling at 45 min exposure (Figure 6.3 B).

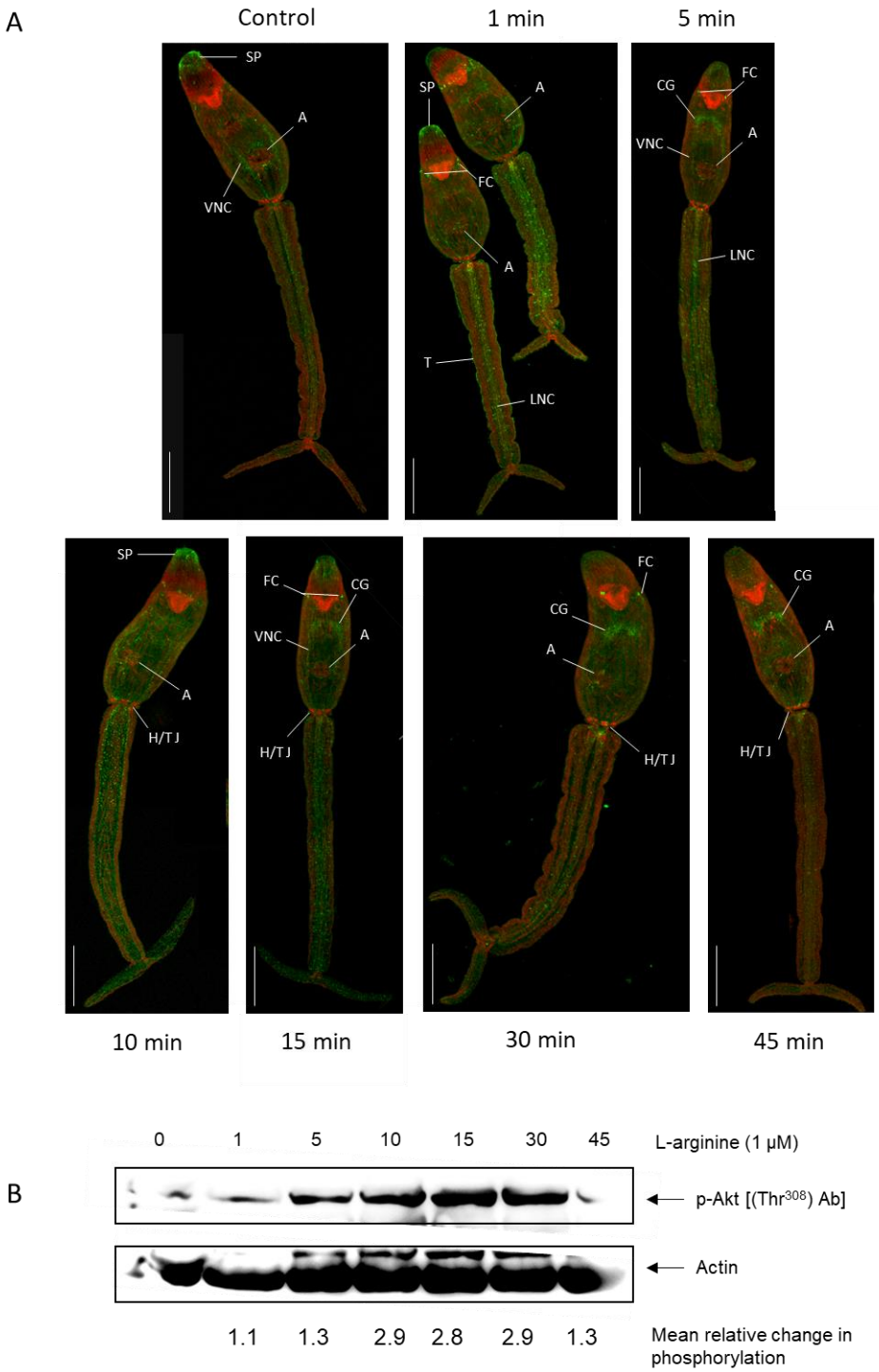

Figure 6.2 **L-arginine stimulates Akt phosphorylation in *S. mansoni* cercariae.** Freshly shed cercariae were exposed to 100 µM L-arginine for increasing durations (1 – 45 min) or not (control). **A.** Cercariae were processed for immunohistochemistry with anti-phospho Akt (Thr^{308}) primary and Alexa Fluor 488 secondary antibodies (Green). Rhodamine phalloidin was used to stain filamentous actin (red). All images are maximum projections, representative of >40 cercariae. Bars: 50 µm **B.** Cercariae were processed for western blotting with anti-phospho Akt (Thr^{308}) antibodies. Blots were then stripped and re-probed with anti-actin antibodies to determine protein loading levels between the lanes. Blot is representative of two experiments. A – acetabulum, CG – cephalic ganglia; FC – flame cell; H/T J – head-tail junction, LNC – longitudinal nerve cord; SP – sensory papillae; T – tegument; VNC – ventral nerve cord.

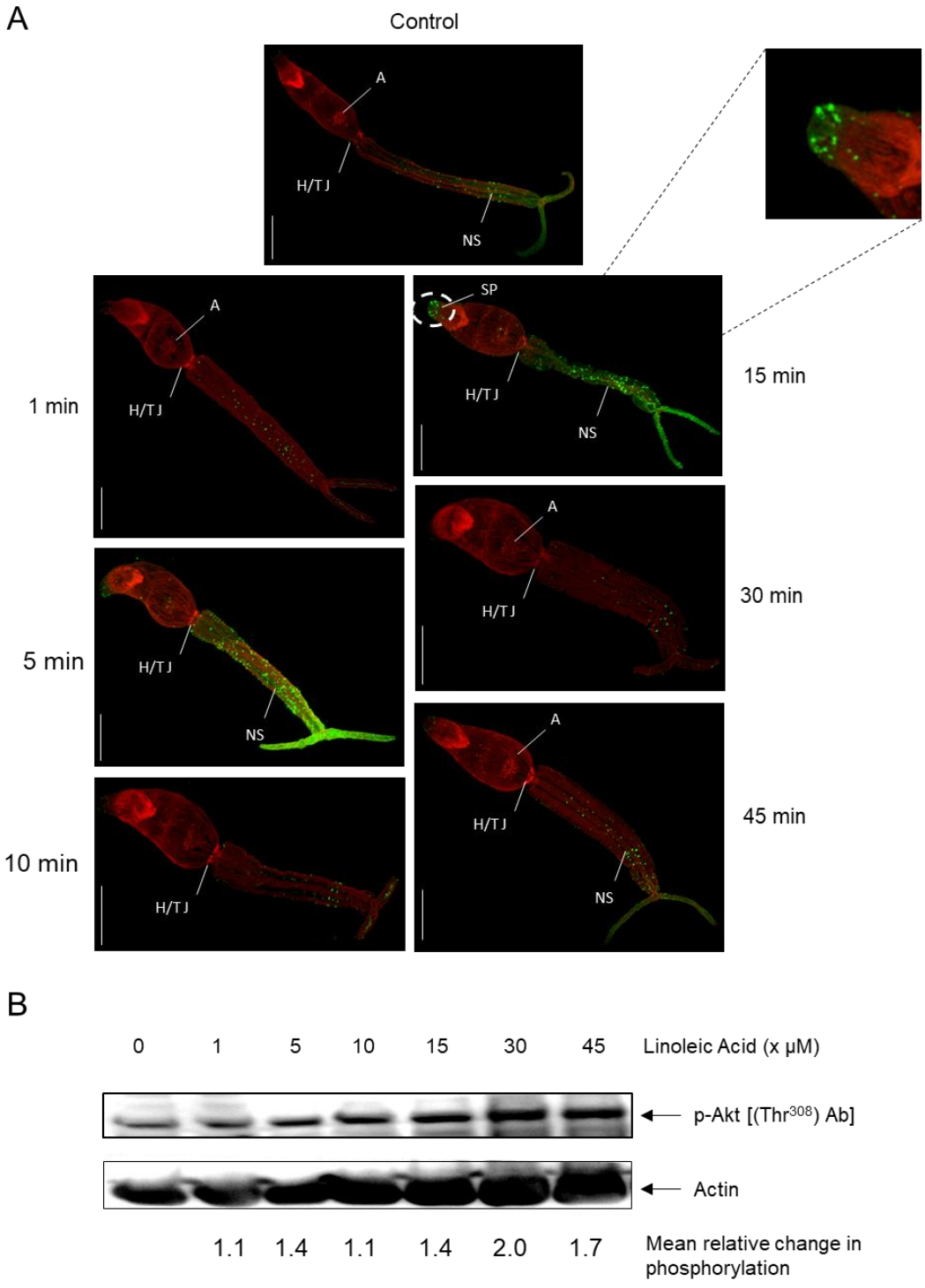

Figure 6.3 **Linoleic acid treatment reveals inconsistent Akt phosphorylation in *S. mansoni* cercariae.** Freshly shed cercariae were added to a well plate previously treated with linoleic acid for increasing times. **A.** Cercariae were processed for immunolocalisation with anti phospho-Akt (Thr^{308}) antibodies. All images are maximum projections, bars: 50 µm. **B.** Cercariae were processed for western blotting with anti phospho-Akt (Thr^{308}) antibodies. Blots were then stripped and re-probed with anti-actin antibodies to determine protein loading. Blot shown is representative of three experiments. A – acetabulum, H/T J – head-tail junction, NS – nervous system, SP – sensory papillae.

6.3 Akt Inhibitor X treatment

Having evaluated the effects of mammalian skin components on the stimulation of cercarial Akt, next, the response to a previously validated inhibitor (Chapter 3) was explored. After exposure of cercariae to 10 µM Akt Inhibitor X for 1 h, phosphorylated Akt was considerably less evident in intact cercariae as determined by immunolocalisation; very little Akt activation remained in the tail and staining was no longer apparent in the head region (Figure 6.4 A). The discrepancy between the levels of Akt phosphorylation seen in the controls of the stimulation and inhibition experiments (Figures 6.2 - 6.4) are likely due to differences in staining performed on different days. However, the control and treated cercariae in each case were stained at the same time, allowing comparisons within, but not between, experiments; in all cases the laser settings remained constant for a specific experiment. Western blotting demonstrated similar

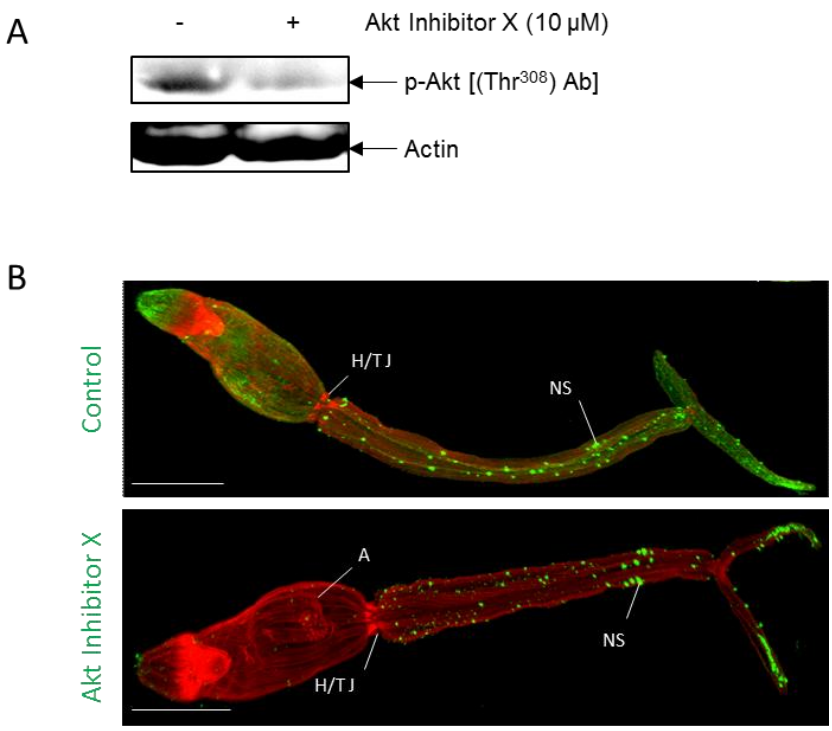

Figure 6.4 **Akt Inhibitor X treatment supresses Akt phosphorylation in *S. mansoni* cercariae.** Freshly shed cercariae were treated with 10 µM Akt Inhibitor X for 1 h. **A.** Cercariae were processed for immunohistochemistry with anti phospho-Akt (Thr^{308}) primary and Alexa Fluor 488 secondary antibodies (green). Rhodamine phalloidin was used to stain filamentous actin (red). Images are maximum projections. Bars: 50 µm. **B.** Cercariae were processed for western blotting with anti phospho-Akt (Thr^{308}) antibodies. Blots were then stripped and re-probed with anti-actin antibodies to determine protein loading between lanes. The blot shown is representative of those obtained in three experiments. A – acetabulum, H/T J – head-tail junction, NS – nervous system.

results to those seen with confocal microscopy; a reduction in Akt phosphorylation of ~61 % was seen, measured over three experiments.

6.4 The Effect of Akt Pathway Stimulation and Inhibition on Cercarial Swimming

Given the localisation of phosphorylated Akt in cercariae and its response to skin components, it was hypothesised that Akt might influence the swimming behaviour of cercariae. Movies were therefore recorded of cercariae exposed to L-arginine, linoleic acid, or Akt Inhibitor X and various parameters analysed.

The parasites were sampled from a beaker of freshly shed cercariae and a 100 µl droplet containing cercariae was pipetted onto the bottom of a Petri dish, to enable video capture of the entire droplet; treatments were delivered *via* a 1 µl drop of appropriately diluted stimulant or inhibitor. For each treatment, videos were taken at 1, 5, 10, 15, 30 and 45 min.

Thirty cercariae were analysed for each duration and the number of seconds each parasite demonstrated positive swimming action within a 30 s period was determined (Figure 6.5). Cercariae demonstrating contractile movements on the plate surface were not counted as swimming. The most effective treatments were L-arginine and Akt Inhibitor X, which had opposite effects on swim duration. The effect of L-arginine was rapidly apparent with the cercariae becoming highly agitated and swimming for significantly longer than the control parasites following exposure at 0 min ($p \leq 0.001$) (Figure 6.5). This lasted until approximately 20 min, after which the mean swim duration of treated cercariae dropped to control levels (Figure 6.5; Video 1).

Conversely, after 5 min treatment with 10 µM Akt Inhibitor X cercariae sank to the base of the Petri dish. Muscular twitching and contractile movements were seen but very few cercariae swam (Figure 6.5; Video 3). This effect was sustained throughout the 45 min of the experiment. When L-arginine was added to cercariae that had already been treated for 1 h with Akt Inhibitor X, no change in the state of the parasites was observed. Cercariae remained relatively non-motile on the plate surface.

Treatment with linoleic acid was performed separately and consequently a second control was done (Figure 6.5). Drops of water containing freshly shed cercariae were pipetted onto LA pre-coated glass cover slips, and movies captured in the same manner as before. Similarly to L-arginine, LA rapidly stimulated cercarial swimming and cercariae displayed an approximate 6-fold increase in swim duration after 1 min. However, this

activity decreased substantially from 5 min onwards, with a mean of 0.57 seconds swim time at 10 min, increasing slightly to 2.2 seconds at 30 min (Figure 6.5; Video 4).

Another curious observation was in control and L-arginine treated cercariae, their tail furcae appeared curled upwards. This was consistent across all cercariae in these treatments. However, in Akt Inhibitor X cercariae tails were unaffected and extended.

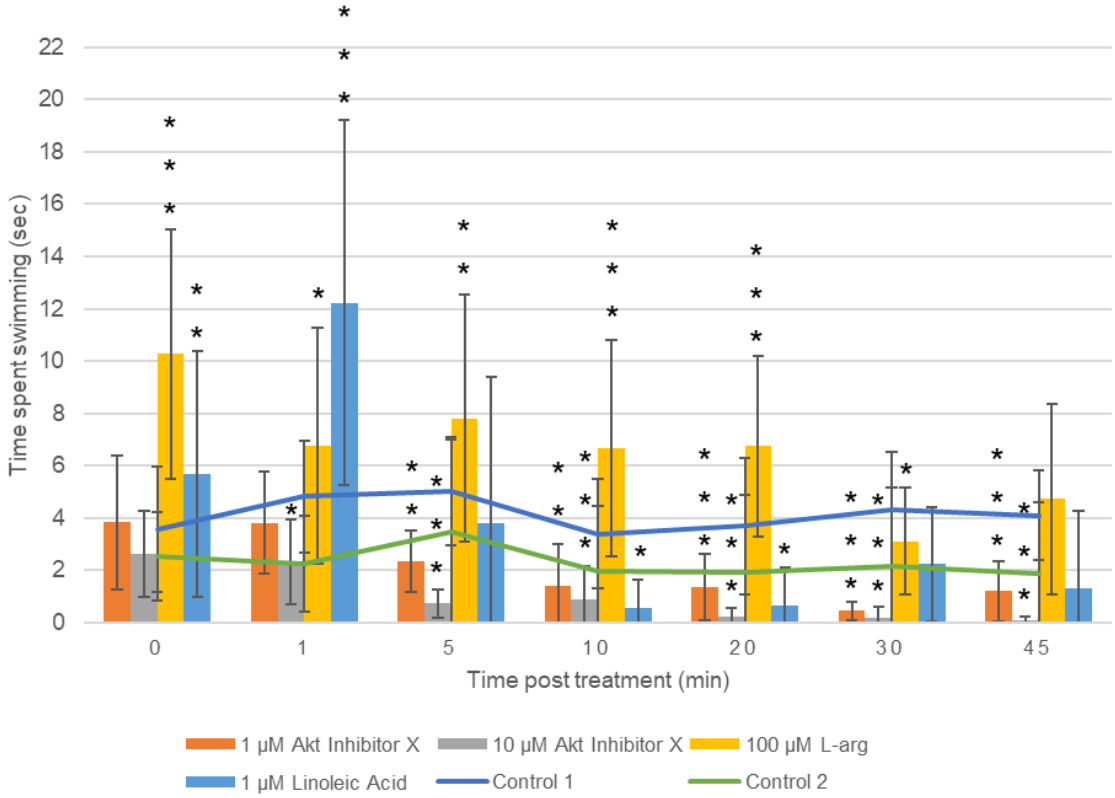

***Figure 6.5* Cercarial swim duration is affected by Akt Inhibitor X, L-arginine, and linoleic acid.** Freshly-shed cercariae were pipetted into a Petri dish, treatments added, and movies were captured immediately (0 min) and after increasing durations. The number of seconds that a cercaria was swimming in a 30 s time frame was then enumerated and the mean swim duration compared with that for the control cercariae (Control 1 for L-arginine and Akt Inhibitor X, and Control 2 for linoleic acid). (±S.D.; n = 30). *p≤0.05, **p≤0.01, ***p≤0.001 (ANOVA).

In addition, the number of swimming cercariae was also calculated at 0, 10, 30 and 45 min (Figure 6.6). Non-swimming cercariae were clearly visible on the bottom of the plate and these were enumerated. At 45 min, no cercariae were left swimming, therefore the number counted was taken as the total amount of cercariae, and percentages were taken for the remaining time points. At 0 min, 81 % of cercariae were actively swimming. This

decreased to 28 % after 10 min, and to 13 % after a further 20 min treatment, indicating the fast effect of the inhibitor on cercarial motility.

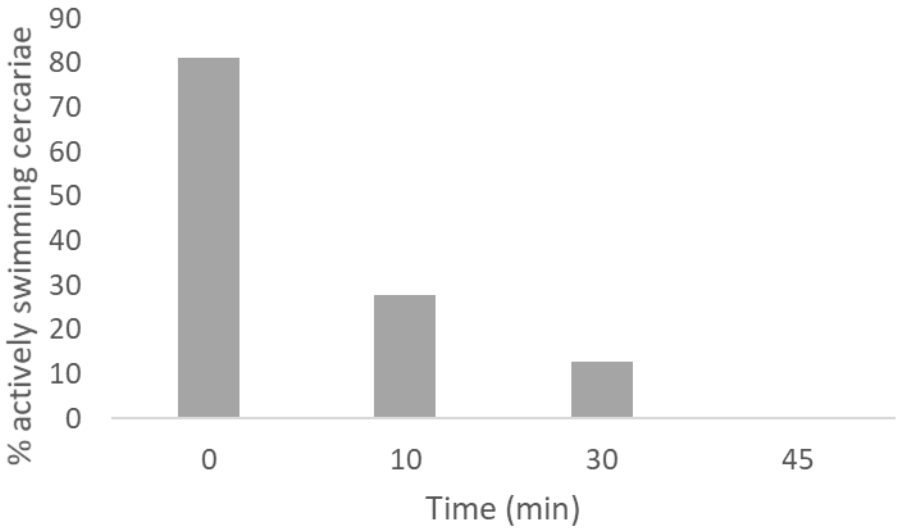

***Figure 6.6 C*ercarial swimming drops 63 % in the first 10 min of treatment with 10 µM Akt Inhibitor X.** The number of cercariae lying on the bottom of the plate in videos of 10 µM Akt Inhibitor X treatment from figure 6.5 were enumerated and calculated as a percentage of total cercariae.

Summary:

Previously validated Akt stimulant and inhibitor, L-arginine, and Akt inhibitor, respectively, were used to determine the patterns of Akt phosphorylation in cercariae. LA was employed as a stimulant given its potential relevance to host finding and skin penetration. Western blotting of both L-arginine and LA treated cercariae revealed an increase in Akt phosphorylation of ~2.9 and 2.0-fold, respectively, at 30 min compared to the controls. Immunohistochemistry of treated cercariae showed a less dramatic increase in Akt phosphorylation although at 15 min LA induced phosphorylation of the sensory papillae on the cercariae head. Akt phosphorylation in the tail also appeared to be modulated in waves following LA treatment. Experiments with Akt inhibitor X showed a significant decrease in cercarial Akt phosphorylation using western blotting and immunohistochemistry techniques.

To ascertain a functional role for Akt in *S. mansoni* cercariae, movies were recorded of cercariae swimming, after incubation with L-arginine, LA and Akt Inhibitor X for increasing durations. Both stimulants resulted in a striking increase in cercarial swimming. L-arginine treatment induced a level of cercarial swimming significantly above control levels ($p \leq 0.5 – 0.001$), until 45 min, whilst LA treated cercariae swimming times decreased to below control levels by 10 min, with a marginal increase again at 30 min. Akt Inhibitor X treatment caused a complete arrest in cercarial swimming after 45 min.

These experiments have uncovered further functional roles for Akt signalling in *S. mansoni*, specifically in the cercarial stage and have furthered our knowledge into the molecular control of cercarial behaviour and host finding/penetration mechanisms.

7

Discussion

Ranked the second most important neglected tropical disease (NTD) after malaria, water-borne schistosomiasis affects the lives of hundreds of millions of people in tropical developing countries. Research into cell signalling pathways of schistosomes provides not only valuable knowledge on the general biology of the parasite but may also reveal promising new avenues for drug development to enhance disease control. Insights gained during this project on the importance of Akt signalling to schistosome homeostasis highlight Akt as a worthy candidate for future drug targeting, particularly in the context of tegumental glucose transport. Figure 7.1 summarises the key findings from the research presented in this thesis.

7.1 Determining the presence of an Akt in *S. mansoni*

As a component of the PI3K signalling pathway, the protein kinase Akt is key to many fundamental processes in mammals including glucose uptake and metabolism, insulin signalling, cell-cycle progression and apoptosis (Brazil *et al.*, 2004). As such, studying Akt in *S. mansoni* was deemed to be a valuable progression in deepening knowledge of signalling kinases of the parasite.

7.1.1 Validating the ~52 kDa protein

The first part of this research project focused on determining the identity of the ~52 kDa protein, detected with anti-phospho Akt (Thr^{308}), anti-phospho Akt (Tyr^{315}) and anti-Akt antibodies, which possessed Akt-like qualities. Whilst the currently published *S. mansoni* genome (Protasio *et al.* 2012) predicts Akt to be 68 kDa as confirmed by Morel *et al.* (2014), the ~52 kDa protein detected in this project across multiple *S. mansoni* life stages displayed convincing Akt activity. Three antibodies were validated, each recognising a similar protein band across three parasite life stages and reciprocal IPs verified that all antibodies bound the same protein. A fourth antibody tested, anti-phospho Akt (Ser^{473}), did not react with *S. mansoni* total protein in several western blots. Protein sequence alignment to human Akt revealed a lack of sufficient conservation around the Ser^{473} residue that would explain the lack or reactivity to *S. mansoni* protein. Within the stretch of 11 amino acids that are recognised by anti-phospho Akt (Ser^{473}) antibodies, only 5 residues (55%) were conserved between the two species, compared to 82% and 100% conservation across the epitope of the anti-phospho Akt (Thr^{308}) and anti-phospho Akt (Tyr^{315}) antibodies, respectively (Figure 3.4).

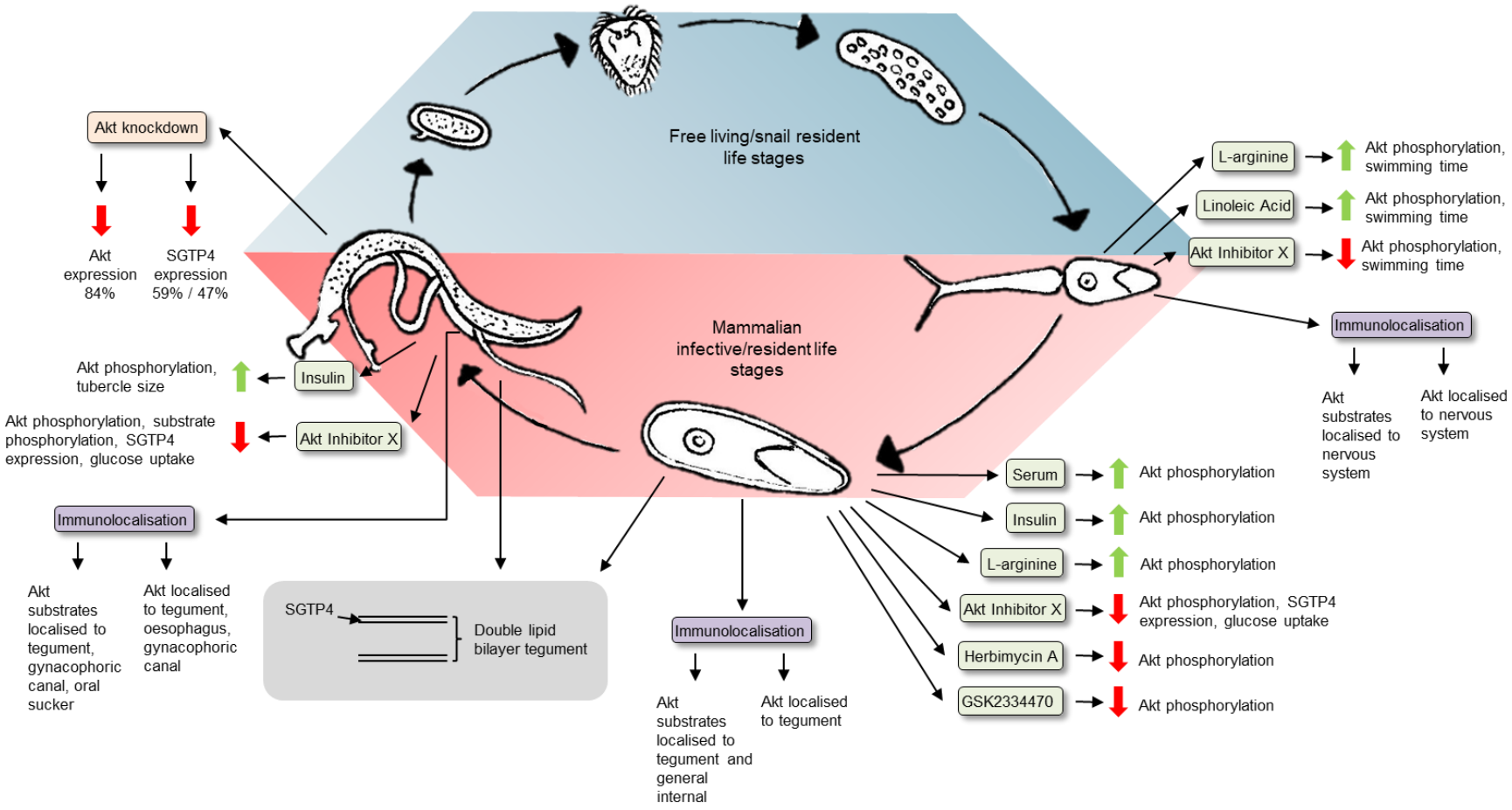

***Figure 7.1* Schematic diagram illustrating the main finding during the current research project.** Effects of all ligands on each life stage, results of immunohistochemistry and notable experiment results.

Experiments in Chapter 3 demonstrated that phosphorylation of the ~52 kDa Akt-like protein was increased by human host ligands and decreased by Akt pathway inhibitors. Furthermore, the protein immunoprecipitated using anti-phospho Akt (Thr^{308}) XP antibodies possessed Akt activity, and RNAi of the Akt gene (Smp_243630) reduced the immunoreactivity to Akt antibodies by ~83%. This figure is comparable to results achieved after the knockdown of other *S. mansoni* proteins, 90% knockdown of SmILK expression (Gelmedin *et al.*, 2017) and 83-85% reduction of SmIR1/2 expression (You *et al.*, 2015). Quantification of the success of RNAi by western blotting is an established and accepted technique, and has been used in many studies (Xia *et al.*, 2002; Seth *et al.*, 2005; Wang *et al.* 2017), including in schistosomes (Patocka *et al.*, 2014; You *et al.*, 2015; Han *et al.*, 2017). Following RNAi, the levels of Akt protein and activated protein were measured using anti-Akt and anti-phospho Akt (Thr^{308}) antibodies, respectively. In contrast to the ~83% reduction seen with the anti-Akt antibodies, the reduction in phosphorylated Akt signal was less stark. This was attributed to hyperactivation of the remaining Akt in the face of reduced overall expression of the protein through RNAi. Nevertheless, RNAi provided unequivocal evidence that the ~52 kDa protein is a bone fide Akt derived from the Akt gene Smp_243630.

Furthermore, the effects of stimulators and inhibitors on Akt were investigated to provide a range of tools for studying functional roles for Akt in schistosomes. Although useful initially, serum was dismissed as a stimulatory agent due to the non-specific binding between serum and the anti-rabbit secondary antibody, often causing a double band effect. Human insulin and the amino acid L-arginine both provided robust and reproducible phosphorylation of Akt, with L-arginine being the more effective. Later, linoleic acid was found to be a stimulator of Akt in cercariae. All successfully trialled stimulants were exogenous factors that would be encountered by the parasite early-on during host invasion, revealing the potential for Akt to play a role in several processes, host localisation and penetration, parasite development and host-parasite communications.

Several candidate molecules were tested to determine their ability to inhibit the phosphorylation (activation) of *S. mansoni* Akt in live somules: LY294002, GSK2334470, Akt Inhibitor X and Herbimycin A. Whilst the latter two compounds were found to robustly inhibit Akt phosphorylation and were chosen for further experiments, LY294002 and GSK2334470 were less effective. The original publication using LY294002 as a specific PI3K inhibitor (Vlahos *et al.*, 1994), tested the effect of the compound on human neutrophils and rabbit smooth muscle cells at 100 μM, but determined an IC_{50} of just 1.40

μM. Vlahos *et al.* (1994) also reported a distinct lack of inhibition of protein kinase A (PKA) and protein kinase C (PKC), among other ATP-requiring enzymes, presumably due to their position not directly downstream of PI3K. In contrast to its protein kinase cousins, Akt (PKB) lies directly downstream of PI3K, hence the choice of LY294002 as an inhibitor. Results of the assays however, indicate a lack of conservation between HuPI3K and SmPI3K, in terms of its interaction with this inhibitor, therefore restricting its effect on downstream Akt phosphorylation, or insufficient penetration of the inhibitor within the intact live parasite. In contrast, Akt Inhibitor X, a phenoxazine, attenuates directly the Akt kinase (Thimmaiah *et al.*, 2005). Thimmaiah *et al.* (2005) reported complete loss of Akt phosphorylation in human cancer cells after treatment of 1 h with 2.5 μM Akt Inhibitor X, measured with anti-phospho Akt (Ser^{473}) antibodies. Although the precise mechanism of protein interaction is unclear, it has been deduced that inhibition is independent of the PH domain, as upstream kinases which promote membrane localisation of Akt are unaffected by Akt Inhibitor X (Thimmaiah *et al.*, 2005).

7.1.2 A putative second Akt isoform

In *D. melanogaster*, a single Akt gene (*DAkt1*) exists, which encodes two forms of the protein, one short (66 kDa) and one long (85 kDa) (Andjelkovic *et al.*, 1995). The source of the two proteins is an alternative initiation codon, ACG, which precedes the usual start site, ATG (Andjelkovic *et al.*, 1995), resulting in the longer protein. A third peptide of 120 kDa was also discovered, derived from a distinct gene, which has a common epitope(s) to *DAkt1* (Andjelkovic *et al.*, 1995). Given the collective evidence acquired in this project, it is proposed that a similar mechanism is occurring in *S. mansoni* through alternative splicing at a region downstream from the published start codon. To achieve a resulting molecular weight of 52 kDa, a sequence of approximately 134 aa would need to be spliced from the currently annotated protein. In alignment with the human gene sequence, *S. mansoni* Akt possesses a leader sequence of 100 aa in addition to HuAkt1 before the beginning of the PH domain, although the putative methionine start point sits at position 92. In addition to potential gene splicing, it is worth noting that proteins can migrate differently within different SDS-PAGE gel systems, possibly accounting for the remaining difference in molecular weight. A molecular characterisation of the *S. mansoni* Akt gene and its regulatory mechanisms is warranted to determine if and where the protein is being spliced. Alternatively, the protein could be post-translationally proteolytically cleaved.

Once it was clear that a second, smaller Akt isoform existed in *S. mansoni*, and antibodies to detect its presence and activation status were validated, work moved to mapping Akt within the three human infective/resident life-stages, cercariae, somules and adult worms. Across all slides of somules and adult worms visualised by confocal microscopy, phosphorylated/non-phosphorylated Akt, measured by anti-Akt antibodies, was located primarily in the tegument, and in adult males it also localised to the tubercles and the gynaecophoric canal. Possible regions demonstrating non-phosphorylated Akt could be localised through comparisons with images probed with anti-phospho Akt antibodies.

Tubercles are exclusive to adult male schistosomes and present as tiny mound-like structures on the surface of the tegument (Hockley, 1973). When male adult worms were incubated in Akt Inhibitor X, the size of tubercles increased significantly over four to five days. A possible reason for this phenomenon could be an increase in surface area in an attempt to compensate for the reduction in SGTP4 expression also seen after adult worm treatment with this inhibitor. The swelling of the tubercles, whether or not intended to actively increase surface area, was possibly regulated by aquaporins. Aquaporins are ubiquitously expressed and are the most abundant transmembrane protein in the schistosome tegument (Castro-Borges *et al.*, 2011). *S. mansoni* aquaporin (SmAQP) serves to transport water across the tegument (Da'dara *et al.*, 2012) but has also been implicated in drug uptake and the excretion of lactate as a by-product of glucose metabolism (Faghiri and Skelly, 2009; Faghiri *et al.*, 2010). Interestingly, Akt has been implicated in the translocation of mammalian aquaporin-2 *via* interaction with the Akt substrate AS160, a Rab GAP protein (Kim *et al.*, 2011). Further evidence for the regulation of aquaporins by Akt has been obtained in chicken hepatocytes (Suh *et al.*, 2008). After the discovery that inhibition of Akt affects the morphology of adult worms at the tegument, several hypotheses for the localisation of Akt in this surface structure were considered, including Akt playing a role in vesicle trafficking and exocytosis, involvement in lipid raft trafficking/maintenance, male-female communication, and glucose uptake. Ultimately, experiments were designed to investigate the role of Akt in glucose transport across the tegument of *S. mansoni* (Chapter 4).

7.1.3 Akt in S. mansoni cercariae

In cercariae, activated and non-activated Akt, measured by anti-phospho Akt and anti-Akt antibodies, localised particularly in the nervous system and punctate regions in the tail. This finding was exploited to study the possible importance of Akt to swimming and

recognition of the mammalian host (Chapter 6). Significant work has been done previously to define the chemical stimulants that attract cercariae to their definitive host (Shiff *et al.*, 1972; Haas, 1992; Shiff and Graczyk, 1994; Haas *et al.*, 1997; Brachs and Haas, 2008; Haas *et al.*, 2008; Ressurreição *et al.*, 2015). From these studies, it is known that L-arginine and LA promote attachment and skin penetration, respectively. Investigating these compounds from a signalling perspective revealed that both are capable of stimulating Akt phosphorylation in cercariae as determined by western blotting, although this change was less pronounced when visualised in intact parasites. Confocal microscopy images revealed only a modest increase in Akt phosphorylation in response to L-arginine not concurrent with the change seen by western blot. In some cases, Akt was detected in punctate regions in the anterior region of the head. These were seen inconsistently in un-treated cercariae and also in L-arginine stimulated parasites (Chapter 6; sections 6.1 - 6.2). It is hypothesised that these punctate regions of Akt activity are flame cells, which appear in pairs in the heads of cercariae (Senft *et al.*, 1961; Skelly and Shoemaker, 2001). Flame cells contain cilia, the movement of which is thought to draw fluid into the protonephridial system from interstitial spaces, acting as a means of body fluid regulation, and also waste excretion (Valverde-Islas *et al.*, 2011). The potential role of Akt in this mechanism is unclear and warrants further investigation.

Another structure observed inconsistently in cercariae was a ring of punctate regions of Akt around the tip of the head, previously seen and named as sensory papillae (Ressurreição *et al.*, 2015). Initially, these sensory papillae were only detected when parasites were stained with anti-Akt antibodies, demonstrating that the Akt present was not active. However, after stimulation with L-arginine and LA, phosphorylated Akt was localised to this region (Figures 6.2 – 6.3), albeit not in every specimen, but indicating that Akt is possibly functionally involved in the response to host factors in cercarial host localisation and penetration.

Akt phosphorylation in cercariae was diminished by Akt Inhibitor X. Inhibitor treatment for 1 h significantly reduced Akt phosphorylation as measured by western blotting, and a decrease in global Akt phosphorylation when visualised by immunohistochemistry, with only punctate regions of activated Akt remaining in the tail. Clear staining of activated Akt of the peripheral nervous system in the tails of cercariae suggest that these regions of Akt activity are nerve ending or sensory receptors. They appear too abundant and irregularly spaced to be flame cells, which have never been reported in the tails of cercariae. This hypothesis provides a rationale for the tail being more than just a

locomotor organ; it may be stimulated by extracellular ligands to influence cercarial behaviour.

As well as western blot and immunohistochemistry analysis, cercarial behaviour in response to LA, L-arginine and Akt Inhibitor X was monitored by video analysis. Movies were recorded in 30 s clips of cercariae after treatment at various time intervals. L-arginine stimulated cercarial swimming immediately (Figure 6.5, Video 1), which was sustained before declining towards the end of the experiment. The sudden and drastic effect of L-arginine on the cercariae indicates a powerful response from sensory papillae in the head and potentially receptors in the tail. A similar response was observed with LA treatment, although the dramatic increase in swimming duration was not seen until 1 min (Figure 6.5, Video 4). In this case however, swim time decreased to below control levels 20 min sooner than seen with L-arginine. This could be due to the different roles (cues) for each compound in the process of host skin penetration by cercariae. L-arginine promotes the initial skin attachment, meaning that cercariae can sense this chemical from a distance, causing them to locate the host. In contrast, LA stimulates the burrowing of cercariae into the skin itself. Video analysis showed many of the LA-treated cercariae lying the on bottom of the treated surface, presumably attempting to penetrate as they would do mammalian skin. LA has previously been shown to stimulate the phosphorylation of PKC and ERK in *S. mansoni*, and the release of acetabular gland contents (Ressurreição *et al.*, 2015), a prerequisite for skin penetration.

When cercariae were treated with 1 µM or 10 µM Akt Inhibitor X, the observed effect was in stark contrast to that seen with the Akt stimulants LA and L-arginine. More pronounced with 10 µM but just as clearly seen with 1 µM Akt Inhibitor X, treatment significantly attenuated the swimming of cercariae, with 63%, 87%, and 100% inhibition at 10, 20 and 45 min respectively. As the locomotion organ of cercariae, these findings indicate that there are sensory receptors on the tails of cercariae and that Akt is in part responsible for motor function.

7.2 Akt in the Bigger Picture of *S. mansoni* Signalling

Every intracellular signalling pathway is composed of protein kinases which all possess connections with other proteins, forming a complex web of interactions (Natarajan *et al.*, 2006). The map of proteins, which are predicted to have a connection with Akt, created with STRINGdb began to reveal how many processes Akt may potentially be involved with in *S. mansoni*.

7.2.1 Glycogen synthase kinase

Glycogen synthase kinase-3 was one of the first identified substrates of Akt in mammals (Lawlor and Alessi, 2001). The primary sites for phosphorylation of mammalian GSK-3 are Ser^{21} for isoform α and Ser^{9} for isoform β. These sites are phosphorylated by Akt, which inactivates GSK-3, downregulating downstream processes (Fang *et al.*, 2000). In addition to Akt, GSK-3α/β is also phosphorylated by cAMP-dependant PKA, independently of PI3K/Akt signalling (Fang *et al.* 2000). In *S. mansoni*, alignment of the GSK-3 gene with its human counterparts reveals that despite an 88% homology across the kinase domain (Osolodkin *et al,* 2011), the $Ser^{9/21}$ residues are missing. This could be due to an error in annotation or, alternatively, the phosphorylated serine residue may appear elsewhere in the *S. mansoni* protein. However, given the specificity of Akt for substrate phosphorylation sites to have an Arg in the -3 and -5 positions, the latter possibility seems unlikely as not a single Ser residue in the *S. mansoni* sequence fits these requirements (Figure 4.18). Concurrent with bioinformatic analyses, western blotting of *S. mansoni* total proteins using antibodies that recognise the region surrounding and including the the $Ser^{9/21}$ residues yielded no results. However, western blotting using antibodies that recognise the $Tyr^{216/279}$ phosphorylation motif, demonstrated phosphorylation of GSK-3 after treatment of somules with Akt Inhibitor X. In mammals, the $Tyr^{216/279}$ residue is autophosphorylated in quiescent cells and results in positive regulation of downstream substrates (Grimes and Jope, 2001). The precise mechanism of tyrosine phosphorylation remains unclear although it has been previously suggested that stimulation of cells results in the dephosphorylation of GSK-3 at the tyrosine residue (Woodgett *et al.*, 1993; Murai *et al.*, 1996). Although there is no prior indication that Akt is involved in the regulation of GSK-3 *via* tyrosine phosphorylation, this insight explains the results seen in Chapter 4; inhibition of Akt by Akt Inhibitor X allowed GSK-3 to remain constitutively phosphorylated, whereas stimulation by insulin and L-arginine caused dephosphorylation of the tyrosine residue detected by the anti-phospho GSK-3 ($Tyr^{216/279}$) antibodies. Given that Akt is a serine/threonine kinase, it cannot directly affect the status of GSK-3 tyrosine phosphorylation, but as GSK-3 is widely known to play a role in insulin signalling (Hughes *et al.*, 1993; Woodgett *et al.*, 1993), it is not inconceivable for Akt to be involved indirectly in regulation of the tyrosine residue. A study of Wnt signalling revealed that in the ameboid protozoan *Dictyostelium discoideum,* GSK-3β is phosphorylated by a kinase, ZAK1, on Tyr^{216} (Kim *et al.*, 1999). However, like in humans, there is no ZAK1 homologue in *S. mansoni*, with the closest

match being abl kinase 2 (31% identity) when ZAK1 was blasted against *S. mansoni* proteins using the NCBI database.

7.2.2 p70^{S6K}

Although reported as being downstream of Akt (Cheatham *et al.*, 1994), p70^{S6K} is not directly phosphorylated by Akt, being activated instead through mTOR complex 1 (mTORC1) (Isotani *et al.*, 1999). One study has suggested that although both proteins are mediated *via* PDK1 signalling, Akt and p70^{S6K} lie on separate pathways (Conus *et al.*, 1998). However, as knowledge of Akt signalling in humans improved over the last two decades, the complex relationship between Akt and mTORC1 has been elucidated (Manning and Cantley, 2007), confirming an indirect link from Akt to p70^{S6K}. Despite this, experiments to activate p70^{S6K} using Akt pathway stimulants were unsuccessful (data not shown), indicating that the complex series of events leading to phosphorylation of p70^{S6K} in humans may not be conserved in schistosomes.

7.2.3 Ras superfamily G proteins

Bioinformatic analysis revealed 342 medium confidence (≥0.40) and 158 high confidence (≥0.70) proteins with putative Akt interacting activity (Appendix 2). Further interrogation of the high confidence protein hit-list resulted in 32 sequences with motifs suitable for phosphorylation by Akt, as determined by at least two phosphorylation site prediction tools. Of perhaps greatest significance was the presence of proteins from the Ras superfamily of small monomeric G proteins. The superfamily encompasses Ras, Rho, Ran, Rab and Arf G proteins (Wennerberg *et al.*, 2005), which are involved in membrane trafficking, including vesicle formation and transport, and vesicle/membrane fusion (Novick and Zerial, 1997). Present within the list of high confidence proteins containing phosphorylation sites predicted by more than one prediction tool were Rac (GTPase) (Smp_130230), Rac GTPase activating protein (Smp_021590) and Ras GTP exchange factor son of sevenless (Smp_242150; formerly Smp_161230) (Table 4.1). Given that these G proteins are ubiquitous in all eukaryotes (Hall, 1990; Ridley, 2006), a moderate level of homology in schistosomes can be assumed and several studies have found this to be true (Loeffler and Bennett, 1996; Kampkötter *et al.*, 1999; Osman *et al.*, 1999). A Ras homologue has been identified in larval and adult *S. mansoni* (Kampkötter *et al.*, 1999; Osman *et al.*, 1999) prompted by its essential role in eukaryotic growth and development signal transduction (McCormick, 1993). Ras has been demonstrated as present in all stages of schistosome and although Osman *et al.* (1999) found Ras to be overexpressed in female worms, levels of the protein were similar between mature and

immature worms and levels in males were the lowest of all life stages, likely indicating several roles in parasite development between stages. Schüßler *et al.* (1997) determined *S. mansoni* Ras and GAP proteins to be developmentally regulated but also involved in the maturation of the adult female *via* male worm interaction. Additionally and more recently, SmRho1 has been demonstrated as active in the gonads of both male and female adult worms, interacting with SmTK3 (Quack *et al.*, 2009).

Despite differences in their specific biological functions, all members of the Ras superfamily share the basic activity of GTP binding in their active form, and hydrolysis of GTP to GDP when inactive (Jiang and Ramachandran, 2006). Rac GTPases belong the Rho subfamily, which is known for the regulation of cell motility and polarity *via* functions regarding cytoskeletal organisation and membrane trafficking (Fransson *et al.*, 2003). *S. mansoni* Rac is 188 aa long and has a putative Akt phosphorylation site at Ser^{71}. The GO terms associated with this protein include "small GTPase mediated signal transduction", "protein transport", "GTP binding", "intracellular" and "plasma membrane"[11]. All GTPase proteins have a corresponding GTPase activating protein (GAP), which participates in the change between active and inactive forms of GTPase (Jiang and Ramachandran, 2006). *S. mansoni* Rac GAP is 610 aa in length and is putatively phosphorylated by Akt on Ser^{181}. The molecular functions associated with this protein include "zinc ion binding", "GTPase activator activity" and "diacylglycerol binding", and locations are primarily intracellular and cytoplasmic[12]. In mammalian fibroblasts, Akt has been shown to co-localise with Rac and cell division control protein 42 homologue (Cdc42) at the leading edge of cells in response to platelet-derived growth factor (PDGF), proving crucial in Rac/Cdc42 regulated cell motility (Higuchi *et al.*, 2001). Cdc42 is another low molecular weight (195 aa) GTPase of the Rho family, also present in the list of sequences putatively phosphorylated by Akt (Table 4.1). Higuchi *et al.* (2001) suggest that Akt is located downstream of Rac and Cdc42 and that the latter proteins induce phosphorylation of Akt at the critical residues Thr^{208} and Ser^{473}. However, this is contradicted by Sánchez-Martin *et al.* (2004) who demonstrate that PI3K/Akt signalling regulates Rac activation. Whilst a connection between Akt and Rac/Cdc42 is present, the precise mechanisms of interaction are uncertain.

The putative *S. mansoni* Ras GTP exchange factor, son of sevenless (Sos) is 1518 aa in length and also possesses just one Akt phosphorylation site at Ser^{541}. Its main biological process is regulation of GTPase-mediated signal transduction and can be

[11] http://www.genedb.org/gene/Smp_130230 [Accessed 29th September 2017].
[12] http://www.genedb.org/gene/Smp_021590 [Accessed 29th September 2017].

localised within cells[13]. Sos is a Ras-specific guanine nucleotide exchange factor protein required for growth factor receptor signalling *via* tyrosine kinases. The exchange factor is recruited to the cell membrane where it activates Ras by converting GDP to GTP (reviewed by Bar-Sagi, 1994). Very little data is published on any interactions between Sos and Akt, although a study by Tumurkhuu *et al.* (2013) reports PI3K/Akt signalling to be negatively affected by a mutant Sos protein, indicating an indirect link between the two proteins. Similarly, Sos in *S. mansoni* has been poorly studied and homology with the mammalian homologue is unknown.

7.2.4 A functional role for small GTPase Rab11 in S. mansoni?

In addition to the aforementioned proteins, Rab11 was identified as a high confidence protein with up to three potential Akt phosphorylation sites, although only confirmed by one prediction tool (Appendix 3). Across organisms, Rab proteins make up the largest subgroup of the Ras superfamily, with 60 members (Stenmark, 2009). There are three isoforms of Rab11 in humans (Rab11a, b and c), which all share high sequence homology (reviewed by Welz *et al.*, 2014). The involvement of Ras superfamily proteins in cellular transport mechanisms was first identified three decades ago (Salminen and Novick, 1987) with one of the primary roles of Rab11 proteins in mammalian cells being the transport of receptors to the cell surface (Stenmark, 2009). Rab GTPase proteins control vesicle trafficking by interacting with the actin cytoskeleton (Peranen *et al.*, 1996). Mammalian Rab11 isoforms have been located in the trans-Golgi network and recycling endosome, and are known to participate in both the endocytic and exocytic trafficking pathways (Urbé *et al.*, 1993). Rab11 is commonly found in complex with motor proteins, *via* interaction with adaptor proteins (Welz *et al.*, 2014). These complexes, such as the exocyst vesicle-tethering complex or SNARE complex, allow Rab11 to act in multiple biological processes aside from vesicle trafficking, including ciliogenesis, cytokinesis and neuritogenesis (Hobdy-Henderson *et al.*, 2003; Shirane and Nakayama, 2006; Knödler *et al.*, 2010).

The putative *S. mansoni* Rab11 (Smp_267200; formerly Smp_173990) comprises 933 aa with putative Akt phosphorylation sites at Thr^{82}, Ser^{649} and Ser^{873}. Comparable with other Ras superfamily G proteins, *S. mansoni* Rab11 is assigned GO terms including "GTP binding", "small GTPase mediated signal transduction" and "protein import into nucleus"[14]. As is its role in mammalian cells, Rab11, along with other small GTPases,

[13] http://www.genedb.org/gene/Smp_242150 [Accessed 29th September 2017].
[14] http://www.genedb.org/gene/Smp_267200 [Accessed 2nd October 2017].

also mediates vesicle transport to the plasma membrane in helminths (Torre-Escudero *et al.*, 2016). In addition to knowledge that Rab11 traffics receptors to the plasma membrane, this GTPase has been specifically shown to co-localise with GLUT4 containing vesicles in cardiomyocytes (Uhlig *et al.*, 2005). Furthermore, Rab11 expression is substantially increased in GLUT4 transporting vesicles in response to insulin stimulation, which also induced the expression of Akt-2 (Kessler *et al.*, 2000). A Rab GAP protein, AS160, has been identified as an Akt substrate in mammalian cells (Larance *et al.*, 2005) and could provide the link between Akt and Rab11. The Rab11 protein provides a rationale for Akt being implicated in vesicle trafficking and furthermore could link Akt not only with the expression of SGTP4, but also its movement within the tegument during the early post-transformation stage of somule development.

7.3 A Functional Role for Akt in *S. mansoni*

Whilst Akt is almost certainly present in other tissues of schistosomes, using the methods described in this project (tegument stripping/western blot, immunolocalisation), Akt was found predominately expressed in the parasite surface layer, adding Akt to the long list of other proteins already discovered in the *S. mansoni* tegument (Braschi and Wilson, 2005; Braschi *et al.*, 2006; Wilson, 2012). As the barrier between parasite and host, the tegument represents a valuable source of information on host-parasite interactions and putative novel drug targets. After three decades of almost exclusive treatment of schistosomiasis with PZQ, fears of developing resistance have stimulated the search for a new method of control (Cioli *et al.*, 2014). Consensus in the scientific community exists that protein kinases are one of the most viable routes to find novel drug targets against schistosomes (Doerig, 2004; Dissous *et al.*, 2007; Beckmann *et al.*, 2012a). Protein kinase is a term encompassing several sub-groups: tyrosine kinases (TKs), receptor tyrosine kinases (RTKs) and serine/threonine kinases (STKs), among others (Andrade *et al.*, 2011). Of particular interest recently have been those kinases already targeted in human cancer research, with a view to discovering if homology with schistosome kinases is sufficient for current drugs to be deployed in the fight against schistosomes (Dissous and Grevelding, 2011). Several studies have also linked protein kinases to *S. mansoni* reproductive processes (reviewed by Morel *et al.*, 2014b), ideal targets to prevent proliferation of the life cycle. Elements of the TGF-β pathways are known to influence female worm reproductive development and egg embryogenesis. *S. mansoni* receptor kinase-1 (SmRK-1) is a receptor serine/threonine kinase present on the surface of the parasite, specifically the dorsal tubercles, from the immature adult stage (Davies *et al.*, 1998). Proposed to be mediated by FK-506 binding protein 12 (FKBP12) (Knobloch *et*

al., 2004), SmRK-1 is a divergent type I receptor; type I receptors form a complex with type II receptors to convey intracellular signals in TGF-β pathways (Davies *et al.*, 1998). Downstream of SmRK-1, receptor-regulated SmSmad1, SmSmad2 and SmSmad4 are phosphorylated, leading to signalling implicated in parasite development and male-female communication (Beall *et al.*, 2000; Osman *et al.*, 2004). Both SmSmad2 and SmSmad4 have been localised to the female reproductive organs, specifically the vitellaria, ovary and developing embryo (Osman *et al.*, 2001; Osman *et al.*, 2004), linking TFG-β signalling and SmRK-1 to female sexual development. In addition to TGF-β signalling, SmTK3 is also known to be present in the female ovary and vitelline glands, as well as the male testes, indicating a role in the cytoskeletal organisation of schistosome gonads (Kapp *et al.*, 2004).

More recently, post genome publication (Berriman *et al.*, 2009; Protasio *et al.*, 2012), many more *S. mansoni* proteins have been shown to regulate functions beyond those of the reproductive system (Andrade *et al.*, 2011). The possibility of insulin signalling in schistosomes was first raised after discovery of two insulin receptor-like RTKs (Vicogne *et al.*, 2003). One of the proteins characterised possessed a C-terminal TK domain, similar to that of other IR family members, but a divergent extracellular N-terminal domain more closely similar to venus flytrap (VFT) modules, such as the ones in bacterial periplasmic binding proteins (PBP) (Vicogne *et al.*, 2003). VFTs possess two lobes that close around the bound ligand, stabilising the conformation (Felder *et al.*, 1999). The newly characterised receptor, termed Venus Kinase Receptor 1 (SmVKR-1), was shown to be a part of a new family of Venus Kinase Receptors (VKRs) (Ahier *et al.*, 2009). Subsequently, VKR homologues were identified in several insect species including seven *Drosophila* species and two mosquito species, evidencing that these receptors are not unique to schistosomes. In several of the insect species, the VKR proteins were primarily expressed in larval stages and in the gonads of the adult form suggesting another kinase with a functional role in reproductive activities, embryogenesis and larval development (Ahier *et al.*, 2009). In *S. mansoni*, *vkr1* and *vkr2* proteins were present in all life stages and presented with very similar structures, indicating origin from a gene duplication event (Gouignard *et al.*, 2012). Among the ligands identified for VKR-1 and VKR-2 were L-arginine (Ahier *et al.*, 2009) and insulin (Gouignard *et al.*, 2012). More recently, VKR proteins expressed in *Xenopus* oocytes demonstrated the capacity to stimulate the endogenous *Xenopus* Akt/PI3K pathway, revealing an alternative to the IRs (Morel *et al.*, 2014a).

In mammalian systems, insulin mediates a wide range of processes and pathways including glucose metabolism, cell growth and differentiation, protein synthesis and DNA synthesis (You *et al.*, 2009). The functions of insulin overlap those of Akt as they are implicated together in PI3K signalling (Alessi *et al.*, 1997; Conus *et al.*, 1998). Knowledge of insulin signalling in schistosomes was driven by the discovery of two insulin receptors, SmIR-1 and SmIR-2, which are part of the RTK family (Khayath *et al.*, 2007). Insulin receptors are ancient RTKs and have been identified in organisms as primitive as marine sponges (Skorokhod *et al.*, 1999). *S. mansoni* insulin receptors bind human insulin (Khayath *et al.* 2007) and the localisation of SmIR-1 at the tegument indicates that insulin receptors play a vital role in host-parasite communication (Ahier *et al.*, 2008). A connection between insulin and glucose uptake was first made in *Schistosoma douthitti* (Cornford, 1974) and insulin has since been shown to increase glucose uptake in *S. mansoni* somules and adult worms by 25% and 50%, respectively (Ahier *et al.*, 2008), as well as in unpaired female *S. japonicum* worms (You *et al.*, 2009). Knockdown of SmIR-1 in somules by the RNAi soaking method (Ndegwa *et al.*, 2007) resulted in a decrease of ~33% glucose uptake although this was independent of global SmIR-1 levels (Ahier *et al.*, 2008). In *S. japonicum*, insulin has been shown to regulate the expression of genes controlling growth and development (You *et al.*, 2009). In mammals, insulin-regulated glucose uptake into adipose tissues is a well-characterised process, due to its dysfunction leading to type II diabetes mellitus (Kahn and Pessin, 2002). Insulin stimulates the translocation of glucose transporter 4 (GLUT4) from intracellular vesicles to the plasma membrane of fat, skeletal and cardiac muscle (Smith *et al.*, 1991) *via* the Akt/PI3K pathway, which subsequently increases glucose uptake (Cheatham *et al.*, 1994; Kotani *et al.*, 1995). An insulin mediated PI3K independent pathway has also been implicated in the translocation of GLUT4, linking this process with actin dynamics (Kahn and Pessin, 2002).

In schistosomes, two glucose transporters have been characterised, SGTP1 and SGTP4 (Zhong *et al.*, 1995) through in-depth research of glucose uptake in schistosomes (Skelly and Shoemaker, 1996; Skelly and Shoemaker, 2001). Glucose in an essential element of schistosome survival in the mammalian host, but the mechanisms behind the control of glucose uptake remain relatively unknown. SGTP1 localises to the basal tegument membrane (Zhong *et al.*, 1995) contrary to SGTP4, which is found in the apical tegument membrane (Skelly and Shoemaker, 1996). SGTP4 has been localised in both bilayers of the apical tegument membrane and also in the multilamellar bodies of adults and the membranous bodies of somules (Jiang *et al.*, 1996). Interestingly, SGTP4 develops in

the parasite only after cercariae start to transform into somules, after which it remains present throughout adulthood (Skelly and Shoemaker, 1996), coinciding with the expression and localisation in the tegument of SmIR-1 (Khayath *et al.*, 2007), and Akt (Chapter 3). Data from the current research demonstrated that insulin could stimulate Akt phosphorylation in somules and adult *S. mansoni*, adding to knowledge already gained in this field (Morel *et al.*, 2014a). Given the crucial nature of Akt in mammalian glucose regulation, the insulin context and immunolocalisation of activated Akt in *S. mansoni* provided the rationale for a series of experiments to determine whether expression of SGTP4 could be influenced by manipulation of the Akt protein. Results revealed that SGTP4 expression can be attenuated by molecular inhibitors of Akt and also Akt siRNA in adult worms. Furthermore, inhibition of Akt in adult male and female worms significantly reduced their ability to uptake glucose, by 38% ($p \leq 0.001$) and 37% ($p \leq 0.01$) respectively. These results, in addition to the data gathered on the evolution of SGTP4 in somules, provide evidence that the Akt pathway is at least in part responsible for SGTP4 expression and translocation to the apical membrane, as it is responsible for GLUT4 translocation in mammals (Cheatham *et al.*, 1994). Collectively, these findings, in addition to data that links L-arginine and insulin to Akt phosphorylation (Figures 3.17 and 3.18) and the functional mapping of the active kinase to the schistosome tegument (Figures 3.12 - 3.14), provides evidence for Akt playing a role in the evolution and subsequent sustained expression of SGTP4 at the parasite surface. As such, a model for the mechanistic function of Akt in schistosome glucose uptake is proposed (Figure 7.2), based on integrated knowledge of the findings presented here and analysis of comparative biology, highlighting the role of Rab and RabGAP proteins in the translocation of SGTP4-containing vesicles to the apical membrane. The precise proposed mechanism is as follows: 1) interaction of host insulin or L-arginine with the IR or VKR, respectively, at the parasite surface, results in receptor phosphorylation/activation; adaptor proteins then bind, which in turn bind PI3K causing the production of PIP3 (PI3K potentially could also interact directly with the receptor). 2) Akt, phosphorylated (activated) by PDK1, can then phosphorylate and inactivate Rab-GAP, in turn 3) enhancing levels of GTP-bound Rab, which then promotes production of SGTP4 vesicles at the trans-Golgi network (TGN) that are shuttled to the parasite surface. 4) SGTP4 gene expression, which also seems to be dependent on Akt activation, is driven by signalling events, which might include mTOR activation. This mechanism provides a sound rationale for conducting additional research on Akt signalling in *S. mansoni* that would be beneficial towards deepening our understanding

of schistosome biology and that may reveal promising candidates for drug target development in the context of glucose uptake.

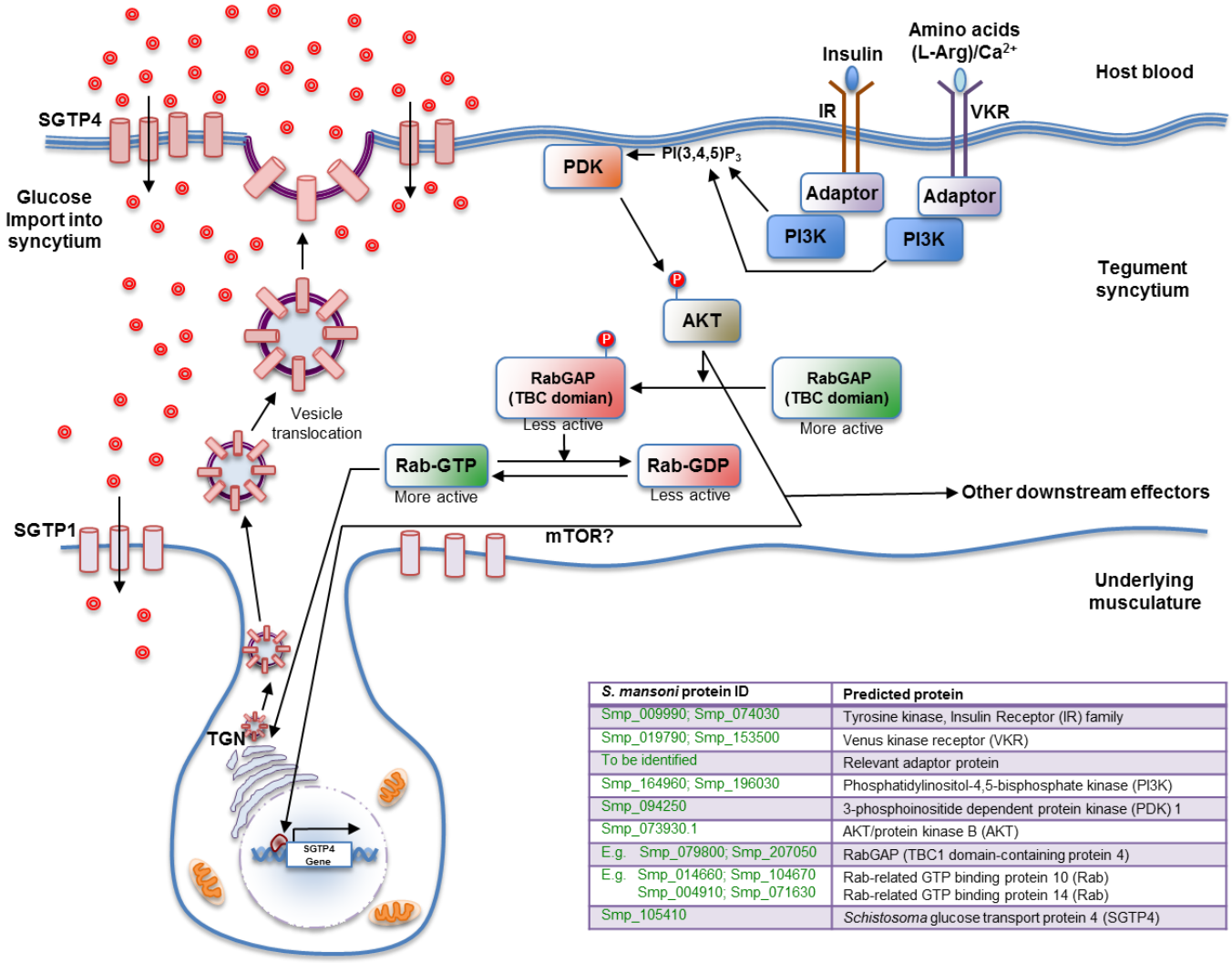

S. mansoni protein ID	Predicted protein
Smp_009990; Smp_074030	Tyrosine kinase, Insulin Receptor (IR) family
Smp_019790; Smp_153500	Venus kinase receptor (VKR)
To be identified	Relevant adaptor protein
Smp_164960; Smp_196030	Phosphatidylinositol-4,5-bisphosphate kinase (PI3K)
Smp_094250	3-phosphoinositide dependent protein kinase (PDK) 1
Smp_073930.1	AKT/protein kinase B (AKT)
E.g. Smp_079800; Smp_207050	RabGAP (TBC1 domain-containing protein 4)
E.g. Smp_014660; Smp_104670 Smp_004910; Smp_071630	Rab-related GTP binding protein 10 (Rab) Rab-related GTP binding protein 14 (Rab)
Smp_105410	*Schistosoma* glucose transport protein 4 (SGTP4)

Figure 7.2 **Schematic diagram of the postulated mechanism of Akt-dependent SGTP4 expression/translocation in *S. mansoni*.** Predicted *S. mansoni* proteins that could play a role in such processes are identified in the box.

7.4 Priorities for Future Work

There are several avenues of research that could be pursued to not only further investigate the importance of Akt signalling in *S. mansoni* but also to expand the current knowledge of Akt substrates and interacting proteins in schistosomes. Primarily, in-depth molecular genetic characterisation of the ~52 kDa protein to identify the putative alternative start site from the currently annotated 70 kDa Akt protein would be the final element to demonstrate that this is the only active form of the kinase in *S. mansoni*. Additionally, investigating the role of Akt in vesicle trafficking would add further support to the glucose transporter translocation model proposed here. Identifying the downstream substrates of Akt and their roles in the parasite life-cycle could lead to exciting insights in host-parasite communication and shed more light on the complex network of signalling pathways that intersect and interact with Akt, implicated by this project. The specific localisation of phosphorylated Akt in the gynaecophoric canal also warrants further investigation as this could indicate that Akt is somewhat involved in male-female communication. Finally, it would be useful to confirm whether the mechanism for SGTP4 translocation proposed here is conserved in other species of schistosome. Regarding Akt as a novel drug target, it is hoped that with advances in research of Akt in human cancer, a drug may become available that is adaptable to use against all three main species of human infecting schistosomes, improving the lives of millions currently battling this devastating NTD.

References

Adamson, E.D. and Rees, A.R. (1981) Epidermal growth factor receptors. *Molecular and Cellular Biochemistry* **34(3)**: 129 – 152.

Adema, C.M., Hillier, L.W., Jones, C.S., Loker, E.S., Knight, M., Minx, P., Oliveira, G., Raghavan, N.,Shedlock, A., do Amaral, L.R., Arican-Goktas, H.D., Assis, J.G., Baba, E.H., Baron, O.L., Bayne, C.J., Bickham-Wright, U., Biggar, K.K., Blouin, M., Bonning, B.C., Botka, C., Bridger, J.M., Buckley, K.M., Buddenborg, S.K., Lima C.R., Carleton, J., Carvalho, O.S., Castillo, M.G., Chalmers, I.W., Christensens, M., Clifton, S., Cosseau, C., Coustau, C., Cripps, R.M., Cuesta-Astroz, Y., Cummins, S.F., di Stephano, L., Dinguirard, N., Duval, D., Emrich, S., Feschotte, C., Feyereisen, R., FitzGerald, P., Fronick, C., Fulton, L., Galinier, R., Gava, S.G., Geusz, M., Geyer, K.K., Giraldo-Calderón, G.I., de Souza G.M., Gordy, M.A., Gourbal, B., Grunau, C., Hanington, P.C., Hoffmann, K.F., Hughes, D., Humphries, J., Jackson, D.J., Jannotti-Passos, L.K., de Jesus J.W., Jobling, S., Kamel, B., Kapusta, A., Kaur, S., Koene, J.M., Kohn, A.B., Lawson, D., Lawton, S.P., Liang, D., Limpanont, Y., Liu, S., Lockyer, A.E., Lovato, T.L., Ludolf, F., M.V., McManus, D.P., Medina, M., Misra, M., Mitta, G., Mkoji, G.M., Montague, M.J., Montelongo, C., Moroz, L.L., Munoz-Torres, M.C., Niazi, U., Noble, L.R., Oliveira, F.S., Pais, F.S., Papenfuss, A.T., Peace, R., Pena, J.J., Pila, E.A., Quelais, T., Raney, B.J., Rast, J.P., Rollinson, D., Rosse, I.C., Rotgans, B., Routledge, E.J., Ryan, K.M., Scholte, L.L.S., Storey, K.B., Swain, M., Tennessen, J.A., Tomlinson, C., Trujillo, D.L., Volpi, E.V., Walker, A.J., Wang, T., Wannaporn, I., Warren, W.C., Wu, X., Yoshino, T.P., Yusuf, M., Zhang, S., Zhao, M. and Wilson, R.K. (2017) Whole genome analysis of a schistosomiasis-transmitting freshwater snail. *Nature Communications* **8(15451)**: 1 – 11.

Ahier, A., Khayath, N., Vicogne, J. and Dissous, C. (2008) Insulin receptors and glucose uptake in the human parasite *Schistosoma mansoni. Parasite* **15(4)**: 573 – 579.

Alessi, D.R., Andjelkovic, M., Caudwell, F.B., Cron, P., Morrice, N., Cohen, P. and Hemmings, B. (1996a) Mechanism of activation of protein kinase B by insulin and IGF-1. *EMBO Journal* **15(23)**: 6541 – 6551.

Alessi, D.R., Caudwell, F.B., Andjelkovic, M., Hemmings, B.A. and Cohen, P. (1996b) Molecular basis for the substrate specificity of protein kinase B; comparison with MAPKAP kinase-1 and p70 S6 kinase. *Federation of European Biochemical Societies Letters* **399(1)**: 333-338.

Alessi, D.R., James, S.R., C. Downes, P., Holmes, A.B., Gaffney, P.R.J., Reese, C.B. and Cohen, P. (1997) Characterization of a 3-phosphoinositide-dependent protein kinase which phosphorylates and activates protein kinase Bα. *Current Biology* **7(4)**: 261 – 269.

Andjelkovic, M., Jones, P.F., Grossniklaus, U., Cron, P., Schier, A.F., Dick, M., Bilbe, G. and Hemmings, B.A. (1995) Developmental Regulation of Expression and Activity of Multiple Forms of the *Drosophila* RAC Protein Kinase. *The Journal of Biological Chemistry* **270(8)**: 4066 – 4075.

Andrade, L.F., Nahum, L.A., Avelar, L.G.A., Silva, L.L., Zerlotini, A., Ruiz, J.C. and Oliveira, G. (2011) Eukaryotic Protein Kinases (ePKs) of the Helminth Parasite *Schistosoma mansoni*. *BMC Genomics* **12(1)**: 215 – 233.

Angeli, V., Faveeuw, C., Roye, O., Fontaine, J., Teissier, E., Capron, A., Wolowczuk, I., Capron, M. and Trottein, F. (2001) Role of the Parasite-derived Prostaglandin D2 in the Inhibition of Epidermal Langerhans Cell Migration during Schistosomiasis Infection. *Journal of Experimental Medicine* **193(10)**: 1135 – 1147.

Ashburner, M., Ball, C.A., Blake, J.A., Botstein, D., Butler, H., Cherry, J.M., Davis, A.P., Dolinski, K., Dwight, S.S., Eppig, J.T., Harris, M.A., Hill, D.P., Issel-Tarver, L., Kasarskis, A., Lewis, S., Matese, J.C., Richardson, J.E., Ringwald, M., Rubin, G.M and Sherlock, G. (The Gene Ontology Consortium) (2000) Gene Ontology: tool for the unification of biology. *Nature Genetics* **25(1)**: 25 – 29.

Ashton, P.D., Harrop, R., Shah, B. and Wilson, R.A. (2001) The schistosome egg: development and secretions. *Parasitology* **122(3)**: 329 – 338.

Bahia, D., Andrade, L.F., Ludolf, F., Mortara, R.A. and Oliveira. G. (2006a) Protein tyrosine kinases in *Schistosoma mansoni*. *Memórias do Instituto Oswaldo Cruz* **101(1)**: 137 – 143.

Bahia, D., Avelar, L., Mortara, R.A., Khayath, N., Yan, Y., Noël, C., Capron, M., Dissous, C., Pierce, R.J. and Oliveira, G. (2006b) SmPKC1, a new protein kinase C identified in the platyhelminth parasite *Schistosoma mansoni*. *Biochemical and Biophysical Research Communications* **345(1)**: 1138 – 1148.

Bahia, D., Avelar, L. G. A., Vigorosi, F., Cioli, D., Oliveira, G. C., and Mortara, R. A. (2006c). The distribution of motor proteins in the muscles and flame cells of the *Schistosoma mansoni* miracidium and primary sporocyst. *Parasitology* **133(3)**: 321-9.

Bahia, D., Mortara, R.A., Kusel, J.R., Andrade, L.F., Ludolf, F., Kuser, P.R., Avelar, L., Trolet, J., Dissous, C., Pierce, R.J. and Oliveira, G. (2007) Schistosoma mansoni: Expression of Fes-like tyrosine kinase SmFes in the tegument and terebratorium suggests its involvement in host penetration. *Experimental Parasitology* **116(1)**: 225 – 232.

Bailek, R. and Knobloch, J. (1999) Katayama fever in a child returning from Malawi. *Monatsschrift Kinderheilkunde* **147(3)**: 265 – 268.

Bar-Sagi. D. (1994) The Sos (Son of sevenless) protein. *Trends in Endocrinology and Metabolism* **5(4)**: 165 – 169.

Basch, P.F. and Rhine, W.D. (1983) *Schistosoma mansoni*: Reproductive Potential of Male and Female Worms Cultured In Vitro. *Journal of Parasitology* **69(3)**: 567 – 569.

Beall, M.J., McGonigle, S. and Pearce, E.J. (2000) Functional conservation of *Schistosoma mansoni* Smads in TGF-b signalling. *Molecular and Biochemical Parasitology* **111(1)**: 131 – 142.

Becker, B., Mehlhorn, H., Andrews, P. and Eckert, T. (1980) Light and Electron-microscopic studies on the effect of Praziquantel on *Schistosoma mansoni, Dicrocoelium dendtriticum* and *Fasciola hepatica* (trematode) *in-vitro***.** *Zeitschrift fur Parasitenkunde – Parasitology Research* **63(2)**: 113 – 128.

Beckmann, S., Quack, T., Burmeister, C., Buro, C., Long, T., Dissous, C and Grevelding, C.G. (2010) *Schistosoma mansoni*: signal transduction processes during the development of the reproductive organs. *Parasitology* **137(1)**: 497 – 520.

Beckmann, S., Hahnel, S., Cailliau, K., Vanderstraete, M., Browaeys, E., Dissous, C., Grevelding, C.G. (2011) Characterization of the Src/Abl Hybrid Kinase SmTK6 of *Schistosoma mansoni*. *Journal of Biological Chemistry* **286(49)**: 42325 – 42336.

Beckmann, S., Leutner, S., Gouignard, N., Dissous, C. and Christoph G. Grevelding, C.G. (2012a) Protein Kinases as Potential Targets for Novel Anti-Schistosomal Strategies. *Current Pharmaceutical Design* **18(1)**: 1 – 16.

Beckmann, S., Quack, T., Dissous, C., Cailliau, K., Lang, G. and Grevelding, C.G. (2012b) Discovery of Platyhelminth-Specific a/b-Integrin Families and Evidence for Their Role in Reproduction in *Schistosoma mansoni*. *PLoS one* **7(12)**: e52519.

Bellacosa, A., Testa, J.R., Staal, S.P. and Tsichlis, P.N. (1991) A Retroviral Oncogene, akt, encoding a Serine-Threonine Kinase Containing an SH2-Like Region. *Science* **254(5029)**: 274 – 277.

Beltran, S., Desdevises, Y., Portela, J. and Boissier, J. (2010) Mating system drives negative associations between morphological features in Schistosomatidae. *BMC Evolutionary Biology* **10(245)**: 1 – 8.

Berriman, M., Haas, B.J., LoVerde, P.T., Wilson, R.A., Dillon, G.P., Cerqueira, G.C., Mashiyama, S.T., Al-Lazikani, B., Andrade, L.F., Ashton, P.D., Aslett, M.A., Bartholomeu, D.C., Blandin, G., Caffrey, C.R., Coghlan, A., Coulson, R., Day, T.A., Delcher, A., DeMarco, R., Djikeng, A., Eyre, T., Gamble, J.A., Ghedin, E., YongGu, Hertz-Fowler, C., Hirai, H., Hirai, Y., Houston, R., Ivens, A., Johnston, D.A., Lacerda, D., Macedo, C.D., McVeigh, P., Ning, Z., Oliveira, G., Overington, J.P., Parkhill, J., Pertea, M., Pierce, R.J., Protasio, A.V., Quail, M.A., Rajandream, M., Rogers, J., Sajid, M., Salzberg, S.L., Stanke, M., Tivey, A.R., White, O., Williams, D.L., Wortman, J., Wu., W., Zamanian, M., Zerlotini, A., Fraser-Liggett, C.M., Barrell, B.G. and El-Sayed, N.M. (2009) The genome of the blood fluke *Schistosoma mansoni*. *Nature* **460(1)**: 352 – 358.

Beurel, E., Michalek, S.M. and Jope, R.S. (2010) Innate and adaptive immune responses regulated by glycogen synthase kinase-3 (GSK3). *Trends in Immunology* **31(1)**: 24 – 31.

Boissier, J., Morand, S. and Moné, H. (1999) A review of performance and pathogenicity of male and female *Schistosoma mansoni* during the life-cycle. *Parasitology* **119(1)**: 447 – 454.

Bordinhão, A.J.R., Evangelista, A.F., Oliveira, R.J.S., Macedo, T., Silveira, H.C., Reis, R.M. and Marques, M.M. (2016) MicroRNA profiling in human breast cancer cell lines exposed to the anti-neoplastic drug cediranib. *Oncology reports* **36(6)**: 3197 – 3206.

Bottieau, E., Clerinx, J., de Vega, M. R., Van den Enden, E., Colebunders, R., Van Esbroeck, M., Vervoort, T., Van Gompel, A. and Van den Ende, J. (2006) Imported Katayama fever: Clinical and biological features at presentation and during treatment. *Journal of Infection* **52(1)**: 339 – 345.

Bozulic, L. and Hemmings, B.A. (2009) PIKKing on PKB: regulation of PKB activity by phosphorylation. *Current Opinion in Cell biology* **21(1)**: 256 – 261.

Brachs, S. and Haas, W. (2008) Swimming behaviour of *Schistosoma mansoni* cercariae: responses to irradiance changes and skin attractants. *Parasitology Research* **102**: 685–690.

Braschi, S., Castro Borges, W. and Wilson, R.A. (2006a) Proteomic analysis of the schistosome tegument and its surface membranes. *Memoria do Instituto Oswaldo Cruz* **101(1)**: 205 – 212.

Braschi, S., Curwen, R.C., Ashton, P.D., Verjovski-Almeida, S. and Wilson, A. (2006b) The tegument surface membranes of the human blood parasite *Schistosoma mansoni*: A proteomic analysis after differential extraction. *Proteomics* **6(5)**: 1471 – 1482.

Braschi, S. and Wilson, R.A. (2006) Proteins Exposed at the Adult Schistosome Surface Revealed by Biotinylation. *Molecular and Cellular Proteomics* **5(2)**: 347 – 356.

Brazil, D.P., Yang, Z., Hemmings, B.A. (2004) Advances in protein kinase B signalling: AKTion on multiple fronts. *TRENDS in Biochemical Sciences* **29(5)**: 233 – 242.

Bueding, E. (1950) Carbohydrate metabolism of *Schistosoma mansoni*. *The Journal of General Physiology* **33(5)**: 475 – 495.

Bustelo, X.R., Sauzeau, V. and Berenjeno, I.M. (2007) GTP-binding proteins of the Rho/Rac family: regulation, effectors and functions in vivo. *Bioessays* **29(4)**: 356 – 370.

Bustinduy, A.L. and King, C.H. (2014) 52 – Schistosomiasis. In: J. Farrar, P.J. Hotez, T. Junghanns, G. Kang, D. Lalloo and N.J. White, ed., *Manson's Infectious Tropical Diseases, 23rd edition*. China: Elesvier., pp. 698 – 725.

Cano, E., Hazzalin, C.A.,and Mahadevan, L.C. (1994) Anisomycin-Activated Protein Kinases p45 and p55 but Not Mitogen-Activated Protein Kinases ERK-1 and -2 Are Implicated in the Induction of c-fos and c-jun. *American Society for Microbiology* **14(11)**: 7352 – 7362.

Castagna, M., Takai, Y., Kaibuchi, K., Sano, K., Kikkawa, U. and Nishizukag, Y. (1982) Direct Activation of Calcium-activated, Phospholipid-dependent Protein Kinase by Tumor-promoting Phorbol Esters. *The Journal of Biologicsl Chemistry* **257(13)**: 7847 – 7851.

Castro-Borges, W., Simpson, D.M., Dowle, A., Curwen, R.S., Thomas-Oates, J., Beynon, R.J. and Wilson, R.A. (2011) Abundance of tegument surface proteins in the human blood fluke *Schistosoma mansoni* determined by QconCAT proteomics. *Journal of Proteomics* **74(9)**: 1519 – 1533.

Cheatham, B., Vlahos, C.J., Cheatham, L., Wang, L., Blenis, J. and Kahn, R. (1994) Phosphatidylinositol 3-Kinase Activation Is Required for Insulin Stimulation of pp7O S6 Kinase, DNA Synthesis, and Glucose Transporter Translocation. Molecular and Cellular Biology **14(7)**: 4902 – 4911.

Chen, R., Kim, O., Yang, J., Sato, K., Eisenmann, K.M., McCarthy, J., Chen, H. And Qiu, Y. (2001) Regulation of Akt/PKB Activation by Tyrosine Phosphorylation. *Journal of Biological Chemistry* **276(34)**: 31858 – 31862.

Chikunguwo, S. M., Kanazawa, T., Dayal, Y. and Stadecker, M.J. (1991) The cell-mediated response to schistosomal antigens at the clonal level. In vivo functions of cloned murine egg antigen-specific CD4+ T helper type 1 lymphocytes. *The Journal of Immunology* **147(11)**: 3921 – 3925.

Chitsulo, L., Engels, D.,Montresor, A. and Savioli, L. (2000) The global status of schistosomiasis and its control. *Acta Tropica* **77(1)**: 41 – 51.

Chitsulo, L., Loverde, P. and Engels, D. (2004) Schistosomiasis. *Nature Reviews Microbiology* **2(1)**: 12 – 13.

Cioli, D., Pica-Mattoccia, L. and Archer, S. (1995) Antischistosomal drugs: Past, Present...and Future? *Pharmacology and Therapeutics* **68(1)**: 35 – 85.

Cioli, D., Pica-Mattoccia, L., Basso, A. and Guidi, A. (2014) Schistosomiasis control: praziquantel forever? *Molecular and Biochemical Parasitology* **195(1)**: 23 – 29.

Clemens, L.E. and Basch, P.F. (1989) *Schistosoma mansoni*: Insulin Independence. *Experimental Parasitology* **68(1)**: 223 – 229.

Coffer, P.J. and Woodgett, J.R. (1991) Molecular cloning and characterisation of a novel putative protein-serine kinase related to the CAMP-dependent and protein kinase C families. *European Journal of Biochemistry* **201(2)**: 475 – 481.

Collins III, J.J., King, R.S., Cogswell, A., Williams, D.L. and Newmark, P.A. (2011) An Atlas for *Schistosoma mansoni* Organs and Life-Cycle Stages Using Cell Type-Specific Markers and Confocal Microscopy. *Plos Neglected Tropical Diseases* **5(3)**: 1 – 17.

Collins III, J.J., Wang, B., Lambrus, B.G., Tharp, M.E., Iyer, H. and Newmark, P.A. (2013) Adult somatic stem cells in the human parasite *Schistosoma mansoni*. *Nature* **494(7438)**: 476 – 479.

Collins III, J.J., Wendt, G.R. Iyer, H. and Newmark, P.A. (2016) Stem cell progeny contribute to the schistosome host-parasite interface. *eLife* **5(1)**: e12473.

Conus, N.M., Hemmings, B.A. and Pearson, R.B. (1998) Differential Regulation by Calcium Reveals Distinct Signaling Requirements for the Activation of Akt and p70S6k. *The Journal of Biological Chemistry* **273(8)**: 4776 – 4782.

Cornford, E.M. (1974) Effects of insulin on *Schistosomatium douthitti*. *General and Comparative Endocrinology 23(3)*: 286 – 293.

Cross, D.A., Alessi, D.R., Cohen, P., Andjelkovich, M., Hemmings, B.A. (1995) Inhibition of glycogen synthase kinase-3 by insulin mediated by protein kinase B. *Nature* **378 (6559)**: 785 – 789.

Da'dara, A., Krautz-Peterson, G., Faghiri, Z. and Skelly, P.J. (2012) Metabolite movement across the schistosome surface. *Journal of Helminthology* **86(2)**: 141 – 147.

Dajani, R., Fraser, E., Roe, S.M., Young, N., Good, V., Dale, T.C. and Pearl, L.H. (2001) Crystal Structure of Glycogen Synthase Kinase 3: Structural Basis for Phosphate-Primed Substrate Specificity and Autoinhibition. *Cell* **105(6)**: 721 – 732.

Davies, S.J., Shoemaker. C.B. and Pearce, E.J. (1998) A Divergent Member of the Transforming Growth Factor β Receptor Family from *Schistosoma mansoni* Is Expressed on the Parasite Surface Membrane. *Journal of Biological Chemistry* **273(18)**: 11234 – 11240.

De Saram, P.S.R., Ressurreição, M., Davies, A.J., Rollinson, D., Emery, A.M. and Walker, A.J. (2013) Functional Mapping of Protein Kinase A Reveals Its Importance in Adult *Schistosoma mansoni* Motor Activity. *PLoS Neglected Tropical Diseases* **7(1)**: e1988

deWalick, S., Tielens, A.G.M. and van Hellemond, J.J. (2012) *Schistosoma mansoni*: The egg, biosynthesis of the shell and interaction with the host. *Experimental Parasitology* **132(1)**: 7 – 13.

Dissous, C., Ahier, A. and Khayath, N. (2007) Protein tyrosine kinases as new potential targets against human schistosomiasis. *BioEssays* **29(12)**: 1281 – 1288.

Dissous, C. and Grevelding, C.G. (2011) Piggy-backing the concept of cancer drugs for schistosomiasis treatment: a tangible perspective? *Trends in Parasitology* **27(2)**: 59 – 66.

Doenhoff, M. J., Kusel, J.R., Coles, G.C. and Cioli, D. (2002) Resistance of *Schistosoma mansoni* to praziquantel: is there a problem? *Transactions of The Royal Society of Tropical Medicine and Hygiene* **96 (5)**: 465 – 469.

Doerig, C. (2004) Protein kinases as targets for anti-parasitic chemotherapy. Biochimica et Biophysica Acta **1697(1-2)**: 155 – 168.

Dorsey, C. H. (1976). *Schistosoma mansoni*: description of the head gland of cercariae and schistosomules at the ultrastructural level. *Experimental Parasitology* **36(3)**: 444–459.

Dorsey, C.H., Cousin, C.E., Lewis, F.A. and Stirewalt, M.A. (2002) Ultrastructure of the *Schistosoma mansoni* cercariae. *Micron* **33(3)**: 279 – 323.

Du, X., McManus, D.P., Cai, P., Hu, W. and You, H. (2017) Identification and functional characterisation of a *Schistosoma japonicum* insulin-like peptide. *Parasites and Vectors* **10(181)**: 1 – 12.

Dunne, D.W., Agnew, A.M., Modha, J. and Doenhoff, M.J. (1986) *Schistosoma mansoni* egg antigens: preparation of rabbit antisera with monospecific immunoprecipitating activity, and their use in antigen characterization. *Parasite Immunology* **8(6)**: 575 – 586.

Dupont, J., Khan, J., Qu, B., Metzler, P., Helman, L. and LeRoith, D. (2001) Insulin and IGF-1 Induce Different Patterns of Gene Expression in Mouse Fibroblast NIH-3T3 Cells: Identification by cDNA Microarray Analysis. *Endocrinology* **142(11)**: 4969 – 4975.

Erasmus, D.A. (1973) A comparative study of the reproductive system of mature, immature and 'unisexual' female *Schistosoma mansoni. Parasitology* **67(1)**: 165 – 183.

Faghiri, Z. and Skelly, P.J. (2009) The role of tegumental aquaporin from the human parasitic worm, *Schistosoma mansoni*, in osmoregulation and drug uptake. *FASEB Journal* **23(8)**: 2780 – 2789.

Faghiri, Z., Camargo, S.M.R., Huggel, K., Forster, I.C., Ndegwa, D., Verrey, F. and Skelly, P.J. (2010) The Tegument of the Human Parasitic Worm *Schistosoma mansoni* as an Excretory Organ: The Surface Aquaporin SmAQP Is a Lactate Transporter. *PLoS One* **5(5)**: e10451.

Fallon, P.G. and Doenhoff, M.J. (1994) Drug-resistant schistosomiasis: resistance to praziquantel and oxamniquine induced in *Schistosoma mansoni* in mice is drug specific. *The American Journal of Tropical Medicine and Hygiene* **51(1)**: 83 – 88.

Fang, X., Yu, X.Y., Lu, Y., Bast, Jr., R.C., Woodgett, J.R. and Gordon B. Mills, G.B. (2000) Phosphorylation and inactivation of glycogen synthase kinase 3 by protein kinase A. *Proceedings of the National Academy of Sciences of the United States of America* **97(22)**: 11960 – 11965.

Felder, C.B., Graul, R.C., Lee, A.Y., Merkle, H. and Sadee, W. (1999) The Venus Flytrap of Periplasmic Binding Proteins: An Ancient Protein Module Present in Multiple Drug Receptors. *AAPS PharmSci* **1(2)**: article 2.

Forrester, S.G., Warfel, P.W. and Pearce, E.J. (2004) Tegumental expression of a novel type II receptor serine/threonine kinase (SmRK2) in *Schistosoma mansoni*. *Molecular and Biochemical Parasitology* **136(1)**: 149 – 156.

Fransson, A., Ruusala, A., and Aspenstrom, P. (2003) A typical Rho GTPases have roles in mitochondrial homeostasis and apoptosis. *Journal of Biological Chemistry* **278(1)**: 6495 – 6502.

Fujinami, A. and Nakamura, G. (1909) The route of infection and the development of the parasite of Katayama disease (Schistosomiasis japonica) in the infected animal. *Kyoto Igakai Zasshi* **6**: 224 - 252.

Fusco, A.C., Salafsky, B. and Delbrook, K. (1986) *Schistosoma mansoni*: Production of Cercarial Eicosanoids as Correlates of Penetration and Transformation. *The Journal of Parasitology* **72(3)**: 397 – 404.

Gelmedin, V., Morel, M., Hahnel, S., Cailliau, K., Dissous, C. and Grevelding, C.G. (2017) Evidence for Integrin ± Venus Kinase Receptor 1 Alliance in the Ovary of *Schistosoma mansoni* Females Controlling Cell Survival. *PLoS Pathogens* **13(1)**: e1006147.

The Gene Ontology Consortium, Ashburner, M., Ball, C.A., Blake, J.A., Botstein, D., Butler, H., Cherry, J.M., Davis, A.P., Dolinski, K., Dwight, S.S., Eppig, J.T., Harris, M.A., P. Hill, D.P., Issel-Tarver, L., Kasarskis, A., Lewis, S., Matese, J.C., Richardson, J.E., Ringwald, M., Rubin, G.M. and Sherlock, G. (2000) Gene Ontology: tool for the unification of biology. *Nature Genetics* **25(1)**: 25–29.

The Gene Ontology Consortium (2006) The Gene Ontology (GO) project in 2006. *Nucleic Acids Research* **34(Database issue)**: D322 – D326.

Giambelluca, M.S., Cloutier, N., Rollet-Labelle, E., Boilard, E. and Pouliot. M. (2013) Expression and regulation of glycogen synthase kinase 3 in human neutrophils. *The International Journal of Biochemistry and Cell Biology* **45(1)**: 2660 – 2665.

Gobert, G.N., Stenzel, D.J., McManus, D.P., Jones, M.K. (2003) The ultrastructural architecture of the adult *Schistosoma japonicum* tegument. *International Journal for Parasitology* **33(14)**: 1561 – 1575.

Gönnert, R. (1955) Schistosomiasis studies. I. Contributions to the anatomy and histology of *Schistosoma mansoni*. *Zeitschrift fur Tropenmedizin und Parasitologie* **6(1)**: 18 – 33.

Gouignard, N., Vanderstraete, M., Cailliau, K., Lescuyer, A., Browaeys, E. and Dissous, C. (2012) *Schistosoma mansoni*: Structural and biochemical characterization of two distinct Venus Kinase Receptors. *Experimental Parasitology* **132(1)**: 32 – 39.

Granzer, M. and Haas, W. (1986) The chemical stimuli of human skin surface for the attachment response of *Schistosoma mansoni* cercariae. *International Journal of Parasitology* **16(1)**: 575 – 579.

Grimes C.A. and Jope, R.S. (2001) The multifaceted roles of glycogen synthase kinase 3_ in cellular signalling. *Progress in Neurobiology* **65(4)**: 391 – 426.

Gryseels, B., Polman, K., Clerinx, J. And Kestens, L. (2006) Human Schistosomiasis. *The Lancet* **368(1)**: 1106 – 1118.

Haas, W. (2003) Parasitic worms: strategies of host finding, recognition and invasion. *Zoology* **106(1)**: 349 – 364.

Haas, W. and Haberl, B. (1997) Host Recognition by Trematode Miracidia and Cercariae. In Fried, B., Graczyk, T. K. *Advances in Trematode Biology*. London: CRC Press, pp197 – 220.

Haas, W., Granzer, M. and Hannappel, E. (1989) Ein Funktionswandel des Signals Arginin bei der Wirtsfindung von schistosoma-Cercarien. *Verhandlungen der Deutschen Zoologischen Gesellschaft* **82**: 241.

Haas, W., Diekhoff, D., Koch, K., Schmalfuss, G. and Loy, C. (1997) *Schistosoma mansoni* cercariae: Stimulation of Acetabular gland secretion is adapted to the chemical composition of mammalian skin. *The Journal for Parasitology* **83(6)**: 1079 – 1085.

Haas, W., Grabe, K., Geis, C., Päch, T., Stoll, K., Fuchs, M., Haberl, B. and Loy, C. (2002) Recognition and invasion of human skin by *Schistosoma mansoni* cercariae: the key-role of l-arginine **124(1)**: 153 – 167.

Haas, W., Haeberlein, S., Behring, S. and Zoppelli, E. (2008) *Schistosoma mansoni*: Human skin ceramides are a chemical cue for host recognition of cercariae. *Experimental Parasitology* **120(1)**: 94 – 97.

Hall, A. (1990) The Cellular Functions of Small GTP-Binding Proteins. *Science* **249(4969)**: 635 – 640.

Han, Q., Jia, B., Hong, Y., Cao, X., Zhai, Q., Lu, K., Li, H., Zhu, C., Fu, Z., Shi, Y. and Lin, J. (2017) Suppression of VAMP2 Alters Morphology of the Tegument and Affects Glucose uptake, Development and Reproduction of *Schistosoma japonicum. Scientific Reports* **7(5121)**: 1 – 12.

Hanada, M., Feng, J. and Hemmings, B.A. (2004) Structure, regulation and function of PKB/AKT—a major therapeutic target*. Biochimica et Biophysica Acta* **1697(1)**: 3 – 16.

Hanks, S.K., Quinn, A.M. and Hunter, T. (1988) The protein kinase family: conserved features and deduced phylogeny of the catalytic domains. *Science* **241(4861)**: 42 – 52.

Haslam, R.J., Koide, H.B. and Hemmings, B.A. (1993) Pleckstrin domain homology. *Nature* **363(1)**: 309 – 310.

He, Y., Chen, L. and K. Ramaswamy, K. (2002) *Schistosoma mansoni, S. haematobium,* and *S. japonicum*: early events associated with penetration and migration of schistosomula through human skin. *Experimental Parasitology* **102(1)**: 99 – 108.

Hernandez, H.J., Edson, C.M., Harn, D.A., Ianelli, C.J. and Stadecker, M.J. (1998) *Schistosoma mansoni:* Genetic Restriction and Cytokine Profile of the CD4 + T Helper Cell Response to Dominant Epitope Peptide of Major Egg Antigen Sm-p40. *Experimental Parasitology* **90(1)**: 122 – 130.

Higuchi, M., Masuyama, N., Fukui, Y., Suzuki, A. and Yukiko Gotoh, Y. (2001) Akt mediates Rac/Cdc42-regulated cell motility in growth factorstimulated cells and in invasive PTEN knockout cells. *Current Biology* **11(24)**: 1958 – 1962.

Hirst, N.L., Lawton, S.P. and Walker, A.J. (2016) Protein kinase A signalling in *Schistosoma mansoni* cercariae and schistosomules. *International Journal for Parasitology* **46(7)**: 425 – 437.

Hobdy-Henderson, K.C., Hales, C.M., Lapierre, L.A., Cheney R.E. and Goldenring, J.R. (2003) Dynamics of the apical plasma membrane recycling system during cell division. *Traffic* **4(10)**: 681 – 693.

Hockley, D.J. (1968) Small spines on the egg shells of Schistosoma. *Parasitology* **58(2)**: 367 – 370.

Hockley, D.J. and McLaren, D.J. (1973) *Schistosoma mansoni*: Changes in the outer membrane of the tegument during development from cercaria to adult worm. *International Journal for Parasitology* **3(1)**: 13 – 25.

Hu, W., Brindley, P.J., McManus, D.P., Feng, Z. and Han, Z. (2004) Schistosome transcriptomes: new insights into the parasite and schistosomiasis. *TRENDS In Molecular Medicine* **10(5)**: 217 – 225.

Huang, Z., Bodkin, N.L., Ortmeyer, H.K., Hansen, B.C. and Shuldiner, A.R. (1994) Hyperinsulinemia Is Associated with Altered Insulin Receptor mRNA Splicing in Muscle of the Spontaneously Obese Diabetic Rhesus Monkey. *The Journal of Clinical Investigation* **94(3)**: 1289 – 1296.

Hughes, K., Hughes, E., Nikolakaki, S.E., Plyte, N.F. and Woodgett, J.T. (1993) Modulation of the Glycogen-Synthase Kinase-3 family by tyrosine phosphorylation. *EMBO Journal* **12(2)**: 803 – 808.

Isotani, S., Hara, K., Tokunaga, C., Inoue, H., Avruch, J. and Yonezawa, K. (1999) Immunopurified Mammalian Target of Rapamycin Phosphorylates and Activates p70 S6 Kinase α in Vitro. *The American Society for Biochemistry and Molecular Biology.* **274(48)**:34493 – 34498.

Jenkins, S.J., Hewitson, J.P., Jenkins, G.R. and Mountford, A.P. (2005) Modulation of the host's immune response by schistosome larvae. *Parasite Immunology* **27(1)**: 385 – 393.

Jiang, J., Skelly, P.J., Shoemaker, C.B. and Caulfield, J.P. (1996) *Schistosoma mansoni:* The Glucose Transport Protein SGTP4 Is Present in Tegumental Multilamellar Bodies, Discoid Bodies, and the Surface Lipid Bilayers. *Experimental Parasitology* **82(1)**: 201 – 210.

Jiang, S. and Ramachandran, S. (2006) Comparative and evolutionary analysis of genes encoding small GTPases and their activating proteins in eukaryotic genomes. *Physiological Genomics* **24(3)**: 235 – 251.

Jo, H., Mondala, S., Tana, D., Nagatac, E., Takizawac, S., Sharmad, A.K., Houe, Q., Shanmugasundaramd, K., Prasada, A., Tunga, J.K., Tejedaa, A.O., Mane, H., Rigbyd, A.C. and Luoa, H.R. (2012) Small molecule-induced cytosolic activation of protein kinase Akt rescues ischemia-elicited neuronal death. Proceedings of the National Academy of Sciences **109(26)**: 10581 – 10586.

Jones, P.F., Jakubowicz, T. Hemmings. B.A. (1991) Molecular cloning of a second form of rac protein kinase. *Cell Regulation* **2(1)**: 1001 – 1009.

Jones, M.K., Lustigman, S. and Loukas, A. (2008) Tracking the Odysseys of Juvenile Schistosomes to Understand Host Interactions. *PLoS Neglected Tropical Diseases* **2(7)**: e257.

Kaboord, B. and Perr, M. (2008) Isolation of Proteins and Protein Complexes by Immunoprecipitation. In: A. Posch, ed., *2D Page: sample preparation and fractionation, Volume 1*. Totowa: Humana Press., pp. 349 – 364.

Kampkötter, A., Ridgers, I., Johnston, D.A., Rollinson, D., Kunz, W. and Grevelding, C.G. (1999) *Schistosoma mansoni*: Cloning and Characterization of the Ras Homologue. *Experimental Parasitology* **91(3)**: 280 – 283.

Kapp, K., Schüßler, P., Kunz, W. and Grevelding, C.G. (2001) Identification, isolation and characterization of a Fyn-like tyrosine kinase from *Schistosoma mansoni. Parasitology* **122(3)**: 317 – 327.

Kapp, K., Knobloch, J., Schüßler, P., Sroka, S., Lammers, R., Kunz, W. and Grevelding, C.G. (2004) The *Schistosoma mansoni* Src kinase TK3 is expressed in the gonads and likely involved in cytoskeletal organization. *Molecular and Biochemical Parasitology* **138(1)**: 171 – 182.

Kardalinou, E., Zhelev, N., Hazzalin, C.A. and Mahadevan, L.C. (1994) Anisomycin and Rapamycin Define an Area Upstream of p70/85S6k Containing a Bifurcation to Histone H3-HMG-Like Protein Phosphorylation and c-fos-c-jun Induction. *American Society for Microbiology* **14(2)**: 1066 – 1074.

Kasinathan, R.S., Sharma, L.K., Cunningham, C., Webb, T.R. and Greenberg, R.M. (2014) Inhibition or Knockdown of ABC Transporters Enhances Susceptibility of Adult and Juvenile Schistosomes to Praziquantel. *PLoS Neglected Tropical Diseases* **9(10)**: e3265.

Kessler, A., Tomas, E., Immler, D., Meyer, H.E., Zorzano, A. and Eckel, J. (2000) Rab11 is associated with GLUT4-containing vesicles and redistributes in response to insulin. *Diabetologia* **43(12)**: 1518 – 1527.

Khalil, M., (1921) The Morphology of the Cercaria of *Schistosoma mansoni* from *Planorbis boissyi* of Egypt. *Proceedings of the Royal Society of Medicine* **15**: 27 – 34.

Khan, A.H. and Pessin, J.E. (2002) Insulin regulation of glucose uptake: a complex interplay of intracellular signalling pathways. *Diabetologia* **45(11)**: 1475 – 1483.

Khayath, N., Vicogne, J., Ahier, A., BenYounes, A., Konrad, C., Trolet, J., Viscogliosi, E., Brehm, K. and Dissous, C. (2007) Diversification of the insulin receptor family in the helminth parasite *Schistosoma mansoni*. *The Federation of European Biochemical Societies Journal* **274(3)**: 659 – 676.

Kim, L., Liu, J. and Kimmel, A.R. (1999) The Novel Tyrosine Kinase ZAK1 Activates GSK3 to Direct Cell Fate Specification. *Cell* **99(4)**: 399 – 408.

Kim, H., Choi, H., Lim, J., Park, J., Jung, H.J., Lee, Y., Kim, S. and Kwon, T. (2011) Emerging role of Akt substrate protein AS160 in the regulation of AQP2 translocation. *American Journal of Physiology – Renal Physiology* **301(1)**: 151 – 161.

Kotani, K., Carozzi, A.J., Sakaue, H., Hara, K., Robinson, L.J., Clark, S.F., Yonezawa, K., James, D.E. and Kasuga, M. (1995) Requirement for Phosphoinositide 3-Kinase in Insulin-Stimulated GLUT4 Translocation in 3T3-L1 *Adipocytes. Biochemical and Biophysical Communications* **209(1)**: 343 – 348.

Knobloch, J., Winnen, R., Quack, M., Kunz, W. And Grevelding, C.G. (2002) A novel Syk-family tyrosine kinase from *Schistosoma mansoni* which is preferentially transcribed in reproductive organs. *Gene* **294(1)**: 87 – 97.

Knobloch, J., Rossi, A., Osman, A., LoVerde, P.T., Klinkert, M., Grevelding, C.G. (2004) Cytological and biochemical evidence for a gonad-preferential interplay of SmFKBP12 and SmT_R-I in *Schistosoma mansoni*. *Molecular and Biochemical Parasitology* **138(2)**: 227 – 236.

Knobloch, J., Kunz, W. and Grevelding, C.G. (2006) Herbimycin A suppresses mitotic activity and egg production of female *Schistosoma mansoni*. *International Journal for Parasitology* **36(1)**: 1261 – 1272.

Knödler, A., Feng, S., Zhang, J., Zhang, X., Das, A., Peränen, J. and Guo, W. (2010) Coordination of Rab8 and Rab11 in primary ciliogenesis. *PNAS* **107(14)**: 6346 – 6351.

Kunz, W. (2001) Schistosome male–female interaction: induction of germ-cell differentiation. *TRENDS in Parasitology* **17(5)**: 227 – 231.

Larance, M., Ramm, G., Stöckli, J., van Dam, E.M., Winata, S., Wasinger, V., Simpson, F., Graham, M., Junutula, J.R., Guilhaus, M. and James, D.E. (2005) Characterization of the Role of the Rab GTPase-activating Protein AS160 in Insulin-regulated GLUT4 Trafficking. *The Journal of Biological Chemistry* **280(45)**: 37803 – 37813.

Lawlor, M.A. and Alessi, D.R. (2001) PKB/Akt: a key mediator of cell proliferation, survival and insulin responses? *Journal of Cell Science* **114(16)**: 2903 – 2910.

Leiper, R.T. (1915) Report on the results of the Bilharzia mission in Egypt, 1915. Part I. Transmission. *Journal of the Royal Army Medical Corps* **26**: 253 – 267.

Lietzke, S.E., Bose, S., Cronin, T., Klarlund, J., Chawla, A., Czech, M.P. and Lambright, D.G. (2000) Structural Basis of 3-Phosphoinositide Recognition by Pleckstrin Homology Domains. *Molecular Cell* **6(1)**: 385 – 394.

Loeffler, I.K. and Bennett, J.L. (1996) A rab-related GTP-binding protein in *Schistosoma mansoni. Molecular and Biochemical Parasitology* **77(1)**: 31 – 40.

Long, T., Vanderstraete, M., Cailliau, K., Morel, M., Lescuyer, A., Gouignard, N., Grevelding, C.G., Browaeys, E., Dissous, C. (2012) SmSak, the Second Polo-Like Kinase of the Helminth Parasite *Schistosoma mansoni*: Conserved and Unexpected Roles in Meiosis. *PloS ONE* **7(6)**: e40045.

Lorenz, W., Henglein, A. and Schrader, G. (1955) The new insecticide O,O-dimethyl-2,2,2-trichloro-l-hydroxyethylphosphonate. *Journal of the American Chemical Society* **77(1)**: 2554.

Loukas, A., Tran, M. and Pearson, M.S. (2007) Schistosome membrane proteins as vaccines. *International Journal for Parasitology* **37(3-4)**: 257 – 263.

LoVerde, P.T., Niles, E.G., Osman, A. and Wu, W. (2004) *Schistosoma mansoni* male–female interactions. *Canadian Journal of Zoology* **82(2)**: 357 – 374.

LoVerde, P.T., Andrade, L.F. and Oliveira, G. (2009) Signal Transduction Regulates Schistosome Reproductive Biology. *Current Opinions in Microbiology* **12(4)**: 422 – 428.

Ludtmann, M.H.R., Rollinson, D., Emery, A.M., Walker, A.J. (2009) Protein kinase C signalling during miracidium to mother sporocyst development in the helminth parasite, *Schistosoma mansoni*. *International Journal for Parasitology* **39(11)**:1223 – 1233.

Machado-Silva, J.R., Galvão, C., de Oliveira, R.M.F., Presgrave, O.A.F. and Gomes, D.C. (1995) *Schistosoma mansoni* Sambon, 1907: comparative morphological studies of some brazilian strains. *Revista do Instituto de Medicina Tropical de São Paulo* **37(5)**: 441 – 447.

Mair, G. R., Maule, A. G., Fried, B., Dayt, T. A. and Haltont, D. W. (2003) Organization of the Musculature of Schistosome Cercariae. *Journal of Parasitology* **89(3)**: 623 – 625.

Manneck, T., Haggenmüller, Y. and Keiser, J. (2010) Morphological effects and tegumental alterations induced by mefloquine on schistosomula and adult flukes of *Schistosoma mansoni*. *Parasitology* **137(1)**: 85 – 98.

Manning, B.D. and Cantley, L.C. (2007) AKT/PKB Signaling: Navigating Downstream. *Cell* **129(1)**: 1261 – 1274.

Matsumura, K., Shimada, M., Sato, K. and Aoki, Y. (1990) Praziquantel-Induced Secretion of Proteolytic Enzyme from *Schistosoma mansoni* Cercariae. *The Journal of Parasitology* **76(3)**: 436 – 438.

McCormick, F. (1993) How receptors turn Ras on. *Nature* **363(6424)**: 15 – 16.

McLaren, D. J. and Hockley, D. J. (1977). Blood flukes have a double outer membrane. *Nature* **269(1)**: 147–149.

McKerrow, J.H. and Doenhoff, M.J. (1988) Schistosome proteases. *Parasitology Today* **4(12)**: 334 – 340.

Meili, R., Ellsworth, C., Lee, S., Reddy, T.B.K., Ma, H. and Firtel, R.A. (1999) Chemoattractant-mediated transient activation and membrane localization of Akt/PKB is required for efficient chemotaxis to cAMP in Dictyostelium. *The EMBO Journal* **18(8)**: 2092 – 2105.

Mora, A., Komander, D., van Aalten, D.M.F. and Alessi, D.R. (2004) PDK1, the master regulator of AGC kinase signal transduction. *Seminars in Cell & Developmental Biology* **15(1)**: 161–170.

Morel, M., Vanderstraete, M., Cailliau, K., Lescuyer, A., Lancelot, J. and Dissous, C. (2014a) Compound library screening identified Akt/PKB kinase pathway inhibitors as potential key molecules for the development of new chemotherapeutics against schistosomiasis. *International Journal for Parasitology: Drugs and Drug Resistance* **4(1)**: 256 – 266.

Morel, M., Vanderstraete, M., Hahnel, S., Grevelding, C.G. and Dissous, C. (2014b) Receptor tyrosine kinases and schistosome reproduction: new targets for chemotherapy. *Frontiers in Genetics* **5(238)**: 1 – 5.

Morel, M., Vanderstraete, M., Cailliau, K., Hahnel, S., Grevelding, C.G. and Dissous, C. (2016) SmShb, the SH2-ContainingAdaptor Protein B of *Schistosoma mansoni* Regulates Venus Kinase Receptor Signaling Pathways. *PLoS ONE* **11(9)**: 1 – 19.

Morris, G.P. and Threadgold, L.T. (1968) Ultrastructure of the tegument of adult *Schistosoma mansoni*. *The Journal of Parasitology* **54(1)**: 15 – 27.

Murai, H., Okazaki, M. and Kikuchi, A. (1996) Tyrosine dephosphorylation of glycogen synthase kinase-3 is involved in its extracellular signal-dependent inactivation. *FEBS Letters* **392(2)**: 153 – 160.

Murillo-Cuesta, S., Rodríguez-de la Rosa, L., Cediel, R., Lassaletta, L. and Varela-Nieto, I. (2011) The role of insulin-like growth factor-I in the physiopathology of hearing. *Frontiers in Molecular Neuroscience* **4(11)**: 1 – 17.

Naguib, F.N.M., and el Kouni, M.H. (2014) Nucleoside kinases in adult *Schistosoma mansoni*: Phosphorylation of pyrimidine nucleosides. *Molecular and Biochemical Parasitology* **194(1-2)**: 53 – 55.

Najafov, A., Sommer, E.M., Axten, J.M., DeYoung, M.P. and Alessi, D.R. (2011) Characterization of GSK2334470, a novel and highly specific inhibitor of PDK1. *Biochemical Journal* **433(1)**: 357 – 369.

Natarajan, M., Lin, K.M., Hsueh, R.C., Sternweis, P.C. and Ranganathan, R. (2006) A global analysis of cross-talk in a mammalian cellular signalling network. *Nature Cell Biology* **8(6)**: 571 – 580.

Ndegwa, D., Krautz-Peterson, G. and Skelly, P.J. (2007) Protocols for gene silencing in schistosomes. *Experimental Parasitology* **117(3)**: 284 – 291.

Nene, V., Dunne, D., Johnson, K., Taylor, D. and Cordingley, J. (1986) Sequence and expression of a major egg antigen from *Schistosoma mansoni*. Homologies to heat shock proteins and alpha-crystallins. *Molecular and biochemical parasitology* **21(2)**:179 – 188.

Norrmén, C. And Suter, U. (2013) Akt/mTOR signalling in myelination. *Biochemical Society Transactions* **41(4)**: 944 – 950.

Novick, P. and Zerial, M. (1997) The diversity of Rab proteins in vesicle transport. *Current Opinion in Cell Biology* **9(4)**: 496 – 504.

Osman, A., Niles, E.G. and LoVerde, P.T. (1999) Characterization of the Ras homologue of *Schistosoma mansoni. Molecular and Biochemical Parasitology* **100(1)**: 27 – 41.

Osman, A., Niles, E.G., and LoVerde. P.T. (2001) Identification and Characterization of a Smad2 Homologue from *Schistosoma mansoni*, a Transforming Growth Factor-b Signal Transducer. *The Journal of Biological Chemistry* **276(13)**: 10072 – 10082.

Osman, A., Niles, E.G., and LoVerde. P.T. (2004) Expression of Functional *Schistosoma mansoni* Smad4: Role in ERK mediated transforming growth factor β (TGF-β) down regulation. The Journal of Biological Chemistry **279(8)**: 6474 – 6486.

Osolodkin, D.I., Zakharevich, N.V., Palyulin, V.A., Danilenko, V.N. and Zefirov, N.S. (2011) Bioinformatic analysis of glycogen synthase kinase 3: human versus parasite kinases. *Parasitology* **138(1)**: 725 – 735.

Pandini, G., Medico, E., Conte, E., Sciacca, L., Vigneri, R. and Belfiore, A. (2003) Differential Gene Expression Induced by Insulin and Insulin-like Growth Factor-II through the Insulin Receptor Isoform A. *The Journal of Biological Chemistry* **278(43)**: 42178 – 42189.

Paradis, S. and Ruvkun, G. (1998) *Caenorhabditis elegans* Akt/PKB transduces insulin receptor-like signals from AGE-1 PI3 kinase to the DAF-16 transcription factor. *Genes and Development* **12(16)**: 2488 – 2498.

Paradis, S., Ailion, M., Toker, A., Thomas, J.H. and Ruvkun, G. (1999) A PDK1 homolog is necessary and sufficient to transduce AGE-1 PI3 kinase signals that regulate diapause in *Caenorhabditis elegans*. *Genes and Development* **13(11)**: 1438 – 1452.

Parasido, E.M., Silvestri, A., Canzonieri, V., Belluco, C., Diodoro, M.G., Milione, M., Melotti, F., De Maria, R., Liotta, L., Petricoin, E.F. and Pierobon, M. (2017) Protein drug target activation homogeneity in the face of intra-tumor heterogeneity: implications for precision medicine. *Oncotarget* **8(30)**: 48534 – 48544.

Patocka, N., Sharma, N., Rashid, M. and Ribeiro, P. (2014) Serotonin Signaling in Schistosoma mansoni: A Serotonin-Activated G Protein-Coupled Receptor Controls Parasite Movement. *PloS Pathogens* **10(1)**: e1003878.

Pearce, E.J., Caspar, P., Grzych, J.M., Lewis, F.A. and Sher, A. (1991) Downregulation of Th1 cytokine production accompanies induction of Th2 responses by a parasitic helminth, *Schistosoma mansoni*. *Journal of Experimental Medicine* **173(1)**:159 – 66.

Peranen, J., Auvinen, P., Virta, H., Wepf, R., Simons, K. (1996) Rab8 promotes polarized membrane transport through reorganization of actin and microtubules in fibroblasts. *Journal of Cell Biology* **135(1):** 153 – 167.

Peterson, R.T. and Schreiber, S.L. (1999) Kinase phosphorylation: Keeping it all in the family. *Current Biology* **9(14)**: R521 – R524.

Pica-Mattoccia, L., Carlini, D., Guidi, A., Cimica, V., Vigorosi, F. and Cioli, D. (2006) The schistosome enzyme that activates oxamniquine has the characteristics of a sulfotransferase. *Memorias do Instituto Oswaldo Cruz* **101(Suppl. 1)**: 307 – 312.

Pica-Mattoccia, L. and Cioli, D. (2004) Sex- and stage-related sensitivity of *Schistosoma mansoni* to in vivo and in vitro praziquantel treatment. *International Journal for Parasitology* **34(4)**: 527 – 533.

Popiel, I. and Basch, P.F. (1984) Reproductive development of female of *Schistosoma mansoni* (digenean Schistosomatidae) following bisexual pairing of worms and worm segments. *Journal of Experimental Zoology* **232(1)**: 141 – 150.

Pottinger, P.S. and Jong. E.C. (2017) Trematodes. In: The Travel and Tropical Medicine Manual, fifth edition. Elsevier pp. 588 – 597.

Protasio, A.V., Tsai, I.J., Babbage, A., Nichol, S., Hunt, M., Aslett, M.A., De Silva, N., Velarde, G.S., Anderson, T.J.C., Clark, R.C., Davidson, C., Dillon, G.P., Holroyd, N.E., LoVerde, P.T., Lloyd, C., McQuillan, J., Oliveira, G., Otto, T.D., Parker-Manuel, S.J., Quail, M.A., Wilson, R.A., Zerlotini, A., Dunne, D.W. and Berriman, M. (2012) A Systematically Improved High Quality Genome and Transcriptome of the Human Blood Fluke *Schistosoma mansoni*. *PLOS Neglected Tropical Diseases* **6(1)**: e1455, 1 – 13.

Quack, T., Knobloch, J., Beckmann, S., Vicogne, J., Dissous, C. and Grevelding, C.G. (2009) The Formin-Homology Protein SmDia Interacts with the Src Kinase SmTK and the GTPase SmRho1 in the Gonads of *Schistosoma mansoni*. *PLoS One* **4(9)**: e6998.

Ramachandran, H.; Skelly, P.J. and Shoemaker, C.B. (1996) The *Schistosoma mansoni* epidermal growth factor receptor homologue, SER, has tyrosine kinase activity and is localized in adult muscle. *Molecular and Biochemical parasitology* **83(1)**: 1 – 10.

Ressurreicao M (2009) *Cell Signalling in Schistosoma mansoni: a role for p38 MAPK*. MSC by Research Thesis, Kingston University, UK.

Ressurreicao M (2013) Protein Kinase Signalling in *Schistosoma mansoni*. PhD Thesis, Kingston University, UK.

Ressurreição, M., Rollinson, D., Emery, A.M. and Walker, A.J. (2011) A role for p38 mitogen-activated protein kinase in early post-embryonic development of *Schistosoma mansoni*. *Molecular and Biochemical Parasitology* **180(1)**: 51 – 55.

Ressurreição, M., De Saram, P., Kirk, R.S., Rollinson, D., Emery, A.M., Page, N.M., Davies, A.J., Walker, A.J. (2014) Protein Kinase C and Extracellular Signal-Regulated Kinase Regulate Movement, Attachment, Pairing and Egg Release in *Schistosoma mansoni*. *PLOS Neglected Tropical Diseases* **8(6)**: e2924, 1 – 21.

Ressurreição, M., Kirk, R.S., Rollinson, D., Emery, A.M., Page, N.M. and Walker. A.J. (2015) Sensory Protein Kinase Signaling in *Schistosoma mansoni* Cercariae: Host Location and Invasion. *Journal of Infectious Diseases* **212(10)**: 1787 – 1797.

Ridley, A.J. (2006) Rho GTPases and actin dynamics in membrane protrusions and vesicle trafficking. *TRENDS in Cell Biology* **16(10)**: 522 – 529.

Roberts, S.M., MacGregor, A.N. Vojvodic, M., Wells, E., Crabtree, J.A. and Wilson, R.A. (1983) Tegument surface-membranes of adult *Schitsosoma mansoni* – Development of a method for their isolation. *Molecular and Biochemical Parasitology* **9(2)**: 105 – 127.

Rogers, S.H. and Beuding, E. (1975) Anatomical localization of glucose uptake by *Schistosoma mansoni* adults*. International Journal for Parasitology* **5(3)**: 369 – 371.

Ross, A.G.P., Bartley, P.B., Sleigh, A.C., Olds, R., Li, Y., Williams, G.M. and McManus, D.P. (2002) Schistosomiasis. *The New England Journal of Medicine* **346(16)**: 1212 – 1220.

Salafsky, B. and Fusco. A.C. (1987) *Schistosoma mansoni:* A comparison of secreted vs nonsecreted eicosanoids in developing schistosomulae and adults. *Experimental Parasitology.* **64(3)**: 361 – 367.

Salminen, A. and Novick, P.J. (1987) A *ras*-like protein is required for a post-Golgi event in yeast secretion. *Cell* **49(4)**: 527 – 538.

Samuelson, J.C. and Caulfield, J.P. (1982) Loss of Covalently Labeled Glycoproteins and Glycolipids from the Surface of Newly Transformed Schistosomula of *Schistosoma mansoni*. *The Journal of Cell Biology* **94(1)**: 363 – 369.

Samuelson, J.C. and Caulfield, J.P. (1985) The Cercarial Glycocalyx of *Schistosoma mansoni*. *The Journal of Cell Biology* **100(1)**: 1423 – 1434.

Sarbassov, D.D., Geurtin, D.A., Ali, S.M. and Sabatini, D.M. (2005) Phosphorylation and Regulation of Akt/PKB by the Rictor-mTOR Complex. *SCIENCE* **307(5712)**: 1098 – 1101.

Sato, H., Kusel, J.R. and Thornhill, J. (2002) Functional visualization of the excretory system of adult *Schistosoma mansoni* by the fluorescent marker resorufin. *Parasitology* **125(6)**: 527 – 535.

Schäke, H., Schröder, H.C., Gamulin, V., Rinkevich, B., Müller, I.M. and Müller, W.E.G. (1994) Molecular cloning of a tyrosine kinase gene from the marine sponge *Geodia cydonium*: a new member belonging to the receptor tyrosine kinase class II family. *Molecular Membrane Biology* **11(2)**: 101 – 107.

Schramm, G., Falcone, F.H., Gronow, A., Haisch, K., Mamat, U., Doenhoff, M.J., Oliveira, G., Galle, J., Dahinden, C.A. and and Haas, H. (2003) Molecular Characterization of an Interleukin-4-inducing Factor from *Schistosoma mansoni* Eggs. *The Journal of Biochemical Chemistry* **278(20)**: 18384 – 18392.

Schueßler, P., Grevelding, C.G. and Kunz, W. (1997). Identifcation of Ras, MAP kinases, and a GAP protein in *Schistosoma mansoni* by immunoblotting and their putative involvement in male-female interaction. *Journal of Parasitology*, **115**: 629-634.

Schultze, S.M., Hemmings, B.A., Niessen, M. and Tschopp, O. (2012) PI3K/AKT, MAPK and AMPK signalling: protein kinases in glucose homeostasis. *Expert reviews in molecular medicine* **14(e1)**: 1 – 21.

Senft, A.W., Philpott, D.E. and Pelofsky, A.H. (1961) Electron Microscope Observations of the Integument, Flame Cells, and Gut of *Schistosoma mansoni*. *The Journal of Parasitology* **47(2)**: 217 – 229.

Seth, R.B., Sun, L., Ea, C. and Chen, Z.J. (2005) Identification and Characterization of MAVS, a Mitochondrial Antiviral Signaling Protein that Activates NF-_B and IRF3. *Cell* **122(5)**: 669 – 682.

Shiff, C. J., Cmelik, S. H. W., Ley, H. E. and Kriel, R. L. (1972) The influence of human skin lipids on the cercarial penetration response of *Schistosoma haematobium* and *Schistosoma mansoni*. *The Journal of Parasitology* **58(3)**: 476 – 480.

Shiff, C.J. and Thaddeus K. Graczyk, T.K. (1994) A Chemokinetic Response in *Schistosoma mansoni* Cercariae. *The Journal of Parasitology* **80(6)**: 879 – 883.

Shirane, M. and Nakayama, K. (2006) Protrudin induces neurite formation by directional membrane trafficking. *Science* **314(5800)**: 818 – 821.

Shuhua, X., Binggui, S., Chollet, J. and Tanner, M. (2000) Tegumental changes in adult *Schistosoma mansoni* harboured in mice treated with praziquantel enantiomers. *Acta Tropica* **76(2)**: 107 – 117.

Skelly, P.J., Kim, J.W., Cunningham, J., and Shoemaker, C.B. (1994) Cloning, Characterisation, and functional expression of cDNAs encoding glucose-transporter proteins from the human parasite *Schistosoma mansoni*. *Journal of Biological Chemistry* **269(6)**: 4247 – 4253.

Skelly, P.J. and Shoemaker, C.B. (1995) A molecular genetic study of the variations in metabolic function during schistosome development. *Memorias do Instituto Oswaldo Cruz* **90(2)**: 281 – 284.

Skelly, P.J. and Shoemaker, C.B. (1996) Rapid appearance and asymmetric distribution of glucose transporter SGTP4 at the apical surface of intramammalian-stage *Schistosoma mansoni*. *Proceedings of the National Academy of Sciences of the United States of America* **93(8)**: 3642 – 3646.

Skelly, P.J. and Shoemaker, C.B. (2001) The *Schistosoma mansoni* host-interactive tegument forms from vesicle eruptions of a cyton network. *Parasitology* **122(1)**: 67 – 73.

Skelly, P.J., Tielens, A.G.M. and Shoemaker, C.B. (1998) Glucose Transport and Metabolism in Mammalian-stage Schistosomes. *Parasitology Today* **14(10)**: 402 – 406.

Skorokhod, A., Gamulin, V., Gundacker, D., Kavsan, V., Muller, I.M. and Muller, W.E.G. (1999) Origin of Insulin Receptor-Like Tyrosine Kinases in Marine Sponges. The Biological Bulletin **197(2)**: 198 – 206.

Smith, R.M., Charron, M.J., Shah, N., Lodish, H.F. and Jarett, L. (1991) Immunoelectron microscopic demonstration of insulin-stimulated translocation of glucose transporters to the plasma membrane of isolated rat adipocytes and masking of the carboxyl-terminal epitope of intracellular GLUT4 (glucose transport/insulin action/epitope masking). *Proceeding of the National Academy of Sciences of the United States of America* **88(15)**: 6893 – 6897.

Smithers, S.R., Terry, R.J. and Hockley, D.J. (1969) Host Antigens in Schistosomiasis. *Proceedings of the Royal Society B* **171(1025)**: 483 – 494.

Stadecker, M.J. (1999) The development of granulomas in schistosomiasis: genetic backgrounds, regulatory pathways, and specific egg antigen responses that influence the magnitude of disease. *Microbes and Infection* **1(7)**: 505 – 510.

Stenmark, H. (2009) Rab GTPases as coordinators of vesicle traffic. *Nature Reviews Molecular Cell Biology* **10(8)**: 513 – 525.

Stirewalt, M.A., Kruidenier, F.J. (1961) Activity of the acetabular secretory apparatus of cercariae of *Schistosoma mansoni* under experimental conditions. *Experimental Parasitology* **11(2-3)**: 191 – 211.

Stirewalt, M.A. (1971) Penetration Stimuli for Schistosome Cercariae. In: T.C. Cheng, Ed., *Aspects of the Biology of Symbiosis, first edition.* Baltimore: University Park Press., pp. 1 – 23.Stroehlein, A.J., Young. N.D., Jex, A.R., Sternberg, P.W., Tan, P., Boag, P.R., Andreas Hofmann, A. and Gasser, R.B. (2015) Defining the Schistosoma haematobium kinome enables the prediction of essential kinases as anti-schistosome drug targets. *Scientific Reports* **5**: article 17759. Suh, H.N., Lee, S.H., Lee, M.Y., Heo, J.S., Lee, Y.J. and Han, H.J. (2008) High glucose induced translocation of aquaporin8 to chicken hepatocyte plasma membrane: Involvement of cAMP, PI3K/Akt, PKC, MAPKs, and microtubule. *Journal of Cellular Biochemistry* **103(4)**: 1089 – 1100.

Swierczewski, B.E. and Davies, S.J. (2009) A Schistosome cAMP-Dependent Protein Kinase Catalytic Subunit Is Essential for Parasite Viability. *PLOS Neglected Tropical Diseases* **3(8)**: e505.

Szklarczyk, D., Franceschini, A., Kuhn, M., Simonovic, M., Roth, A., Minguez, P., Doerks, T., Stark, M., Muller, J., Bork, P., Jensen, L.J. and von Mering, C. (2011) The STRING database in 2011: functional interaction networks of proteins, globally integrated and scored. *Nucleic Acids Research* **39(Database issue)**: D561 – D568.

Teleman, A.A. (2010) Molecular mechanisms of metabolic regulation by insulin in *Drosophila*. *Biochemical Journal* **425(1)**: 13 – 26.

Thimmaiah, K.N., Easton, J.B., Germain, G.S., Morton, C.L., Kamath, S., Buolamwini, J.K. and Houghton, P.J. (2005) Identification of *N*10-Substituted Phenoxazines as Potent and Specific Inhibitors of Akt Signaling. *The Journal of Biological Chemistry* **280(36)**: 31924 – 31935.

Tielens, A.G.M. (1997) Biochemistry of Trematodes. In: B. Fried and T.K. Graczyk, ed., *Advances in trematode biology, 1st edition*. New York: CRC Press., pp 309 – 344.

Tumurkhuu, M., Saitoh, M., Takita, J., Mizuno, Y. and Mizuguchi, M. (2013) A novel *SOS1* mutation in Costello/CFC syndrome affects signaling in both RAS and PI3K pathways. *Journal of Receptors and Signal Transduction* **33(2):** 124 – 128.

Torre-Escudero, E., Bennett, A.P.S., Clarke, A., Brennan, G.P. and Robinson, M.W. (2016) Extracellular Vesicle Biogenesis in Helminths: More than One Route to the Surface? *Trends in Parasitology* **32(12)**: 921 – 929.

Uglem, G.L. and Read, C.P. (1975) Sugar transport and metabolism in *Schistosoma mansoni*. *The Journal of Parasitology* **61(3)**: 390- 397.

Uhlig, M., Passlack, W. and Eckel, J. (2005) Functional role of Rab11 in GLUT4 trafficking in cardiomyocytes. *Molecular and Cellular Endocrinology* **235(1-2)**: 1 – 9.

Urbé, S., Huber, L.A., Zerial, M., Tooze, S.A. and Parton, R.G. (1993) Rab11, a small GTPase associated with both constitutive and regulated secretory pathways in PC12 cells. *FEBS Letters* **334(2):** 175 – 182.

Valverde-Islas, L.E., Arrangoiz, E., Vega, E., Robert, L., Villanueva, R., Reynoso-Ducoing, O., Willms, K., Zepeda-Rodríguez, A., Fortoul, T.I., Ambrosio, J.R. (2011) Visualization and 3D Reconstruction of Flame Cells of *Taenia solium* (Cestoda). *PLoS ONE* **6(3)**: e14754.

van Balkom,B.W.M. van Gestel,R.A. Brouwers,J.F.H.M., Krijgsveld, J., Tielens, A.G.M., Heck, A.J.R. and van Hellemond, J.J. (2005) Mass Spectrometric Analysis of the *Schistosoma mansoni* Tegumental Sub-proteome. *Journal of Proteome Research* **4(3)**: 958 – 966.

Vanderstraete, M., Gouignard, N., Cailliau, K., Morel, M., Lancelot, J., Bodart, J., Dissous, C. (2013) Dual Targeting of Insulin and Venus Kinase Receptors of *Schistosoma mansoni* for novel anti-schistosome therapy. *PLoS Neglected Tropical Diseases* **7(5)**: e2226.

Van Hellemond, J.J., Retra, K., Brouwers, J.F.H.M., van Balkom, B.W.M., Yazdanbakhsh, M., Shoemaker, C.B. and Tielens, A.G.M. (2006) Functions of the tegument of schistosomes: Clues from the proteome and lipidome. *International Journal for Parasitology* **36(1)**: 691 – 699.

Van Liempt, E., van Vliet, S.J., Engering, A., Vallejo, J.J. G., Bank, C.M.C., Sanchez-Hernandez, M., van Kooyk, Y. and van Die, I. (2007) *Schistosoma mansoni* soluble egg antigens are internalized by human dendritic cells through multiple C-type lectins and suppress TLR-induced dendritic cell activation. *Memorias do Instituto Oswaldo Cruz* **44(10)**: 2605 – 2615.

Vanhaesebroeck, B. and Alessi, D.R. (2000) The PI3K–PDK1 connection: more than just a road to PKB. *Biochemical Journal* **346(3)**: 561 – 576.

Vicogne, J., Pin, J., Lardans, V., Capron, M., Noël, C. and Dissous, C. (2003) An unusual receptor tyrosine kinase of *Schistosoma mansoni* contains a Venus Flytrap module. *Molecular and Biochemical Parasitology* **126(1)**: 51 – 62.

Vlahos, C.J., Matter, W.F., Hui, K.Y. and Brown, R.F. (1994) A Specific Inhibitor of Phosphatidylinositol 3-Kinase, 2-(4-Morpholinyl)-8-phenyl-4H-l-benzopyran-4-one (LY294002). *The Journal of Biological Chemistry* **269(7)**: 5241 – 5248.

Walker, A.J. (2011) Insights into the functional biology of Schistosomes. *Parasites and Vectors* **4(203)**.

Wang, H., Hong, J. and Yang, C.S. (2016) d-Tocopherol Inhibits Receptor Tyrosine Kinase-Induced AKT Activation in Prostate Cancer Cells. *Molecular Carcinogensis* **55(11)**: 1728 – 1738.

Wang, Y., Fan, C., Chen, B. and Jun, S. (2017) Resistin-Like Molecule Beta (RELM-beta) Regulates Proliferation of Human Diabetic Nephropathy Mesangial Cells via Mitogen-Activated Protein Kinases (MAPK) Signaling Pathway. *Medical Science Monitor* **23(1)**: 3897-3903.

Welz, T., Wellbourne-Wood, J. and Kerkhoff, E. (2014) Molecular Orchestration of cell surface proteins by Rab11. *Trends in Cell Biology* **24(7)**: 407 – 415.

Wennerberg, K., Rossman, K.L. and Der, C.J. (2005) The Ras superfamily at a glance. *Journal of Cell Science* **118(5)**: 843 – 846.

Wheater, P.R. and Wilson, R.A. (1979) *Schistosoma mansoni:* a histological study of migration in the laboratory mouse. *Parasitology* **79(1)**: 46 – 62.

Wilson, R.A. and Barnes, P.E. (1974) The tegument of *Schistosoma mansoni:* observations on the formation, structure and composition of cytoplasmic inclusions in relation to tegument function. *Parasitology* **68(2)**: 239 – 258.

Wilson, R.A. (2012) Proteomics at the schistosome-mammalian host interface: any prospects for diagnostics or vaccines? *Parasitology* **139(9)**: 1178 – 1194.

Woicke, E. and Haas, W. (1989) *Schistosoma mansoni*: Stimuli der menschlichen Haut fuir die Verbleibereaktion der Cercarie. *Verhandlungen der Deutschen Zoologischen Gesellschaft* **82**: 250.

Woodgett, J.R., Plyte, S.E., Pulverer, B.J., Mitchell, J.A. and Hughes, K. (1993) Roles of glycogen synthase kinase-3 in signal transduction. *Biochemical Society Transactions* **21(4)**: 905 – 907.

Xia, H., Mao, Q., Paulson, H.L. and Davidson, B.L. (2002) siRNA-mediated gene silencing *in vitro* and *in vivo. Nature Biotechnology* **20(10)**: 1006 – 1010.

Yan, Y., Tulasne, D., Browaeys, E., Cailliau, K., Khayath, N., Pierce, R.J., Trolet, J., Fafeur, V., Younes, A.B. and Dissous, C. (2007) Molecular cloning and characterisation of SmSLK, a novel Ste20-like kinase in *Schistosoma mansoni*. *International Journal for Parasitology* **37(1)**: 1539 – 1550.

Yang, J., Cron, P., Good, V.M., Thompson, V., Hemmings, B.A. and Barford, D. (2002) Crystal structure of an activated Akt/Protein Kinase B ternary complex with GSK3-peptide and AMP-PNP. *Nature Structural Biology* **9(12)**: 940 – 944.

Yoshiyama, M., Bache, R.J., Merkle, H., Garwood, M., Ugurbil, K., Zhang, J. and Arthur, H.L. (1995) Transmural distribution of 2-deoxyglucose uptake in normal and post-ischemic canine myocardium. *NMR in Biomedicine* **8(1)**: 9 – 18.

You, H., Zhanga, W., Moertel, L., McManusa, D.P. and Gobert, G.N. (2009) Transcriptional profiles of adult male and female *Schistosoma japonicum* in response to insulin reveal increased expression of genes involved in growth and development. *International Journal for Parasitology* **39(1)**: 1551 – 1559.

You, H., Gobert, G.N., Jones, M.K., Zhang, W. and McManus, D.P. (2011) Signalling pathways and the host-parasite relationship: Putative targets for control interventions against schistosomiasis Signalling pathways and future anti-schistosome therapies. *Bioessays* **33(3)**: 203 – 214.

You, H., Gobert, G.N., Cai, P., Mou, R., Nawaratna, S., Fang, G., Villinger, F. and McManus, D.P. (2015) Suppression of the Insulin Receptors in Adult *Schistosoma japonicum* Impacts on Parasite Growth

and Development: Further Evidence of Vaccine Potential. *PloS Neglected Tropical Diseases* **9(5)**: UNSP e0003730.

Zhao, G., Ma, H., Shen, X., Xu, G.F., Zhu, Y.L., Chen, B., Tie, R., Qu, P., Lv, Y., Z, H. And Yu, J. (2013) Role of glycogen synthase kinase 3b in protective effect of propofol against hepatic ischemia-reperfusion injury. *Journal of Surgical Research* **185(1)**: 388 – 398.

Zhong, C., Skelly, P.J., Leaffer, D., Cohn, R.G., Caulfield, J.P. and Shoemaker, C.B. (1995) Immunolocalization of a *Schistosoma mansoni* facilitated diffusion glucose transporter to the basal, but not the apical, membranes of the surface syncytium. *Parasitology* **110(4)**: 383 – 394.

Appendices

Antibody Name	Monoclonal/Polyclonal	Manufacturer/Source	Product No.
Anti-Akt 1/2/3 (total)	Polyclonal	Abcam	126811
Alexa Fluor 488 goat anti-rabbit IgG		Life Technologies (Thermo Fisher Scientific)	A11008
Anti-phospho GSK3α/β (Tyr^{279}/Tyr^{216})	Polyclonal	Millipore	05413
HRP-conjugated actin	Polyclonal	Santa Cruz Biotechnology	B1815
Anti-phospho Akt 1/2/3 ($Tyr^{315/316/312}$)	Polyclonal	Santa Cruz Biotechnology	29309
Anti-SGTP4	Polyclonal	Patrick Skelly – Tufts University, USA)	N/A
Anti-mouse IgG HRP-linked secondary		Cell Signalling Technology	7076
Anti-rabbit IgG HRP-linked secondary		Cell Signalling Technology	7074
Anti-rabbit IgG conformation-specific mouse	Monoclonal	Cell Signalling Technology	3678
Anti-phospho Akt (Thr^{308})	Monoclonal	Cell Signalling Technology	2965
Anti-phospho Akt substrates (RXXS*/T*)	Monoclonal	Cell Signalling Technology	9614
Anti-phospho Akt (Thr^{308}) XP	Monoclonal	Cell Signalling Technology	13038
Anti-phospho p70 S6 Kinase (Thr^{389})	Monoclonal	Cell Signalling Technology	9234
Anti-phospho GSK-3α/β ($Ser^{9/21}$)	Monoclonal	Cell Signalling Technology	9327

Appendix 1. **Antibodies.**Tabulated form of antibodies from Chapter 2, section 2.1.1 for easy referral.

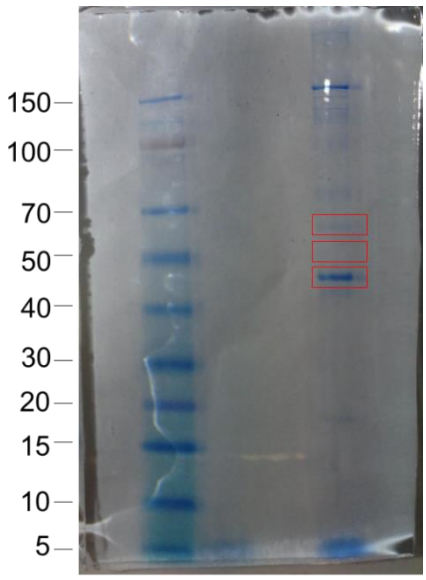

Appendix 2 **Stained gel for sequencing analysis.** 20 worm pairs were processed for IP using the crosslinking IP method. The electrophoresed gel was incubated in Gel Code Blue stain to reveal protein bands. The red boxes indicate the three slices of gel that were excised and sent for protein sequencing at Nottingham University. The middle box surrounds the area of the gel at 50 kDa, where a band would have been expected.

Smp_073930.2__mRNA	Rac-alpha serine/threonine-protein kinase (Ec 2.7.1.37) (Rac-pk-alpha)(Akt1 kinase) (Protein kinase b) (Pkb) (C-akt) (Thymoma viral proto-oncogene) (776 aa)	Neighborhood	Gene Fusion	Cooccurence	Coexpression	Experiments	Databases	Textmining	[Homology]	Score
Predicted Functional Partners:										
Smp_094250	Serine/threonine kinase (484 aa)					●	●	●	●	0.993
Smp_122910	Ataxia telangiectasia mutated (Atm)-related (2611 aa)					●	●	●		0.989
Smp_079760.1__mRNA	Protein kinase (491 aa)					●	●	●		0.988
Smp_154470	Pten, putative (597 aa)				●	●		●		0.986
Smp_072330.2__mRNA	Heat shock protein, putative (718 aa)					●	●	●		0.984
Smp_074390	Eukaryotic translation initiation factor 4e-binding protein, putative (121 aa)					●	●	●		0.977
Smp_053130	40S ribosomal protein S6 (248 aa)					●	●	●		0.973
Smp_099930	F-box and wd40 domain protein, putative (863 aa)					●		●		0.966
Smp_164960	Phosphatidylinositol-4,5-bisphosphate 3-kinase catalytic subunit alpha PI3K (1340 aa)					●	●	●		0.964
Smp_159000	Expressed protein (1610 aa)					●	●	●		0.950
Smp_064010	Camp-response element binding protein-related (825 aa)					●	●	●		0.950
Smp_142710	Fkbp-rapamycin associated protein, putative (4023 aa)					●	●	●		0.948
Smp_008260	Glycogen synthase kinase 3-related (Gsk3) (Cmgc group III) (463 aa)					●	●	●	●	0.945
Smp_023550	Beta-catenin, putative (989 aa)	●				●	●	●		0.941
Smp_159560	Transcription factor GATA-1, putative (735 aa)					●		●		0.939
Smp_018590	Endothelial transcription factor GATA-2, putative (565 aa)					●		●		0.939
Rac	Rac gtpase, putative (188 aa)					●	●	●		0.938
Smp_139630	Protein kinase (619 aa)				●	●		●		0.934
Smp_133020	Serine/threonine kinase (237 aa)					●	●	●		0.933
Smp_047900	Serine/threonine kinase (201 aa)					●	●	●		0.933
Smp_032000	Caspase-7 (C14 family) (379 aa)					●	●	●		0.925
Smp_193170	Putative uncharacterized protein (79 aa)					●	●	●		0.924
Smp_073560.2__mRNA	G beta-like protein gbl (317 aa)					●	●	●		0.922
Smp_081410	Ste20-related kinase (452 aa)					●		●		0.915
Smp_039490.1__mRNA	Expressed protein (954 aa)					●		●		0.913
Smp_156680	Fyve finger-containing phosphoinositide kinase, fyv1, putative (2289 aa)							●		0.911
SER	Tyrosine kinase (1600 aa)					●	●	●		0.908
Smp_073210	ADP-ribosylation factor interacting protein, putative (341 aa)					●		●		0.906
Smp_028500	Caspase-3Caspase-3 (C14 family) (296 aa)					●	●	●		0.904
Smp_056440	Superoxide dismutase; Destroys radicals which are normally produced within the cells and which are toxic to bi...	●				●	●	●		0.899
Smp_104030.3__mRNA	Scribble complex protein (Cell polarity protein) (Leucine-rich repeat protein) (1456 aa)					●		●		0.896
Smp_012050	Bola-like protein my016 (77 aa)	●			●	●		●		0.894
Smp_167400	Myogenic factor, putative (864 aa)						●	●		0.893
Smp_178480	Wd and tetratricopeptide repeat protein, putative (220 aa)							●		0.884
Smp_123420	Aryl hydrocarbon receptor nuclear translocator homolog (Darnt)„ putative (783 aa)						●	●		0.882
Smp_105910	CREB-binding protein 1 (SmCBP1) (2093 aa)					●	●	●		0.880
Cdc42	Cell polarity protein (Regulator of photoreceptor cell morphogenesis) (Cdc42, putative) (195 aa)					●	●	●		0.871
Smp_005880	Phosphoenolpyruvate carboxykinase, putative (626 aa)						●	●		0.871
Smad4	Smad4, putative (738 aa)					●		●		0.867
Smp_036270.2__mRNA	Arginine/serine-rich splicing factor, putative (371 aa)					●		●		0.860
Smp_085700	cAMP-dependent protein kinase catalytic subunit, putative (104 aa)					●		●		0.857
Smp_078230	Protein kinase, cgmp-dependent, type I, putative (488 aa)					●		●		0.857
Smp_139930	Protein tyrosine phosphatase, non-receptor type nt1, putative (628 aa)					●	●	●		0.850
Smp_075450	Heparan sulfate 2-o-sulfotransferase, putative (206 aa)							●		0.850
Smp_191040	P38 MAPk, putative (74 aa)					●		●		0.847
Smp_062950	Growth factor receptor-bound protein, putative (234 aa)					●	●	●		0.846
Smp_044530	Growth factor receptor-bound protein, putative (317 aa)					●	●	●		0.846
hsp70	Heat shock 70 kDa protein homolog; Major immunogen in Schistosoma mansoni infections. Possibly plays an i...					●		●		0.839
Smp_166290	Phosphotyrosyl phosphatase activator, putative (373 aa)					●		●		0.834
SOD	Superoxide dismutase [Cu-Zn]; Destroys radicals which are normally produced within the cells and which are to...					●	●	●		0.830
Smp_142450	Rap1 and, putative (183 aa)					●	●	●		0.830
Smp_071250	Rap1 and, putative (184 aa)					●	●	●		0.830
Smp_048990	Beclin, putative (494 aa)							●		0.830
Smp_172010	Caspase-7Caspase-7 (C14 family) (329 aa)					●	●	●		0.830
Smp_182250	Serine/threonine-protein phosphatase (211 aa)					●	●	●		0.828
Smp_165490	Serine/threonine-protein phosphatase (423 aa)					●	●	●		0.828
Smp_030710	Serine/threonine-protein phosphatase (307 aa)					●	●	●		0.828
Smp_150430	Forkhead protein/ forkhead protein domain, putative (504 aa)					●		●		0.826
Smp_018240.3__mRNA	Cell division control protein 48 aaa family protein (Transitional endoplasmic reticulum atpase), putative (803 aa)					●		●		0.824
Smp_017900	Serine/threonine kinase (806 aa)				●	●	●	●	●	0.823
Smp_085680	Guanylate cyclase (584 aa)					●		●		0.818
Smp_136750	Serine/threonine kinase (1767 aa)				●	●	●	●	●	0.817
Smp_082030	Family C56 non-peptidase homologue (C56 family) (184 aa)				●	●		●		0.813
Smp_138640	Chromatin regulatory protein sir2, putative (618 aa)					●		●		0.812
Smp_152900	Protein Wnt; Ligand for members of the frizzled family of seven transmembrane receptors (By similarity) (1435...					●		●		0.807
Smp_072110.1__mRNA	Programmed cell death, putative (534 aa)					●	●	●		0.804
Smp_165570.2__mRNA	Ras-dva small gtpase, putative (394 aa)					●	●	●		0.802
Smp_171530	Beta-parvin-related (383 aa)						●	●		0.802
Smp_035390	Protein tyrosine phosphatase n11 (Shp2), putative (708 aa)						●	●		0.801
Smp_170550.1__mRNA	Granulin, putative (748 aa)					●		●		0.799
Smp_173990	Rab11, putative (933 aa)					●	●	●		0.798
Smp_078040	Tubulin beta chain, putative; Tubulin is the major constituent of microtubules. It binds two moles of GTP, one at...					●		●		0.797
Smp_035760	Tubulin beta chain, putative; Tubulin is the major constituent of microtubules. It binds two moles of GTP, one at...					●		●		0.797
Smp_030730	Tubulin beta chain, putative (443 aa)					●		●		0.797

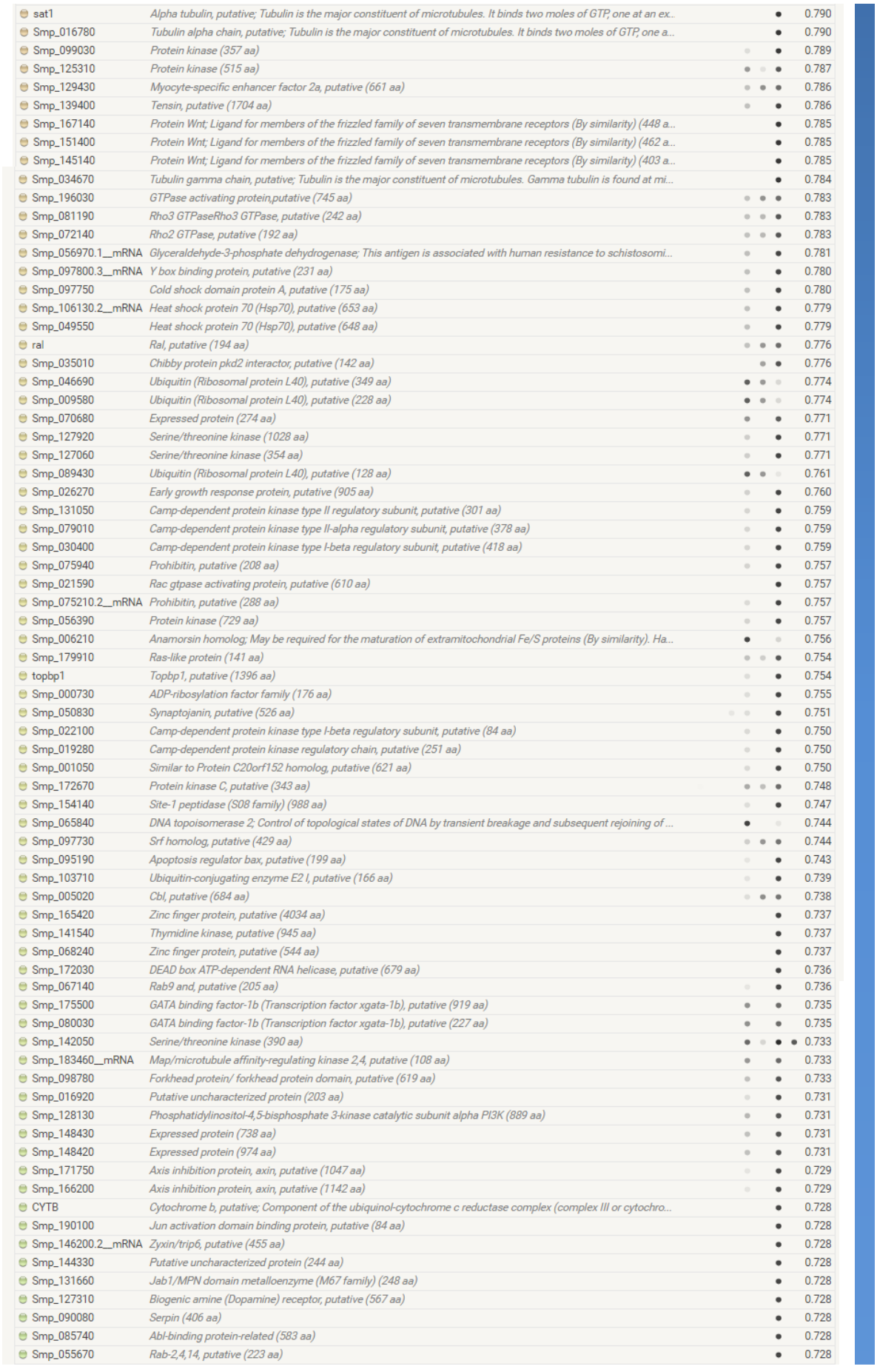

sat1	Alpha tubulin, putative; Tubulin is the major constituent of microtubules. It binds two moles of GTP, one at an ex...	0.790
Smp_016780	Tubulin alpha chain, putative; Tubulin is the major constituent of microtubules. It binds two moles of GTP, one a...	0.790
Smp_099030	Protein kinase (357 aa)	0.789
Smp_125310	Protein kinase (515 aa)	0.787
Smp_129430	Myocyte-specific enhancer factor 2a, putative (661 aa)	0.786
Smp_139400	Tensin, putative (1704 aa)	0.786
Smp_167140	Protein Wnt; Ligand for members of the frizzled family of seven transmembrane receptors (By similarity) (448 a...	0.785
Smp_151400	Protein Wnt; Ligand for members of the frizzled family of seven transmembrane receptors (By similarity) (462 a...	0.785
Smp_145140	Protein Wnt; Ligand for members of the frizzled family of seven transmembrane receptors (By similarity) (403 a...	0.785
Smp_034670	Tubulin gamma chain, putative; Tubulin is the major constituent of microtubules. Gamma tubulin is found at mi...	0.784
Smp_196030	GTPase activating protein,putative (745 aa)	0.783
Smp_081190	Rho3 GTPaseRho3 GTPase, putative (242 aa)	0.783
Smp_072140	Rho2 GTPase, putative (192 aa)	0.783
Smp_056970.1__mRNA	Glyceraldehyde-3-phosphate dehydrogenase; This antigen is associated with human resistance to schistosomi...	0.781
Smp_097800.3__mRNA	Y box binding protein, putative (231 aa)	0.780
Smp_097750	Cold shock domain protein A, putative (175 aa)	0.780
Smp_106130.2__mRNA	Heat shock protein 70 (Hsp70), putative (653 aa)	0.779
Smp_049550	Heat shock protein 70 (Hsp70), putative (648 aa)	0.779
ral	Ral, putative (194 aa)	0.776
Smp_035010	Chibby protein pkd2 interactor, putative (142 aa)	0.776
Smp_046690	Ubiquitin (Ribosomal protein L40), putative (349 aa)	0.774
Smp_009580	Ubiquitin (Ribosomal protein L40), putative (228 aa)	0.774
Smp_070680	Expressed protein (274 aa)	0.771
Smp_127920	Serine/threonine kinase (1028 aa)	0.771
Smp_127060	Serine/threonine kinase (354 aa)	0.771
Smp_089430	Ubiquitin (Ribosomal protein L40), putative (128 aa)	0.761
Smp_026270	Early growth response protein, putative (905 aa)	0.760
Smp_131050	Camp-dependent protein kinase type II regulatory subunit, putative (301 aa)	0.759
Smp_079010	Camp-dependent protein kinase type II-alpha regulatory subunit, putative (378 aa)	0.759
Smp_030400	Camp-dependent protein kinase type I-beta regulatory subunit, putative (418 aa)	0.759
Smp_075940	Prohibitin, putative (208 aa)	0.757
Smp_021590	Rac gtpase activating protein, putative (610 aa)	0.757
Smp_075210.2__mRNA	Prohibitin, putative (288 aa)	0.757
Smp_056390	Protein kinase (729 aa)	0.757
Smp_006210	Anamorsin homolog; May be required for the maturation of extramitochondrial Fe/S proteins (By similarity). Ha...	0.756
Smp_179910	Ras-like protein (141 aa)	0.754
topbp1	Topbp1, putative (1396 aa)	0.754
Smp_000730	ADP-ribosylation factor family (176 aa)	0.755
Smp_050830	Synaptojanin, putative (526 aa)	0.751
Smp_022100	Camp-dependent protein kinase type I-beta regulatory subunit, putative (84 aa)	0.750
Smp_019280	Camp-dependent protein kinase regulatory chain, putative (251 aa)	0.750
Smp_001050	Similar to Protein C20orf152 homolog, putative (621 aa)	0.750
Smp_172670	Protein kinase C, putative (343 aa)	0.748
Smp_154140	Site-1 peptidase (S08 family) (988 aa)	0.747
Smp_065840	DNA topoisomerase 2; Control of topological states of DNA by transient breakage and subsequent rejoining of ...	0.744
Smp_097730	Srf homolog, putative (429 aa)	0.744
Smp_095190	Apoptosis regulator bax, putative (199 aa)	0.743
Smp_103710	Ubiquitin-conjugating enzyme E2 I, putative (166 aa)	0.739
Smp_005020	Cbl, putative (684 aa)	0.738
Smp_165420	Zinc finger protein, putative (4034 aa)	0.737
Smp_141540	Thymidine kinase, putative (945 aa)	0.737
Smp_068240	Zinc finger protein, putative (544 aa)	0.737
Smp_172030	DEAD box ATP-dependent RNA helicase, putative (679 aa)	0.736
Smp_067140	Rab9 and, putative (205 aa)	0.736
Smp_175500	GATA binding factor-1b (Transcription factor xgata-1b), putative (919 aa)	0.735
Smp_080030	GATA binding factor-1b (Transcription factor xgata-1b), putative (227 aa)	0.735
Smp_142050	Serine/threonine kinase (390 aa)	0.733
Smp_183460__mRNA	Map/microtubule affinity-regulating kinase 2,4, putative (108 aa)	0.733
Smp_098780	Forkhead protein/ forkhead protein domain, putative (619 aa)	0.733
Smp_016920	Putative uncharacterized protein (203 aa)	0.731
Smp_128130	Phosphatidylinositol-4,5-bisphosphate 3-kinase catalytic subunit alpha PI3K (889 aa)	0.731
Smp_148430	Expressed protein (738 aa)	0.731
Smp_148420	Expressed protein (974 aa)	0.731
Smp_171750	Axis inhibition protein, axin, putative (1047 aa)	0.729
Smp_166200	Axis inhibition protein, axin, putative (1142 aa)	0.729
CYTB	Cytochrome b, putative; Component of the ubiquinol-cytochrome c reductase complex (complex III or cytochro...	0.728
Smp_190100	Jun activation domain binding protein, putative (84 aa)	0.728
Smp_146200.2__mRNA	Zyxin/trip6, putative (455 aa)	0.728
Smp_144330	Putative uncharacterized protein (244 aa)	0.728
Smp_131660	Jab1/MPN domain metalloenzyme (M67 family) (248 aa)	0.728
Smp_127310	Biogenic amine (Dopamine) receptor, putative (567 aa)	0.728
Smp_090080	Serpin (406 aa)	0.728
Smp_085740	Abl-binding protein-related (583 aa)	0.728
Smp_055670	Rab-2,4,14, putative (223 aa)	0.728

Smp_027610	*40S ribosomal protein S3, putative (230 aa)*	0.728
Smp_149150	*Acyl-CoA-binding protein (Acbp) (Diazepam binding inhibitor) (Dbi) (Endozepine), putative (343 aa)*	0.727
Smp_166010	*Ankyrin repeat-containing, putative (1291 aa)*	0.726
Smp_173810	*Protein phosphatase pp2a regulatory subunit B, putative (490 aa)*	0.726
Smp_172290	*Serine/threonine protein phosphatase 2a regulatory subunit A, putative (392 aa)*	0.716
Smp_172280	*Serine/threonine protein phosphatase 2a regulatory subunit A, putative (535 aa)*	0.716
Smp_153410	*Serine/threonine protein phosphatase 2a regulatory subunit A, putative (821 aa)*	0.716
Smp_056760	*Protein disulfide-isomerase, putative (482 aa)*	0.715
Smp_151420	*Phospholipase D (906 aa)*	0.712
Smp_161230	*Ras GTP exchange factor, son of sevenless, putative (1518 aa)*	0.706
Smp_196040	*Shc transforming protein, putative (409 aa)*	0.705
Smp_023150	*Serine/threonine-protein phosphatase (302 aa)*	0.704
Smp_145810.1__mRNA	*Poly [ADP-ribose] polymerase, putative (536 aa)*	0.703
Smp_129260	*Poly [ADP-ribose] polymerase, putative (977 aa)*	0.703
Smp_082490	*Cyclin B, putative (414 aa)*	0.702
Smp_176990	*Serine/threonine kinase (771 aa)*	0.699
Smp_156740	*Ocrl type II inositol 5-phosphatase, putative (796 aa)*	0.697
Smp_064190	*Ocrl type II inositol 5-phosphatase, putative (600 aa)*	0.697
Smp_130310	*Prolyl oligopeptidase (S09 family) (1693 aa)*	0.696
Smp_111120	*Insulin receptor tyrosine kinase substrate, putative (51 aa)*	0.696
Smp_127200	*Putative uncharacterized protein (390 aa)*	0.694
Smp_105410	*Glucose transport protein, putative (505 aa)*	0.694
Smp_046790	*Glucose transport protein, putative (492 aa)*	0.694
Smp_012440	*Glucose transport proteinGlucose transport protein, putative (521 aa)*	0.694
Smp_147260	*Ras-like family (359 aa)*	0.692
Smp_129070	*Rap1 and, putative (186 aa)*	0.692
Smp_084940.3__mRNA	*GTP-binding protein rit, putative (199 aa)*	0.692
Smp_046010__mRNA	*Diras family, GTP-binding ras-like (213 aa)*	0.692
Smp_046000	*Diras family, GTP-binding ras-like (240 aa)*	0.692
Smp_045990	*Diras family, GTP-binding ras-like (75 aa)*	0.692
Smp_168730	*Carbonic anhydrase, putative (303 aa)*	0.690
Smp_150290	*Map-kinase activating death domain protein, putative (705 aa)*	0.690
Smp_080680	*Map-kinase activating death domain protein, putative (765 aa)*	0.690
aPKC	*Serine/threonine kinase (Cell polarity protein) (Atypical protein kinase c) (673 aa)*	0.689
Smp_042440	*(Dihydro)ceramide Synthase (LAG1) (331 aa)*	0.688
Smp_127730	*ATP-citrate synthase, putative (1164 aa)*	0.688
Smp_151850	*Inositol 1,4,5-trisphosphate receptor, putative (987 aa)*	0.687
Smp_066760.2__mRNA	*Merlin/moesin/ezrin/radixin, putative (543 aa)*	0.687
Smp_060940.1__mRNA	*Protein kinase (1068 aa)*	0.686
Smp_143170	*Mannosyl-oligosaccharidealpha-1,2-mannosidase-r el ated (737 aa)*	0.684
Smp_113620.3__mRNA	*Serine/arginine rich splicing factor, putative (151 aa)*	0.683
Smp_155030	*Putative uncharacterized protein (1413 aa)*	0.683
Smp_109550	*Serine/threonine protein phosphatase 2a regulatory subunit A, putative (54 aa)*	0.683
Smp_133500	*Serine/threonine kinase (724 aa)*	0.682
Smp_139200	*Nuclear hormone receptor nor-1/nor-2, putative (704 aa)*	0.682
Smp_133490	*Serine/threonine kinase (503 aa)*	0.681
Smp_134260	*Serine/threonine kinase (610 aa)*	0.680
Smp_142380	*Expressed protein (1555 aa)*	0.680
Smp_030300.4__mRNA	*Endoplasmin, putative (2172 aa)*	0.679
Smp_126080	*Beta-arrestin 1,, putative (560 aa)*	0.679
Smp_122900	*Beta-arrestin 1,, putative (281 aa)*	0.679
Smp_054240	*Translationally-controlled tumor protein homolog; Involved in calcium binding and microtubule stabilization (By...*	0.679
Smp_179800	*Serine/threonine kinase (567 aa)*	0.678
Smp_151860	*Inositol 1,4,5-trisphosphate receptor, putative (1476 aa)*	0.677
Smp_017010.4__mRNA	*Expressed protein (1013 aa)*	0.671
Smp_146710	*Putative uncharacterized protein (276 aa)*	0.671
Smp_008500.2__mRNA	*Transcription factor IWS1, putative (625 aa)*	0.671
Smp_156700	*Putative uncharacterized protein (894 aa)*	0.670
Smp_152170	*Expressed protein (1643 aa)*	0.670
Smp_176600	*Protein phosphatase 2a regulatory subunit, putative (627 aa)*	0.669
Smp_146790	*Tgf-beta family, putative (677 aa)*	0.669
Smp_176330	*Twist, putative (120 aa)*	0.668
Smp_166910	*Calcium-activated potassium channel (1263 aa)*	0.668
Smp_157100	*Sphingoid long chain base kinase (424 aa)*	0.668
Smp_173060	*Pak-interacting exchange factor, beta-pix/cool-1, putative (749 aa)*	0.665
HSF	*Heat shock transcription factor, putative (671 aa)*	0.664
Smp_099630	*Fragile X related 1, frx1 (598 aa)*	0.661
Smp_016050	*Fragile X related 2, frx2 (777 aa)*	0.661
Smp_020080.1__mRNA	*GTP-binding protein (l) alpha-1subunit, gnai1, putative (353 aa)*	0.658
Smp_016630.1__mRNA	*Trimeric G-protein alpha o subunit, putative (355 aa)*	0.658
Smp_016250.2__mRNA	*GTP-binding protein (l) alpha-2 subunit, gnai2, putative (362 aa)*	0.658
Smp_027300	*Histone-lysine n-methyltransferase, suv9, putative (586 aa)*	0.655
Smp_035430.2__mRNA	*Protein phosphatase 2a regulatory subunit, putative (487 aa)*	0.654
Smp_153660	*Cyclin d, putative (410 aa)*	0.653
Smp_007630.1__mRNA	*Polyadenylate binding protein, putative (223 aa)*	0.652

Smp_078900	*Enhancer of zeste, ezh, putative (1026 aa)*	0.650
SmHDAC3	*Histone deacetylase (418 aa)*	0.648
SmHDAC1	*Histone deacetylase (469 aa)*	0.648
Smp_147210	*Ubiquitin (Ribosomal protein L40), putative (153 aa)*	0.648
Smp_123260	*Ubiquitin 1,, putative (595 aa)*	0.648
Smp_146600	*Gtpase_rho, putative (264 aa)*	0.646
Smp_161530	*Myocyte-specific enhancer factor 2a, putative (717 aa)*	0.645
Smp_095150	*Eukaryotic translation initiation factor 2 gamma subunit (Eif-2-gamma), putative (462 aa)*	0.646
Smp_129180	*Dyrk, putative (109 aa)*	0.645
Smp_129170	*Dual specificity kinase (1084 aa)*	0.645
Smp_079230	*Immunophilin FK506 binding protein FKBP12Immunophilin FK506 binding protein FKBP12, putative (108 aa)*	0.639
Smp_157540	*Smad, putative (559 aa)*	0.637
Smp_085910	*TGF-beta signal transducer Smad2, putative (649 aa)*	0.637
Smp_013060	*Smad1Smad1, 5, 8, and, putative (455 aa)*	0.637
gli2a	*Zinc finger transcription factor gli2 (2492 aa)*	0.636
Smp_152000	*Ubiquitin carboxyl-terminal hydrolase (1027 aa)*	0.632
Smp_179230	*Protein disulfide-isomerase, putative (592 aa)*	0.626
Smp_179230__mRNA	*Protein disulfide-isomerase, putative (97 aa)*	0.626
Smp_172110	*Shc transforming protein, putative (363 aa)*	0.626
Smp_155420	*Putative uncharacterized protein (593 aa)*	0.626
Smp_144840	*BWK4-like protein (230 aa)*	0.626
Smp_079770.1__mRNA	*Probable protein disulfide-isomerase ER-60 (484 aa)*	0.626
Smp_054470	*Thioredoxin (104 aa)*	0.626
Smp_037530	*Thioredoxin m(Mitochondrial)-type, putative (108 aa)*	0.626
Smp_028930	*Thioredoxin domain containing protein 9-related (238 aa)*	0.626
Smp_008070	*Thioredoxin (106 aa)*	0.626
Smp_001500	*Eukaryotic translation initiation factor 4e, putative (203 aa)*	0.625
Smp_130170	*Ubiquitin 1,, putative (77 aa)*	0.624
Rad23	*DNA repair proteinUv excision repair protein rad23, putative (354 aa)*	0.624
Smp_010290	*Ubiquilin 1,2, putative (543 aa)*	0.624
Smp_063260	*WD-repeat protein, putative (421 aa)*	0.621
Smp_157820	*Ataxia telangiectasia mutated (Atm), putative (3138 aa)*	0.613
Smp_069130.2__mRNA	*Heat shock protein 70 (Hsp70)-4, putative (847 aa)*	0.613
Smp_186050	*Heat shock protein, putative (70 aa)*	0.612
Smp_130080	*Ankrd45 protein , putative (207 aa)*	0.612
Smp_094680	*Heat shock protein 70 (Hsp70), putative (201 aa)*	0.612
Smp_088950	*Hypoxia upregulated 1 (Hyou1)-related (845 aa)*	0.612
Smp_072320	*Heat shock protein 70 (Hsp70), putative (97 aa)*	0.612
Smp_158770	*Expressed protein (619 aa)*	0.611
Smp_146220	*Calcium-binding protein, putative (181 aa)*	0.611
Smp_135980	*Calcium-binding protein, putative (156 aa)*	0.611
Smp_028210	*Calcyphosine/tpp, putative (207 aa)*	0.611
Smp_019640.1__mRNA	*Calcyphosine/tpp, putative (208 aa)*	0.611
Smp_151100	*Serine/threonine kinase (881 aa)*	0.609
Smp_178910	*Uridine cytidine kinase I, putative (181 aa)*	0.607
Smp_134000	*Plakoglobin, putative (493 aa)*	0.607
Smp_095810	*Uracil phosphoribosyltransferase, putative (249 aa)*	0.607
Smp_160760	*Serine/threonine kinase (1077 aa)*	0.607
Smp_130230	*Rac gtpase, putative (168 aa)*	0.605
Smp_107540	*Gtpase_rho, putative (103 aa)*	0.605
Smp_104110	*Gtpase_rho, putative (192 aa)*	0.605
Rho1	*Rho GTPase, putative (172 aa)*	0.605
Smp_025740	*Gtpase_rho, putative (336 aa)*	0.605
Smp_148460	*Neurofibromin, putative (3013 aa)*	0.604
Smp_162800.2__mRNA	*Protein kinase (1429 aa)*	0.602
Smp_176360	*Serine/threonine kinase (1008 aa)*	0.601
Smp_050380	*Protein kinase (1793 aa)*	0.600
Smp_067520	*Jun-related protein (945 aa)*	0.600
Smp_174810	*Superoxide dismutase [Cu-Zn] (156 aa)*	0.598
Smp_095980	*Extracellular superoxide dismutase [Cu-Zn]; Destroys radicals which are normally produced within the cells and...*	0.598
Smp_074030	*Tyrosine kinase (1502 aa)*	0.597
Smp_009990	*Tyrosine kinase (1736 aa)*	0.597
Smp_147450	*Serine/threonine kinase (1245 aa)*	0.595
Smp_168670	*Serine/threonine kinase (1183 aa)*	0.594
Smp_131700	*Serine/threonine kinase (860 aa)*	0.594
Smp_135790	*Dynamin-associated protein, putative (1594 aa)*	0.594
Smp_159720	*Atpase, class VI, type 11c, putative (1347 aa)*	0.593
Smp_013860	*Glutamate-cysteine ligase (444 aa)*	0.591
Smp_128480	*Serine/threonine kinase (657 aa)*	0.590
TPx-2	*Thioredoxin peroxidase, putative (194 aa)*	0.589
Smp_062900	*Peroxiredoxins, prx-1, prx-2, prx-3, putative (194 aa)*	0.589
Smp_059480	*Thioredoxin peroxidase, putative (185 aa)*	0.589
TPx3	*Thioredoxin peroxidase 3, putative (219 aa)*	0.589
Smp_159900.1__mRNA	*Lamin, putative (2086 aa)*	0.589

Smp_140310	*Paxillin-related (126 aa)*	0.587
Smp_145640	*Forkhead protein/ forkhead protein domain, putative (433 aa)*	0.585
Smp_135710	*Forkhead protein/ forkhead protein domain, putative (787 aa)*	0.585
Smp_143150	*Eukaryotic translation elongation factor, putative (544 aa)*	0.584
Smp_168390	*Tnf receptor-associated factor, putative (452 aa)*	0.583
Smp_141270	*Subfamily C14A unassigned peptidase (C14 family) (707 aa)*	0.581
Smp_034840.2__mRNA	*14-3-3 epsilon (250 aa)*	0.581
Smp_046500.1__mRNA	*Proliferating cell nuclear antigen; This protein is an auxiliary protein of DNA polymerase delta and is involved in ...*	0.580
Smp_154230.2__mRNA	*Expressed protein (332 aa)*	0.577
Smp_004910	*Rab-2,4,14, putative (225 aa)*	0.573
Smp_170990	*Vinculin, putative (1577 aa)*	0.566
vav2	*Vav2, putative (1027 aa)*	0.566
Smp_148190	*T-cell specific transcription factor, tcf, putative (526 aa)*	0.566
Smp_131280	*Bcl-2 homologous antagonist/killer (Bak), putative (987 aa)*	0.566
Smp_131260	*Pangolin, putative (683 aa)*	0.566
Smp_125630	*Pangolin, putative (1010 aa)*	0.566
Smp_093670	*Putative uncharacterized protein (135 aa)*	0.566
Smp_018260	*Glycogen synthase (706 aa)*	0.566
Smp_192110	*Tubulin beta chain, putative (459 aa)*	0.565
Smp_164770	*Apg5-related (583 aa)*	0.565
Smp_164480	*Tubulin beta chain, putative (267 aa)*	0.565
Smp_152200	*M-phase inducer phosphatase(Cdc25), putative (355 aa)*	0.565
Smp_145930	*Matrix metallopeptidase-7 (M10 family) (454 aa)*	0.565
Smp_134890	*ATP-binding cassette, sub-family B, member 6, mitochondrial (Abc6), putative (260 aa)*	0.565
acc1	*Acetyl-CoA carboxylase (2576 aa)*	0.565
Smp_116630	*ATP-binding cassette, sub-family B, member 6, mitochondrial (Abc6), putative (106 aa)*	0.565
Smp_102510	*Peripheral-type benzodiazepine receptor, putative (159 aa)*	0.565
Smp_087930	*ATP-binding cassette, sub-family B, member 7, mitochondrial (Abc7), putative (745 aa)*	0.565
Smp_079970	*Tubulin beta chain, putative; Tubulin is the major constituent of microtubules. It binds two moles of GTP, one at...*	0.565
Smp_079960	*Tubulin beta chain, putative; Tubulin is the major constituent of microtubules. It binds two moles of GTP, one at...*	0.565
Smp_046810	*M-phase inducer phosphatase(Cdc25), putative (565 aa)*	0.565
Smp_028360	*Tubulin epsilon chain, putative (466 aa)*	0.565
Smp_023570	*ATP-binding cassette, sub-family B, member 6, mitochondrial (Abc6), putative (91 aa)*	0.565
Smp_140260	*Expressed protein (2059 aa)*	0.564
Smp_172890	*Protein tyrosine phosphatase, putative (368 aa)*	0.564
Smp_158400	*Receptor protein tyrosine phosphatase r (Pcptp1), putative (984 aa)*	0.564
Smp_075810	*Pcd6 interacting protein-related (1913 aa)*	0.564
Smp_160630	*DNA repair protein rad51 homolog 3, r51h3, putative (999 aa)*	0.563
Smp_005670	*Rab11, putative (218 aa)*	0.562
Smp_142990	*Serine/threonine kinase (830 aa)*	0.559
Smp_164380	*cAMP-dependent protein kinase catalytic subunit, putative (191 aa)*	0.559
Smp_093830.1__mRNA	*Expressed protein (112 aa)*	0.559
Smp_126460	*Serine/threonine kinase (332 aa)*	0.558
Smp_155720	*Serine/threonine kinase (594 aa)*	0.556
Smp_123610	*Serine/threonine kinase (1764 aa)*	0.554
faa3	*FAA1 Long-chain-fatty-acid--CoA ligase 1 (Faa3 long-chain-fatty-acid--coa ligase 3) (Faa4 long-chain-fatty-acid--...*	0.554
Smp_191310	*Histone deacetylase 4, 5,, putative (291 aa)*	0.551
Smp_138770	*Histone deacetylase hda2, putative (1132 aa)*	0.551
Smp_069380	*Histone deacetylase 4, 5,, putative (701 aa)*	0.551
Smp_149950	*Dephospho-CoA related kinases (558 aa)*	0.548
Smp_125060	*Serine/threonine kinase (537 aa)*	0.544
Smp_150690.1__mRNA	*Proliferation-associated protein 2G4, 38kDa (M24 family) (385 aa)*	0.535
Smp_044550.8__mRNA	*Far upstream (Fuse) binding protein, putative (530 aa)*	0.532
Smp_070190	*Gcn5proteinral control of amino-acid synthesis 5-like 2, gcnl2 (899 aa)*	0.532
Smp_162410	*Dishevelled, putative (854 aa)*	0.531
Smp_020300	*Dishevelled, putative (980 aa)*	0.531
calmodulin	*Calmodulin, putative (183 aa)*	0.531
Smp_077180	*Serine/threonine kinase (571 aa)*	0.531
Smp_068170.1__mRNA	*Pyruvate dehydrogenase, putative (386 aa)*	0.530
Smp_194610	*Serine/threonine kinase (361 aa)*	0.530
Smp_049760	*Protein kinase (780 aa)*	0.530
Smp_172270	*Carbon catabolite repressor protein, putative (658 aa)*	0.529
Smp_063640	*G-protein, beta subunit, putative (340 aa)*	0.527
Smp_010230	*Guanine nucleotide-binding protein beta 1, 4 (G protein beta1, 4), putative (340 aa)*	0.527
Smp_188470	*Forkhead protein/ forkhead protein domain, putative (95 aa)*	0.527
Smp_187740	*Putative uncharacterized protein (147 aa)*	0.527
Smp_158750	*Forkhead protein/ forkhead protein domain, putative (744 aa)*	0.527
Smp_158200	*Forkhead protein/ forkhead protein domain, putative (282 aa)*	0.527
Smp_155010	*Forkhead protein/ forkhead protein domain, putative (1156 aa)*	0.527
Smp_145650	*Expressed protein (208 aa)*	0.527
Smp_133520	*FREAC-7-like protein (899 aa)*	0.527
Smp_133480	*Forkhead protein/ forkhead protein domain, putative (113 aa)*	0.527
Smp_127090	*Forkhead protein/ forkhead protein domain, putative (286 aa)*	0.527
Smp_086270	*Forkhead protein/ forkhead protein domain, putative (987 aa)*	0.527
Smp_076300	*Forkhead protein/ forkhead protein domain, putative (758 aa)*	0.527

Smp_054350	*Forkhead protein/ forkhead protein domain, putative (674 aa)*	0.527
Smp_130130	*Nck2/grb4, putative (375 aa)*	0.526
Smp_014850	*Dreadlocks/dock, putative (309 aa)*	0.526
Smp_188400	*NADPH flavin oxidoreductase, putative (374 aa)*	0.524
Smp_034220	*5-methyl tetrahydrofolate-homocysteine methyltransferase reductase, putative (578 aa)*	0.524
Smp_030760	*Cytochrome P450 reductase, putative (594 aa)*	0.524
Smp_162010	*Serine/threonine kinase (794 aa)*	0.523
Smp_085690	*Serine/threonine kinase (238 aa)*	0.522
Smp_152330	*Serine/threonine kinase (351 aa)*	0.519
Smp_080770	*Serine/threonine kinase (214 aa)*	0.517
Smp_170340	*Collagen alpha-1(V) chain, putative (1794 aa)*	0.515
Smp_170330	*Collagen alpha-1(V) chain, putative (2991 aa)*	0.515
Smp_159600	*Collagen alpha-1(V) chain, putative (1377 aa)*	0.515
Smp_154870	*Signal transduction protein Ink-related (836 aa)*	0.514
Smp_087320	*Zinc finger protein, putative (273 aa)*	0.514
Smp_169900.2__mRNA	*Serine/threonine kinase (910 aa)*	0.512
Smp_062490	*Dhand, putative (251 aa)*	0.512
Smp_014170.2__mRNA	*Serine/threonine kinase (1024 aa)*	0.511
Smp_183460	*Serine/threonine kinase (1165 aa)*	0.510
Smp_172200	*Tyrosine kinase (801 aa)*	0.507
Smp_047560	*Peptide chain release factor, putative (1202 aa)*	0.504
Smp_186400	*cGMP-dependent protein kinase, putative (50 aa)*	0.503
Tk5	*Term=tyrosine kinase 5;db_xref=PMID-11289068;with=UniProt-Q9NH62;evidence=tracea ble author statement ...*	0.501
Smp_157150	*Expressed protein (1356 aa)*	0.499
Smp_087940.2__mRNA	*Gaba(A) receptor-associated protein, putative (119 aa)*	0.499
Smp_073790	*Gaba(A) receptor-associated protein, putative (124 aa)*	0.499
Smp_158460	*Putative uncharacterized protein (506 aa)*	0.495
Smp_035980	*Histone H2A (264 aa)*	0.493
Smp_057360	*Serine/threonine kinase (455 aa)*	0.491
Smp_194640	*Serine/threonine kinase (448 aa)*	0.491
Smp_089230	*Polycomb complex protein bmi-1, putative (353 aa)*	0.491
Smp_045610	*Rho GDP-dissociation inhibitor-related (200 aa)*	0.489
Smp_157650	*Putative uncharacterized protein (539 aa)*	0.487
Smp_004780.1__mRNA	*Immunophilin, putative (430 aa)*	0.483
Smp_137540	*Disulfide oxidoreductase, putative (691 aa)*	0.481
Smp_124360	*Glutathione peroxidase (175 aa)*	0.480
Smp_058690	*Glutathione peroxidase (169 aa)*	0.480
Smp_066930	*Transcription factor sp8,sp9, putative (834 aa)*	0.478
Smp_040190	*Serine/threonine kinase (351 aa)*	0.473
Smp_196120	*Choline/ethanolaminephosphotransferase 1 (Ethanolaminephosphotransferase) (2431 aa)*	0.473
Smp_190600	*Phosphatidylinositol 3-kinase class, putative (58 aa)*	0.473
Smp_172400	*Phosphatidylinositol-4,5-bisphosphate 3-kinase catalytic subunit alpha PI3K (2003 aa)*	0.473
Smp_162340	*Phosphatidylinositol 3-and 4-kinase, putative (2788 aa)*	0.473
Smp_150660	*Phosphatidylinositol 4-kinase (1020 aa)*	0.473
Smp_024190	*Expressed protein (2574 aa)*	0.473
Smp_137190	*Frataxin homolog, mitochondrial, putative (161 aa)*	0.471
Smp_165470	*Tyrosine kinase (1693 aa)*	0.467
Smp_152680	*Tyrosine kinase (1766 aa)*	0.467
Smp_047190	*Serine/threonine kinase (1472 aa)*	0.467
Smp_102040.1__mRNA	*Receptor for activated PKC, putative (315 aa)*	0.461
Smp_020800	*Cysteine and histidine-rich domain (Chord)-containing, zinc binding protein, putative (343 aa)*	0.461
Smp_175650	*E3 ubiquitin-protein ligase nedd-4, putative (965 aa)*	0.459
Smp_116320	*14-3-3 protein, putative (273 aa)*	0.458
Smp_009760	*14-3-3 protein homolog 1 (252 aa)*	0.458
Smp_002410	*14-3-3 epsilon 2 (249 aa)*	0.458
Smp_172700	*Serine/threonine kinase (831 aa)*	0.457
Smp_155740	*Heat shock protein, putative (704 aa)*	0.451
HDAC8	*Histone deacetylase 1, 2 ,3, putativeHistone deacetylase 8 (440 aa)*	0.451
Smp_026510	*Protein kinase (544 aa)*	0.449
Smp_135950	*Cell polarity protein (Lethal giant larvae homolog 2) (Inorganic pyrophosphatase, putative) (1647 aa)*	0.449
Smp_080730	*Serine/threonine kinase (410 aa)*	0.447
Smp_096640	*Serine/threonine kinase (621 aa)*	0.447
Smp_159620	*Expressed protein (1151 aa)*	0.446
Smp_049970.5__mRNA	*Zinc finger protein, putative (276 aa)*	0.446
Smp_028630	*Exocyst complex component sec6, 3' (565 aa)*	0.444
Smp_177250	*Histone deacetylase, putative (292 aa)*	0.442
Smp_138780	*Histone deacetylase hda2, putative (204 aa)*	0.442
Smp_072340	*26S protease regulatory subunit 6b, putative (415 aa)*	0.439
Smp_169230	*Tyrosine kinase (1194 aa)*	0.438
Smp_128790	*Tyrosine kinase (1057 aa)*	0.437
Smp_120800	*DNAj homolog subfamily C member, putative (369 aa)*	0.433
Smp_000850	*DnaJ domain, putative (356 aa)*	0.433
Smp_161110.2__mRNA	*Fh1/fh2 domains-containing protein (Formin homolog overexpressed in spleen) (Fhos), putative (1247 aa)*	0.432
Smp_188360	*26S protease regulatory subunit 6b, putative (154 aa)*	0.431
Smp_170130	*Fos transcription factor-related (833 aa)*	0.429

Smp_080420	*Expressed protein (442 aa)*	0.429
Smp_192550	*Rab2, putative (92 aa)*	0.428
Smp_190370	*Rab2, putative (103 aa)*	0.428
Smp_104310	*Rab11, putative (213 aa)*	0.428
Smp_090890	*Serine/threonine protein kinase (705 aa)*	0.426
Smp_137370	*Serine/threonine kinase (926 aa)*	0.425
Smp_086690	*Kinase (384 aa)*	0.425
Smp_172240	*Serine/threonine kinase (450 aa)*	0.425
Smp_155330	*Serine/threonine kinase (1535 aa)*	0.425
Smp_134910.1__mRNA	*Serine/threonine kinase (1511 aa)*	0.422
Smp_095350	*Zinc finger protein, putative (353 aa)*	0.415
Smp_129120	*Shoc2, putative (532 aa)*	0.415
Smp_142610	*Serine/threonine kinase (1608 aa)*	0.415
PFK	*6-phosphofructokinase (797 aa)*	0.414
MYH	*Myosin heavy chain (1937 aa)*	0.413
Smp_046060.1__mRNA	*Myosin-10 (Myosin heavy chain, nonmuscle IIb) (Nonmuscle myosin heavy chain IIb) (NMMHC II-b) (NMMHC-II...*	0.413
Smp_125360	*Tyrosine kinase (670 aa)*	0.412
Smp_079490	*Eukaryotic translation initiation factor 4b/4h, putative (293 aa)*	0.412
Smp_041820	*Serine/threonine kinase (429 aa)*	0.411
Smp_027390	*Exocyst componenet sec8, putative (1263 aa)*	0.411
Smp_125640	*Syntaxin-12, putative (240 aa)*	0.411
Smp_161120	*Actin bundling/missing in metastasis-related (1050 aa)*	0.410
Smp_135520	*Dock, putative (2485 aa)*	0.407
Smp_128740	*Sec24-related A, B (594 aa)*	0.407
Smp_128730	*Sec24-related A, B (675 aa)*	0.407
Smp_055130.1__mRNA	*Zinc finger protein, putative (297 aa)*	0.407
Smp_113470	*Putative uncharacterized protein (1268 aa)*	0.403
Smp_113460	*Receptor-type adenylate cyclase, putative (1197 aa)*	0.403
Smp_112590	*Putative uncharacterized protein (1269 aa)*	0.403
Smp_160500	*Nalp (Nacht, leucine rich repeat and pyrin domain containing)-related (1691 aa)*	0.402
Smp_151670	*Protein kinase (489 aa)*	0.402
Smp_055090	*Chromatin regulatory protein sir2, putative (305 aa)*	0.402
Smp_021870	*Ccr4-associated factor, putative (291 aa)*	0.400

Appendix 3 **Medium confidence analysis parameters reveals 342 putative Akt interacting proteins.** STRING analysis was performed using Smp_079360 with parameters set to ≥0.40 (medium confidence).

Protein ID	Protein Name	KinasePhos				Scansite3		HPRD	
		Amino Acid	Predicted Phosphosite	HMM Bit Score	E-value	Amino Acid	Predicted Phosphosite	Amino Acid	Predicted Phosphosite
Smp_094250	Serine/threonine kinase (484 aa)	198	RQSDSTPNS	-1.3	20	•		•	
Smp_122910	Ataxia telangiectasia mutated (Atm)-related (2611 aa)	1765	ARTLSKVNS	-2.8	1.80E+02	•		•	
		2470	RRANSPNRV	-0.7	66	2099	PRKLTITGS	2099	PRKLTITGS
Smp_079760.1_mRNA	Protein kinase (491 aa)	None				•		182	RARDAT
Smp_154470	Pten, putative (597 aa)	478	DRDVSSDEE	-1.7	29	•		•	
Smp_072330.2_mRNA	Heat shock protein, putative (718 aa)	457	YSSASGDEM	-2.3	37	•		•	
Smp_074390	Eukaryotic translation initiation factor 4e-binding protein, putative (121 aa)	None				•	-	•	-
Smp_053130	40S ribosomal protein S6 (248 aa)	96	RRRKSVRGC	1.9	1.1	233	KRSRSHSLR	•	
		235	SRSHSLRES	0	3	•	-	•	
Smp_099930	F-box and wd40 domain protein, putative (863 aa)	289	SRTQSIPFS	0.6	14	•	-	•	
		853	SSKSSFISS	-2.8	71	•		•	
Smp_164960	Phosphatidylinositol-4,5-bisphosphate 3-kinase PI3K (1340 aa)	None				•	-	646	RIRRPT
Smp_159000	Expressed protein (1610 aa)	533	GRNDSVRDF	-2.5	1.20E+02	•	-	•	-
		766	LRKSSNREV	-1	62	•	-	•	-
		933	SSNTSTDNV	-2.9	1.50E+02	•	-	•	-
Smp_064010	Camp-response element binding protein-related (825 aa)	134	PRSPSASSS	1.8	8.4	•		•	
		137	PSASSSTSN	-2.5	72	•		•	
		209	RRRSSTLAP	-1.1	38	210	RRSSTLAPP	210	RRSSTLAPP
		339	SRNTSSVPH	-0.3	25	•	-	•	
		574	ARFSSESDR	-0.2	23	•	-	•	
		614	QRRRSVFTA	-2.5	74	•	-	•	-
		817	ESESSAPES	-1.2	39	•	-	•	
Smp_142710	Fkbp-rapamycin associated protein, putative (4023 aa)	481	TSSFSARFS	-2.3	2.80E+02	•		•	
		1246	LSHPSTSAS	-2.7	3.30E+02	•		•	
		1543	IRQKSESAN	-2	2.40E+02	•		1545	RQKSES
		1815	QSSNSFPGS	-2.6	3.20E+02	•		•	

		1822	GSSTSWTNR	-1.3	1.70E+02	●	_	●	
		2308	KRVSSKHSI	-2.2	2.70E+02	2473	PRLCSIQFE	●	
		2906	RQHASFIKT	-1.5	1.90E+02	2578	ARTYSVTPL	●	
		3309	IRISSCAIT	-1.2	1.70E+02	●	_	●	
		3858	RRSTSSESC	0.9	55	●	_	●	
Smp_008260	Glycogen synthase kinase 3-related (Gsk3) (Cmgc group III) (463 aa)	427	IRLTSNNSN	-1.7	18	●	_	282	RPRVPS
Smp_023550	Beta-catenin, putative (989 aa)	None				906	SCVGSISSS	●	_
Smp_159560	Transcription factor GATA-1, putative (735 aa)	20	SRQESDCRA	-1	28	195	NRKLTMTEG	●	
		478	HQSQSMNSM	-2.7	64	255	RRTGTICSN	309	RNRKVS
		571	AQLRSTPNQ	-2.6	62	●		●	
		669	ISSSSTSSE	-2.1	48	●		●	
Smp_018590	Endothelial transcription factor GATA-2, putative (565 aa)	334	KRRISANRK	-1.6	30	●	_	395	RNRKLT
Rac	Rac gtpase, putative (188 aa)	None				71	LRPLSYPQT	71	RXRXXS
Smp_139630	Protein kinase (619 aa)	None				377	YRHSTLDAT	●	_
Smp_133020	Serine/threonine kinase (237 aa)	133	IRDISKCEP	-2.4	12	●		●	
Smp_047900	Serine/threonine kinase (201 aa)	None				138	DRLLTFNPT	●	_
Smp_032000	Caspase-7 (C14 family) (379 aa)	159	NRHGSSHDA	-2.8	26	●		●	
Smp_193170	Putative uncharacterized protein (79 aa)	None				●	_	●	_
Smp_073560.2_mRNA	G beta-like protein gbl (317 aa)	255	TRQGSPSGH	-2.3	19	●		●	
Smp_081410	Ste20-related kinase (452 aa)	131	QQQTSAPDT	-1.5	16	●	_	●	_
		179	VRSNSTSNR	-2.9	30	●	_	●	_
Smp_039490.1_mRNA	Expressed protein (954 aa)	187	ASTPSLSSE	-2	68	●		495	KIKSSS
		680	SRHSSHQSE	0.7	17	●		●	
		832	KRRYSKTDS	-1.4	51	●	_	●	
		850	QSRPSLTSS	-0.8	38	●		●	
		853	PSLTSSGDS	-2.8	98	●		●	
		885	HRRRSSSNR	-1.1	44	●		●	
		886	RRRSSSNRP	-2.1	71	●		915	KDKTDS
		887	RRSSSNRPS	1.5	12	●	_	●	
		927	GRRRSRSFN	-2.6	89	●		●	

		929	RRSRSFNQR	0.7	17	●	-	●	
		938	HRSRSTDRR	-1	42	●	-	●	-
		945	RRDRSSSNR	-1.4	50	947	DRSSSNRYR	947	RDRSSS
Smp_156680	Fyve finger-containing phosphoinositide kinase, fyv1, putative (2289 aa)	160	QRACSYCAE	0	57	●			
		213	TRPKSVPSH	-1.7	1.30E+02	●			
		266	TSTSSADEC	-1.7	1.30E+02	508	SRRKTVDFT		
		870	DRLMSNPSR	-1.1	1.00E+02	591	MRDCSLESL	591	RMRDCSL
		876	PSRKSDNNT	-2.1	1.60E+02	1062	GRLLSVSPS		
		995	SRVKSLNKM	-1.6	1.30E+02	●	-	●	-
		1756	ARTHSNSIS	-1.9	1.50E+02	●	-	●	-
		2048	QSEISMANN	-2.7	2.10E+02	1758	THSNSISSV		
SER	Tyrosine kinase (1600 aa)	1260	HRNNSLHRH	-1.1	57	●		190	KEKTVS
		1401	ESRSSVALS	-2.2	95	●		●	
Smp_073210	ADP-ribosylation factor interacting protein, putative (341 aa)	None				●	-	●	-
Smp_028500	Caspase-3Caspase-3 (C14 family) (296 aa)	None				●	-	●	-
Smp_056440	Superoxide dismutase (217 aa)	None				●	-	●	-
Smp_104030.3_mRNA	Scribble complex protein (Cell polarity protein) (1456 aa)	575	LSTSSAHSS	-2.3	95	74	IRLLTLSDN	74	RIRLLT
		658	SSSESLNDG	-2.9	1.20E+02	652	DGTGSASSS	495	KNRSIS
		891	KRFASPFGG	-2.4	1.00E+02	848	ARIQSKTAD	848	RARIQS
						1288	LRRITVTKR		
Smp_012050	Bola-like protein my016 (77 aa)	24	ARLVSVSDV	-0.4	1.1	●	-	●	-
Smp_167400	Myogenic factor, putative (864 aa)	348	RSSSSLGNA	-2.4	88	●		●	
		465	KRTKSMMQS	-0.6	36	●		●	
		791	DQLNSMPNS	-2.2	78	●		●	
Smp_178480	Wd and tetratricopeptide repeat protein, putative (220 aa)	None				207	RRKLTLSTY	●	-
Smp_123420	Aryl hydrocarbon receptor nuclear translocator homolog, putative (783 aa)	254	QRRNSPANL	-2.6	70	●		●	
		717	SSSISTSES	-2	55	●		●	
Smp_105910	CREB-binding protein 1 (SmCBP1) (2093 aa)	577	HRFKSDSGT	-1.4	98	●	-	577	RHRFKS
		1266	HRHNSAASL	-2.7	1.80E+02	●	-	579	RFKSDS
		1399	DRRISIEGC	-2.5	1.70E+02	1499	RRISTMHRG	1499	RRRIST

		1994	GRQSSTPQA	1	29	●	-	●	
Cdc42	Cell polarity protein (Regulator of photoreceptor cell morphogenesis) (195 aa)	None				75	LRPLSYPQT	75	RLRPLS
Smp_005880	Phosphoenolpyruvate carboxykinase, putative (626 aa)	None				●	-	624	RERIQS
Smad4	Smad4, putative (738 aa)	241	GSHTSCSKN	-1.7	38	●			
		375	YSSNSTPVC	-2.2	49	●			
Smp_036270.2_mRNA	Arginine/serine-rich splicing factor, putative (371 aa)	187	QRSRSGSYR	-2.8	34	196	SRSDSRHSH	31	RSRSGS
		189	SRSGSYRSR	-0.2	9.8	●	-	33	RSRSGS
		194	YRSRSDSRH	0	8.7	●	-	38	RSRSDS
		204	HRSRSRDSH	-2.4	28	●	-	40	RSRSDS
		233	QRSESGNDS	2.6	2.2	●	-	57	RQKSRS
		252	PRSRSPSRR	-1.9	23	●	-	75	RQRSES
		257	PSRRSGTNR	-1.6	20	●	-	77	RQRSES
		284	SRSPSCNGR	-0.8	13	●	-	96	RSRSPS
		304	SRSRSISHS	-2.2	26	●	-	98	RSRSPS
		316	SRSRSVESR	-1.6	20	●	-	146	RSRSRS
		337	SRSRSMSHR	-1.9	22	●	-	148	RSRSRS
		339	SRSMSHRSE	-1	15	●	-	181	RSRSMS
		344	HRSESGTPR	0.6	6.5	●	-	183	RSRSMS
Smp_085700	cAMP-dependent protein kinase catalytic subunit, putative (104 aa)	None				●	-	●	-
Smp_078230	Protein kinase, cgmp-dependent, type I, putative (488 aa)	236	TRTASVKAI	-1.6	20	●	-	●	-
Smp_139930	Protein tyrosine phosphatase, non-receptor type nt1, putative (628 aa)	67	YRDVSPFDS	0.1	12	244	GRSGTFVLI	●	-
Smp_075450	Heparan sulfate 2-o-sulfotransferase, putative (206 aa)	None				●	-	●	-
Smp_191040	P38 MAPk, putative (74 aa)	None				●	-	●	-
Smp_062950	Growth factor receptor-bound protein, putative (234 aa)	147	HRKTSISRN	-1.4	6.4	155	NRLLTLVDL	155	RNRLLT
Smp_044530	Growth factor receptor-bound protein, putative (317 aa)	None				●	-	●	-
hsp70	Heat shock 70 kDa protein homolog (637 aa)	138	GRTVSDAVI	-1.6	23	●	-	●	-
Smp_166290	Phosphotyrosyl phosphatase activator, putative (373 aa)	None				●	-	●	-
SOD	Superoxide dismutase [Cu-Zn] (153 aa)	None				●	-	●	-
Smp_142450	Rap1 and, putative (183 aa)	None				●	-	●	-

Smp_071250	Rap1 and, putative (184 aa)	None				•	-	•	-
Smp_048990	Beclin, putative (494 aa)	None				•	-	•	-
Smp_172010	Caspase-7Caspase-7 (C14 family) (329 aa)	101	PRNGSLVDV	-0.9	11	•	-	•	-
Smp_182250	Serine/threonine-protein phosphatase (211 aa)	None				•	-	•	-
Smp_165490	Serine/threonine-protein phosphatase (423 aa)	None				•	-	•	-
Smp_030710	Serine/threonine-protein phosphatase (307 aa)	None				•	-	•	-
Smp_150430	Forkhead protein/ forkhead protein domain, putative (504 aa)	181	RRTNSLQRS	1.2	7.2	•	-	•	
		194	LRLASYYAS	-2.7	52	•		56	RKRKLT
								179	RRRTNS
Smp_018240.3_mRNA	Cell division control protein 48 aaa family protein (803 aa)	586	ARGGSVGDA	-1.8	23	744	RRSVTENDV	•	
Smp_017900	Serine/threonine kinase (806 aa)	302	KRTPSNRLG	-1.7	33	221	DRTYSFCGT	107	RDRLRT
						794	VRAKSILTN	794	RVRAKS
Smp_085680	Guanylate cyclase (584 aa)	390	ISSSSTPFE	-0.7	17	124	LRRDSIPLS	•	
Smp_136750	Serine/threonine kinase (1767 aa)	319	RRLGSGPSD	-1.6	78	282	DRRQTIDLI	•	
		423	SRRRSGISS	0.7	24	•	-	•	
		430	SSSSSPGFV	-2.7	1.30E+02	•	-	•	
		575	TRLVSPSSS	0.7	24	•	-	•	
		697	KRLISAASE	-0.1	38	•	-	•	
		781	QRFDSDAEE	-1.5	77	•	-	•	
		934	HRQSSLRLR	-0.9	54	•	-	•	
		1243	QSTPSTPQS	-0.9	55	1297	ARPGTVTTS	•	
		1416	QRKSSLTSP	0.7	24	•	-	1496	RRKSQS
Smp_082030	Family C56 non-peptidase homologue (C56 family) (184 aa)	123	KRLTSYPGF	-1	4.4	•	-	•	
Smp_138640	Chromatin regulatory protein sir2, putative (618 aa)	143	RRINSLEKV	-1.6	31	•	-	•	-
Smp_152900	Protein Wnt (1435 aa)	1406	SSSSSVPIH	-2.1	95	585	PRMRTLGTL	723	RIRMHS
								900	KSKTTS
								1164	KSKTTS
Smp_072110.1_mRNA	Programmed cell death, putative (534 aa)	51	KRFHSASFS	-1.9	26	•	-	•	-
		319	TRNFSDSSS	1	6	•	-	•	-
		520	KRFISETDS	0.1	9.8	•	-	•	-

Smp_165570.2_mRNA	Ras-dva small gtpase, putative (394 aa)	85	QRRASAFVL	-2.6	26	•		•	
		205	ERRASAFAV	1.6	3.2	•		•	
		284	RREPSIIKP	-2.5	25	•		•	
		356	IRKSSKMSS	-2.9	29	•		•	
Smp_171530	Beta-parvin-related (383 aa)	None				•	-	•	-
Smp_035390	Protein tyrosine phosphatase n11 (Shp2), putative (708 aa)	424	TRDSSVSTK	-2.3	49	708	PRTKS****	708	RPRTKS
								405	RVRHLS
								706	RPRTKS
Smp_170550.1_mRNA	Granulin, putative (748 aa)	647	SQRQSTSNH	-2.6	55	•	-		
Smp_173990	Rab11, putative (933 aa)	649	RQSTSNHNI	-2.1	43	82	YRAITAAYY		
						873	RRRLSLELR		
Smp_078040	Tubulin beta chain, putative (444 aa)	None				285	YRSLTVPEL		
Smp_035760	Tubulin beta chain, putative (444 aa)	None				285	YRSLTVPEL		
Smp_030730	Tubulin beta chain, putative (443 aa)	None				285	YRSLTVPEL		
sat1	Alpha tubulin, putative (451 aa)	None				•	-		
Smp_016780	Tubulin alpha chain, putative (451 aa)	None				•	-		
Smp_099030	Protein kinase (357 aa)	None				•	-		
Smp_125310	Protein kinase (515 aa)	460	DQRSSMSSI	-1.5	24	•	-		
		462	RSSMSSIFS	-2.9	44	•	-		
Smp_129430	Myocyte-specific enhancer factor 2a, putative (661 aa)	139	TSSVSMALE	-3	74	20	NRQVTFTKR		
		262	NRGSSLIDP	-2.2	53	•			
		341	TQRSSLTSS	0.3	15	•			
		374	SRSRSPILP	-2.3	54	•			
		490	SSTPSMQER	-1.9	46	•			
Smp_139400	Tensin, putative (1704 aa)	530	MRQTSDPLS	-2.6	1.40E+02	•	-		
		542	IRGRSPQSS	1.4	19	•	-		
		870	QRTRSLLNE	-1.6	89	•	-		
		1002	RRIYSDSEM	-2.3	1.30E+02	•	-		
		1121	GRAFSGSPT	-0.2	46	•	-		

		1409	LRGSSNEPI	-2.9	1.70E+02	●	-
		1561	RSNRSPPAV	-1.8	99	●	-
Smp_167140	Protein Wnt (448 aa)	None				●	-
Smp_151400	Protein Wnt (462 aa)	367	TSSTSLSPS	-2.1	25	●	-
Smp_145140	Protein Wnt (403 aa)	None				●	-
Smp_034670	Tubulin gamma chain, putative (493 aa)	None				●	-
Smp_196030	GTPase activating protein,putative (745 aa)	90	LRSKSTDRI	-2.7	65	●	
		264	SSSISTTEQ	-2.1	49	●	
		503	NRSNSFSES	-0.2	19	●	-
		671	VRDASGSSS	-1.5	38	●	
Smp_081190	Rho3 GTPaseRho3 GTPase, putative (242 aa)	207	HRKKSISNG	-0.2	4.8	55	GRHLTLGLW
		224	TRRSSGLKR	-2.3	13	●	-
Smp_072140	Rho2 GTPase, putative (192 aa)	None				73	LRPLSYPDT
Smp_056970.1_mRNA	Glyceraldehyde-3-phosphate dehydrogenase (338 aa)	None				●	-
Smp_097800.3_mRNA	Y box binding protein, putative (231 aa)	114	GRGRSPRVF	0.3	2.4	154	GRGGSEMYG
Smp_097750	Cold shock domain protein A, putative (175 aa)	None				●	-
Smp_106130.2_mRNA	Heat shock protein 70 (Hsp70), putative (653 aa)	None				●	-
Smp_049550	Heat shock protein 70 (Hsp70), putative (648 aa)	300	SKRPSTTVE	-2.8	35	●	-
ral	Ral, putative (194 aa)	None				48	RRKMTLDGV
Smp_035010	Chibby protein pkd2 interactor, putative (142 aa)	None				●	-
Smp_046690	Ubiquitin (Ribosomal protein L40), putative (349 aa)	None				●	-
Smp_009580	Ubiquitin (Ribosomal protein L40), putative (228 aa)	None				●	-
Smp_070680	Expressed protein (274 aa)	117	KRTRSETSI	-0.9	10	●	-
						119	TRSETSICL
Smp_127920	Serine/threonine kinase (1028 aa)	374	SRKTSSIEQ	-1.3	42	823	NRTGSLPGP
						954	IRKLTSTIE
						956	KLTSTIEVT
Smp_127060	Serine/threonine kinase (354 aa)	None				●	-
Smp_089430	Ubiquitin (Ribosomal protein L40), putative (128 aa)	None				●	-

Smp_026270	Early growth response protein, putative (905 aa)	435	RRRKSTTRN	2.1	8.2	•	
		511	QREFSRSDH	-2.6	87	•	
Smp_131050	Camp-dependent protein kinase type II regulatory subunit, putative (301 aa)	132	SRAASIIAT	-0.4	7.1	•	-
		254	PRAASAYAV	-2.2	17	•	-
Smp_079010	Camp-dependent protein kinase type II-alpha regulatory subunit, putative (378 aa)	None				•	-
Smp_030400	Camp-dependent protein kinase type I-beta regulatory subunit, putative (418 aa)	None				•	-
Smp_075940	Prohibitin, putative (208 aa)	114	GREFSEAVE	-1.5	8	94	QRASSFGIL
Smp_021590	Rac gtpase activating protein, putative (610 aa)	181	GRASSVSHT	-1	21	•	-
		401	LRSRSTPSL	-2.6	44	228	QRLGTINRL
						257	GRRITFGKA
						345	SRNLSLSLL
Smp_075210.2_mRNA	Prohibitin, putative (288 aa)	None				82	PRKITSPTG
Smp_056390	Protein kinase (729 aa)	45	PRISSNFGR	-2.1	37	•	-
		121	PKHESWFSS	-2.3	41	•	-
		603	KRNPSERPN	-2.2	40	•	-
Smp_006210	Anamorsin homolog (1264 aa)	544	QRISSAHPS	1.7	13	•	
Smp_179910	Ras-like protein (141 aa)	None				•	-
topbp1	Topbp1, putative (1396 aa)	35	KRLSSCEVI	-1.7	68	960	ARVASLNLF
		242	TRQASGTKY	-2.4	94	1372	PRNYSWLRI
Smp_000730	ADP-ribosylation factor family (176 aa)	None				•	-
Smp_050830	Synaptojanin, putative (526 aa)	276	QRQASPSRR	-0.6	13	341	PRWFSLPVK
		468	HRKNSVSSA	-1.2	18	•	-
Smp_022100	Camp-dependent protein kinase type I-beta regulatory subunit, putative (84 aa)	None				41	PRAATVVAQ
Smp_019280	Camp-dependent protein kinase regulatory chain, putative (251 aa)	14	ARRQSVAAE	0.3	3.8	•	
Smp_001050	Similar to Protein C20orf152 homolog, putative (621 aa)	34	HRISSSRST	-0.1	15	•	-
		37	SSSRSTDDK	-2.2	42	•	-
		183	HSSSSLSNS	-0.8	22	•	-
		221	TSSSSSFNE	-2.4	47	•	-
Smp_172670	Protein kinase C, putative (343 aa)	None				•	-

Smp_154140	Site-1 peptidase (S08 family) (988 aa)	583	SSRFSGVAE	-2.1	58	●	-
		676	LRRKSYFIE	-0.4	25	●	-
Smp_065840	DNA topoisomerase 2 (1599 aa)	1464	SRGASAIVS	1.5	13	901	GFTGTIEDL
		1482	GRQFSAPPK	-0.7	41	●	
		1493	PSIKSMFPS	-2.4	94	1313	GKGRTVPTS
Smp_097730	Srf homolog, putative (429 aa)	102	TQQPSFTDE	-1.6	26	●	-
		302	GRTVSFCNN	1.7	4.8	●	-
Smp_095190	Apoptosis regulator bax, putative (199 aa)	55	RRRTSTDME	0.8	2	56	RRTSTDMET
Smp_103710	Ubiquitin-conjugating enzyme E2 I, putative (166 aa)	None				●	-
Smp_005020	Cbl, putative (684 aa)	None				●	
Smp_165420	Zinc finger protein, putative (4034 aa)	326	TRDSSIALR	-2.3	3.00E+02	●	-
		391	SRSVSVALS	0	99	●	-
		468	TRLSSSKAV	-2	2.60E+02	●	-
		3874	SRAMSGHLS	0.4	81	2259	TRLTTQTNN
		4020	SSSPSPVPS	-2.8	3.80E+02	●	-
Smp_141540	Thymidine kinase, putative (945 aa)	54	QRRWSVPFQ	-1.9	62	●	
		147	ARNRSGEED	-2.7	85	●	
		305	SRSISSCTR	-2.5	79	●	
		382	PSNNSMASS	-0.9	38	●	
		489	PRMNSYCND	-2.4	77	●	
		877	LQRSSYGNT	-2.2	70	●	
Smp_068240	Zinc finger protein, putative (544 aa)	522	SRNISKTGE	-1.1	24	●	-
Smp_172030	DEAD box ATP-dependent RNA helicase, putative (679 aa)	None				●	
Smp_067140	Rab9 and, putative (205 aa)	None				●	-
Smp_175500	GATA binding factor-1b (Transcription factor xgata-1b), putative (919 aa)	13	LSTSSKTSS	-3	98	●	
		36	CRSPSTTSS	-1.2	45	●	
		226	SSSSSNSEV	-2.8	94	●	
		880	SSSSSNNDN	-2.2	70	●	
Smp_080030	GATA binding factor-1b (Transcription factor xgata-1b), putative (227 aa)	None				●	-
Smp_142050	Serine/threonine kinase (390 aa)	None				●	

Smp_183460_mRNA	Map/microtubule affinity-regulating kinase 2,4, putative (108 aa)	95	RRRSSLDTS	1.1	1.3	●		-
Smp_098780	Forkhead protein/ forkhead protein domain, putative (619 aa)	80	PRTTSSSSL	-2	45	●		
Smp_016920	Putative uncharacterized protein (203 aa)	153	RRTRSIGPS	1.4	1.9	●		-
		162	RRSNSMNIF	0.6	2.9	●		-
		179	RRGNSVTAI	0.7	2.8	●		-
Smp_128130	Phosphatidylinositol-4,5-bisphosphate 3-kinase PI3K (889 aa)	None				●		
Smp_148430	Expressed protein (738 aa)	320	YRNGSSSKS	-1.2	31		300	ERLLSMHRQ
		486	SRLSSDRFT	1.3	8.7	●		-
		570	SRSSSLCYN	-0.6	23	●		-
Smp_148420	Expressed protein (974 aa)	226	ERSVSTVSL	-2.6	58		214	SRSKTLGPT
		597	KRLDSLTDE	-1.9	44	●		
		766	RKTISMPPN	-2.3	51	●		
Smp_171750	Axis inhibition protein, axin, putative (1047 aa)	289	HRSTSRHQF	-2.7	1.00E+02		200	TKHKSFSEY
		626	YRSFSRPNK	-2.3	84	●		-
		638	RSIASWDSG	-1.4	56		760	LRRRSKQCE
		898	RSHSSTRLN	-1.5	58	●		-
		960	PSSSSISSS	-2.4	89	●		-
Smp_166200	Axis inhibition protein, axin, putative (1142 aa)	53	GSTASYEVG	-2.4	1.00E+02	●		
		147	IRGASSSLA	-2.7	1.20E+02	●		
		178	IRLRSETRH	-2.4	1.10E+02		180	LRSETRHAI
		585	RRGASSRPF	1	20	●		
		635	SRSYSMAEH	0	33	●		
		778	DRTPSSGDG	-0.9	51	●		
		1038	SSSTSAVSG	-2.5	1.10E+02	●		
CYTB	Cytochrome b, putative (199 aa)	None				●		-
Smp_190100	Jun activation domain binding protein, putative (84 aa)	None				●		
Smp_146200.2_mRNA	Zyxin/trip6, putative (455 aa)	38	MRSSSERDN	-1.5	26		120	FRTSSVLTA
		236	SSTNSPTES	-1.8	30	●		-
		243	ESASSMCNS	1.7	5	●		-

		421	RRVVSGNSN	-0.6	16	379	SRPFTIDVH
Smp_144330	Putative uncharacterized protein (244 aa)	None				●	
Smp_131660	Jab1/MPN domain metalloenzyme (M67 family) (248 aa)	100	IRTISSGKV	-2.1	15	●	-
Smp_127310	Biogenic amine (Dopamine) receptor, putative (567 aa)	None				●	
Smp_090080	Serpin (406 aa)	75	IRLKSTSSS	0.9	4.6	●	-
Smp_085740	Abl-binding protein-related (583 aa)	171	TRRGSSSAS	-0.7	19	●	
		172	RRGSSSASG	1.7	5.3	●	
		184	GRQHSTVAC	-1.6	29	●	
		288	SRKSSGSSG	1	7.7	●	
		291	SSGSSGTGS	-2.2	38	●	
		515	PRQPSDPAW	-2.8	51	●	
Smp_055670	Rab-2,4,14, putative (223 aa)	74	ERFRSVARS	0.1	4.1	205	PKFGSIPQV
		194	RQSSSLTFN	-0.3	5.1	●	-
Smp_027610	40S ribosomal protein S3, putative (230 aa)	None				●	
Smp_149150	Acyl-CoA-binding protein (Acbp) (Diazepam binding inhibitor) (Dbi) (343 aa)	125	DRGFSLSKV	-1.2	14	●	-
						22	TRWNTIQVV
Smp_166010	Ankyrin repeat-containing, putative (1291 aa)	515	GSVTSNPNS	-3	1.00E+02	●	
		1174	SSSSSTSAS	-3	1.00E+02	●	
		1182	SSSSSGNNV	-2	66	●	
Smp_173810	Protein phosphatase pp2a regulatory subunit B, putative (490 aa)	None				●	-
Smp_172290	Serine/threonine protein phosphatase 2a regulatory subunit A, putative (392 aa)	None				●	
Smp_172280	Serine/threonine protein phosphatase 2a regulatory subunit A, putative (535 aa)	None				●	-
Smp_153410	Serine/threonine protein phosphatase 2a regulatory subunit A, putative (821 aa)	None				●	
Smp_056760	Protein disulfide-isomerase, putative (482 aa)	None				●	-
Smp_151420	Phospholipase D (906 aa)	109	NRFGSYAPS	-1.9	38	●	
		240	RRIRSLRKR	0.2	13	●	
		601	HRQASDHLQ	-1	25	●	
Smp_161230	Ras GTP exchange factor, son of sevenless, putative (1518 aa)	10	SRHTSTVSL	-1.2	66	●	-
		385	KRFPSDDDR	-1.2	68	●	-

		408	HRNISNNNS	0.5	29	●	-
		539	PRRRSTSTT	-0.3	44	●	-
		541	RRSTSTTAT	3.6	5.2	●	-
		700	GSHVSCASM	-2	98	●	-
		1356	LRRESIHNP	-2	1.00E+02	●	-
		1367	QRTSSSSSS	0.5	28	●	-
Smp_196040	Shc transforming protein, putative (409 aa)	75	PSNRSADKS	-2.5	27	●	
		213	SQNTSMPNN	-0.5	11	●	
Smp_023150	Serine/threonine-protein phosphatase (302 aa)	None				251	GRLITIWSA
Smp_145810.1_mRNA	Poly [ADP-ribose] polymerase, putative (536 aa)	280	IRTMSEVKS	-0.7	14	●	
Smp_129260	Poly [ADP-ribose] polymerase, putative (977 aa)	None				108	TRKFTVKLS
						705	TRFYTLIPH
Smp_082490	Cyclin B, putative (414 aa)	None				388	GRVASLPQL

Appendix 4 **Analysis of interacting proteins revealed 48 with putative Akt phosphorylation sites.** Phosphorylation prediction tools Kinasephos, Scansite and HRPD were used to search for putative Ser/Thr phosphorylation motifs with an arginine (R) in the -3 and -5 position, suitable for Akt.

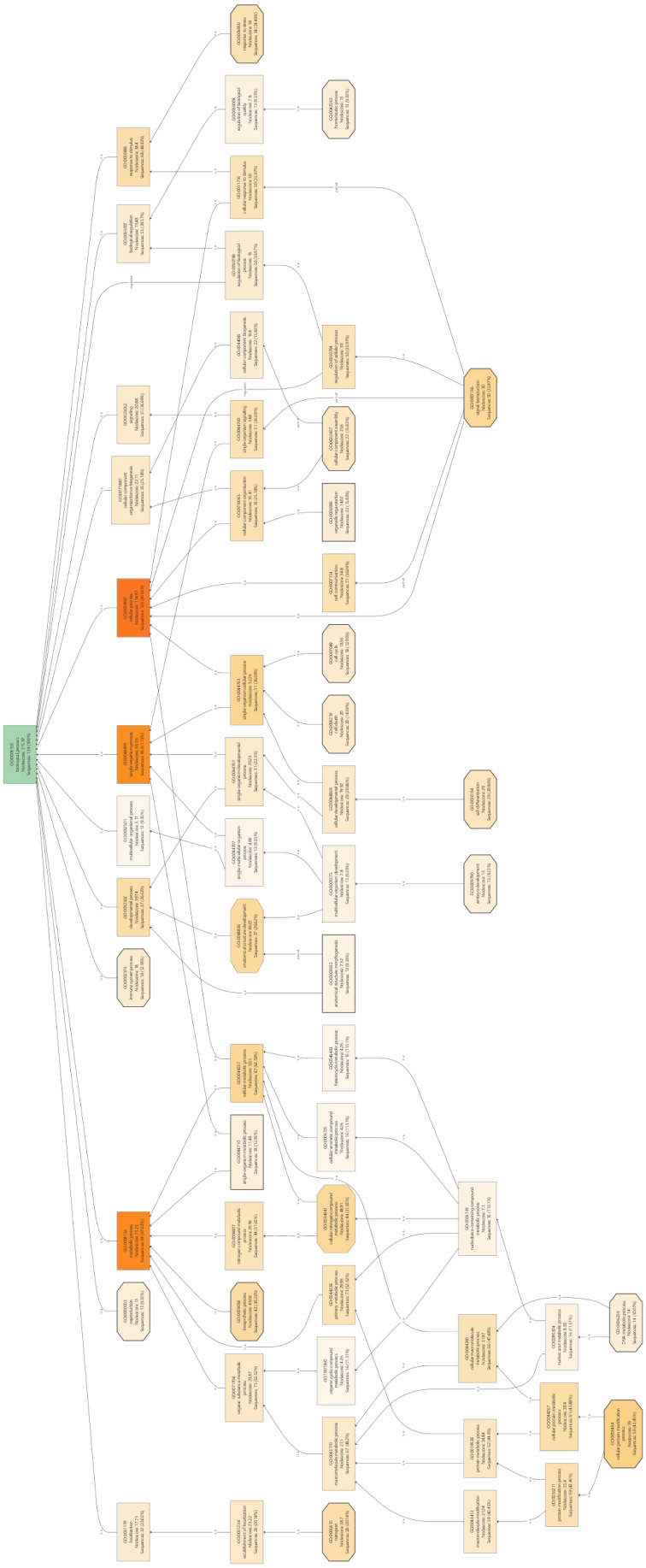

***Appendix 5* Combined graph of the biological process root term.** Blast2GO software was used to create a combined graph revealing all terms under the umbrella biological process. Seven generations of terms are visible.

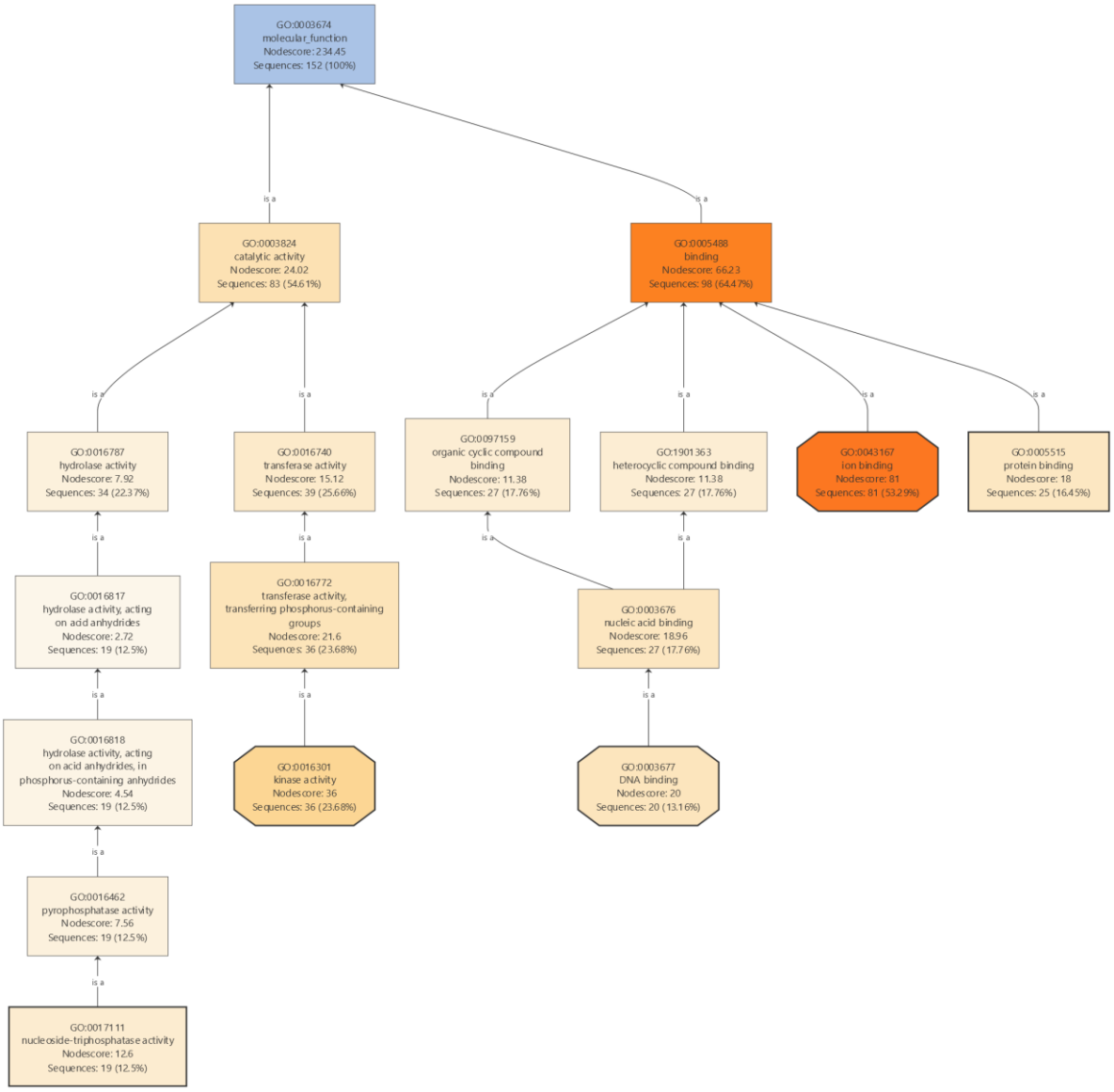

***Appendix 6* Combined graph of the molecular function root term.** Blast2GO software was used to create a combined graph revealing all terms under the umbrella molecular function. Seven generations of terms are visible.

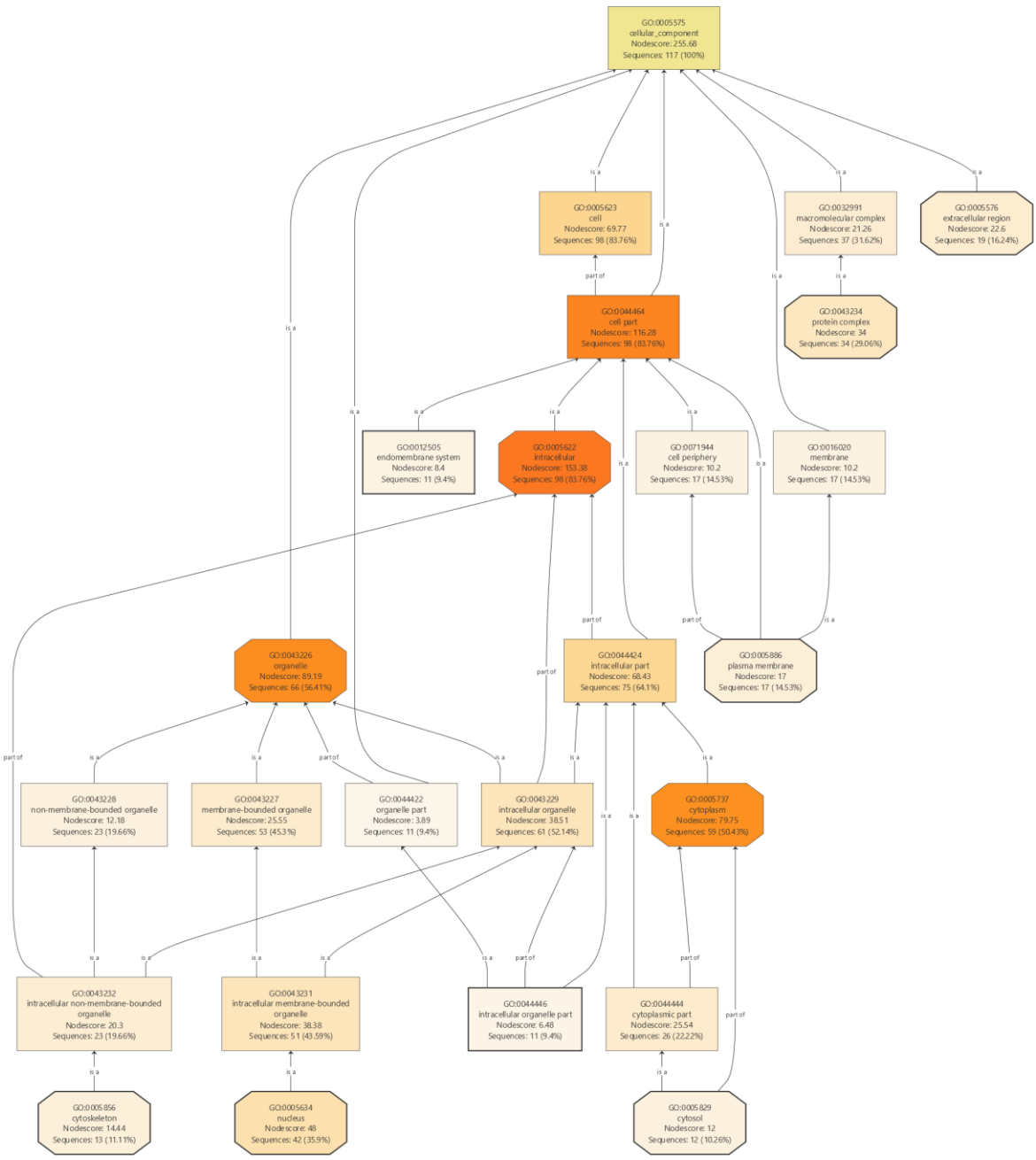

***Appendix 7* Combined graph of the cellular component root term.** Blast2GO software was used to create a combined graph revealing all terms under the umbrella cellular component. Eight generations of terms are visible.